**Lateral Cartilage Tissue Integration**

**Evaluation of Bonding Strength and Tissue Integration *in vitro* Utilizing Biomaterials and Adhesives**

**Laterale Knorpelintegration**

**Beurteilung der Adhäsionskraft und der Gewebeintegration *in vitro* unter Verwendung verschiedener Biomaterialien und Gewebekleber**

DOCTORAL THESIS FOR A DOCTORAL DEGREE

AT THE GRADUATE SCHOOL OF LIFE SCIENCES,

JULIUS-MAXIMILIANS-UNIVERSITÄT WÜRZBURG,

SUBMITTED BY

OLIVER BERBERICH

FROM

HARDHEIM, GERMANY

MÜNCHEN, 2023

Submitted on: …………………………………………………………………………………………………

**Members of the Promotionkomitee:**

Chairperson: Prof. Dr. Thomas Dandekar

Primary Supervisor: Prof. Dr. Torsten Blunk

Supervisor (Second): Dr. Jörg Teßmar

Supervisor (Third): Prof. Dr. Robert Luxenhofer

Date of Public Defence: …………………………………………………………………………………

Date of Receipt of Certificates: …………………………………………………………………………

In Liebe und Dankbarkeit für meine Eltern

# Table of Contents

# Summary

Articular cartilage defects represent one of the most challenging clinical problem for orthopedic surgeons and cartilage damage after trauma can result in debilitating joint pain, functional impairment and in the long-term development of osteoarthritis. The lateral cartilage-cartilage integration is crucial for the long-term success and to prevent further tissue degeneration. Tissue adhesives and sealants are becoming increasingly more popular and can be a beneficial approach in fostering tissue integration, particularly in tissues like cartilage where alternative techniques, such as suturing, would instead introduce further damage. However, adhesive materials still require optimization regarding the maximization of adhesion strength on the one hand and long-term tissue integration on the other hand. *In vitro* models can be a valuable support in the investigation of potential candidates and their functional mechanisms. For the conducted experiments within this work, an *in vitro* disc/ring model obtained from porcine articular cartilage tissue was established. In addition to qualitative evaluation of regeneration, this model facilitates the implementation of biomechanical tests to quantify cartilage integration strength. Construct harvesting for histology and other evaluation methods could be standardized and is ethically less questionable compared to *in vivo* testing. The opportunity of cell culture technique application for the *in vitro* model allowed a better understanding of cartilage integration processes.

Tissue bonding requires chemical or physical interaction of the adhesive material and the substrate. Adhesive hydrogels can bind to the defect interface and simultaneously fill the gap of irregularly shaped defect voids. Fibrin gels are derived from the physiological blood-clot formation and are clinically applied for wound closure. Within this work, comparisons of different fibrin glue formulations with the commercial BioGlue® were assessed, which highlighted the need for good biocompatibility when applied on cartilage tissue in order to achieve satisfying long-term integration. Fibrin gel formulations can be adapted with regard to their long-term stability and when applied on cartilage disc/ring constructs improved integrative repair is observable. The kinetic of repairing processes was investigated in fibrin-treated cartilage composites as part of this work. After three days *in vitro* cultivation, deposited extracellular matrix (ECM) was obvious at the glued interface that increased further over time. Interfacial cell invasion from the surrounding native cartilage was detected from day ten of tissue culture. The ECM formation relies on molecular factors, e.g., as was shown representatively for ascorbic acid, and contributes to increasing integration strengths over time. The experiments performed with fibrin revealed that the treatment with a biocompatible adhesive that allows cartilage neosynthesis favors lateral cartilage integration in the long term. However, fibrin has limited immediate bonding strength, which is disadvantageous for use on articular cartilage that is subject to high mechanical stress. The continuing aim of this thesis was to further

develop adhesive mechanisms and new adhesive hydrogels that retain the positive properties of fibrin but have an increased immediate bonding strength.

Two different photochemical approaches with the advantage of on-demand bonding were tested. Such treatment potentially eases the application for the professional user. First, an UV light induced crosslinking mechanism was transferred to fibrin glue to provide additional bonding strength. For this, the cartilage surface was functionalized with highly reactive light-sensitive diazirine groups, which allowed additional covalent bonds to the fibrin matrix and thus increased the adhesive strength. However, the disadvantages of this approach were the multi-step bonding reactions, the need for enzymatic pretreatment of the cartilage, expensive reagents, potential UV-light damage, and potential toxicity hazards. Due to the mentioned disadvantages, no further experiments, including long-term culture, were carried out. A second photosensitive approach focused on blue light induced crosslinking of fibrinogen (RuFib) via a photoinitiator molecule instead of using thrombin as a crosslinking mediator like in normal fibrin glue. The used ruthenium complex allowed inter- and intramolecular dityrosine binding of fibrinogen molecules. The advantage of this method is a one-step curing of fibrinogen via visible light that further achieved higher adhesive strengths than fibrin. In contrast to diazirine functionalization of cartilage, the ruthenium complex is of less toxicological concern. However, after *in vitro* cultivation of the disc/ring constructs, there was a decrease in integration strength. Compared to fibrin, a reduced cartilage synthesis was observed at the defect. It is also disadvantageous that a direct adjustment of the adhesive can only be made via protein concentration, since fibrinogen is a natural protein that has a fixed number of tyrosine binding sites without chemical modification.

An additional cartilage adhesive was developed that is based on a mussel-inspired adhesive mechanism in which reactivity to a variety of substrates is enabled via free DOPA amino acids. DOPA-based adhesion is known to function in moist environments, a major advantage for application on water-rich cartilage tissue surrounded by synovial liquid. Reactive DOPA groups were synthetically attached to a polymer, here POx, to allow easy chemical modifiability, e.g. insertion of hydrolyzable ester motifs for tunable degradation. The possibility of preparing an adhesive hybrid hydrogel of POx in combination with fibrinogen led to good cell compatibility as was similarly observed with fibrin, but with increased immediate adhesive strength. Degradation could be adjusted by the amount of ester linkages on the POx and a direct influence of degradation rates on the development of integration in the *in vitro* model could be shown.

Hydrogels are well suited to fill defect gaps and immediate integration can be achieved via adhesive properties. The results obtained show that for the success of long-term integration, a good ability of the adhesive to take up synthesized ECM components and cells to enable regeneration is

required. The degradation kinetics of the adhesive must match the remodeling process to avoid intermediate loss of integration power and to allow long-term firm adhesion to the native tissue.

Hydrogels are not only important as adhesives for smaller lesions, but also for filling large defect volumes and populating them with cells to produce tissue engineered cartilage. Many different hydrogel types suitable for cartilage synthesis are reported in the literature. A long-term stable fibrin formulation was tested in this work not only as an adhesive but also as a bulk hydrogel construct. Agarose is also a material widely used in cartilage tissue engineering that has shown good cartilage neosynthesis and was included in integration assessment. In addition, a synthetic hyaluronic acid-based hydrogel (HA-SH/P(AGE/G)) was used. The disc/ring construct was adapted for such experiments and the inner lumen of the cartilage ring was filled with the respective hydrogel. In contrast to agarose, fibrin and HA-SH/P(AGE/G) gels have a crosslink mechanism that led to immediate bonding upon contact with cartilage during curing. The enhanced cartilage neosynthesis in agarose compared to the other hydrogel types resulted in improved integration during *in vitro* culture. This shows that for the long-term success of a treatment, remodeling of the hydrogel into functional cartilage tissue is a very high priority. In order to successfully treat larger cartilage defects with hydrogels, new materials with these properties in combination with chemical modifiability and a direct adhesion mechanism are one of the most promising approaches.

## Zusammenfassung

Gelenkknorpeldefekte stellen eines der größten klinischen Probleme für orthopädische Chirurgen dar, und Knorpelschäden nach einem Trauma können zu starken Gelenkschmerzen, Funktionseinschränkungen und langfristig zur Entwicklung von Arthrose führen. Die laterale Knorpel-Knorpel-Integration ist entscheidend für den langfristigen Behandlungserfolg, um eine weitere Degeneration des Gewebes zu verhindern. Gewebekleber und -versiegelungen erfreuen sich zunehmender Beliebtheit und können einen vorteilhaften Ansatz zur Förderung der Gewebeintegration darstellen. Insbesondere bei einem avaskulären Gewebe wie Knorpel können alternative Fixierungstechniken wie Nähte eher zu weiteren Schäden führen. Aktuelle Klebstoffe bedürfen jedoch noch der Optimierung im Hinblick auf die Maximierung der Klebekraft einerseits und der langfristigen Gewebsintegration andererseits. *In vitro* Modelle können eine wertvolle Unterstützung bei der Untersuchung potenzieller Kleber-Kandidaten und derer Funktionsmechanismen sein. Für die im Rahmen dieser Arbeit durchgeführten Experimente wurde ein *in vitro* Disc/Ring-Modell aus porcinem Gelenkknorpel hergestellt. Neben der qualitativen Bewertung der Regeneration erleichtert dieses Modell die Durchführung biomechanischer Tests zur Quantifizierung der Knorpelintegrationskraft. Die Herstellung von Konstrukten für die Histologie und anderer analytischer Verfahren ist standardisierbar und ist im Vergleich zu *in vivo* Versuchen ethisch weniger bedenklich. Die Möglichkeit der Anwendung von Zellkulturtechniken mit dem *in vitro* Modell ermöglicht eine bessere Untersuchung von Knorpelintegrationsprozessen.

Das Verkleben von Gewebe erfordert eine chemische oder physikalische Wechselwirkung zwischen dem Klebstoff und dem Substrat. Adhäsive Hydrogele können sich an die Defektoberfläche binden und gleichzeitig die Lücke unregelmäßig geformter Defekthohlräume füllen. Fibrin-Gele sind von der physiologischen Blutgerinnung abgeleitet und werden seit langem klinisch zum Wundverschluss eingesetzt. Innerhalb dieser Arbeit wurden Vergleiche verschiedener Fibrinkleberformulierungen mit dem kommerziellen BioGlue® durchgeführt, welche gezeigt haben, dass bei der Anwendung auf Knorpelgewebe eine gute Biokompatibilität erforderlich ist, um eine zufriedenstellende Langzeitintegration zu erreichen. Fibrinformulierungen können im Hinblick auf ihre Langzeitstabilität angepasst werden, und bei der Anwendung auf Knorpel Disc/Ring-Konstrukten ist eine verbesserte integrative Reparatur zu beobachten. Im Rahmen dieser Arbeit wurde die Kinetik der Reparaturprozesse in fibrinbehandelten Knorpelkompositen untersucht. Nach dreitägiger *in vitro*-Kultivierung war eine Ablagerung von extrazellulärer Matrix (ECM) an der verklebten Grenzfläche zu erkennen, welche mit der Zeit weiter zunahm. Ab dem zehnten Tag der Gewebekultur wurde das Einwandern von Zellen aus dem umgebenden nativen Knorpel an der Grenzfläche festgestellt. Die ECM-Bildung hängt von Stoffwechselfaktoren ab, wie es beispielhaft für Ascorbinsäure gezeigt wurde.

Dabei trug neue ECM zu einer mit der Zeit zunehmenden Integrationsstärke bei. Die mit Fibrin durchgeführten Experimente haben gezeigt, dass der Ansatz mit einem biokompatiblen Klebstoff und dem Potenzial zur Knorpelneosynthese die laterale Knorpelintegration langfristig begünstigt. Allerdings hatte Fibrin nur eine begrenzte anfängliche Klebekraft, was für den Einsatz auf mechanisch stark belastetem Gelenkknorpel nachteilig ist. Das weiterführende Ziel dieser Arbeit war es unter anderem Haftmechanismen und neue adhäsive Hydrogele zu entwickeln, welche die positiven Eigenschaften von Fibrin beibehalten, aber eine höhere Klebekraft aufweisen.

Es wurden zwei verschiedene photochemische Ansätze getestet, die den Vorteil einer zeitlich festlegbaren Verklebung haben und somit dem Anwender eine einfache Applizierung ermöglichen. Zunächst wurde ein UV-Licht-induzierter Vernetzungsmechanismus zur Bereitstellung zusätzlicher Klebestellen zum Fibrinkleber entwickelt. Die Knorpeloberfläche wurde dabei mit hochreaktiven, lichtempfindlichen Diazirin-Molekülen funktionalisiert, die zusätzliche kovalente Bindungen an die Fibrinmatrix ermöglichten und damit die direkte Adhäsionskraft erhöhten. Die Nachteile dieses Ansatzes waren jedoch die mehrstufigen Vernetzungsreaktionen, die Notwendigkeit einer enzymatischen Vorbehandlung des Knorpels, teure Reagenzien, eine mögliche Schädigung durch UV-Licht und potentielle toxikologische Risiken. Wegen den erwähnten Nachteilen wurde auf zusätzliche Untersuchungen verzichtet und der Fokus auf die Alternativenfindung gelegt. Ein weiterer Ansatz konzentrierte sich auf die Vernetzung von Fibrinogen durch blaues Licht (RuFib) mittels eines Photoinitiaor-Moleküls statt über Thrombinzugabe wie bei gewöhnlichen Fibrinklebern. Der verwendete Rutheniumkomplex ermöglichte die inter- und intramolekulare Dityrosinbindung von Fibrinogenmolekülen. Der Vorteil war dabei die einstufige lichtinduzierte Vernetzung von Fibrinogen mit höheren Haftkräften als bei Fibrin. Im Gegensatz zur Diazirin-Funktionalisierung von Knorpel ist der Rutheniumkomplex auch toxikologisch weniger bedenklich. Nach *in vitro* Kultivierung der RuFib geklebten Disc/Ring-Konstruktes kam es jedoch zu einer Abnahme der Integrationskraft. Im Vergleich zu Fibrin wurde eine verminderte Knorpelsynthese am Defekt beobachtet. Nachteilig ist auch, dass eine Modifizierung des Klebers einzig über die Proteinkonzentration erfolgen kann, da Fibrinogen als natürliches Protein eine feste Anzahl von Tyrosin-Bindungsstellen hat und alternativ chemisch verändert werden müsste.

Ein zusätzlich entwickelter Klebstoff basiert auf einem von Muscheln inspirierten Haftmechanismus, bei dem die Reaktivität zu einer Vielzahl von Substraten über freie DOPA-Aminosäuren ermöglicht wird. Es ist bekannt, dass die DOPA-basierte Adhäsion in einer feuchten Umgebung funktioniert, ein großer Vorteil für die Anwendung auf stark wasserhaltigem Knorpelgewebe und im feuchten Synovium. Reaktive DOPA-Gruppen wurden synthetisch an ein Polymer, in diesem Fall POx, gebunden, um eine einfache chemische Modifizierbarkeit zu ermöglichen.

Mögliche Anpassungen sind z.B. das Einfügen von hydrolysierbaren Esterbindungen um veränderte Degradationsraten zu erreichen. Die Möglichkeit der Herstellung eines adhäsiven Hybridhydrogels aus POx in Kombination mit Fibrinogen führte zu einer erhöhten Zellkompatibilität, wie sie bereits bei Fibrin beobachtet wurde, jedoch mit erhöhter direkter Klebekraft. Die angepasste Degradationskinetik über die Menge an Esterbindungen am POx hatte einen direkten Einfluss auf die Entwicklung der Integration im *in vitro* Modell gezeigt.

Hydrogele sind gut geeignet, um Defektlücken zu füllen. Bei intrinsischen Adhäsionseigenschaften kann eine gewisse sofortige Integration erreicht werden. Die erzielten Ergebnisse zeigen, dass für den Erfolg einer langfristigen Integration eine gute Fähigkeit des Klebstoffs zur Aufnahme von synthetisierten ECM-Komponenten und Zellen erforderlich ist. Die Abbaukinetik des Klebstoffs muss dabei mit dem Umbauprozess im Gleichgewicht sein, um einen zwischenzeitlichen Verlust der Integrationskraft zu vermeiden und eine langfristige feste Adhäsion an das native Gewebe zu ermöglichen. Hydrogele sind nicht nur als Klebstoffe für kleinere Defekte wichtig, sondern auch als Tissue-Engineering Material um große Defektvolumina aufzufüllen und mit Zellen zu besiedeln.

In der Literatur werden verschiedene Hydrogelarten für die Knorpelsynthese berichtet. Eine langzeitstabile Fibrinformulierung wurde in dieser Arbeit nicht nur als Klebstoff, sondern auch als größeres Hydrogelkonstrukt getestet. Agarose ist ebenfalls ein im Knorpel-Tissue-Engineering häufig verwendetes Material, das bereits eine gute Knorpelneosynthese gezeigt hat. Darüber hinaus wurde ein synthetisches Hyaluronsäure-basiertes Hydrogel (HA-SH/P(AGE/G)) untersucht. In durchgeführten Experimenten wurde das Disc/Ring Modell adaptiert und das innere Lumen des Knorpelrings mit dem jeweiligen Hydrogel gefüllt. Im Gegensatz zu Agarose verfügen Fibrin und das HA-SH/P(AGE/G)-Gel über einen Vernetzungsmechanismus, der beim Kontakt mit dem Knorpel während der Aushärtung zu einer sofortigen Bindung führte. Die verstärkte Knorpelneosynthese in Agarose im Vergleich zu den anderen Hydrogeltypen führte zu einer erhöhten Integration während der *in vitro* Kultur. Dies zeigt, dass für den langfristigen Erfolg eines Therapieansatzes der Umbau des Hydrogels in funktionelles Knorpelgewebe eine sehr hohe Priorität hat. Um größere Knorpeldefekte erfolgreich mit Hydrogelen behandeln zu können, sind neue Materialien mit diesen Eigenschaften in Kombination mit chemischer Modifizierbarkeit und einem direkten Adhäsionsmechanismus einer der vielversprechendsten Ansätze.

# 1  Introduction

## 1.1    Articular Cartilage Tissue

Articular cartilage refers to hyaline cartilage that overlies the interacting bony surfaces in diarthrodial joints and is separated by synovial fluid. Hyaline cartilage mainly consists of type II collagen and proteoglycans. The location of the articular cartilage and specification of the surrounding structures is exemplified for the knee joint in Figure 1. Within the knee joint, the fibrocartilaginous meniscus additionally divides the joint cavity and further serves to disperse load and friction.

In order to ensure that joints and bone move together, a high specialization of the articular cartilage tissue is required. This type of connective tissue is providing a smooth and lubricated surface for articulation and facilitates the transmission of loads. Articular cartilage tissue is avascular and is devoid of nerves and lymphatics, thus leading to a limited capacity of intrinsic healing and repair. The environment of healthy cartilage is hypoxic, with oxygen tensions ranging between 1 and 5 %, as
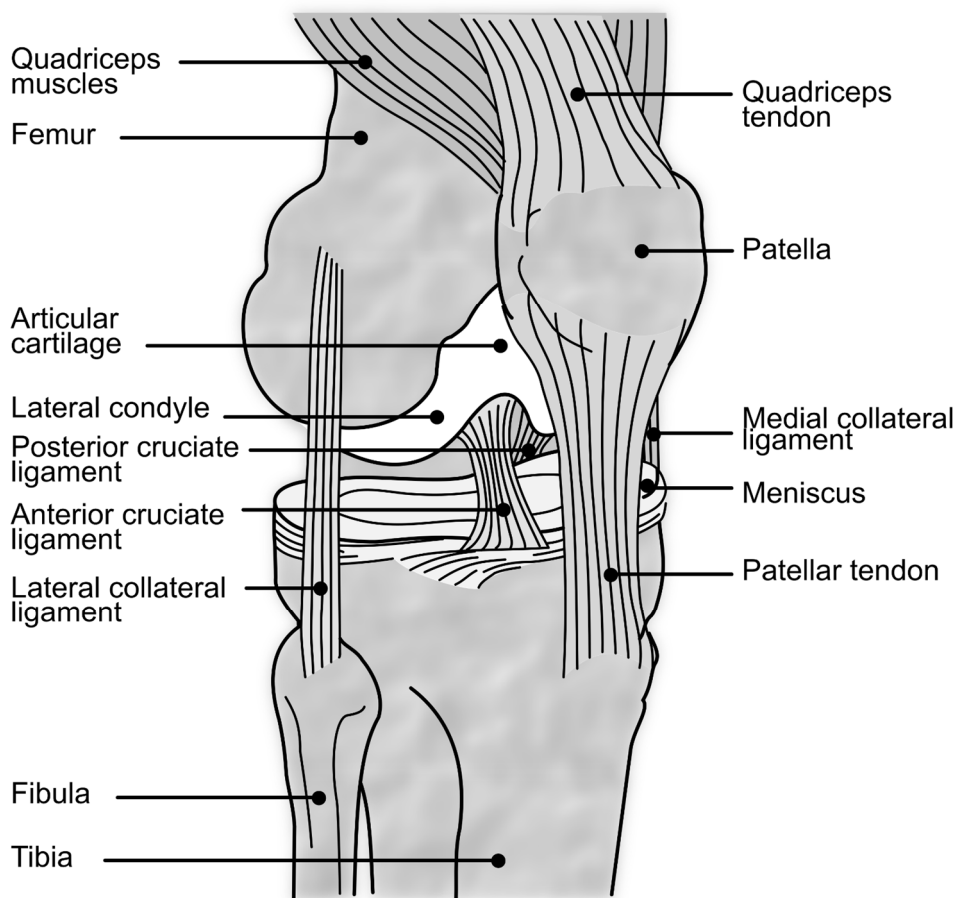


**Figure 1: Schematic overview of the knee joint.**

Graphic created with royalty free components

compared with 21 % in ambient air [1]. However, there is still controversy in the literature as to which oxygen content has a beneficial effect on cartilage formation (e.g. in tissue engineering approaches) [2].

Even minor injuries to the cartilage tissue often result in osteoarthritis (OA) and musculoskeletal morbidity. With the demographic change and the increasing number of patients with overweight, the prevalence of osteoarthritis is likely to rise in the near future. The current surgical intervention for end-stage degenerative joint pathologies is the total joint replacement with artificial prostheses. Although there are other ways of treatment, including repair and tissue engineering strategies. However, the complex structure of articular cartilage makes repair and/or restoration of the defects difficult. To preserve to the function of the tissue it is mandatory to maintain its organized architecture.

### 1.1.1    Cartilage Tissue Structure and Function

Articular cartilage primarily consists of a single cell type, the chondrocyte. The chondrocyte has a hypoxic metabolism and produces abundant extracellular matrix (ECM). The ECM production is controlled through cytokines and proteases. Chondrocytes originate from mesenchymal stem cells of the bone marrow [3]. Proliferation of chondrocytes appears steadily during embryogenesis but decreases or ceases in adulthood. Thus, cartilage cells usually last a lifetime unless damaged through trauma or disease. Chondrocytes have a spherical phenotype and can occur either as single cells or aggregated into chondrons. Chondrocytes are covered by a pericellular matrix, which in turn is surrounded by the territorial matrix, although the greatest volume in cartilage tissue is occupied by the interterritorial matrix which fills the space between the single chondrocytes. Components of the ECM mainly are type II collagen and the proteoglycan aggrecan. About 60 % of the cartilage dry weight is credited to the collagens, 80 % of which is represented by type II collagen. Another 15 % are composed of the remaining isoforms type IX and XI collagen. About 5 % are credited to other collagen types like types III, XII and VI. The collagen fibrils provide for resistance to the mechanical compression forces that occur in joints, most of all in the knee joint [4]. The rest of the cartilage dry weight is partitioned to proteoglycans (5-10 %) and non-collagenous proteins like the transmembrane proteins anchorin CII and integrins. These proteins are involved in anchoring the chondrocyte to its pericellular space via interaction with collagen and fibronectin molecules [5] (see Figure 2).
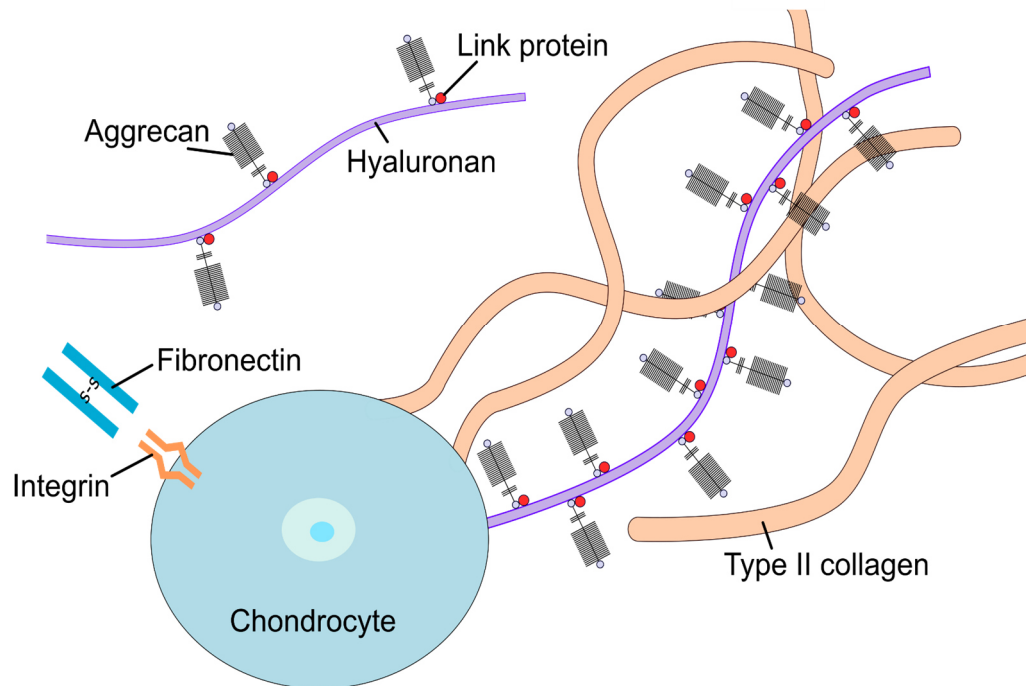
**Figure 2: Schematic illustration of the macromolecular composition in the extracellular matrix of cartilage tissue.**

Graphic created with royalty free components

Aggregating proteoglycans that fill the interfibrillar space are referred to as aggrecans. Aggrecan is the largest and most abundant proteoglycan that is present in articular cartilage. It is composed of many sulfated glycosaminoglycans (GAG) chains with high negative charges such as chondroitin sulfate and keratin sulfate that are covalently attached to a core protein. Additionally, these proteoglycans have the ability to bind to hyaluronan via link proteins. The resulting osmotic properties of aggrecan are also recognized to contribute to the mechanical functions of articular cartilage. The attraction of large amounts of water results in a high viscoelasticity and allows the distribution of stress across the joint during loading [6]. The amount of water in the cartilage depends on the concentration of proteoglycans and the organization of the collagen network and ranges between 65 and 80 % in different cartilage regions [3]. The non-aggregating proteoglycans decorin, biglycan and fibromodulin are much smaller than aggrecan and are characterized by their ability to interact with collagen and play an important role in fibrillogenesis and interfibril interactions of collagens.

A compromised collagen network present in OA or introduced by traumatic lesions is accompanied by loss of mechanical function of the cartilage tissue. As the anatomic alignment of the collagen fibers in articular cartilage determines the mechanical function of the tissue and varies with the different layers of the tissue, it is also mandatory to understand differences in the zonal architecture of articular cartilage.

## 1.1.2    Cartilage Zones

Articular cartilage is partitioned into a superficial, middle, deep and calcified zone with each layer providing different tensile and shear strength to the tissue due to variation of cellular and macromolecular organization (see Figure 3). For example, the compressive modulus of bovine articular cartilage differs in depth from 0.079 MPa to 2.10 MPa [7]. The collagen fibers in the superficial zone are packed tightly and aligned parallel to the articular surface thus protecting the deeper layers from shear-stress. It makes up to 10 % to 20 % of the cartilage thickness. Chondrocytes in this layer also have a flattened phenotype. The middle zone below anatomically and functionally links the superficial zone with the deeper zones. This zone represents 40 % to 60 % of the total cartilage volume and its characteristic for its high proteoglycan content and thick collagen fibers that are organized obliquely.
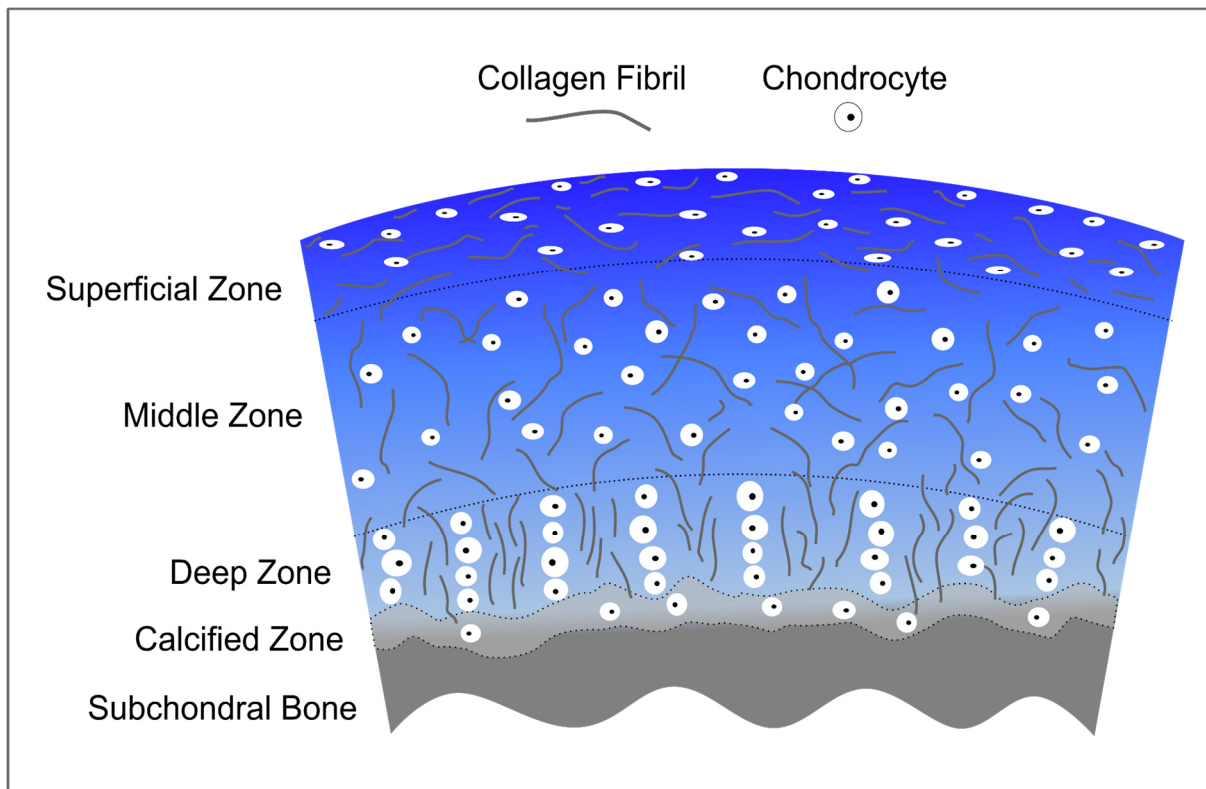


**Figure 3: Schematic diagram showing the zonal organization and collagen structure of articular cartilage.**

Redrawn and simplified with kind permission from reference [10,409].

The interplay of collagens and proteoglycans in the middle zone provide for resistance to compressive forces. Chondrocytes in this layer appear spherical and at low density. Most of the compressive forces is compensated in the deep zone where the collagen fibers have a perpendicular orientation, and the proteoglycan content is the highest. The deep zone counts to about 30 % of the total cartilage volume. In contrast to the top layers, here the chondrocytes are arranged in a columnar pattern perpendicular to the articular surface and parallel to the collagen fibers. From the deep zone

highly aligned type II collagen fibers span to the calcified layer which helps to anchor the cartilage to the subchondral bone. In the calcified zone chondrocytes are scarce and have a hypertrophic metabolism [6,8]. Besides high contents of proteoglycans, mineral and collagen II, the calcified layer also contains type IX and type X collagen [9,10]. The zonal origin of cells may play a crucial role for regenerative approaches, as it has been shown that cells from the deep zone most of all contribute to neocartilage formation at chondral wound edges [11].

### 1.1.3    Cartilage Injuries

In healthy cartilage it is known that there appear age-related changes. Concomitant with aging processes the cartilage thickness and its cellularity decrease with differences between cartilage zones. With a decreasing cell concentration the risks of fibrillation and development of OA are likely to increase [12]. These processes can be initiated by age-related wear or by trauma to the cartilage. It is reported that even with current treatments more than 40 % of people who suffered traumatic knee joint injuries will develop OA [13]. When impact forces to the cartilage surfaces are too heavy or appear too rapidly it may surpass the compression resistance of the tissue and the ECM framework ruptures accompanied by cell damage [14]. Different types of cartilage injuries with different repair responses can be classified in three types according to applied impact energy: (1) damage to cells and/or matrices that does not include macroscopic structural disruption of cartilage or bone; (2) damage to cells and/or matrices along with macroscopic structural disruption of articular cartilage without displaced bone fracture. These injuries can be associated with microfractures in the calcified cartilage or into the subchondral bone; (3) displaced fractures of the articular surface extending through cartilage and bone [15]. For the patient the direct outcome of cartilage damage is joint swelling and pain [16].

In healthy cartilage there is a balance between ECM synthesis and breakdown. Chondrocytes are thereby responsible for both matrix generation and the balanced decomposition of the ECM via a group of degenerative enzymes. The turnover of ECM components is reported to take up to 25 years for proteoglycans [17] and several decades up to even 400 years for collagen [18]. One of the earliest outcomes of cartilage injury is the loss or decrease of aggregation of proteoglycans. This may be attributable to increased molecular degradation or decreased synthesis [15]. Proinflammatory cytokines such as interleukin-1 (IL-1) and tumor necrosis factor−α (TNF−α), growth factors (e.g. transforming growth factor-β (TGF-β) and insulin-like growth factors (IGF)) have been implicated in the regulation of proteoglycan metabolism and are crucial for the degradation and synthesis of ECM components. Although, the exact mechanisms of the interplay of these factors yet remains unclear [3,6]. The increased degradation of proteoglycans and the collagen network after cartilage injuries is attributed to elevated

activities of degrading enzymes like matrix metalloproteinases (MMPs) and aggrecanases [19,20]. For example, members of the MMP family (MMP1, 3, 7, 9, 13) cleave type II collagen at the C-telopeptide domain generating the specific neoepitope CTX-II, which is an established indicator for cartilage damage and progress in OA [21–23]. Even though the MMPs are believed to cleave in the C-terminal regions of aggrecan as well, the most sensitive region for MMPs and ADAMTS (short for A Disintegrin And Metalloproteinase with ThromboSpondin motifs) for site specific cleavage of aggrecan is the G1-G2 interglobular domain of aggrecan. Amongst the known neoepitopes resulting from aggrecan cleavage are the MMP-related C-terminal DIPEN and the aggrecanase-related C-terminal NITEGE [24,25]. Inflammatory responses vary with the severity of cartilage defects and cytokines such as IL-1 or TNF-α may accelerate the progress of OA [20,26]. Other factors that influence the progression of cartilage lesions are the size and location of the lesion, patient age, limb alignment, associated meniscal and ligament injuries and body mass index [27,28]. Because of the multitude of risk factors, the time course of OA in affected patients can range from two to five years in the case of certain articular fractures, to decades for less severe joint injuries [13].

Due to the lack of vascularization and access of progenitor cells to chondral lesions, there is limited repair after cartilage trauma. Despite that, it was observed that small < 3 mm diameter full-thickness cartilage defects showed spontaneous healing in rabbits [29]. Larger defects however do not possess the ability to heal and lead to a progressive degeneration at the lesion site, as shown in a goat defect model [30]. In osteochondral or full-thickness defects that span to the vascularized subchondral bone a hematoma composed of a fibrin clot is formed at the defect site. This clot can fill defects of up to 2 to 3 mm in diameter. Mesenchymal stem cells (MSCs) from the vasculature or the bone marrow can penetrate this clot and build up a repair tissue. However, neither does this repair tissue possess the typical biomacromolecular composition of hyaline cartilage nor its zonal organization [31,32]. Because of its high content of type I collagen this repair tissue is also referred as fibrocartilage. Additionally, fibrocartilage does not have equivalent mechanical properties compared to hyaline cartilage, which leads to lateral discontinuities between the host and repair tissue [29,31,33]. Because of the missing integration, chondrocytes from the neighboring host tissue do not contribute to the defect filling but undergo apoptosis over time leaving back an acellular region at the defect interface [30].

### 1.1.4 Clinical Presentation of Cartilage Injuries

Osteoarthritis is highly prevalent around the globe. It causes disability and not only negatively affects patient's mobility but also their mental wellbeing [34]. The 2010 Global Burden of Disease Study reports that the burden of musculoskeletal disorders is much larger than estimated in previous

assessments and an estimated 10 % to 15 % of all adults aged over 60 have some degree of OA, with prevalence higher among women than men. The global prevalence of radiographically confirmed symptomatic knee OA in 2010 was estimated to be 3.8 %. Prevalence peaked at around 50 years of age [35]. Amongst EU member states the prevalence of diagnosed OA prevalence varied from 2.8 % in Romania to 18.3 % in Hungary [36]. According to estimations of the United Nations, in the year 2050 people aged over 60 will account for more than 20 % of the world's population. Of that 15 % to 20 % will have symptomatic OA, and one-third of these people will be severely disabled. In other words, in 2050 about 130 million people will suffer from OA worldwide, of whom 40 million will be severely disabled by the disease [37]. Additionally, OA is a risk factor for the development of cardiovascular diseases. The risk of myocardial infarction and coronary heart disease is reported to be significantly elevated in patients with OA [38–40].

Besides the severe impacts on patient's life, OA healthcare is also an important cost factor in healthcare systems. Much effort has been devoted to quantify the burden of OA and it is believed that the cost of OA account for between 0.25 % and 0.50 % of a country's gross domestic product [41]. Precise global precisions remain unfeasible as most of this data has been surveyed in developed countries. In addition, the progressive development of OA makes it difficult to break down the costs more precisely [42]. However, according to estimates the average direct cost of osteoarthritis in Canada increased between 2003 and 2010 from 577 $ to 811 $ per patient and year with joint replacement surgeries as the main factor [43]. In the United States, the estimated total annual average direct per
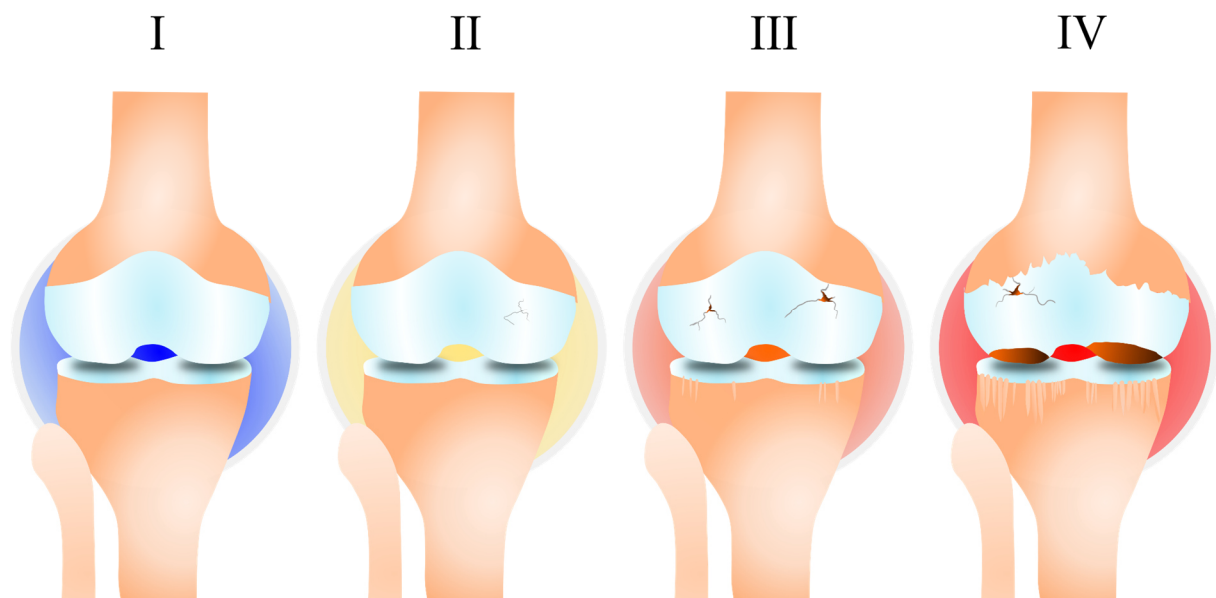


**Figure 4: Exemplary illustration of the Outerbridge classification for cartilage defects.**

(Grade I: cartilage with softening and swelling, Grade II: fissures on the cartilage surface that do not exceed 1.3 cm in diameter, Grade III: like grade II, but in an area with a diameter more than 1.3 cm, Grade IV: erosion of cartilage down to the subchondral bone). Graphic created with royalty free components

patient cost had huge variations from 1442 $ to 21335 $ [44]. Despite the variations in reports, these numbers clearly demonstrate the need for successful treatment of cartilage defects, ideally at early stages before the onset of OA.

In clinical evaluation cartilage defects are graded routinely using the Outerbridge classification (Grade 0: normal cartilage, Grade I: cartilage with softening and swelling, Grade II: fissures on the cartilage surface that do not exceed 1.3 cm in diameter, Grade III: like grade II, but in an area with a diameter more than 1.3 cm, Grade IV: erosion of cartilage down to the subchondral bone) [45] (see Figure 4). The display of chondral lesions differs is of great variability which affects the clinical outcome. In general, lesions are separated in superficial, partial thickness that span into deeper cartilage zones and full thickness lesions that cross the osteochondral junction. Arthroscopy of patients suffering pain revealed the incidence chondral injuries to be about 60 % with 2/3 described as localized focal lesions and 1/3 as osteoarthritic defects [46,47] Another study found that the incidence of treatable full thickness cartilage injuries was of 11 % [48]. Partial and full thickness lesions mostly count to Grade III and IV defects and often need surgical intervention [47,49].

### 1.1.4.1 Clinical Approaches for the Treatment of Cartilage Defects

In clinics, initial treatment of cartilage injuries commonly is focused on non-surgical techniques such as physical therapy, weight loss, and anti-inflammatory medications. However, as the defect progresses, these treatment options become ineffective, eventually requiring surgical intervention. Current procedures are aimed at either stimulating a healing response or replacing and regenerating the articular cartilage. The various strategies used in clinical practice today include those aimed at spontaneous repair (microfracturing, chondroplasty), those that reconstruct injured cartilage and replace it with donor cartilage (mosaicplasty and allograft), and, more recently, biologically based approaches (autologous chondrocyte implantation (ACI) and bioengineered scaffolds). All of these strategies are less invasive than prosthetic joint replacement and potentially more durable. Most surgeons attempt to limit total knee replacement to patients in their sixth decade of life or older because the lifespan of an artificial knee prosthesis is approximately 15 years [50,51], after which the failure rate increases [52]. In the following, the surgical procedures that are most commonly performed by orthopedic surgeons to treat cartilage injuries are described.

## 1.1.4.2    Scaffold-Free Clinical Approaches

Amongst the current approaches for clinical treatment of cartilage defects are bone marrow-stimulating microfracture, mosaicplasty with autologous or allogeneic osteochondral implants [53], as well as cell-based autologous chondrocyte implantation (ACI), which Brittberg introduced in 1994 [54]. In the case of breaching the subchondral bone, MSCs are allowed to migrate from the underlying cavity into the defect [31]. The resulting fibrous repair tissue misses satisfying biomechanical properties but may remain durable for several years [55]. However, long-term results show that this fibrocartilage is incapable of withstanding the high mechanical forces in the knee joint and fails over time [56,57]. Regarding the pain release of patients, mosaicplasty seems beneficial compared to microfracture techniques in the middle-term [58]. The long-term results also remain unsatisfactory though, with little evidence of integrative repair [59–62] and a failure rate of 55 % [63]. For this procedure osteochondral grafts from a healthy low weight-bearing area of the knee are isolated and transferred towards the defective site [53]. For this reason, additional defects are created and donor site morbidity in the patient is enhanced. Another option to treat focal lesions is ACI. A small cartilage tissue biopsy is taken arthroscopically followed by enzymatic digestion to obtain the incorporated chondrocytes. The cells are subsequently expanded in cell culture *in vitro* and finally re-implanted into the cartilage defect covered by a periosteal flap [54]. The resulting repair tissue after ACI treatment reportedly is of variable quality. Studies showed that in only 15-25 % of the patients hyaline-like cartilage was formed, whereas in the rest biomechanically instable fibrocartilage was built up [64,65]. Attending issues are hypertrophy and delamination [66], although some integration with the host tissue was observed in short-termed animal studies [67]. Since its first clinical application many modifications of ACI were carried out, most of all to potentially minimize the risk of hypertrophy and ossification associated with the periosteal tissue. For example, collagen membranes were used as substitution of the periosteal flap [66,68] and various matrices as carrier for the chondrocytes (matrix-induced autologous chondrocyte implantation - MACI) were used to improve the clinical outcome. This technique is described in more detail in Chapter 1.1.4.3.

## 1.1.4.3    Cell- and Scaffold-Based Clinical Approaches

Almost any cell-based clinical approach for the treatment of cartilage defects starts with a tissue biopsy from the patient to obtain chondrocytes which can be expanded *in vitro*. These cells are then seeded within or onto an appropriate scaffold before being implanted back to the patient. One mayor drawback of the expansion of chondrocytes is the inevitable dedifferentiation and the change to a more fibroblastic phenotype during passaging under 2D cell culture conditions. This hampers the

synthesis of cartilage specific ECM and thus the regenerative potential. Additionally, the isolation of chondrocytes from cartilage causes considerable damage to the donor site. In contrast, stem cells isolated from mesenchymal tissues can be harvested without introducing further damage to the cartilage and are capable of neocartilage formation under the right conditions [69]. Studies utilizing MSCs to investigate cartilage repair commonly are however constrained to the use of regulatory factors such as transforming growth factor-beta (TGF-β) to induce chondrogenic differentiation [70], although it has been shown that mechanical loading triggers the upregulation of TGF-β secretion by MSCs and thus stimulates chondrogenesis without the need of growth factor supplementation [71–73]. Despite the increasing understanding of MSCs and their regenerative abilities, clinical translation remains difficult and MSCs have yet not been used routinely in clinical tissue engineering approaches for the treatment of cartilage defects. As chondrocytes are the cells originating from cartilage tissue, they may be the most suitable choice for studies that investigate basic principles in cartilage regeneration, but it is important that future studies include cells from all clinically relevant sources to determine the effectiveness of tissue engineering strategies.

The use of scaffolds for cell delivery rather than just the introduction of cells to the lesion by drilling has the benefit to hinder the invasion of fibroblasts that could otherwise induce fibrous repair [74,75]. Scaffold-based approaches have the major advantages that they provide the possibility to better fill the cartilage defect, increase the graft stability, are less technically challenging to the surgeon and have fewer donor site complications. Additionally they counteract the dedifferentiation of chondrocytes because they provide a 3D environment [76]. First case series focusing on MACI application showed good clinical and histological outcome [77,78], however the superiority of this technique to others is still questioned. So it was also shown in competitive studies that there was little to no advantage or even a setback of MACI compared to ACI [79,80]. As the overall outcome of a matrix-assisted approach is highly dependent on the performance of the scaffold material, many current investigations focus on that matter. For functional cartilage regeneration applied materials need to balance biomechanical properties, the capability for ECM deposition and cell proliferation, as the cells seeded into the scaffolding material are responsible for synthesis and metabolism of ECM. A plethora of biomaterials that provide a functional three-dimensional environment for tissue engineering approaches is available [81,82] and much investigation is conducted to improve their capability to form cartilaginous repair tissue [2,83–85]. Biomaterials have been used in various application forms, such as sponges, electrospun fibers, microparticles and hydrogels and all have different features for cartilage regeneration [86]. Biomaterials can be separated into naturally derived offspring either from polymers (e.g. agarose, hyaluronate and alginate) or from proteins (e.g. fibrin, collagen, gelatin and silk). Natural polymers commonly are biocompatible but often have poor mechanical strength and relatively high

degradation rates. In contrast synthetic polymers can be designed to achieve some distinct advantages like controllable degradation rate, high reproducibility, high mechanical strength, and easy technical handling. A significant drawback of these materials however is the usually missing cell interaction [81], which is why modifications have been explored to fabricate composite biomimetic scaffolds that combine the advantages of synthetic and natural materials [87–89]. Amongst different biomaterial application forms, hydrogels well replicate the high water content of native cartilage tissue and have become a popular option for scaffold-based cartilage treatments. Hydrogels are described in more detail in Chapter 1.1.5.

## 1.1.5    Hydrogels for Cartilage Tissue Engineering

Hydrogels are defined as networks of crosslinked polymers with high water contents and native cartilage tissue obtains hydrogel-like properties. The composition of hydrogels for wound treatments is highly modular concerning the choice of polymer, the crosslinking mechanism as well as the degradation products and rate. These factors affect parameters like crosslinking density, the mechanical loading regimen and the integration with the adjacent host tissue [85]. Although hydrogels are widely considered biocompatible, there can be immune responses to some polymer-types, degradation products and crosslinking methods. Thus, proven biocompatibility and missing cytotoxicity is of particular interest in most studies and necessary for potential market release [90,91]. A common disadvantage of hydrogels is the poor mechanical stability compared to stiff scaffolds. On the other side, hydrogels are prone to some important factors that make them suitable for clinical approaches. In general, the ability of direct cell-encapsulation improves the seeding procedure and the seeding efficiency, which results in homogeneous cell distributions. Additionally, the permeability for liquids that allows a good gas exchange and nutrient supply of the encapsulated cells is beneficial in an avascular surrounding like cartilage tissue.

Based on their polymer composition, hydrogels can be classified into natural or synthetic origin, although hybrids are also investigated. Natural polymers are isolated from both plant or animal sources and can be further divided into two categories as protein based and polysaccharide-based biomaterials. Several of these polymers can provide suitable environments to maintain the phenotype of encapsulated chondrocytes *in vitro*. Further, they can possess inherent features like cell-triggered proteolytic degradation, natural remodeling capacity, and the ability to present receptor-binding ligands to cells [92]. A variety of synthetic biomaterials are also being used for cartilage repair. Prominent synthetic materials to fabricate hydrogels are polyethylene glycol (PEG), poly(glycidol)s (PG) and poly(oxazoline)s (POx). They are pathogen-free, have low potential for immunological rejection and

can be manufactured with good control of compositional, structural and mechanical properties. Synthetic polymers have certain disadvantages such as hydrophobicity and lack of intrinsic cell attachment moieties. In addition, they undergo degradation mainly through hydrolysis that in some cases generates acidic byproducts, and elevated levels of foreign body response [5,93]. In recent years the trend to combine natural and synthetic biomaterials to a hybrid has emerged in cartilage tissue engineering. Researchers aim to exploit the advantages of both classes to adapt the composition, architecture and mechanical properties with benefit to chondrogenesis [94]. For the use as biocomposite hydrogels, the easy and standardized functionalization of synthetic polymers with versatile chemical groups is of great help to customize crosslinking and degradation profiles of biocomposite hydrogels [95,96].

In orthopedic surgery it is also important to minimize the severity of intervention. Hydrogels can be applied in an arthroscopic procedure instead of open joint surgery since they can be designed as injectable precursor solutions. This not only shortens procedural duration but also helps to reduce the infection risk and shorten the recovery time of the patient [97]. Hydrogels are also a basic part for tissue engineered constructs. 3D bioprinting with hydrogels gained considerable attention over the last years and is also investigated for the treatment of cartilage defects [98–101]. It can provide precise control of the initial structure including a zonal setting of tissue-engineered cartilage constructs. Studies showed that the deposition of an appropriate pericellular environment by 3D printing helped to mimic the specific zonal structure of cartilage tissue [102–104]. Cui et al. could also prove in an *ex vivo* study that bioprinting directly into a created cartilage defect can achieve some level of cartilage integration and mechanical competence [105]. In order to yield stiffer hydrogels the polymer concentrations are most commonly increased, but this can also lead to inhibited cell growth, migration and ECM synthesis [106]. To overcome this issue, other groups combined a hydrogel with mechanical support structures like a rigid scaffold of biodegradable fibers to improve overall mechanical properties [107]. For example, the inclusion of additional polycaprolactone (PCL) strands has been widely used as structural support in cartilage biofabrication [99,100,104,108]. Despite the ongoing development of scaffold materials, a remaining key problem is the integration of different biomaterials with the surrounding cartilage. Different types of hydrogels that have been tested for cartilage integration in the scope of this work will be described in more detail in the following.

### 1.1.5.1    Fibrin

Fibrin is the key component in physiological blood coagulation. Already in 1944 an unprocessed form of fibrin was introduced for skin grafting [109]. Although many alterations of fibrin were published,
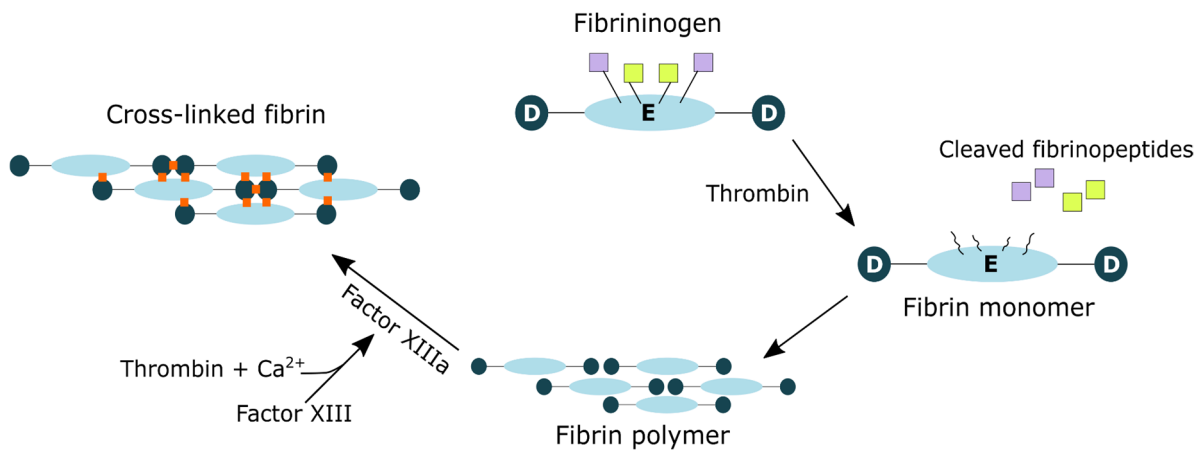
**Figure 5: Schematic illustration of the physiological fibrin clot formation.**

Fibrinogen has a central E domain joined by segment coils to two D outer domains. Thrombin cleavage of fibrinopeptides from the central E domain of fibrinogen activates polymerization by forming a fibrin monomer. The strong affinity of the exposed E-domain for the D-domain subsequently drives fibrin clot formation. The activated transglutaminase factor XIIIa causes fibrin matrix maturation and stabilization via covalently crosslinking the fibrin polymers. Redrawn and simplified with kind permission from [111]

the actual principle remains unchanged. Generally, applied forms of fibrin consist of two major component solutions, fibrinogen in combination with Factor XIII and thrombin together with $Ca^{2+}$. Fibrinogen molecules have a length of about 45 nm and is divided in two outer D domains, each of them connected by a coiled-coil segment to the central E domain. Thrombin is a serine protease that converts the soluble fibrinogen into insoluble strands of fibrin. Briefly, thrombin cleaves the fibrinopeptides A and B from the α and β chains of fibrinogen to form the fibrin monomer. A single E domain can interact with 4 D domains of other fibrin monomers to form staggered oligomers. These oligomers aggregate to protofibrils that can build up to a 3D network of entangled multi-stranded fibers and form a fibrin clot. In the presence of $Ca^{2+}$ thrombin also activates Factor XIII. The resultant activated Factor XIIIa crosslinks in the form of amide bonds between glutamine residues on one fibrin molecule and lysine residues on another fibrin molecule. This stabilization of the fibrin clot increases resistance to solubilization and proteolytic cleavage [110,111] (see Figure 5). Because of its versatility fibrin was used for different tissue engineering applications in the last decades [112]. With regard to cartilage tissue engineering, Homminga et al. reported already in 1993 that chondrocytes encapsulated in fibrin retained their morphology and produced cartilaginous ECM [113]. There are numerous clinically fibrin products commercially available (e.g. TissuCol, Artiss and Evicel®). However, these commercial products have the tendency to shrink and disintegrate *in vitro* and *in vivo* after a few days up to complete dissolution after 3-4 weeks [114–118]. The use of protease inhibitors like aprotinin or tranexamic acid is one approach to extend the longevity of fibrin constructs. As a supplement to the gel or the cell culture medium they slow down degradation and partially stabilize shape fidelity [119–121]. Still, the

resulting stability does not suffice the demands for applications where long-term shape fidelity is desired, most apparently in tissues with restricted regeneration like cartilage. To address this issue, long-term stable fibrin formulations have been developed [84,118,122]. Adaptations of the final fibrinogen concentration (25 mg/ml or higher), $Ca^{2+}$ (20 mM) concentration and the pH (between 6.8 and 9) result in transparent hydrogels that maintain their original form over several weeks. Additionally, chondrocytes showed proliferation and distinct homogeneously distributed ECM deposition in long-term stable fibrin gels [122]. Yet, up to date the integration of these materials to the adjacent cartilage remains to be investigated.

### 1.1.5.2      Agarose

Agarose is a linear polysaccharide derived from red seaweed. Because it is thermoreversible and can be modified to melt and gel at a variety of temperatures complicated chemical crosslink mechanisms are not necessary. Although it is non-degradable under physiological conditions, agarose is recognized as biocompatible. These features made agarose a popular product for the use in myriad applications across fields ranging from food industry, molecular biology and microbiology [123]. But above all, it is still widely used in cartilage tissue engineering yielding *in vitro* cartilaginous tissues with some of the most consistent, mechanically functional properties reported in the literature [124,125]. The total agarose concentration of a hydrogel determines its stiffness and pore size. The general rule with higher agarose concentration is that the strength increases with accompanying decrease of pore size diffusivity. For tissue engineering a 2 % weight/volume (w/v) agarose gel has been regularly used as it combines the desired mechanical properties and the correct pore size to trap matrix constituents with efficient nutrient and waste exchange [126–130].

Despite agarose does not enable cell attachment it has been shown that the physical entrapment of cells inside agarose hydrogels is sufficient to prevent loss of chondrocyte morphology or phenotype. Furthermore, chondrocytes previously grown in monolayer cell culture reversed dedifferentiation and increased the production of cartilage-specific proteoglycans and collagen type II [131–135]. In a 2010 canine study, allogenic passaged chondrocytes seeded in agarose-based grafts showed promising recovery of a non-weight bearing cartilage defect. Whereas empty defect controls grew fibrous tissue with poor outcome, a reported 90 % of the defect felling in the agarose group showed good integration with the host cartilage tissue [125]. Taken together, the unique properties of agarose make it still a good reference material for cartilage tissue engineering and accompanying integration studies.

### 1.1.5.3 Hyaluronic Acid-Based Hydrogels for Cartilage Tissue Engineering

Hyaluronic acid (HA) is a linear polysaccharide that is found abundantly in the ECM of native articular cartilage. This has led many investigations to design hydrogels consisting of HA. A not to be neglected advantage of HA is the interaction and attachment of cells, including chondrocytes, via CD44 (Homing Cell Adhesion Molecule: HCAM), CD168 (Receptor for Hyaluronan Mediated Motility: RHAMM) and CD54 (Intercellular Adhesion Molecule 1: ICAM-1) cell surface receptors [136,137]. Additionally, HA reportedly triggered chondrogenic differentiation and ECM production of MSCs [138–140]. Due to its excellent biocompatibility, injectable HA-based hydrogels have already been used for different tissue engineering approaches [141], but also for the treatment of OA [139]. HA also has some limitations, such as insufficient mechanical integrity and a rapid degradation by MMPs in inflamed defects [142]. Nonetheless, HA is highly versatile regarding physical and chemical modifications helping to adapt material properties to specific demands. Thiol-, haloacetate-, dihydrazide-, aldehyde- and tyramine-functionalized HA have all been used in various tissue engineering approaches [83,100,140]. Amongst reported improvements for the outcome of cartilage-like tissue in HA-based hydrogels were the inclusion of fibrin [143] or the covalent binding of cell regulating factors like TGF-β [83].

Most commonly, HA hydrogels are prepared by photogelation triggered by the incorporation of a methacrylate group to the polymer backbone [144,145]. Photocrosslinking is often a rapid process and the use of focused light sources facilitates good spatial and temporal control of the reaction [146]. Many of these reactions have proven biocompatibility to facilitate cell encapsulation [147,148]. Our group recently published investigations on another HA-based hydrogel utilizing a different UV-light crosslinking mechanism that was also applied in 3D printing of tissue engineered constructs for cartilage applications [100,149]. Instead of the widely used PEG as a counterpart for HA this hydrogel system consists
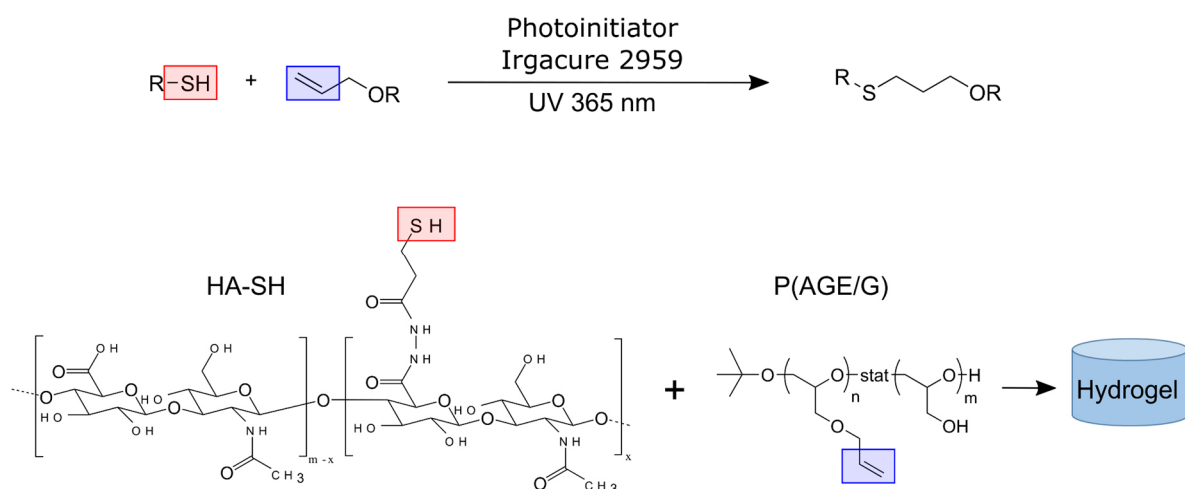


**Figure 6: Crosslinking scheme of the generation of UV-crosslinked HA-SH/P(AGE/G) hydrogels by using thiol-ene reaction.**

of an allyl-functionalized poly(glycidol) crosslinker (P(AGE/G)). Poly(glycidol)s (PG) are chemically similar to the FDA approved PEG but feature additional hydroxyl methylene side groups at each repeating unit which can be further chemically functionalized, e.g. with carboxylates, allyl and thiol groups. Furthermore, the use of distinct chemical protective groups during polymer synthesis allows for the preparation of polymers with different functionalities along a single PG chain [150,151].

In this case the allyl-functionalized PG can react with thiol-functionalized HA (HA-SH) via thiol-ene click reaction to form the hydrogel (see Figure 6). However, this HA-SH/P(AGE/G) hydrogel has never been tested in an integration model to investigate transition to the host cartilage.

## 1.1.6    The Importance of Cartilage Integration

In order to achieve successful repair of a cartilage defect, the filling of the defect with hyaline neocartilage is needed but the integration of repair cartilage with the surrounding host cartilage is necessary to the same extent. One source of consistent failure of cartilage repair procedures mentioned before is the missing transition of the repair tissue to the host cartilage on a permanent basis [152]. Although some integration of repair cartilage to the subchondral bone is reported frequently [8,61,153], integrative repair at the lateral defect interface remains a huge obstacle in all different approaches [29,62,154–157]. Khan et al. excellently summarized many known factors that affect cartilage integration and highlighted the importance to gain understatement on how these factors impede cartilage fusion for the development of improved strategies [152]. Some of the major issues are described in the following.

As chondrocytes are essential for the metabolism of cartilage-specific ECM components, the cell death at the defect site or within a graft is unambiguously a hindrance for the long-term success of a treatment. Studies evaluating different methods of cartilage wounding *in vitro* found that cells $100 - 200\,\mu m$ from the defect site immediately undergo necrosis and following apoptosis further contributes to an acellular region at the margin [14,158]. It has therefore been supposed to increase the number of viable chondrocytes at the defect site in order to improve tissue continuity [159,160]. Treatment of cartilage tissue with pharmacological cell death inhibitors during wound repair is reported to help in increasing numbers of viable cells at the wound edge, prevent matrix loss and improve lateral cartilage integration [161]. Other studies utilized proteolytic enzymes to disrupt the dense ECM network of the native cartilage and foster chondrocyte migration to the defect interface and thus improve long-term integration strength [158,159,162–167]. Additionally, it could be shown that the delivery of migrating and dividing chondrocytes with appropriate scaffolds adjacent to the wound edge helped in fusion of the cartilage tissue [168,169].

The patient's age or the age of donor material has also influence on the intrinsic healing capacity. There is proof of loss in chondrocyte function related to the developmental stage of the cartilage tissue [164,170–174]. Especially in tissue engineering strategies with expanded chondrocyte cultures there are-related symptoms that need to be taken into consideration. Estimations based on telomere length observations reveal that *in vitro* expansion of chondrocytes can accelerate chondrocyte aging equal up to 30 years [172]. The use of MSCs as cell source in cartilage tissue engineering can circumvent this problem but also introduces other obstacles (see also Chapter 1.1.4.3). More recently, chondrocyte progenitor cells isolated from cartilage tissue have been introduced as a promising cell source for cartilage tissue engineering. They have been described with the ability to maintain their chondrogenic phenotype even after extensive monolayer expansion [175]. Levato et al. showed that multipotent articular cartilage-resident chondroprogenitor cells (ACPCs) have a high potential in terms of neocartilage formation in hydrogels and are also suitable for 3D bioprinting applications [101]. However, up to date these cells received limited attention and more information needs to be gained to clarify how these cells can counteract age-related issues in integrative cartilage repair.

Although the developmental stage of chondrocytes may limit their regenerative potential, other *in vitro* studies demonstrated that chemical messenger molecules can also influence cartilage integration success. For example, Englert et al. showed in an *in vitro* integration model that supplementation with steroid hormones increases cartilage integration strength [176]. Other studies showed that different growth factors in cartilage tissue culture have chemotactic properties and can increase the cellularity at a defect site [158]. A member of the TGF-β growth factor family was also reported to be a regulator for cell-growth. In combination with a chondrocyte-seeded hydrogel adjacent to cartilage tissue, ECM production was elevated and the integration strength increased [177]. Proinflammatory cytokines are widely recognized to provoke degradative signaling cascades that promote ECM disintegration in cartilage tissue. Particularly the factors IL-1β and TNF-α were shown to reduce ECM deposition of chondrocytes in tissue engineered constructs and thus hinder tissue integration [176,178]. Interestingly another study using a bovine *in vitro* integration model could significantly increase integration strength by transient exposure of the cartilage tissue to IL-1β. They found that the temporal treatment with the catabolic cytokine only transiently upregulates matrix degrading enzymes which lead to better migration of chondrocytes to defect site and better integration outcome [179]. Chondrocytes are also known to be sensitive to mechanical force. The synthesis rates and tissue accumulation of cartilage-specific ECM components is elevated in both *in vitro* and *in vivo* studies in the presence of appropriate mechanical force [180–187]. A more recent study could also demonstrate that mechanical stimulation increased the integration of tissue-engineered cartilage and native cartilage [188]. Although there is variation in models and the application of

mechanical stimulus, it can be suggested that future studies will improve the understanding of mechanical stimulation for cartilage integration.

Chondrocytes and their production of ECM are vital for integrative cartilage repair. To better understand exact mechanisms, one must investigate the process of ECM deposition at a cartilage defect. DiMicco et al. could relate different low and high integrative phenotypes in part to different levels of collagen synthesis [189]. β-aminopropionitrile (BAPN) is a known inhibitor of lysyl oxidase, an enzyme that is crucial for the establishment of crosslinks in collagen networks [190]. Addition of BAPN to tissue culture medium results in almost complete inhibition of integration between pairs of cartilage explants, despite the overall biosynthesis of matrix components is not affected [170,191]. These results indicate that formation of collagen crosslinks in cartilage explants is critical in integrative cartilage repair. Experiments of our own group could further determine the importance of unbiased 3D formation of collagen fibrils on cartilage integration. The enzyme prolyl-4-hydroxylase is essentially involved in the synthesis of procollagens. It converts proline residues to 4(R)-hydroxyproline and thus allows the triple-helical assembly of collagens and subsequent secretion into the extracellular space. Inhibition of the collagen triple helix formation leads to nonfunctional proteins which are rapidly degraded both in the intracellular and extracellular space [192,193]. Ethyl-3,4-dihydroxybenzoate (EDHB) is a structural analogue to ascorbate, which is an essential co-factor for enzyme activity. EDHB can therefore act as an inhibitor of prolyl-4-hydroxylase [192,194,195]. Our group could show that omitting ascorbate from tissue culture results in drastic loss of interfacial ECM deposition and integration strength. Addition of EDHB counteracts available ascorbate in a dose-dependent manner and sufficient concentrations lead to complete failure of cartilage integration [196].

Aforementioned factors unmistakably have influences on long-term cartilage integration. On a shorter scale one desires immediate integration, as missing integration in cartilage lesions or with grafts results in progress of the lesion or in break-off of the neocartilage. A study by Englert et al. investigated the ability of different chemical crosslinkers to facilitate immediate bonding of articular cartilage explants [197]. Large increases in adhesive strength could be achieved by crosslinking opposing cartilage collagen fibers, but cytotoxic properties of most of these agents remain a major obstacle for clinical application. For this reason, much attention has been focused on the use of biocompatible adhesive materials for immediate cartilage integration. A variety of such surgical glues and adhesive materials are described in more detail in Chapter 1.1.8.

## 1.1.7    Integration Model

As mentioned before, cartilage integration is dependent on numerous factors. In order to gain understanding of cartilage integration investigators utilized different models in pre-clinical studies. Both *in vivo* and *in vitro* experiments have been conducted, including variations in species for tissue and cell harvests. The most common practices to evaluate integration are macroscopic morphological assessment, microscopic evaluation in sections of the wound margin and biomechanical measurement of integration strength and combinations of those. Generally speaking, *in vivo* models, especially those where an experimental articular cartilage defect is prepared in the joint, best reflect the environment that is present in a human patient [198]. However, it is this highly variable and complex environment that bring along several problems for the investigation of particular factors. The multi-cellular environment (e.g. the synovium or subchondral bone) allows the settlement of non-cartilaginous cells in the defect thus changing the dynamics and the final outcome of repair tissue formation. In addition, the nutritional and biomechanical circumstances in a moving joint *in vivo* may compromise neocartilage formation, as well as the commonly undefined cocktail of pro-inflammatory factors that is present in synovial joints after trauma [11]. So far most *in vivo* studies focused on rating cartilage integration with histological scores based on maintained cellularity and continuity of tissue at the interface. Quantitative assessment of integration strength in *in vivo* experiments is rare. In case of subcutaneous implantation into mice, the harvested cartilage explant constructs can also easily be processed for biomechanical measurement [159,199–202]. The subcutaneous implantation site however does not simulate the environment of the synovial joint and the presence of highly proliferative cells such as fibroblasts could harness integration strength increases without building up functional hyaline cartilage tissue. Although biomechanical analysis of integrative repair has also been performed on samples retrieved from *in vivo* defects in the knee joint [203], the high practical effort makes this approach unsuitable for most studies on integrative cartilage repair.

Alternatively, cartilage tissue explants for *in vitro* experiments can provide more controllable model systems to investigate specific mechanisms of cartilage-cartilage integration. Isolated cartilage



**Sandwich model**                    **Single-lap model**                    **Disc/ring model**
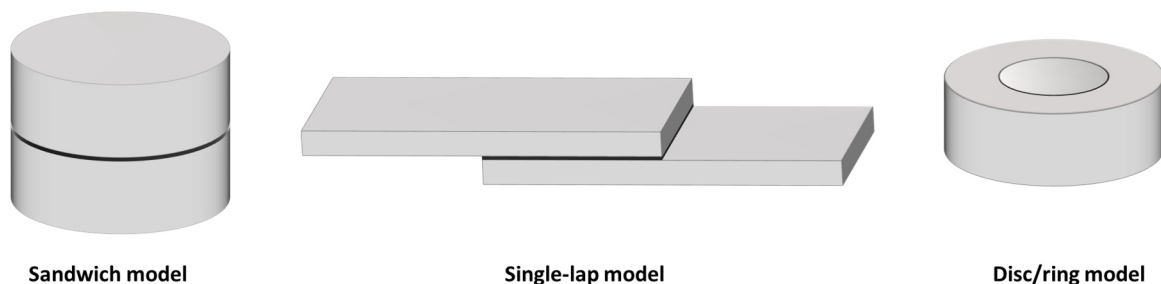
**Figure 7: Schematic illustration of frequently used in vitro models for cartilage integration evaluation.**

Graphic created with royalty free components

explants have been embedded in hydrogels or used in a co-culture with pelleted chondrocytes to investigate cellularity at the cartilage interface [163,204]. The *in vitro* models used there, however, lack the opportunity of biomechanical assessment of integration strength. Other models, e.g. the sandwich model, the single-lap model and the disc/ring model, have been developed that are frequently used in biomechanical tests (see Figure 7). The named models are described in detail within the following subchapters.

### 1.1.7.1 Sandwich Model

Cylindrical constructs that are assembled in a sandwich-like fashion can be used for biomechanical measurements for integration strength both in tensile and shear settings [168,205]. Sandwich-like constructs can vary in their layer and material composition. Besides the use of *in vivo* models to investigate integrative cartilage repair, Wang et al. additionally utilized a sandwich-like *in vitro* setting for biomechanical measurement. In this case a top layer consisting of a hydrogel was adjacent to a cylindrical cartilage disc. The outer surfaces were fixed to rods at which different force directions were applied in order to obtain both tensile and shear strength [206]. Another study used chondrocyte-seeded collagen that were placed between two cylindrical cartilage discs. After *in vitro* culture of 40 days tissue continuum between cartilage and scaffold was analyzed histologically and integrations strength was quantified in a biomechanical tensile test [168]. These layered constructs offer some distinct advantages for investigations on cartilage integration, as they are easily adaptable in their layer composition. Regarding cartilage integration with tissue engineered constructs, the volume of the material can be varied to simulate filling different defect sizes. Additionally, these constructs appear suitable to observe cell migration and ECM deposition at the cartilage-scaffold interface [168].

### 1.1.7.2 Single-Lap Model

Since its introduction to *in vitro* cartilage analysis by Reindel et al. in 1995, the most frequently used *in vitro* test model is composed of uniform cartilage blocks that are assembled with an overlapping area. The objective of this model was to use a single-lap joint configuration to measure adhesive strength. This model is highly variable and single cartilage blocks of different developmental stages, viability, and cartilage zones haven been combined and formulations of culture media have been diversified [160,189,207]. The high reproducibility of this model allowed comparison between studies investigating different factors that influence cartilage integration, such as enzymatic treatment of the cartilage ECM and supplementation of culture medium with different active ingredients, such as

steroid hormones or cytokines [176,197]. The single-lap constructs can be analyzed histologically but have also been used for scanning electron microscopy (SEM) analysis of the interface zone [176]. For quantification of adhesive strength, the sample composites have to be attached to jaws with which a positive uniaxial displacement force is applied. In recent years, the ease of construct fabrication made this test model particularly popular for studies in which immediate bonding of cartilage tissue is investigated [197,208–211]. Regarding this, the possibility to apply load on the overlapping integration area during fabrication proved advantageous when chemical crosslinkers of small molecular structure were used and intimate contact between both cartilage blocks was needed [197,211]. The quality of biomechanical data in this model is very much dependent on the fabrication and its geometry, as in the single-lap configuration the stress varies over the integration area even with perfect parallel alignment. The applied forces to the two cartilage blocks are not simply colinear, as both in-plane tension and a bending moment are applied to the joint. This effects the estimate of strength, since the shear and normal stress are not completely proportional to the applied load [160,212]. Still, biomechanical measurements proved solid for the detection of even relatively small integration strengths and are thus suitable to evaluate immediate bonding principles. However, as the harvested cartilage blocks were approximately parallel to the articular surface, the simulating cartilage defect may be more relevant to fissures that extend horizontally in fractured or osteoarthritic cartilage. In contrast, cartilage failure might occur more frequently because of joint loads in normal direction to the articular surface and also in *in vivo* experiments missing cartilage integration is commonly reported for the lateral orientation [29,60–62,157,213]. Since the orientation of the collagen fibers may modulate the repair process, an integration model that mimics a lateral cartilage defect and simultaneously considers the hierarchical structure of cartilage tissue is very likely better suited for investigations on long-term cartilage repair processes [212].

### 1.1.7.3    Disc/Ring Model

In 2001, Obradovic et al. presented a new cartilage integration model with the aim to adapt the presentation of *in vivo* cartilage defects to better controllable *in vitro* conditions without systemic effects [162]. They assembled a doughnut-shaped cartilage explant with a tissue-engineered inner disc. These disc/ring constructs could easily be cultured for several weeks under variable conditions and the model also allowed histological analysis of the lateral defect interface both in the sagittal (cross-section) and the transverse plane (*en face*). To biomechanically quantify the adhesive strength at the disc-ring interface of the tissue composites, a plunger is used to separate the central disc from the cartilage annulus with a load cell recording the force until failure of the composite. In a following study

with disc/ring constructs consisting solely of native cartilage tissue, the processing was modified in order to obtain more accurate and reproducible biomechanical push-out tests. The feasibility to obtain an interface between the disc and ring that is perpendicular to both the top and bottom surfaces of the composites has been approved, which assures the collinearity of the interface axis with the mechanical testing device's plunger and eliminates potential measurement artifacts [214].

Over the years, the disc/ring model has been successfully utilized for investigations on the effects of synovial fluid components [215], enzymatic treatments [159,162,165–167], cytokines [167,178,179,216] and ECM crosslinking on cartilage integration [211,217]. Further, the disc/ring model is highly variable regarding its composition and can easily be used in combinations with scaffold materials and tissue engineered cartilage. The interfacial gap size between the cartilage disc and ring can be varied by sequentially coring that enables the insertion of scaffolds at the defect site [177]. However, in most cases where cartilage-material integration is investigated with a disc/ring model, the inner cartilage disc is completely exchanged with the tested material or TE-cartilage [178,218–221]. In addition, the disc/ring model is not limited to just chondral explants. Tam et al. developed an *in vitro* osteochondral disc/ring model to investigate integrative repair with an intact adjacent calcified tissue layer. Remarkably, they were able to cut-off the intact bony layer and biomechanically quantify the lateral cartilage-cartilage integration in push-out tests [164]. In recent years, several other studies used adaptions of annular osteochondral explants in *in vitro* systems to evaluate chondral integration [169,188,222–225].

Taken together, the disc/ring model has become increasingly important in integrative cartilage research. In future studies its versatility and the combination of structural and functional analyses will undoubtedly help to gain further knowledge in underlying cellular and molecular processes for enhanced cartilage repair and in the development of adhesive materials for defect filling. For improved treatment of patients, further knowledge is needed and sophisticated *in vitro* models clearly help to diminish animal tests on this way.

### 1.1.8    Adhesives for the Treatment of Cartilage Defects

Even small lesions in articular cartilage can erode over time because of the limited self-healing capacity of cartilage. The direct repair of focal defects may stop the progress to bigger osteoarthritic defects. The outcome of cartilage defect treatments, ranging from small fissures to transplantation of large osteochondral plugs is dependent on the integration of opposing cartilaginous surfaces. Because of the slow and restricted self-repair of cartilage, approaches that allow for immediate tissue fixation and simultaneously promote long-term regeneration are highly desired. Generally, the gold standard for wound closure in clinics is still suturing, however the application of sutures will introduce further

damage to the cartilage tissue. It has been shown that small-sized agents are capable to immediately integrate opposing cartilage surfaces enabled by their reactiveness to ECM molecules [197,205]. Because of their small molecular size, these agents need intimate contact of tissue surfaces and cannot bridge larger defects. Therefore, the application of polymerizing adhesives for surgical integration of tissues has become more and more popular over the last years as an emerging alternative. Regarding adhesives for clinical application, some important definitions and classifications are needed: A hemostat causes blood-clotting, whereas a sealant is self-polymerizing and creates a sealing barrier that prevents leakage of gas or a liquid from a structure. An adhesive is also self-polymerizing and is capable of gluing structures together. Both sealants and adhesives may also have hemostatic properties, but do not necessarily cause active blood-clotting. So far, the only commercial material for clinical application with FDA approvals in all three of these groupings is fibrin [226]. Fibrin is widely used as a hydrogel material in several TE applications, but its crosslink mechanism is also acknowledged for its tissue adhesive properties (see Chapter 1.1.5.1). Already in the 1980s fibrin was used as an adhesive to fix loose chondral and osteochondral bodies after trauma [227] and was subsequently used in a wide range of orthopedic cartilage surgeries [226,228]. However, a frequently reported characteristic of commercial fibrin is a limited adhesion strength [229], especially when applied in a wet environment and with increasing instability and solubility over time. This can represent a problem for the application on cartilage defects where long-term mechanical integrity and stability may be beneficial.

Other commercially available surgical adhesives like cyanoacrylate glues and aldehyde crosslinked gelatins form a solid bond to tissue surfaces but are highly discussed in literature regarding their biocompatibility. Additionally, they can form a rigid matrix with little degradability which may act as a barrier for neocartilage formation [95,230,231]. Recently, there has been increased interest in the challenging development of adhesive materials with good immediate bonding strength combined with biocompatibility for successful long-term integration. Generally, natural and synthetic hydrogels can exhibit excellent biocompatibility and are also broadly investigated matrices for cartilage regeneration approaches. They facilitate the diffusion of nutrients and metabolites similar to the native cartilage ECM because of their highly hydrated nature [85]. Further, the possibility of functionalization with tissue-adhesion moieties, injectability and *in situ* gelation enables their use as tissue adhesives in minimally invasive procedures in the clinic. So far, a variety of hydrogel adhesives has been published including polysaccharides, polypeptides, proteins or synthetic polymer-based systems [95]. Strehin et al. designed a tissue glue based on chondroitin sulfate that has been functionalized with amine-reactive N-hydroxysuccinimide. Gelation started by mixing the chondroitin sulfate component with amine-functionalized PEG but could be controlled by the initial pH value of the solutions [232]. In another approach of the same group chondroitin sulfate was chemically functionalized with methacrylate and

aldehyde groups and was successfully used to chemically bond a bulk hydrogel into a cartilage defect [206]. Adhesive materials have been developed that are based on a plethora of different materials and adhesion mechanisms [233,234]. Adhesion reactions that are temporarily controllable enable the surgeon better handling and easy positioning of the treated surfaces. Sitterle et al. first reported of increased immediate bonding strength in cartilage explants using photochemical induced crosslinking [211]. More recently, photopolymerizable hyaluronan as the basis of adhesive materials for cartilage application was reported [209,220]. Most photochemical approaches require the presence of photosensitizer that catalyze light-induced crosslinking. In contrast to other routinely used photosensitizer that require UV irradiation, ruthenium trisbipyridyl chloride ($[RuII(bpy)_3]^{2+}$) has been used for photogelation of fibrinogen-based adhesives under less problematic blue light [235]. Tough, this adhesive has not been tested on suitability for cartilage tissue integration.

In general, the functionalization of naturally derived biopolymers for adhesives is popular due to their inherent biocompatibility and degradability, but they often lack uniformity, tunability and reproducibility. A possible alternative are water soluble synthetic polymers like poly(oxazoline)s (Pox), which have become increasingly popular in the biomedical field due to their improved and accelerated synthesis using microwave heating. In contrast to the more prominent polyethylene glycols (PEG), POx do not only offer end-terminal functionalization via functional initiators or terminating agents, but also allow for a tunable side chain functionalization, which can be varied through a range of different functional monomers or further post-polymerization functionalization [236]. POx has also been associated with good hemocompatibility, low cytotoxicity and low immunogenicity [237–239]. Accordingly, hydrogels based on different POx derivatives were already used for drug delivery, as cell culture scaffolds, or as hemostatic wound dressings [240,241].

For the use as a tissue adhesive, an emerging functionality is the catechol group. This reactive moiety naturally occurs in the amino acid 3,4-dihydroxyphenylalanine (DOPA). This amino acid plays a key role in the mussel foot protein, which allows mussels to attach to many different types of surfaces with fast curing kinetics even in wet environments. Under oxidizing conditions the catechol group becomes highly reactive and can self-polymerize or react with a variety of nucleophiles like amino or thiol groups undergoing Michael addition or Schiff base formation [242–244]. Therefore, it is a perfect candidate for reactions with nucleophiles like cysteinyl, histidyl or lysyl groups that are present on many natural tissue surfaces [245]. The catechol functionality has already been attached to PEG [246,247], silk fibroin [248] and gelatin [210] or was polymerized as dopamine acrylamide or dopamine hydrochloride to form three-dimensional networks [249,250]. However, POx enabling the attachment of multiple catechol functions at the side chain, which will increase adhesion and stability, has not yet been investigated.

Taken together, an ideal cartilage adhesive should have strong wet tissue adhesion, balanced stability under physiological conditions, rapid curing, nontoxicity and cytocompatibility. Additionally, biodegradability should be adjusted to the demands of the surrounding cartilage tissue for neocartilage formation. Up to now, there is no clinically available adhesive material that implements all these factors. Thus, the aim of this work was to contribute to the ongoing research of biomaterial-guided cartilage integration.

## 1.2 Goals of the Thesis

For the treatment of articular cartilage defects there still exists a tremendous need for adequate approaches to obtain integrative repair. Adhesive hydrogels are a promising tool to both allow immediate bonding of a defect interface and provide a biomaterial matrix for progressing tissue formation. Due to the plethora of available hydrogel materials and their versatility with regard to chemical modifications, possible combinations with different cell types and other physical and biological factors, suitable *in vitro* models are needed for screening and pre-clinical evaluations.

***This work included the following objectives:***

1. The development and testing of different adhesive biomaterials for cartilage defect treatment utilizing *in vitro* models

2. The evaluation of long-term *in vitro* cartilage integration with hydrogel adhesives and

3. The investigation of cartilage integration to tissue-engineering hydrogel constructs in an *in vitro* model

## 1.2.1 Evaluation of Bonding Capacities of Adhesive Hydrogels *in vitro*

The main functions of biological adhesives and sealants are to repair injured tissue, reinforce surgical wounds or even replace conventional suturing techniques. In general surgery, adhesives must meet several requirements, taking into account clinical needs, biological effects, and material properties. These requirements can be met by specific polymers. Natural or synthetic polymeric materials can be used to form three-dimensional networks that physically or chemically bond to the target tissue [251]. Particularly in tissues like cartilage where alternative techniques, such as suturing, would introduce further damage, utilizing adhesive hydrogels provide an elegant approach for integrative repair of defects [8]. So far, a variety of hydrogel adhesives has been published including polysaccharides, polypeptides, proteins or synthetic polymer-based systems [95]. In general, for cartilage defect treatments, high mechanical stability and bonding strengths are required for adhesives to withstand present forces in the joint during motion. These properties can vary depending on the materials applied, which is why different types of hydrogels with varying adhesive crosslink mechanisms were investigated in this work. Commercially available adhesives, namely TissuCol and BioGlue® were compared against each other. Additionally, several chemical modifications to established adhesive materials together with hydrogels of varying crosslinking chemistry were assessed for their immediate bonding strength in the *in vitro* cartilage disc/ring model. Specifically, different formulations of long-term stable fibrin gels, photocrosslinking approaches of fibrinogen, and

catechol-functionalized poly(oxazoline)s were investigated for their capability to improve cartilage bonding.

## 1.2.2 Investigation of the Long-Term Lateral Cartilage Integration Using *in vitro* Models

Surgical adhesives must fulfill several requirements to meet the variable demands of different tissue types and their specific mechanical load and stress profiles [95,251,252]. Due to the poor self-healing capacity of cartilage, adhesive materials need to balance the need for immediate integration as well as favorable tissue regeneration for a successful long-term integration. Appropriate hydrogel degradation is essential to allow cell migration and formation of new tissue at the defect site. Synthesized components of cartilage ECM that integrate with native cartilage and chondrocytes that can freely migrate across the interface have been shown to enhance mechanical stability of tissue repair in cartilage, both in short-term and long-term [81,162,168,169,176,177,253]. In the course of this work, the different investigated candidates of adhesive hydrogels were further assessed for their capacity to form successful tissue integration in the long-term by using *in vitro* tissue cultivation techniques. The influence of hydrogel degradation rates on the long-term cartilage integration outcome was considered in conducted experiments.

## 1.2.3 *In vitro* Investigation on Integrative Cartilage Repair with Tissue-Engineered Hydrogel Constructs

For the treatment of large chondral defects, high-volume formation of functional cartilage tissue is required. Using hydrogels, cartilage tissue has been engineered *in vitro* before, achieving appearances and properties similar to native cartilage [85]. However, for a successful clinical treatment, integration of tissue engineered constructs to the native tissue is required. Cartilage remodeling within a hydrogel alone is not necessarily sufficient for successful integration, and with standard *in vitro* culture setups, the potential influence from native tissue on regenerative development is not considered. Therefore, various tissue-engineered hydrogel constructs, including adhesive materials (fibrin- and hyaluronic acid-based) as well as agarose, were applied to an *in vitro* defect model with native cartilage to observe tissue formation and integrative effects in an environment that simulates clinical use.

# 2 Materials

## 2.1 Instruments

**Table 1: Overview of instruments.**

| Instrument | Supplier | Central office |
|---|---|---|
| Accu-jet® pro | Brand | Wertheim, Germany |
| Analytical scale | Ohaus | Zurich, Switzerland |
| Analytical scale XA 105 | Mettler-Toledo | Columbus, USA |
| Bending Load Cell Z6FD1 | Hottinger Baldwin Messtechnik | Darmstadt, Germany |
| Blue-light LED hand lamp | HQRP | Harrison, USA |
| Centrifuge Rotina 420 R | Hettich | Tuttlingen, Germany |
| Centrifuge SIGMA 1-14 | SIGMA Laborzentrifugen GmbH | Osterode, Germany |
| $CO_2$ incubator | IBS Integra Biosciences | Fernwald, Germany |
| $CO_2$ incubator (hypoxia) | Binder | Tuttlingen, Germany |
| Cryostat CM 3050S | Leica | Wetzlar, Germany |
| Custom-made tools and Teflon hydrogel molds | Feinmechanik Sauer | Würzburg, Germany |
| Dynamic mechanical testing device ElectroForce 5500 | TA Instruments | Eden Prairie, USA |
| FACSCanto flow cytometer | BD Biosciences | Heidelberg, Germany |
| Freezer (-20°C) | Liebherr | Bulle, Switzerland |
| Freezer TTS 500 (-80°C) | Thalheim Kühlung | Ellwangen, Germany |
| Fridges | Liebherr | Bulle, Switzerland |
| Genesys 10S Bio spectrophotometer | Thermo Fisher Scientific | Waltham, USA |
| HandyStep® dispenser | Brand | Wertheim, Germany |
| Hemacytometer Neubauer | Paul Marienfeld GmbH | Lauda, Germany |
| Laminar flow box Typ-HS18 | Heraeus | Hanau, Germany |
| Magnetic stirrer | VWR | Darmstadt, Germany |
| Mastercycler® Gradient | Eppendorf | Hamburg, Germany |
| Microscope BX51/DP71 camera | Olympus | Hamburg, Germany |

| Instrument | Supplier | Central office |
| --- | --- | --- |
| Microscope camera DigiMicro Profi | dnt | Dietzenbach, Germany |
| Microscope IX51/XC30 camera | Olympus | Hamburg, Germany |
| Microwave Micromat 1000W | AEG | Frankfurt am Main, Germany |
| Orbital shaker Unimax 1010 | Heidolph | Schwabach, Germany |
| pH-meter HI2210 | Hanna Instruments | Kehl am Rhein, Germany |
| Pipette displacement Microman™ | Gilson | Middleton, USA |
| Pipette multistep | Brand | Wertheim, Germany |
| Pipettes Research® Plus | Eppendorf | Hamburg, Germany |
| Roll mixer RM5 | Hartenstein | Würzburg, Germany |
| Silicon hydrogel molds | FMZ, Chair: Prof. Jürgen Groll, University of Würzburg (collaboration) | Würzburg, Germany |
| Sledge microtome SM2000R | Leica | Nussloch, Germany |
| Stereomicroscope SteREO Discovery.V12 | Carl Zeiss | Jena, Germany |
| Tecan GENios pro spectrofluorometer | Tecan | Crailsheim, Germany |
| Thermomixer comfort MTP | Eppendorf | Hamburg, Germany |
| Thermomixer MHR 23 | DITABIS | Pforzheim, Germany |
| TissueLyser | Qiagen | Hilden, Germany |
| Universal testing machine BZ020/TH2A | Zwick-Roell | Ulm, Germany |
| UV hand lamp VL-4 with filter | Hartenstein | Würzburg, Germany |
| Vortex, IKAR MS3 basic | IKAR | Staufen, Germany |
| Vortex-centrifuge Combi-Spin | Hartenstein | Würzburg, Germany |
| Water bath | Memmert | Schwabach, Germany |
| Zeiss SteREO Discovery.V20 stereo microscope | Carl Zeiss | Jena, Germany |

## 2.2    Consumables

**Table 2: Overview of used consumables.**

| Consumable | Supplier | Central office |
| --- | --- | --- |
| Bottle top-filter Nalgene® | Thermo Scientific | Waltham, USA |
| Cell culture plates 96-well | TPP | Trasadingen, Switzerland |
| Cell culture plates 96-well (black) | Thermo Scientific | Waltham, USA |
| Cell culture plates Cellstar 6-, 12-, 24-, 48-, 96-well | Greiner Bio-One | Frickenhausen, Germany |
| Coverslip 24 x 60 mm | MENZEL | Braunschweig, Germany |
| Cryovials CryoPure 2.0 mm | Sarstedt | Nümbrecht, Germany |
| Dispenser tips 12.5 ml/25 ml | nerbe plus | Winsen, Germany |
| Disposable forceps ratiomed® | Megro GmbH | Wesel, Germany |
| Falcon cell strainers 100 µm | BD Biosciences | Heidelberg, Germany |
| Filter paper | Hartenstein | Würzburg, Germany |
| Microtome blades type N35 | Feather | Osaka, Japan |
| PAP pen liquid blocker | Sigma-Aldrich | Munich, Germany |
| Parafilm | Pechiney | Chicago, USA |
| PCR-strips 8 tubes 0.2 ml | Carl Roth GmbH | Karlsruhe, Germany |
| pH indicator paper | Carl Roth | Karlsruhe, Germany |
| Pipette filter tips | Starstedt | Nümbrecht, Germany |
| Pipette tips | nerbe plus | Winsen, Germany |
| Pipettes serological | Greiner Bio-One | Frickenhausen, Germany |
| Polypropylene Tubes 15 ml/50 ml | Greiner Bio-One | Frickenhausen, Germany |
| Porcine knee joints | Hollerbach | Rimpar, Germany |
| SafeSeal micro tubes 1.5 ml/2.0 ml | Sarstedt | Nümbrecht, Germany |
| SafeSeal micro tubes 5 ml | nerbe plus | Winsen, Germany |
| Sample cup (urine cup) | nerbe plus | Winsen, Germany |
| Sample cup PE 2.5 ml | Hartenstein | Würzburg, Germany |
| Scalpels | Feather | Osaka, Japan |
| Single-edged razor blades | GEM/Personna | Verona, USA |
| Stainless steel beads, Ø 5 mm | Quiagen | Hilden, Germany |
| Stiefel biopsy punches | GlaxoSmithKline | Munich, Germany |
| Superfrost™ ultra plus glass slide | Thermo Scientific | Waltham, USA |

| Consumable | Supplier | Central office |
|---|---|---|
| SuperFrost™ plus glass slide | R. Langenbrinck | Emmendingen, Germany |
| Syringe Filter Minisart® 0.2 µm | Sartorius AG | Göttingen, Germany |
| Syringes | BD Biosciences | Heidelberg, Germany |
| Syringes Omnican40 | B. Braun | Melsungen, Germany |
| Tissue culture flasks T25/ T75/ T175 | Greiner Bio-One | Frickenhausen, Germany |

## 2.3 Chemicals

If not otherwise stated in Table 3 or the Methods section (Chapter 3), all chemicals and reagents utilized for the preparation of buffers and solutions were obtained from Sigma-Aldrich/Merck (Darmstadt, Germany) and Carl Roth GmbH (Karlsruhe, Germany).

**Table 3: Overview of used chemicals.**

| Chemical | Supplier | Central office |
|---|---|---|
| 2-propanol | VWR | Poole, UK |
| Acetone, 99.5% | AppliChem | Darmstadt, Germany |
| Antibody diluent, Dako REAL™ | Dako | Hamburg, Germany |
| Aqua ad iniectabilia | B. Braun | Melsungen, Germany |
| BioGlue® | CryoLife | Kennesaw, USA |
| DAPI mounting medium ImmunoSelect® | Dako | Hamburg, Germany |
| Distilled water (DNase/RNase free) | Life Technologies | Karlsruhe, Germany |
| DMSO | Thermo Scientific | Waltham, USA |
| Dulbecco's phosphate-buffered saline (DPBS) no calcium, no magnesium | Life Technologies | Karlsruhe, Germany |
| Entellan® | Merck | Darmstadt, Germany |
| EnVision G|2 Doublestain System | Dako | Hamburg, Germany |
| Ethanol absolute, 99.8 %, for molecular biology | AppliChem | Darmstadt, Germany |
| FACS clean solution | BD Biosciences | Franklin Lakes, USA |
| FACS sheath solution | BD Biosciences | Franklin Lakes, USA |
| FACS shutdown solution | BD Biosciences | Franklin Lakes, USA |
| FCS (fetal calf serum) | Thermo Scientific | Waltham, USA |
| Formaldehyde, 37 % | Th. Geyer | Renningen, Germany |

## Materials

| Chemical | Supplier | Central office |
|---|---|---|
| Glycergel® Mounting Medium | Dako | Hamburg, Germany |
| Hematoxylin | Bio Optica | Milan, Italy |
| Hoechst 33258 dye | Polysciences | Warrington, USA |
| Keratanase I | Seikagaku | Tokyo, Japan |
| Live/Dead Cell Staining Kit II | PromoKine | Heidelberg, Germany |
| MTT (3-(4,5-dimethylthiazol-2-yl)-2,5 diphenyltetrazoliumbro-mid) | Serva Electrophoresis | Heidelberg, Germany |
| Non-essential amino acids (NEAA), | Thermo Scientific | Waltham, USA |
| Papain | Worthington | Lakewood, USA |
| PBS (Dulbecco A) | Thermo Scientific | Waltham, USA |
| Penicillin/streptomycin (100 U/ml penicillin, 0.1 mg/ml streptomycin) | Thermo Scientific | Waltham, USA |
| Pepsin (Digest All™-3) | Invitrogen, | Karlsruhe, Germany |
| Phosphate buffered saline (Dulbecco A) tablets | Thermo Scientific | Waltham, USA |
| Photoinitiator Irgacure 2959 | BASF | Ludwigshafen, Germany |
| Proteinase K (Digest-All 4) | Life Technologies | Karlsruhe, Germany |
| Sulfo-NHS-LC-Diazirine (sulfosuccinimidyl 6-(4,4-azipentanamido)hexanoate) | Thermo Scientific | Waltham, USA |
| Terralin Liquid® disinfectant | Schülke | Norderstedt, Germany |
| Tissue-Tek® O.C.T. compound | Sakura Finetek | Zoeterwonde, Netherlands |
| Trypsin-EDTA 0.25% | Life Technologies | Karlsruhe, Germany |
| Tween® 20 | AppliChem | Darmstadt, Germany |
| Type II Collagenase | Worthington | Lakewood, USA |
| Xylene | VWR | Poole, UK |
| **Chemical** | **Supplier** | **Central office** |

## 2.4    Antibodies

**Table 4: Overview of used antibodies.**

| Antibody | Type/Source | Application/Dilution | Supplier |
|---|---|---|---|
| Alexa Fluor™ 488 anti-rabbit | Polyclonal IgG goat | IHC: 1:400 | Jackson Immuno (111-545-003) |
| Alexa Fluor™ 488 anti-rat | Polyclonal IgG goat | FC: 1:400 | Jackson Immuno (112-545-003) |
| Anti CD44 | Monoclonal IgG rat | FC 1:100 | Abcam (ab119348) |
| Anti-Aggrecan | Monoclonal IgG mouse | IHC 1:300 | Thermo Scientific (Clone 969D4D11) |
| Anti-Collagen I | Polyclonal IgG rabbit | IHC 1:800 | Abcam (ab34710) |
| Anti-Collagen II | Monoclonal IgG mouse | IHC 1:100 | Acris (Clone II-4C11) |
| Anti-Collagen X | Monoclonal IgG mouse | IHC 1:200 | eBioscience (Clone X53) |
| Anti-CTX-II | Polyclonal IgG rabbit | IHC 1:200 | USCN Life Science |
| Anti-MMP13 | Polyclonal IgG rabbit | IHC 1:100 | Abcam |
| Cy™3 anti-mouse | Polyclonal IgG donkey | IHC: 1:400 | Dako (22-165-003) |
| Cy™3 anti-rabbit | Polyclonal IgG goat | IHC: 1:400 | Jackson Immuno (711-165-152) |
| DAB Enhancer Kit EnVision | -- | -- | Dako (P05022) |
| HRP anti-mouse | Polyclonal IgG rabbit | IHC 1:1,00 | Dako (P0161) |
| HRP anti-rabbit | Polyclonal IgG goat | IHC 1:1,00 | Dako (P0448) |
| IgG1 isotype control | Polyclonal IgG rabbit | IHC: according to primary antibody concentration | Dianova Clone pAK (DLN-13121) |
| IgG1 negative control | Polyclonal IgG mouse | IHC: according to primary antibody concentration | Dako (X0931) |

## 2.5 Hydrogel Components

**Table 5: Overview of hydrogel components.**

| Component | Specification |
| --- | --- |
| Aprotinin from bovine lung | Lyophilized powder, 3-8 TIU/mg solid; Sigma-Aldrich, Munich, Germany |
| Fibrinogen from bovine plasma | Type I-S, 65-85% protein (≥75% of protein is clottable); Sigma-Aldrich, Munich, Germany |
| HA-SH | Thiolated hyaluronic acid was synthesized at the Department for Functional Materials in Medicine and Dentistry (FMZ), University Hospital Würzburg with a Mn=1.58MDa and 58% SH-functionality (HA-SH; AK Groll, Würzburg, Germany). |
| Low-Melt Agarose | Carl Roth, Karlsruhe, Germany. Melting temperature ≤65,5 °C, gelation temperature ≤28 °C, |
| P(AGE/G) | Linear allyl-modified poly(glycidol) was synthesized at the FMZ with a $M_n$=4760 Da and 10% allyl-functionality (P(AGE/G); (AK Groll, Würzburg, Germany). |
| PCL scaffold | 3D-printed thermoplastic poly(ε-caprolactone) (PCL) with grid structure fabricated at the FMZ. |
| PEOD$_{amide}$ | PEtOx-co-ButEnOx (POx, EtOx building block) was synthesized at the FMZ with 91.5 repeating units and 6.6 % allyl-functionality. The polymer was functionalized with 4.6 % catechol groups using an amide-based chemistry (AK Groll, Würzburg, Germany). |
| PEOD$_{ester}$ | PEtOx-co-ButEnOx (POx, EtOx building block) was synthesized at the FMZ with 91.5 repeating units and 6.6 % allyl-functionality. The polymer was functionalized with 4.3 % catechol groups using a ester-based chemistry (AK Groll, Würzburg, Germany). |
| PMOD$_{amide}$ | PMeOx-co-ButEnOx (POx, MeOx building block) was synthesized at the FMZ with 79 repeating units and 10 % allyl-functionality. The polymer was functionalized with 8.7 % catechol groups using an amide chemistry (AK Groll, Würzburg, Germany). |
| PMOD$_{ester}$ | PMeOx-co-ButEnOx (POx, MeOx building block) was synthesized at the FMZ with 79 repeating units and 10 % allyl-functionality. The polymer was functionalized with 5.3 % catechol groups using an amide chemistry (AK Groll, Würzburg, Germany). |
| TissuCol Duo S | Baxter, Unterschleißheim, Germany; Component 1: Fibrinogen: 70-110 mg/ml, Faktor XIII: 10-50 I.E./ml, plasma fibronectin: 2-9 mg/ml, aprotinin (bovine): 3 000 KIE/ml, Component 2: thrombin (human): 500 I.E./ml, calcium chloride: 5,88 mg/ml |

## 2.6 Cell Culture Media

**Table 6: Overview of used culture media.**

| Medium | Composition |
| --- | --- |
| Chondrocyte proliferation medium | Dulbecco's Modified Eagle's medium high glucose 4.5 g/l (DMEM) supplemented with 10 % FBS, 100 U/ml penicillin and 100 mg/ml streptomycin. |
| Cartilage growth medium | Dulbecco's Modified Eagle's medium high glucose 4.5 g/l (DMEM) supplemented with 10 % FBS, 10 mM HEPES, 0.1 mM non-essential amino acids (NEAA; Thermo Fisher Scientific, Waltham, USA), 0.4 µg/ml L-proline, 50 mg/l L-ascorbic acid 2-phosphate sequimagnesium salt hydrate, 100 U/ml penicillin and 100 mg/ml streptomycin. |
| Chondrocyte cryopreservation medium | Chondrocyte proliferation medium, supplemented with 5% DMSO |

## 2.7 Buffers and Solutions

**Table 7: Overview of used buffers and solutions.**

| Buffer / Solution | Composition |
| --- | --- |
| Blocking solution (IHC) | 1.5% BSA dissolved in PBS. |
| Buffered formalin | 3.7% formalin (37% stock solution) diluted in PBS. |
| Chloramine T solution | 141 mg chloramine T, 8 ml citric acid buffer, and 1 ml 2-propanol. |
| Collagenase buffer | 0.1 M Hepes, 0.12 M NaCl, 0.05 M KCl, 0.001 M $CaCl_2$, and 0.005 M glucose are dissolved in $ddH_2O$. Adjust carefully to pH 7.4 and store at 4 °C. For digestion freshly add 10 % FCS and 0.15 % type II collagenase from *Clostridium histolyticum* and sterilized with a 0.2 µm bottle top-filter. |
| DAB solution | 1.5 g p-dimethylamino-benzaldehyde (DAB), 6 ml 2-propanol, and 2.6 ml 60 % perchloric acid. |
| DMMB solution | 16 mg dimethylmethylene blue (DMMB) is dissolved for 16 h in 5 ml absolute ethanol. Afterwards, it is added to a prepared NaCl-glycine solution, consisting of 900 ml ddH2O, 3.04 g glycine, 2.37 g NaCl. Adjust to pH 3.0 and bring volume to 1 l with ddH2O. |
| FC buffer | 1 % BSA is dissolved in PBS. |
| Hoechst 33258 stock solution | 2 mg/ml is dissolved in $ddH_2O$. |

## Materials

| Buffer / Solution | Composition |
|---|---|
| Papain digestion buffer | 20 ml PBE buffer, 17 mg L-cysteine, 2U/ml papain, and sterilize with a 0.2 µm syringe-filter. |
| PBE buffer | 6.53 g $Na_2HPO_4$, 6.48 g $NaH_2PO_4$, 10 ml 500 mM EDTA in 900 ml $ddH_2O$. Adjust to pH 6.5 and bring volume to 1 l with $ddH_2O$ and sterilize with a 0.2 µm bottle top-filter. |
| PBS | 10 PBS (Dulbecco A) tablets are dissolved in 1 L $ddH_2O$. |
| PBST | 0.1% Tween® 20 dissolved in PBS. |
| TEN buffer | 0.1 M NaCl, 1 mM EDTA, 10 mM Tris is dissolved in $ddH_2O$; adjust to pH 7.4. |
| Thrombin dilution buffer | 40 mM $CaCl_2$, 171 mM NaCl and 40 mM glycine dissolved in $ddH_2O$. Adjust to pH 7.4. |
| L-ascorbic acid 2-phosphate sequimagnesium salt hydrate stock solution | 50 mg/ml L-ascorbic acid 2-phosphate sequimagnesium salt hydrate dissolved in PBS and sterile filtered. |
| L-proline stock solution | 40 mg/ml L-proline dissolved in PBS and sterile filtered. |
| PBE/Cysteine buffer | 0.85 mg/ml L-cysteine dissolved in PBE. |
| Safranin O (SafO) staining solution (0.1 %) | 1 mg/ml safranin O dissolved in $ddH_2O$. |
| Fast green staining solution (0.02 %) | 0.2 mg/ml fast green dissolved in $ddH_2O$. |
| Hoechst 33258 stock solution | mg/ml Hoechst 33258 dye dissolved in $ddH_2O$. |
| Hydroxyproline stock solution | 1 mg/ml Hydroxyproline dissolved in PBE/Cysteine buffer |

## 2.8    Software

**Table 8: Overview of used software.**

| Software/Version | Supplier | Central office |
|---|---|---|
| Origin 2018b Pro | OriginLab | Northampton, USA |
| Microsoft Office 2016/365 | Microsoft | Redmond, USA |
| Inkscape v.0.92 | Open source | |
| CellSense™ 1.16 | Olympus | Hamburg, Germany |
| FlowJo v.10.0.7 | Treestar | San Carlos, USA |
| Chemdraw 20.0 | PerkinElmer | Waltham, USA |

# 3   Methods

## 3.1   Cartilage Isolation

The donor tissue used to generate the cartilage slices was extracted from the hind legs of pigs. The pigs were between 8 and 12 weeks old and were sourced from a regional slaughterhouse (Metzgerei Hollerbach, Rimpar, Germany). The animals were under the legally required veterinary control. After slaughter, the knees were cooled and processed within a few hours. During animal separation, care was taken to ensure that the joint capsule remained intact so that the cartilage could neither dry out nor be damaged and contamination was prevented. The further cartilage isolation procedures were conducted aseptically in the laboratory. To open the joint capsule, a lateral capsulotomy was performed, while preserving the cartilage surface. For a better overview of the knee anatomy see Figure 1. After draining the synovia, the articular surface of the tibia (lateral condyle) was carefully incised with a scalpel and then removed by lever movements using a blunt spatula. This step was carried out with high care to prevent damaging to the cartilage tissue. During the work on the open knee, 1 % penicillin and 1 % streptomycin in PBS was used to keep the cartilage surface moist and to prevent possible contamination of the tissue culture. The isolated cartilage pieces were stored or kept moist in a Falcon tube filled with PBS until further processing (cutting, punching).

## 3.2   Fabrication of the Cartilage Disc/Ring Model

The establishment of the disc/ring model was performed cooperatively with two medical doctoral students and a detailed description of the methodology can be found in their respective dissertations [196,254]. The main points are described below.

After cartilage extraction, a cartilage cylinder with a diameter of 6 mm was punched out of the cartilage surface using a biopsy punch. During the excision, it was very important to consider the anatomical shape of the cartilage and thus taking the samples from suitable condyle locations providing sufficient cartilage thickness. As a next step, the cartilage cylinders were cut to unified heights using a custom-made trimming device and razor blades (see Figure 8). The trimming device has different slits, which allowed parallel cuts superficially and basally to be made at different distances. In this way it was reproducibly possible to remove the uppermost cartilage layer as well as calcified layers.
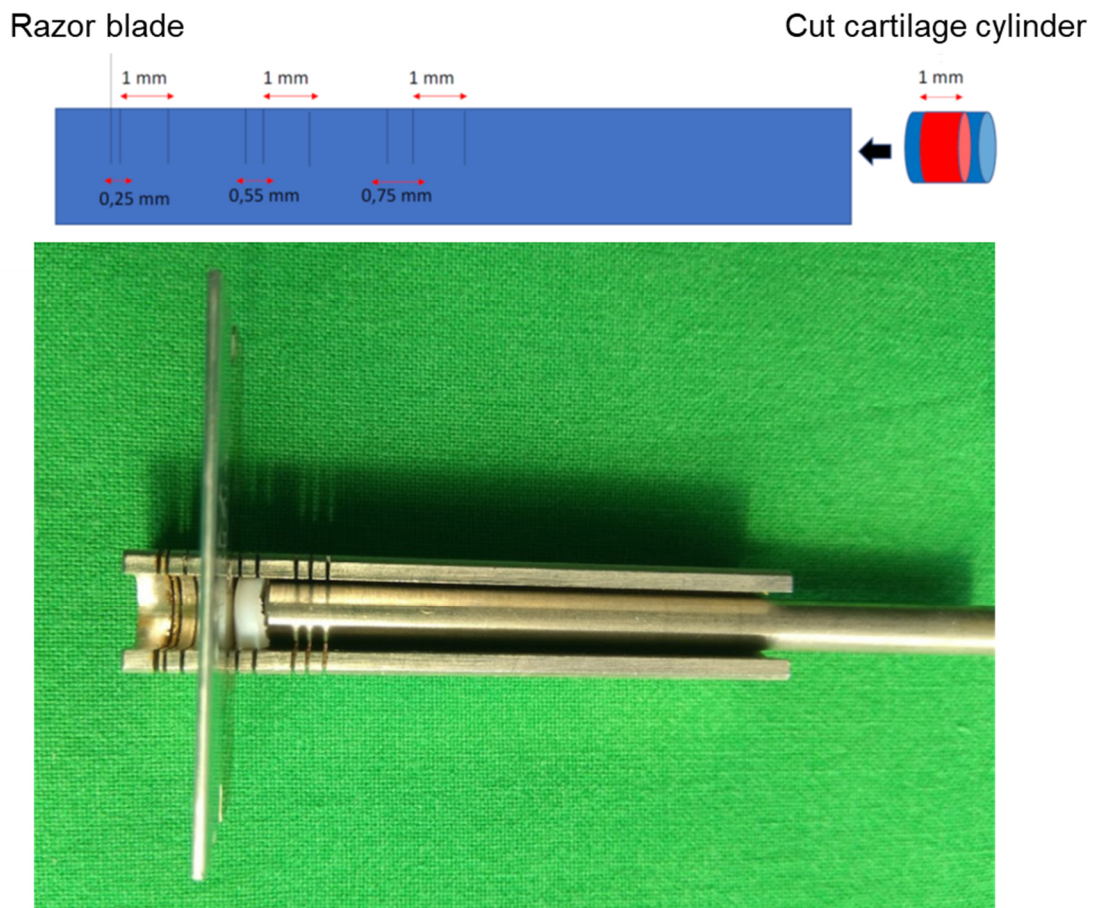
**Figure 8: Custom-made cutting tool for sectioning superficial and deep-layer zones from isolated cartilage cylinders.**

Accomplished, this method ensured that the cartilage discs produced were predominantly from the middle layer of articular cartilage. For cartilage constructs used in gluing experiments, a fine line with pathological dye, which does not diffuse into the tissue, was carefully drawn on one surface in order to be able to recognize the zonal alignment of the cartilage pieces in the further procedure (see Figure 9 upper image). This line was later used as a reference point for reinserting the detached cartilage part and guaranteed that the cartilage core could be glued back into the ring with the correct surface and alignment. The marked cartilage disc was inserted into the custom-made punching device made to punch out a centered middle section (see Figure 9 lower image).

A biopsy punch (3 mm diameter) was then used to separate the cartilage core. It was thus possible to achieve a reproducible, central and right-angled punching of the middle section. At the end of the working steps, a cartilage ring with an outer diameter of 6 mm, as well as a core disc with a diameter of 3 mm were available and related parts (disc with correlating ring) were stored in individual culture plate wells to avoid mixing. In the further course of the procedure, the cartilage core could be re-inserted or glued into the cartilage ring using a bioadhesive (see Chapter 3.6). Alternatively, for

biomaterial integration studies, the cartilage core can be disposed and the inner lumen be filled exclusively with a biomaterial (see Chapter 3.9).
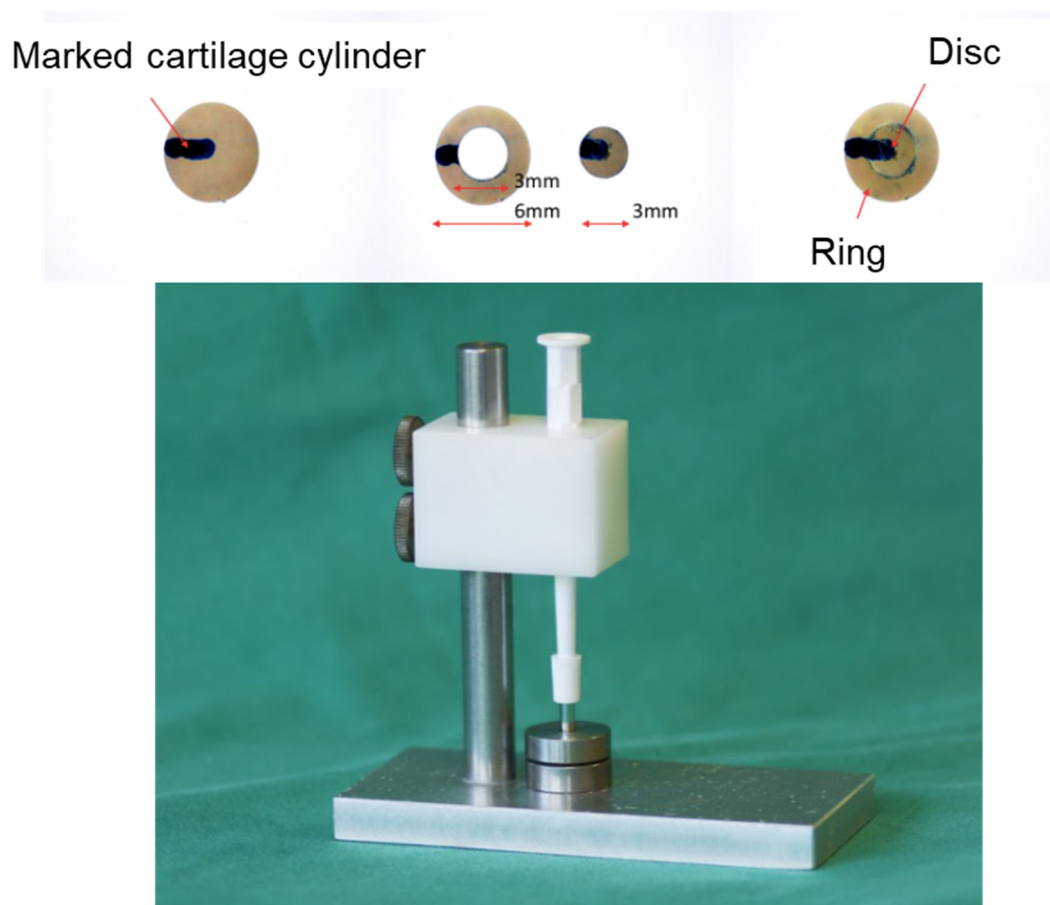


**Figure 9: Marking and punching of cartilage disc/ring construct.**

## 3.3    Fabrication of Cartilage Sandwich Constructs

Porcine cartilage discs with a diameter of 6 mm were fabricated as described before (see Chapter 3.2). In order to obtain a layered construct, about 20 µl of an adhesive material or a hydrogel was applied with a pipette on the sagittal interface of the cartilage disc. A second cartilage disc was put on top of the material. Then the intermediate material was cured with the respective mechanism to obtain a three-layer construction

## 3.4    Isolation and Culture of Chondrocytes

Articular cartilage tissue samples were isolated from porcine knee joints as described in Chapter 3.1. A scalpel was used to remove the calcified parts of the cartilage tissue. Following cell

isolations steps were conducted under sterile conditions and under laminar airflow. The articular cartilage samples were transferred to petri dishes, moistened with PBS and minced with razor blades to pieces (< 1 mm²). The cartilage pieces were then transferred to a 0.15 % collagenase II solution with a ratio of 10 ml digestion solution per each gram of cartilage. Enzymatic digestion was allowed for 16 h at 37°C on an orbital shaker. In the following, the digestion solution was filtrated through a 40 µm cell strainer, before a two-times washing procedure including centrifugation (320 g, 10 min) and resuspending the cell pellet in PBS. The washed cell pellet was resuspended in chondrocyte proliferation medium and the cell yield was determined. The freshly isolated chondrocytes (P0) were either used directly in subsequent experiments or transferred to chondrocyte cryopreservation medium with a cell density of about 1 Mio/ml and stored in liquid nitrogen until further use. For the cultivation of chondrocytes thawed or freshly isolated chondrocytes were resuspended in chondrocyte proliferation medium and plated in culture flasks with a density of about 10000 cells/cm². Cells were harvested by trypsinization and used for experiments or cultivation of further passages under aforementioned conditions.

## 3.5    3D Cell and Tissue Culture

For the *in vitro* cultivation of cartilage and chondrocyte-seeded hydrogel constructs (see also Chapter 3.9), the constructs were placed in sterile well plates (48-well for disc/ring and hydrogel constructs, 24-well for cartilage sandwich constructs). For the creation of chondrocyte pellets, chondrocytes (passage 1) were suspended in cartilage growth medium. $2 \times 10^5$cells were seeded per well in 96-well plates (conical bottom), centrifuged at 300 g for 5 min, and allowed to form dense cell pellets overnight in an incubator (37°C, 5 % $CO_2$, 21 % $O_2$). The plates were placed in an incubator and were cultivated under normoxic conditions at 21 % $O_2$/5 % $CO_2$ by default. In specific cases, separate constructs were cultivated under hypoxic conditions (2 % $O_2$/5 % $CO_2$) in a different incubator with otherwise unchanged parameters. Constructs were maintained *in vitro* with cartilage growth medium for durations as indicated for the respective experiments (up to six weeks). In experiments with chondrocyte pellets the ascorbic acid content of the cartilage growth medium was adapted. The medium was either deprived of ascorbic acid (w/o ascorbate) or supplemented with 50 µg/ml or 100 µg/ml ascorbic acid. Medium was exchanged every two to three days in all experiments.

## 3.6 Gluing of Disc/Ring Constructs

Freshly isolated cartilage discs and rings (see Chapter 3.2) were used for gluing experiments. In an aseptic working environment, the individual cartilage pieces were removed from the isotonic saline solution and excess liquid was absorbed with a paper towel before the cartilage pieces were placed on a Teflon pad. About 7 µl of the respective adhesive was pipetted into the inner lumen of the cartilage ring for initiating the gluing. The corresponding inner cartilage core was then immediately pressed into the cartilage ring, taking care to ensure the best possible original alignment with the aid of the marking line. Spilled adhesive liquid was collected with a paper tissue. Glued constructs were transferred into 48 well plates with sterile PBS and cultivated submerged until subsequent measurements.

### 3.6.1 BioGlue®

BioGlue® is a two-component adhesive consisting of BSA (bovine serum albumin) and glutaraldehyde. This commercially available surgical adhesive is approved for the treatment of aortic dissections. For the clinical application, a 45 % BSA in PBS solution and a 10 % glutaraldehyde in PBS solution are prepared separately in a two-chamber syringe. The mixing of the two components is done by a special syringe tip. For practical reasons the two components were prepared with the raw substances before the experiments as described earlier [255]. For the application as cartilage adhesive, the BSA solution and the glutaraldehyde solution were carefully mixed with a pipette in a ratio of 4:1 and then applied to the cartilage surface. The constructs were allowed to polymerize for 10 min at 37°C, 5 % CO2.

### 3.6.2 Fibrin Glue

Fibrin is derived from blood clotting agents, in particular fibrinogen, Factor XIII and thrombin. Depending on its composition also an antifibrinolytic agent (aprotinin) and calcium chloride may be included in the formulation. The starting material for the experiments performed here was fibrin glue consisting of two ready-mixed solutions (shortly referred to "fibrinogen solution" and "thrombin solution"). By thorough pipette-mixing in a ratio of 1:1 the polymerization is started, and an adhesive hydrogel is formed. The fibrin constructs were allowed to polymerize for 30 min in an incubator at 37°C and 5 % $CO_2$.

### 3.6.2.1 TissuCol

The commercially available TissuCol Duo S Kit served as basis for the generation of TissuCol adhesive hydrogels in conducted experiments. The individual components were prepared according to the manufacturer's instructions and then fractioned into aliquots and stored at -28°C until use.

### 3.6.2.2 Long-term Stable Fibrin

To further investigate cartilage integration with fibrin. Variations of fibrin formulations with long-term stability were included to the experiments. The composition of the stable fibrin gels was described earlier by our group [122]. Bovine fibrinogen was dissolved in 10,000 KIU/ml aprotinin (from bovine lung) solution. To study the influence of fibrinogen concentration we used either a 50 mg/ml or a 100 mg/ml stock solution resulting in hydrogels with total fibrinogen content of 25 mg/ml or 50 mg/ml, respectively (referred as stable fibrin (25/50) in the course of this document). For the preparation of the thrombin solution, components of the TissuCol Duo S Kit were used. Thrombin was prepared at a concentration of 5 U/ml in 40 mM $CaCl_2$ (500 U/ml thrombin stock diluted 1:100 in Baxter dilution buffer containing 40 mM $CaCl_2$). This preparation procedure resulted in final $CaCl_2$ and thrombin concentrations of 20 mM and 2.5 U/ml, respectively.

## 3.6.3 Diazirine Enhanced Bonding of Fibrin Glue

In order to provide a larger number of binding moieties on the cartilage surface, the harvested disc/ring cartilage samples were functionalized with a photoreactive diazirine group. To achieve this, a heterobifunctional diazirine was chosen that can bind to free amines on the cartilage surface via the NHS group, whereby an additional charge (sulfo group) prevents possible diffusion into the cytoplasm and thus undesirable side reactions. To further enhance the binding efficiency of the diazirine molecule to the cartilage, a pre-treatment with Chondroitinase ABC (Ch-ABC) was conducted with separate experimental groups. The affected constructs were incubated for 20 min in a 1 U/ml Ch-ABC solution at 37°C, then rinsed three times with sterile PBS. Small aliquots of the NHS-diazirine were freshly dissolved in sterile PBS to obtain a 10 mM solution, of which about 10 µl were carefully applied to the defect interface of the cartilage disc and ring with a pipette and then incubated in the dark in a humid chamber for 10 min. The disc/ring constructs primed in this way were afterwards rinsed in sterile PBS three times and then either directly assembled or additionally treated with fibrin glue (long-term stable formulation with 50 mg/ml fibrinogen, see also Chapter 3.6.2). The assembled constructs were then illuminated from both sides for 10 min each with a UV hand lamp (365 nm) to start the diazirine

reaction. Fibrin treated constructs were additionally incubated for 30 min at 37°C in a humid chamber afterwards to ensure complete crosslinking of the fibrin.

### 3.6.4    Ruthenium Crosslinked Fibrinogen (RuFib)

A 100 mg/ml fibrinogen stock solution was prepared aseptically and stored at -20°C in the dark until use. Sodium persulphate (SPS) was freshly prepared as a 0.5 M stock in water. Ruthenium trisbipyridyl chloride $[RuII(bpy)_3]^{2+}$ (partially named ruthenium complex or abbreviated as "ruthenium" in the course of this document) was prepared as a 50 mM stock solution in water, aliquoted to 20 µl portions and stored in the dark at -20°C until use. All subsequent steps were carried out in a darkened room and the solutions were additionally protected from light with aluminum foil. An adhesive precursor solution was mixed under addition of sterile PBS, resulting in final concentrations of 50 mg/ml fibrinogen, 2 mM $[RuII(bpy)_3]^{2+}$ and 20 mM SPS. The adhesive precursor solution was pipetted into the lumen of the cartilage ring and the corresponding cartilage disk was inserted. The adhesive was then cured by placing the constructs under a blue-light LED hand lamp at a distance of 10 cm for 30 s from both sides.

### 3.6.5    Poly(oxazoline)s/Fibrinogen Adhesives

Based on the here presented work, the use of poly(oxazoline)s/fibrinogen adhesive hydrogels in cartilage treatment was recently published [256]. Poly(2-alkyl-2-oxazoline) (POx)-based polymers equipped with L-DOPA functional groups as mussel-inspired adhesion moieties (labelled PEOD or PMOD) were synthesized in cooperation with the Department for Functional Materials in Medicine and Dentistry (FMZ), University Hospital Würzburg. Starting from two different precursor polymers, adhesive components with different catechol functionalization were obtained.

Depending on the used POx in the final hydrogel formulation different amounts of reactive moieties and different degradation profiles are obtained. The adhesive precursor solution was prepared by addition of fibrinogen to a PMOD or PEOD stock solution in PBS. Polymerization was initiated by mixing a small amount of 300 mM sodium periodate ($NaIO_4$) in PBS to the PMOD/PEOD-fibrinogen solution. The overall polymer concentration was 7.5 % (w/v), fibrinogen was concentrated at 7.5 % (w/v) and the sodium periodate concentration was 60 mM in the final adhesive. Because of the fast polymerization reaction, the adhesive precursor was placed in the lumen of the cartilage ring and polymerization in contact with the cartilage was started by adding the periodate before plugging

in the cartilage disc. Adhesives were allowed to cure for 30 min on PBS-soaked tissue paper in a humid chamber at 37°C.

## 3.7 Adhesive Strength Measurement

The establishment of this measurement was performed cooperatively with two medical doctoral students and a detailed description of the methodology can be found in their respective dissertations [196,254]. The main points are described below.

For biomechanical adhesive strength measurements, a Zwick Z020 testing machine (Zwick Roell, Ulm, Germany) was utilized. Load was applied to the central 3 mm core of the constructs using a plunger. A custom-made sample holder functioned as alignment unit thus allowing for a centered contact point while the annulus rested on a rigid ring with a center hole (see Figure 10).
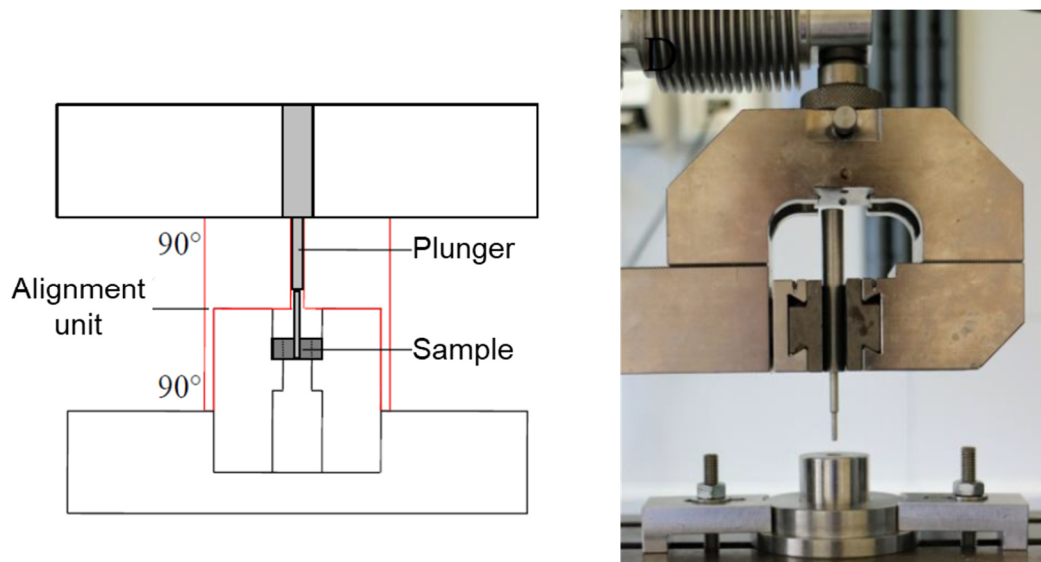


**Figure 10: Schematic illustration (left) and photograph (right) of the push-out setting used in biomechanical testing of cartilage integration strength.**

All specimens were tested to failure with a displacement rate of 0.5 mm/min and the axial force was recorded with a 100 N load cell. The exact height of each construct (h) was measured with an indicating caliper to an accuracy of 0.01 mm. Together with the uniform radius of the punched out defect (r = 1.5 mm) and the individually determined sample height, the interface area was calculated using the lateral cylindrical area formula (2 * π * r * h). The adhesive strength was calculated with the recorded peak push-out force divided by the interface area as follows:

$$Adhesive\ strength\ [kPa] = 1000 \times \frac{Force\ at\ failure\ (Fmax)_{specimen}\ [N]}{Interface\ area_{specimen}\ [mm^2]}$$

## 3.8    Flow Cytometric Characterization of Chondrocytes

Flow cytometry was used to analyze the existence and quantity of the cell surface receptor CD44 in isolated chondrocytes. Chondrocytes were resuspended in FC buffer and viable cells were counted (trypan blue exclusion). $1 \times 10^5$ cells were transferred to FC tubes, washed twice with 1 ml FC buffer and centrifuged (400 g, 4°C, 7 min). FC receptor blocking solution (5 % goat serum, FC buffer) was added for 20 min at 4°C. After washing with FC buffer, cells were incubated with monoclonal antibodies against CD44 (Jackson Immuno) for 25 min at 4°C; a corresponding isotype control was employed. Afterwards, cells were washed two times with FC buffer and incubated with the secondary (goat) antibody (Alexa 488) for 20 min at 4 °C in the dark. Stained cells were washed twice prior to analysis using a FACSCanto flow cytometer (BD Biosciences, Palo Alto, USA). One tube of unstained cells was used to adjust the settings of the flow cytometer. Data analysis was carried out using FlowJo v.10.0.6 software (Treestar, San Carlos, USA).

## 3.9    Preparation of Hydrogels

Hydrogels were either prepared for cell culture experiments with or without cells or for material characterization. For this purpose, 40 µl gels were fabricated using glass/Teflon rings or silicone molds. In order to investigate integration of a distinct hydrogel material with cartilage tissue, about 15 – 20 µl hydrogel solution were pipetted into the lumen of a cartilage ring (see also Chapter 3.2) and cured in direct contact, thus using the cartilage as a mold. For respective controls, the hydrogels were cured in Teflon or silicon molds and then plugged into the cartilage ring to create a composite construct. Cell-laden hydrogels were prepared so that a final cell concentration of $15 \times 10^6$/ml was achieved.

### 3.9.1    Preparation of Fibrin Hydrogels

TissuCol or long-term stable fibrin gels were prepared the same way as when used as cartilage glue and as described in Chapter 3.6.2.

For the preparation of cell-laden fibrin hydrogels, pelleted cells were resuspended in the diluted fibrinogen solution, and equal volumes (1:1) of diluted thrombin and cell-containing fibrinogen were mixed. Fibrin gels were allowed to polymerize for 30 min at 37°C, 5 % $CO_2$.

### 3.9.2 Agarose

A stock solution of 4 % (w/v) Low Melt Agarose was prepared, sterilized and stored as aliquots at 4°C in the dark until further use. For the generation of hydrogels an aliquot of agarose was melted at 70°C and then equilibrated to 40°C. Cell-free hydrogels were fabricated by mixing the liquid agarose 1:1 with sterile PBS (37°C). For cell-laden hydrogels instead PBS a cell suspension in culture medium was used. Hydrogels were solidified by cooling for 10 min at 4°C in a refrigerator.

### 3.9.3 Thiol-Ene Clickable Hyaluronic Acid-based Hydrogels

Allyl-functionalized poly(glycidol)s (P(AGE/G)) and thiol-functionalized hyaluronic acid (HA-SH) were synthesized as described before [149] and were provided by the Department for Functional Materials in Medicine and Dentistry (FMZ), University Hospital Würzburg. 10 % (w/v) (5 % P(AGE/G) and 5 % HA-SH) hydrogel solutions, containing 0.05 % (w/v) photoinitiator Irgacure, were prepared. The pH of the slightly acidic hydrogel solutions was neutralized with 5M NaOH. For the generation of cell-laden hydrogels, the respective cell number was pelleted by centrifugation and subsequently resuspended in the hydrogel precursor solution. To investigate the influence of a structural support scaffold within the hydrogel on cartilage integration outcome, a rigid thermoplastic poly(ε-caprolactone) (PCL) was used. Cylinders of a 3D-printed PCL grid (provided by the FMZ) were obtained by punching with a sharp biopsy punch. The PCL scaffold was then placed inside the cartilage ring before the hydrogel solution was added. In order to cure the constructs, the hydrogel precursor solution was UV irradiated with an UV hand lamp VL-4 at 365nm for 10 min (~1mW/cm$^2$).

### 3.9.4 Poly(oxazoline)s/Fibrinogen

Poly(oxazoline)s/fibrinogen gels were prepared the same way as when used as cartilage glue and as described in Chapter 3.6.5. 50 µl gels with varying POx concentrations, a fixed fibrinogen concentration (5 % / 50 mg/ml) and a sodium periodate concentration of 60 mM were prepared in silicone molds (diameter 4 mm or 6 mm) and stored in sterile PBS until further investigations.

#### 3.9.4.1 Determination of Swelling Behavior

The swelling behavior of POx/fibrinogen hydrogels was determined by weighing the hydrogel specimens (6x2 mm) before they were immersed into PBS ($w_0$) and stored at 37 °C. The weight of the same hydrogel specimen ($w_s$) was recorded at the specific time points (d1, d3, d7, d14, d21), for which

they were taken out of solution and blotted on tissue paper to remove excess PBS. The percentage of swelling was calculated as follows: Swelling (%) = (w$_s$-w$_0$)/w$_0$ x 100. All measurements were performed in triplicate. Additionally, at each timepoint macroscopic images of the hydrogels were taken with a Zeiss SteREO Discovery.V20 stereo microscope (Carl Zeiss, Jena, Germany) or an portable microscope camera DigiMicro Profi (dnt, Dietzenbach, Germany).

### 3.9.4.2 Determination of Iodine Release

In the POx/fibrinogen hydrogel formation process, periodate is reduced to iodine. Over time, brown iodine was released from the hydrogels indicating network degradation. To record the iodine release, hydrogel discs (6 x 2 mm) were incubated over three weeks in 2 ml of PBS at 37°C; measurements were performed in triplicate. A sample of 50 ml was withdrawn and diluted with 0.950 ml deionized water for the measurement. After each sample withdrawal, 50 ml of fresh PBS was added to the hydrogel. The UV/Vis spectrum of the diluted sample solution was recorded between 200 and 600 nm on a Genesys 10S Bio spectrophotometer (Thermo Fisher Scientific, Waltham, MA, USA).

## 3.10 Determination of Elastic Modulus

The elastic modulus, also Young's modulus, was measured using a dynamic electromechanical test instrument (ElectroForce 5000, TA Instruments, Eden Prairie, MN, USA) with a load cell of 250 g. The specimens were compressed with a speed of 0.0025 mm/s until a displacement of -1.25 mm. cylinders of the respective hydrogel formulation with a dimension 4x4 mm were measured. A sliding caliper was used before each measurement to record the dimensions of each specimen. The strain was calculated by dividing the displacement during the measurement by the original height of the specimen before compression. The load was converted from Gram into Newton by multiplication with the gravitational acceleration (9.81 m/s$^2$). The true stress was then calculated as follows:

$$true\ stress\ [MPa] = load\ [N] \times \frac{height_{specimen}[mm] - displacement\ [mm]}{volume_{specimen}[mm^3]}$$

The Young's modulus was obtained by plotting the strain versus the true stress and applying a linear fit from 0.1 to 0.2 strain. The Young's modulus of each specimen was calculated from the slope of the linear fit.

## 3.11 Cell Viability Assays

### 3.11.1 Live/Dead Staining

Cell viability was evaluated using a live/dead cell staining kit from PromoKine (Heidelberg, Germany). At the observation timepoints as mentioned in the respective result section, whole cartilage constructs or hydrogels were washed three times with PBS and stained by applying 0.5 ml of staining solution containing 4 µM ethidium bromide homodimer III (EthD-III) and 2 µM calcein acetoxymethyl ester (calcein-AM) in PBS. After 1 hour, the dye was removed and the specimens were washed with PBS. From the native cartilage samples, thin slices were made at right angles to the integration interface using razor blades. Hydrogels were investigated without further processing. The specimens were subsequently viewed under an inverse fluorescence microscope (ex/em 460-490 nm/520 nm and ex/em 510-550 nm/590 nm, respectively) and the resulting images overlaid (Olympus cellSens™ Dimension Microscope Imaging Software; Olympus, Hamburg, Germany).

### 3.11.2 MTT Staining

Articular cartilage disc/ring composites were incubated for 24 h in cartilage growth medium after adhesive treatment. 3-(4,5-dimethylthiazol-2-yl)-2,5-diphenyltetrazolium bromide (MTT) was used to stain cells for their metabolic viability. Culture medium was removed and MTT solution (1 mg/ml in PBS) was added to the constructs and further cultured with 5 % $CO_2$ at 37 °C for 4 h, allowing the yellow dye to be transformed into dark-blue formazan crystals by mitochondrial dehydrogenases. For qualitative cytotoxicity evaluation, the disc/ring constructs were fixed in 3.7 % buffered formalin, snap-frozen, cryo-sectioned to 12 µm and covered in water-based mounting medium. Cell viability in the tissue sections was assessed microscopically directly at the adhesive-treated defect interface. In order to quantify cell viability in the bulk cartilage tissue, MTT-stained disc/ring samples were rinsed twice with PBS (pH 7.4). Then, 400 ml dimethyl sulfoxide (DMSO) was added to dissolve the formazan crystals. 200 ml of the supernatant were placed in a 96-well plate. The optical density of the solution was recorded using a microplate reader (Infinite M200, Tecan, Crailsheim, Germany) at a wavelength of 570 nm and normalized to the wet weight (mg) of the disc/ring sample. The mean value of control constructs without adhesive treatment was taken as reference and set as 100 % viability

## 3.12   Paraffin Sectioning

Samples for histological analyses were fixed in 3.7 % formalin in PBS overnight, rinsed two times in PBS for 5 min and then embedded in paraffin. An automatic embedding machine was used for the embedding. The following steps were performed for one hour each in a vacuum: 2 x formalin 3 %, 2 x EtOH 80 %, 4 x EtOH absolute, 2 x xylene, 4 x paraffin. Cross-sections of 2 µm thickness were collected on Superfrost™ Ultra Plus glass slides (Thermo Fisher Scientific, Waltham, USA).

## 3.13   Histology and Immunohistochemistry

Before staining, the paraffin present in the construct must be dissolved out. This was achieved by means of a descending alcohol series. The dewaxing was carried out according to the following protocol: 3 x 3 min xylene, 3 x 3 min EtOH absolute, 2 x 3 min EtOH 90 %, 2 x 3 min EtOH 80 %, 1 x 3 min EtOH 70 %, 1 x 3 min EtOH 50 %, 2 x 3 min demineralized water.

### 3.13.1   Safranin O Staining for GAG

Sections of the constructs were stained for glycosaminoglycans with safranin O together with Weigert's hematoxylin and fast green [257]. Briefly, sections were sequentially immersed for 5 min in Weigert's hematoxylin, 5 min under running tap water, 4 min in 0.02 % fast green, 10 sec in 1 % acetic acid, and 6 min in 0.1 % safranin O, dehydrated in an alcohol series up to xylene, mounted with Entellan® and images were captured with a microscope (Microscope BX51/DP71 camera).

### 3.13.2   Chromogenic Immunohistochemical Staining

Immunohistochemical staining was performed using the EnVision G|2 Doublestain System (Dako) according to the protocol of the manufacturer with slight modifications. Prior to the blocking step with 1 % BSA in PBS for 30 min at room temperature to prevent unspecific binding, sections were incubated in Proteinase K (Digest-All 4) for 10 min. Primary antibodies against collagen type II (Col2), aggrecan (ACAN) and collagen type X (ColX) were diluted in Antibody diluent Dako REAL and incubated overnight. Samples were counterstained with Mayer's hematoxylin for 3 min., dehydrated in an alcohol series, cleared in xylene, and finally mounted with Entellan® and images were captured with a microscope (Microscope BX51/DP71 camera).

### 3.13.3   Fluorescence-Based Immunohistochemical Staining

Antigen retrieval was generally performed for using Proteinase K (Digest-All 4) for 10 minutes at room temperature. Slides were washed three times in PBS for 3 min and all sections were blocked with 1 % BSA in PBS for 30 min at room temperature. Primary antibodies were diluted in Antibody diluent Dako REAL. Antibodies against collagen type I (Col1), collagen type II (Col2), aggrecan (ACAN) were incubated overnight in a humidified chamber at room temperature. Immunohistochemical staining for neoepitopes occurring after cleavage of collagen type II by MMPs (crosslinked C- telopeptide of type II collagen, CTX-II neoepitope) was utilized by digestion of the slides with 0.1 units/ml protease-free chondroitinase ABC and 0.1 units/ml of keratanase I (Seikagaku, Tokyo, Japan), prior to overnight incubation with polyclonal rabbit antibody to CTX-II). Slides were thoroughly washed with PBS, and a Cy3-conjugated AffiniPure goat anti-rabbit secondary antibody (Jackson Immuno Research, West Grove, PA, USA) was added for 2 h in the dark. Nuclei were counterstained with IS Mounting Medium DAPI (Dako). Equivalent concentrations of species-matched immunoglobulins on identically treated sections were used as negative controls. The stained slides were imaged using an Olympus BX51 fluorescent and bright-field microscope and the CellSens™ imaging software from Olympus (Olympus, Hamburg, Germany).

## 3.14   Macroscopical Imaging

Macroscopic imaging was performed either with a USB microscope (DigiMicro Profi; dnt®) using the corresponding Micro Capture software on an LED light pad (HUION), a (stereo microscope Zeiss SteREO Discovery.V20) or with a Sony RGBW sensor camera.

## 3.15   Scanning Electron Microscopy

Immediately after adhesive application and curing, the cartilage constructs were fixed in 5 % glutaraldehyde and 3.7 % formalin in PBS. Constructs were washed five times with PBS and gradually dehydrated with acetone. Following that, constructs were critical point-dried and freeze-fractured in liquid nitrogen. After sputter-coating with platinum, specimens were analyzed with a Zeiss Crossbeam 340 Scanning Electron Microscope (SEM) equipped with a GEMINI e-Beam column (Carl Zeiss, Jena, Germany).

## 3.16   Biochemical Assays

### 3.16.1    Papain Digestion

Prior to biochemical analysis, the respective constructs were digested using papain. Therefore, the constructs were removed from medium, at indicated time points, and washed two times in PBS for 10 min, transferred into 2ml SafeSeal micro tubes, and 500 µl of sterile PBE-cysteine buffer was added. In case of cell pellets, three pellets from the same experimental group were pooled in a single tube. Subsequently, 500 µl of PBE-cysteine buffer containing papain 3U/ml was added to the homogenized PBE/construct solution, and incubated for 10 h to 16 h at 60°C. The digested samples were stored at -20°C until used in biochemical assays.

### 3.16.2    DNA Assay

For DNA content measurement, a solution of Hoechst 33258 DNA intercalating dye was used. Therefore, 10 µl of papain digested samples were added to 200 µl of a Hoechst 33258 dye solution and the DNA quantification was carried out with the Tecan GENios pro spectrofluorometer at 340nm and 465nm, using salmon testis as standard [258].

### 3.16.3    GAG Assay

The amount of sulfated glycosaminoglycans (GAGs) was measured as chondroitin sulfate using the dimethylmethylene blue (DMMB) assay adapted to 96-well plate format [259]. Therefore, 10 µl of papain digested samples were added to 40 µl of PBE-cysteine buffer and finally 200 µl DMMB solution were added and the GAG amount was determined spectrophotometrically at 525 nm with a microplate reader, using bovine chondroitin sulfate as standard.

### 3.16.4    Collagen Assay

The hydroxyproline content was determined spectrophotometrically after acid hydrolysis and reaction with p-dimethylamino-benzaldehyde (DAB) and chloramine T. The hydroxyproline assay was adapted to 96-well plate format [260]. Therefore, 100 µl of 36 % HCl were added to 100 µl of papain digested samples, and hydrolyzed for 16 h at 105°C. Afterwards, HCl was allowed to evaporate, and pellets were resuspended in 500 µl ddH$_2$O. For quantification, 50 µl chloramine T solution, and 50 µl

DAB solution were added to 100 µl of the water resuspended samples, and quantification was carried out with the MRX microplate reader at 570 nm, using L-hydroxyproline as standard. The amount of total collagen was calculated using a hydroxyproline to collagen ratio of 1:10 [261].

## 3.17   Statistical Analysis

Statistical significance was assessed by one-way or two-way analysis of variance (ANOVA) assuming confidence level of 95 % ($p < 0.05$) in conjunction with Bonferroni adjustment for multiple comparisons. Statistical analysis was performed using Origin Pro, Version 2018b (OriginLab, Northampton, USA). Analyses were performed in triplicate, if not stated otherwise.

# 4  Results and Discussion

## 4.1  Fabrication and *in vitro* Cultivation of Native Cartilage Tissue Explants and Chondrocyte Pellets

In this chapter the production and cultivation of 3D tissue or cell culture models were investigated to determine the suitability and applicability in subsequent experiments.

### 4.1.1  Fabrication and Characterization of Disc/Ring Test Model

For the investigation of lateral cartilage integration, a disc/ring model obtained from porcine explants was chosen. With the use of custom-made devices, it was able to fabricate a standardized cartilage tissue defect model with a centered defect. The reproducibility of this model and the susceptibility to errors during its fabrication were investigated as part of the medical doctoral thesis of two students (see dissertation Alexander Kossmann and Felix Kiepe, University of Würzburg [196,254]). By using sharp biopsy punches a lateral defect interface was introduced to a 6 mm cartilage disc. To investigate the influence of punching on cell viability in the vicinity of the defect, constructs were stained using both MTT and the live/dead assay (see Figure 11A and B). The constructs were cultivated for 24 hours before staining in order to take into account later cell death by apoptosis. With the MTT-colored constructs, a white border can be seen limited to the direct vicinity of the set defect. The absence of a dark staining in this area indicates the absence or decrease of cell viability. In contrast, the dark staining of the overall construct indicates that the majority of the construct has good vitality 24 hours after isolation. Microscopic examination of complete live/dead stained constructs proved to be impracticable, as the thickness of the construct and the fluorescence intensity did not allow sharp images of defined areas with the existing equipment. For this reason, it was necessary to prepare with fresh razor blades the thinnest possible sections of the area to be examined after the constructs were already stained (see Figure 11B). With this procedure, it could be shown that a necrotic area at the punch channel occurs in a range of about 50 - 200 µm. In the same radius, the CTX-II marker also revealed the lesion of collagen type II fibrils in the extracellular matrix of native tissue (see Figure 11C).
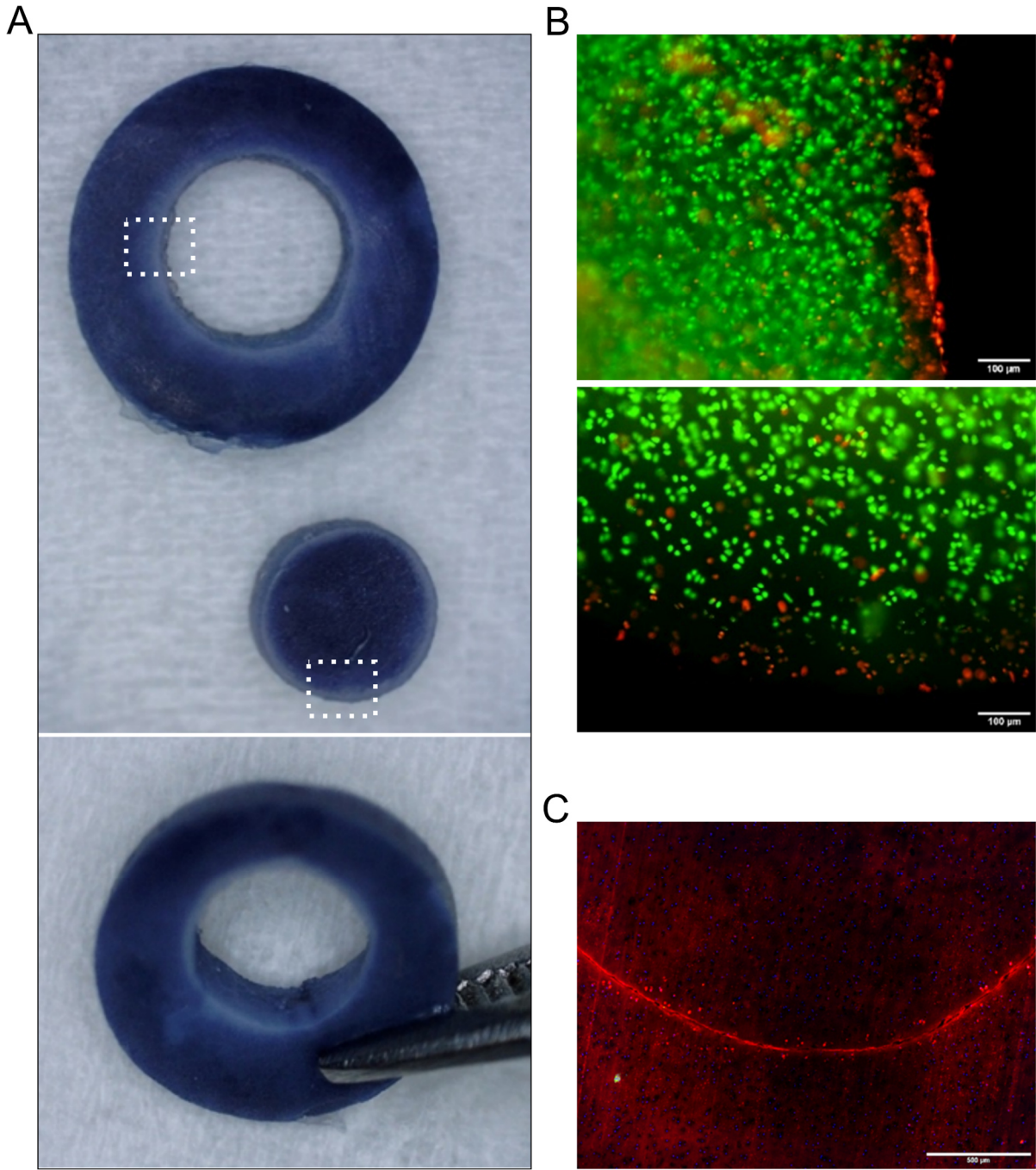
A



B



C



**Figure 11: Classification of the lateral defect in the disc/ring model.**

Microscopical captures of the defect interface after MTT staining (A). The areas marked with a box were stained in separate constructs with the live/dead assay and examined with a fluorescence microscope (B). CTX II staining of the lateral defect in the disc/ring model (C).

## 4.1.2    *In vitro* Cultivation of Native Cartilage Explants

A sufficient cell viability of the cartilage explants after isolation is crucial for the possibility to conduct long-term experiments with these tissue constructs utilizing *in vitro* cultivation. During long-term cultivation, it is also of particular interest how the whole cartilage tissue responses to certain conditions. For that reason, full-thickness cartilage explants were harvested similar to a first step of the disc/ring model fabrication, but without further punching or slicing. The obtained 6 mm cartilage discs were *in vitro* cultivated for 21 days in cartilage growth medium that contains 10 % FCS as a standard or medium were the FCS was substituted by 1 % ITS premix. Visual evaluation of the constructs after 21 days was supported by MTT staining. Between the two experimental groups it was observed that the constructs that were cultivated with FCS had increased in mass and volume in comparison to the ITS cultivated specimens. In both culture media the samples remained viable (see Figure 12). A macroscopic comparison of the two groups suggests that FCS leads to an increased ECM formation. It was particularly noticeable that in constructs cultivated with FCS, strong tissue growth occurred in the deep zone and the calcified zone. Immunohistochemical staining for the Col X revealed that areas in the calcified layer of constructs cultivated with FCS are positive for this hypertrophy marker.
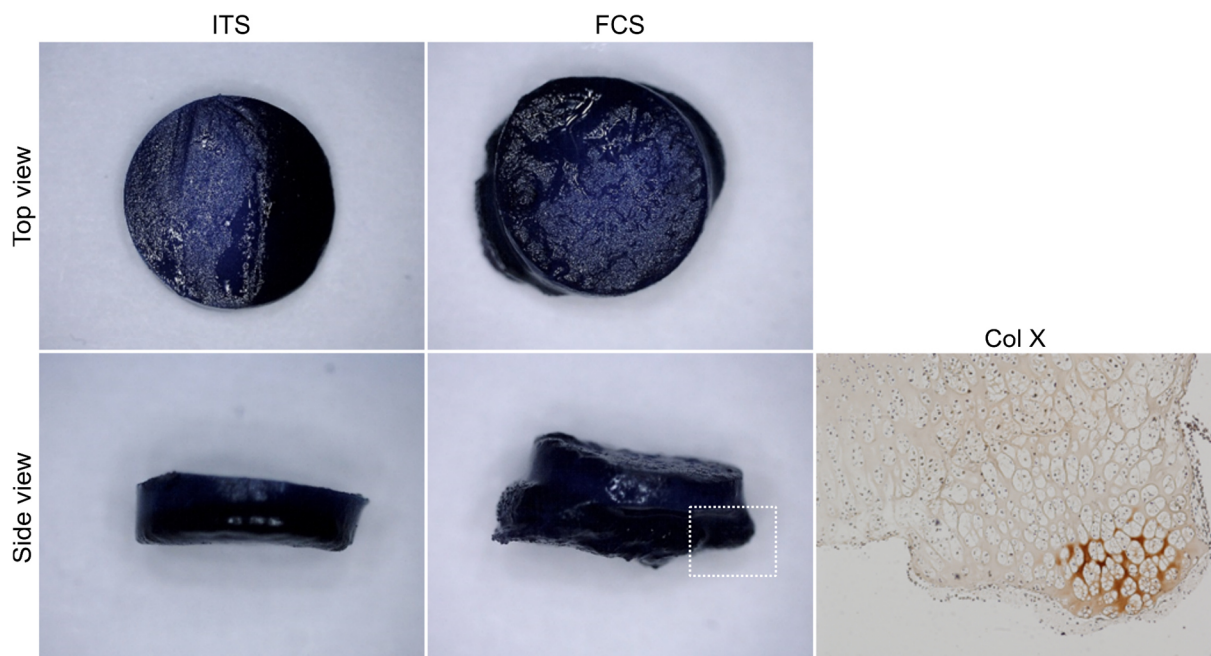


**Figure 12: Comparative evaluation of constructs cultured with ITS or FCS medium supplementation.**

Macroscopic captures of MTT-stained full-thickness cartilage explants after 21 days in vitro cultivation in medium either containing ITS or FCS supplementation (left). The area highlighted with a box (deep/calcified zone) showed partly positive in a Col X immunostaining (right).

### 4.1.3    Effects of Ascorbic Acid on Chondrocytes in a 3D Pellet Model

A widely used model for the investigation of cartilage related ECM formation under *in vitro* conditions are chondrocyte pellets. In this chapter, isolated porcine chondrocytes were cultivated for five days with chondrocyte proliferation medium *in vitro*. Afterwards the cells were trypsinized and pellets of 2 x 10$^5$cells were formed via centrifugation. The influence of ascorbic acid on the formation of a cartilaginous phenotype of the pellets was investigated for up to 28 days. Groups without the presence of ascorbic acid (w/o ascorbate) in the medium or with either 50 µg/ml or 100 µg/ml have been split up. Samples of the different groups were harvested after 14 and 28 days of *in vitro* culture. The constructs were stained for GAG with Safranin O (SafO) and for collagen type II with immunofluorescence. Results of the biochemical analyses are depicted in Figure 13B.

In the w/o ascorbate group the cell number decreased over the course of the cultivation period as determined via pellet DNA contents after 14 and 28 days. A significant increase in cell number was observed in both ascorbate containing groups after 14 days. The DNA content almost stagnated until day 28 of the *in vitro* culture. In contrast to the ascorbate-deprived group significant increases in the total GAG and collagen contents of the pellets was observed in the groups cultured with ascorbate compared to d0 values. In the 100 µg/ml ascorbate group, a decrease in GAG content from d14 to d28 was observed along with a sharp increase in total collagen content. At d14, the collagen content was highest in pellets of the 50 µg/ml ascorbate group without any additional increase being observed. In the 100 µg/ml, collagen deposition at d14 was less than in the 50 µg/ml group, but a strong increase in the further course provided the highest total amount of collagen at d28 in this group. Normalized to the DNA content, the GAG/DNA content was significantly higher in both ascorbate groups than in the w/o ascorbate group. When both GAG and collagen synthesis are considered, the 50 µg/ml ascorbate group showed a consistent increase already after 14 days, whereas collagen deposition in the 100 µg/ml group picked up with a delay and was above the level of the 50 µg/ml group after 28 days, but with a weaker GAG signal. Also in the w/o ascorbate group, GAG and collagen deposition was not completely eliminated, but due to the relatively lower cell number, the DNA normalized GAG and collagen values should be interpreted with caution. The histologic and immunohistochemical images (see Figure 13A) support the overall picture that ascorbic acid withdrawal from the medium prevents pellet growth and hyaline ECM formation. Qualitatively similar increases in pellet sizes and their GAG and collagen type II content were detected in both ascorbate groups.
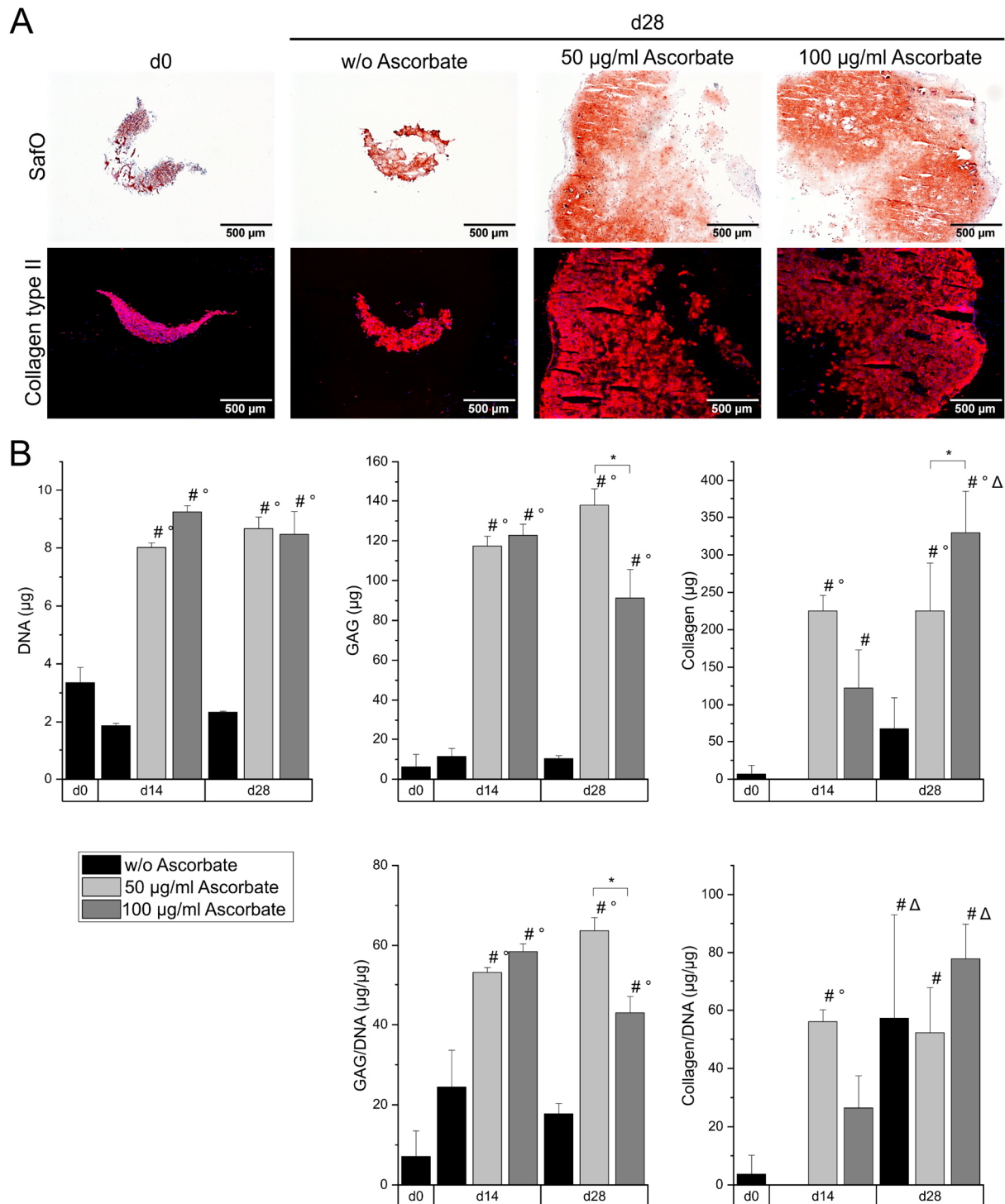
**Figure 13: Effect of varying ascorbic acid concentrations in 3D chondrocyte pellet culture.**

Pellets were stained for GAG and collagen type II (A). The effect on total DNA amount as well as total GAG and collagen per sample (n=3 pellets) or normalized to DNA amount was examined biochemically after 14 and a are 28 days and compared to the d0 values (B). Data are presented as means ± standard deviation (n= 3-5). (* = $p < 0.05$ between groups of different concentrations, # = $p < 0.05$ to d0 and Δ = $p < 0.05$ between d14 and d28 of equal concentrations).

## 4.1.4    Discussion

Articular cartilage damage is a major problem in the population and even small defects can degenerate into osteoarthritis if left untreated. For decades, new treatment approaches were solely tested in animal experiments. With the development of better cell and tissue culture facilities and the fabrication of *in vitro* cartilage defect models, the spectrum of scientific methods has been greatly expanded.

### *In vitro* cartilage models

As *in vivo* models better mimic the natural surroundings of the knee joint, they are well suited for observing the overall effects of a treatment. However, the non-defined environment with cellular and molecular influences from the surrounding tissue also has its drawbacks. Investigating basic influences of single factors on cartilage regeneration or integration necessitates more defined settings. Regarding the evaluation of cartilage integration typical *in vivo* models commonly rely on the rating with histological scores based on maintained cellularity and tissue continuity at the defect interface [153,157]. Alternatively, experiments have been conducted with subcutaneous implantation of cartilage explants into mice [159,200,262]. For those cases the implantation site does not correspond to the environment of the synovial joint and the presence of highly proliferative cells such as fibroblasts could harness integration strength increases without building up functional hyaline cartilage tissue. In general, the use of animal models can have further negative aspects like ethical difficulties, the need for personnel experienced in animal handling and financial expenses. *in vitro* approaches never quite match the actual environmental conditions in the joint, but their use also offers great advantages. Additionally to structural evaluation of tissue responses, these models facilitate the implementation of biomechanical tests to quantify cartilage integration strength [160,162,164,168,263]. Although biomechanical analysis of integrative repair has also been performed on samples retrieved from *in vivo* defects in the knee joint [203], the high practical effort makes this approach unsuitable for most studies on integrative cartilage repair. The variation of animals, particularly the different mechanical exposures makes it additionally hard to compare the findings of concerning studies.

Construct harvesting for histology and other evaluation methods is far plainer from *in vitro* cultivation and the possibility to isolate required tissue material from the abattoir makes it ethically less questionable. Inclusion of cell culture techniques and cartilage *in vitro* models vastly contribute to a better understanding of cartilage integration processes and thus also overall cartilage repair. Defined *in vitro* studies help to understand influences of single factors in the context of cartilage integration. Over the years, different test models have been developed and a large number of studies have been conducted that have expanded the basic understanding of cartilage integration and alternative

treatment options. While considering how best to objectify or measure the adhesion strength of a cartilage adhesive as a main goal for further experiments, various experimental setups were considered. An *in vitro* push-out model was chosen. On the one hand, other research groups have successfully demonstrated this concept, e.g. Obradovic et al. [162] or also Hunter et al. [264]. On the other hand, the measuring plunger hitting the specimen perpendicularly corresponds most closely to the force exerted on the joint surface by the body weight and by the typical motion sequence [212]. These disc/ring constructs were used in experiments with *in vitro* culture for several weeks under variable conditions and the model also allowed histological analysis of the lateral defect interface both in the sagittal (cross-section) and the transverse plane (*en face*). The feasibility to obtain an interface between the disc and ring that is perpendicular to both the top and bottom surfaces of the composites has been approved, which assures the collinearity of the interface axis with the mechanical testing device's plunger and eliminates potential artifacts [214,254]. Non-collinearity could yield an overestimated stress measurement resulting from the disk being pushed at an angle along the surface of the ring. In order to prevent misalignments in the fabrication of the disc/ring model and the mechanical testing, custom-made tools were utilized, facilitating a more accurate and reproducible evaluation.

**Tissue viability**

For reproducible and meaningful results, however, there are fundamental requirements for *in vitro* models in general. In the long term, integrative cartilage repair is dependent on the formation of hyaline cartilage matrix. The introduction of foreign cell types, e.g. by microfracturing, can lead to the development of fibrocartilage, which differs from hyaline cartilage in structural composition and mechanical resistance. Native cartilage tissue is avascular and has comparatively low proliferation and regeneration capacities. For this reason, maintaining the cell vitality of the tissue is of particular importance. In healthy cartilage tissue, chondrocytes ensure a constant turnover of the extracellular matrix and through their ability to regenerate cartilage-specific ECM components, they can also contribute to defect closure. For studies on immediate cartilage integration strategies, e.g. by means of adhesives, the vitality of chondrocytes is rather unimportant. For the investigation of cartilage integration over time, however, a high vitality of the tissue is required in order to be able to consider the effects of ECM formation and cell metabolism in the evaluation.

The starting material for both the generation of the *in vitro* test models and the isolation of chondrocytes for the experiments performed was porcine cartilage from a local slaughterhouse. During the isolation of articular cartilage from the knee, careful attention was paid to ensure that the joint capsule was not previously damaged, leading to contamination, desiccation, and ultimately devitalization of the cartilage tissue.

MTT and Live/dead staining were used to verify whether the isolation procedure used results in vital cartilage tissue samples and whether *in vitro* culture conditions used maintained cell viability. The tetrazolium salt MTT forms a yellow solution that is reduced to purple formazan in living cells. Cell viability staining with MTT is also suggested by ISO 10993-5:2009 for the assessment of cytotoxicity in medical devices. More recently, similar to the method applied here, MTT staining on a 3D tissue construct (reconstructed human epidermis models) was validated for irritation assessment of medical devices and included in the ISO 10993-23:2021 standard. The Live/dead staining is a assay for determining the viability of a cell population based on plasma membrane integrity and esterase activity. In contrast to the MTT staining, its evaluation is via fluorescence-based microscopy. The analysis of the wound edge revealed a clear band of cell death up to a depth of about 100 μm from the wound edge with isolated dead cells down to a depth of 200 μm. The necrotic area also roughly corresponds to the band in which damage to collagen fibrils could be observed via CTX-II staining. (see Figure 11C). The CTX-II neoepitope is generated after MMP cleavage (MMP1, 3, 7, 9, 13) in the C-telopeptide domain of type II collagen fibrils, gives information about cartilage damage and is also used as a marker for the progress in OA as CTX-II levels are increased in the serum of patients [22,23].

This is consistent with results for experimental wounding of cartilage in the literature [155,165,214,265]. It was shown that the extent of the necrotic zone also depends on mechanical influences. Wounds made with a sharp scalpel showed restricted cell death compared to blunt wounds made with a trephine [14]. The problem of necrotic cells also exists in the treatment of large defects by cartilage grafting and is comparable to the fabrication of the disc/ring model. Clinically, surgical preparation for cartilage graft placement involves the removal of damaged cartilage that directly surrounds a lesion to ensure that the graft is well shouldered by healthy tissue [8]. The zone of cell death in isolated osteochondral grafts has also been investigated comparing an isolation via a biopsy punch or via the osteochondral autograft transfer system (OATS). In this study, the biopsy punch harvesting resulted in a zonal death zone with a depth of 26 μm compared to 173 μm with the OATS harvesting system [158]. However, when comparing the results of different studies and transferring them to the clinical treatment of cartilage defects, various factors must be taken into account. Human articular cartilage explants from healthy donors showed considerably less chondrocyte death in lesion edges than was observed in bovine explants. Therefore, in human articular cartilage, the reduced amount of cell death in reaction to wounding may require less adjustment for integrative repair. However, since chondrocyte density in adult human cartilage is low compared with the cell density in most animal models, increased densities of viable chondrocytes may improve integration in human cartilage as well [165].

The extend of cell death present in the clinical observation after trauma depends on the magnitude and nature of load. Cell death after impaction on cartilage occurred around impact induced cracks, but not in impacted areas without cracks [266]. It is generally acknowledged that a decrease in living chondrocytes is a major driving agent in the progress of osteoarthritis and stabilization of the damaged area may prevent late sequelae that lead to OA. The *in vitro* cartilage disc/ring model therefore well reflects the clinical situation of injured cartilage with the presence of cell death related to tissue lesions and is a suitable model to investigate treatment approaches to improve regeneration. The design of the disc/ring model also allows conclusions to be drawn about the integration development of the damaged tissue via the possibility of microscopic and mechanical examination of the wound interface. For example, by using this model it was shown that the number of viable cells and improved cartilage-cartilage integration can be achieved by a brief activation of a catabolic cascade via cytokines or the treatment with cell death inhibitors [161,179].

**Culture conditions**

Not only do harvesting or fabrication techniques of *in vitro* cartilage models influence cell viability and ECM synthesis capacity, but also the conditions under which the constructs are cultivated. A directly controllable factor in culture conditions is the composition of the medium. As a gold standard, bovine serum is added to the medium for the culture of cartilage explants and chondrocytes. In experiments with cartilage explants it was shown before that incubation in medium containing fetal bovine serum stimulates the chondrocytes to increase synthesis and decrease degradation of matrix proteoglycan. Reindel et al. additionally reported the filling of the defect gap in their used single-lap model with an acellular matrix. After 3-6 weeks *in vitro* culture cells began to populate the newly formed matrix. This effect was dependent on the medium being supplemented with serum. Lower proteoglycan content and decreased integration strength was obtained when the explants were cultivated in serum-free basal medium with or without 0.1 % bovine serum albumin. A combination of basic fibroblast growth factor and transforming growth factor supplemented to the basal medium, stimulated regeneration processes as a substitute for serum [160].

Growth factors that are present as a mixture in serum for medium supplementation, play a crucial role in cartilage homeostasis and regeneration. For example, insulin-like growth factor-1 is the component within serum that is predominantly responsible for stimulating chondrocytes to synthesize proteoglycan [267,268]. However, the pathogenesis of cartilage loss in joint degenerative diseases is also influenced in various ways by growth factors. Many of the signaling pathways identified in endochondral ossification are also believed to be important in OA progression through regulation of chondrocyte hypertrophy. Abnormal subchondral bone turnover and cartilage calcification affects the integrity of the articular cartilage structure. In particular, hypertrophic differentiation of chondrocytes,

leading to cartilage calcification, is a key event of the deep layer of the cartilage in early joint deterioration [269]. Articular chondrocytes found in the articular joint surface represent a stable and permanent phenotype which maintains joint function throughout life and produces all ECM components of articular cartilage necessary to provide the tissues functional properties. The transient chondrocytes found in the growth plates display a very dynamic phenotype, undergo proliferation, maturation, hypertrophy and apoptosis followed by the replacement by bone cells during endochondral ossification. Aggrecan expression increases as chondrocytes differentiate and become hypertrophic. When terminally differentiated chondrocytes become hypertrophic, their expression of articular cartilage-specific collagens decreases and the production of collagen X begins, a process that is accompanied by massive ECM remodeling [270].

In a conducted experiment within this work, the cultivation with medium containing 10 % FCS or with a defined serum-free ITS containing medium were compared with isolated full-thickness cartilage discs (see Figure 12). ITS is a defined mixture of insulin, transferrin and selenium that is used frequently as media supplement to reduce or omit serum to better control culture conditions und decrease possible variability e.g. via unknown serum component concentrations and serum batch differences. After a three-week cultivation period, macroscopic differences between serum and ITS cultured explants were clearly visible. The harvested explants were stained with MTT to demonstrate viability of the tissue. A distinct increase in overall explant thickness was observed in the serum cultivated group which was not or only strongly reduced visible in the ITS group. In contrast to the FCS group, no size increase was seen in ITS explants. Strikingly, the increase in tissue size was not uniform in the FCS group. Especially in deeper zones, an outgrowth both in the subchondral and lateral orientation could be seen. In these areas, the dark MTT staining is particularly pronounced, indicating increased metabolic activity or number of cells. Microscopic images show increased cell clusters with large lumens in the deeper cartilage zones, indicating progressive hypertrophy. In addition, in outgrowth areas the hypertrophy marker collagen type X is detectable via immunological staining.

Growth plate chondrocyte proliferation and hypertrophy in endochondral ossification are regulated by pathways of the bone morphogenic protein (BMP) signaling, fibroblast growth factor (FGF) signaling and systemic factors like thyroid hormone together with a negative feedback loop like IHH/PTHrP. BMP2 is suggested to be a strong mediator of chondrocyte hypertrophy, which is characterized by increased collagen type X and alkaline phosphatase (ALP) expression. In addition, the effect of tri-iodothyronine (T3) on terminal differentiation of chondrocytes was confirmed. Furthermore, ascorbic acid combined with β-glycerophosphate show a potency to induce chondrocyte hypertrophy. Nevertheless, the detailed mechanisms of signaling pathways or factors modulating chondrocyte hypertrophy in the pathogenesis of OA are still not completely elucidated [271].

Serum-free medium formulations containing ITS are frequently used for the maturation of chondrocytes or mesenchymal stem cells in tissue engineering approaches. However, in most cases growth factors (e.g. TGF-β) are additionally supplemented [272]. In experiments with isolated human chondrocytes, it was shown that in in serum-free ITS containing medium without addition of further growth factors the cells were unable to grow. With a stepwise addition of FCS, chondrocytes proliferated increasingly in response to the concentration of FCS [273]. In most of the studies performed in the literature, the cell culture of cartilage explants was done with serum. As previously discussed, this also demonstrated increased ECM synthesis, which provides a better basis for well-developed cartilage integration. For these reasons, in the course of further experiments in this work, *in vitro* culture was performed with the addition of serum to the media. Despite the variable influence of serum on the outcome, this approach allows a better comparison of the results with literature values. To prevent falsification of measurement results, especially in biomechanical testing, constructs with hypertrophic outgrowths had to be avoided during the course of the tests. New tissue formation is generally desired for cartilage integration [160], a hypertrophic character with restriction to deep zones of the constructs, however, would not correspond to the desired goal for the clinical treatment of defects. In the fabrication of the cartilage constructs, specially fabricated devices were used to trim both the superficial zone and the calcified deep zone of isolated cartilage cylinders. It was previously described that by changing the geometry of the disc/ring constructs, overestimated integration strengths can be measured in the push-out test [214]. To counteract this, during construct fabrication sharp razor blades were used to make parallel cuts and obtain constructs of middle layers and without curved surfaces. A standardized defect was placed at right angles to the trimmed surfaces of the cartilage cylinders with a custom-made holder and sharp biopsy punches. Accordingly, a falsified experimental read-out due to hypertrophic outgrowths was best avoided by cutting off deep zones. Disc/ring constructs in which a discernible shape change occurred during *in vitro* culture were also excluded from further investigations. For the biomechanical push-out test, custom-made fixtures were also used, which allowed a precisely aligned orientation of the punch and avoided tilting of the test specimens.

The integrative repair processes triggered in the presence of serum in the medium can partly be attributed to an increased proteoglycan synthesis of chondrocytes. Insulin-like growth factor-1 is the component within serum that is predominantly responsible for stimulating chondrocytes to synthesize proteoglycan [160]. The exact interplay of proteoglycan synthesis, structural and enzymatic factors, and influences of other ECM components needs further investigation. In the basic structure of native cartilage, proteoglycans provide the viscoelasticity of the tissue through their water-binding properties. A framework of collagen fibers, in hyaline cartilage mainly type II collagen, provides the

mechanical stability of the tissue. It is therefore logical that a collagen scaffold spanning the defect is required for successful defect healing and stable long-term integration. In experiments with chemical crosslinkers, it has already been shown *in vitro* that re-linking of collagen fibers at the cartilage defect interface leads to an increase in integration strength [197,217]. Without the use of chemical crosslinkers or adhesives, natural regeneration requires synthesis of new collagen fibers that can fill the gap. 80-95 % of the collagen fibers in hyaline articular cartilage consist of type II collagen. The remaining proportion is formed from type I, VI, IX, X, and XI collagen [274]. The anatomical arrangement of collagen fibers in a triple-helix structure is responsible for its mechanical function.

Collagen type II in its final form consists of three molecular chains of equal size, which are arranged helically and form a triple helix. The synthesis and formation of collagen fibrils happens in a cascade of both intracellular and extracellular processes. Intracellularly formed polypeptide chains contain specific sequences of the amino acids proline and lysine which are subsequently converted by the enzymes prolyl and lysyl hydroxylase to form the procollagen molecule. The hydroxylation step requires as co-factor the presence of ascorbic acid (vitamin C). Following, twisting of the procollagen into a triple helix is allowed and is transported to the extracellular matrix by exocytosis. Subsequently procollagen is converted into collagen by endopeptidases. The now insoluble molecules are further covalently crosslinked via their hydroxylysine residues, which permanently fix the resulting collagen fibrils in the course of fibrillogenesis. The final step is the formation of fibers, in which several fibrils combine with the aid of intermediary matrix-specific enzymes to form collagen fibers [276].

The stability of collagen depends on the above-mentioned post-translational modifications. One of the most important steps in this process is the hydroxylation of collagen by the enzyme collagen prolyl 4-hydroxylase (CP4H). In this step, ascorbic acid is responsible for the reactivation of CP4H by the reduction of iron in the reactive center of the enzyme from $Fe(III)$ to $Fe(II)$ [276–278]. In experiments conducted in the course of a doctorate within our group, the disc/ring model and biomechanical testing were utilized to investigate the influence of ascorbic acid on integrational strength [196]. Additionally, ethyl 3,4-dihydroxybenzoate (EDHB) as inhibitor on mechanical crosslinking and the production of collagen and glycosaminoglycans was utilized. EDHB is an inhibitor of CP4H, which was used in cell culture experiments before [279]. Omission of ascorbic acid or alternatively addition of EDHB to the culture medium resulted in decrease in integration strength and deposition of ECM in the defect gap. It was also reported in literature that ascorbic acid at concentrations around 100 µM can protect chondrocytes from oxidative stress in cell cultures and also inhibits the production of fibrocartilage, which is not as resistant in the joint as hyaline cartilage. In contrast, at high concentrations above 150 µg/ml ascorbic acid, the induction of apoptosis of chondrocytes is also reported in the literature [280,281].

To further investigate the influence of ascorbic acid on ECM synthesis, *in vitro* culture experiments using a chondrocyte pellet model were used here. Pellet cultures with high cellular density are the gold standard to keep chondrocytes in a differentiated stage and are well suited to investigate medium supplements and their impact on ECM synthesis rates [282]. For the pellets, just as for the disc/ring cartilage model, porcine knee joints from the slaughterhouse were used for isolation. The isolated chondrocytes were taken into *in vitro* culture for five days. In this way, cells that were necrotic or apoptotic due to the isolation procedure could be removed via plastic adherence. Additionally, due to culture-expansion the number of viable cells available for the creation of a tissue engineered graft increases. A problem of 2D plate culture of chondrocytes is the increasing dedifferentiation of the chondrocytes. Consequently, chondrocytes form a fibroblast-like character and gradually lose the ability to synthesize articular cartilage-specific ECM molecules. However, this effect is contributed to serial passaging of chondrocytes [283]. By limiting the culture period to a short period of several days, potential dedifferentiation of chondrocytes is estimated to be at a minimum. Furthermore, chondrocytes were found to have the intrinsic ability to redifferentiate when transferred to a 3D culture system [284,285].

In the literature different forms of ascorbate such as l-ascorbate, sodium l-ascorbate, and l-ascorbate-2-phosphate are frequently reported for the cultivation of chondrocytes whereby different concentrations ranging from 30 µM up to 600 µM are used. The different ascorbate forms are all potent antioxidants. L-ascorbate is acidic in aqueous solutions such as culture medium. l-ascorbate-2-phosphate is not only non-acidic, but also characterized by a longer half-life in aqueous solutions compared to the other derivatives. It is internalized, dephosphorylated, and highly concentrated in the aqueous phase of the cells [286]. Due to the aforementioned advantages, the use of l-ascorbate-2-phosphate in the culture of chondrocytes and MSCs for tissue engineering approaches is frequently found in the literature. L-ascorbate-2-phosphate has become established for cell culture at an applied concentration of 50 µg/ml. As the molecular weight of l-ascorbate-2-phosphate is 256.1 g/mol this corresponds to a concentration of 195 µM and lies in between the range of concentration reported to suppress oxidative stress and induce apoptosis, as mentioned before. By using the chondrocyte pellet model, the goal was to evaluate and compare the effect of different ascorbate concentrations on *in vitro* cartilage formation of porcine chondrocytes that were isolated from the same tissue source as for the production of the disc/ring composites in other experiments.

In the evaluation of the pellet experiment (see Chapter 4.1.3), it was found that without the addition of ascorbate, a small amount of GAG and collagen was present in the pellet after d14 and d28, but no increase in size of the pellet and no increase in cell number per pellet was measured. Since, apart from ascorbate, nothing was removed from the ordinary culture medium, it is confirmed that

ascorbate is essential for cartilage neosynthesis. It is conceivable that the limited possibility of ECM synthesis at ascorbate deficiency also prevents proliferation. Collagens are known to modulate cell behavior and function singularly or through interactions with integrins and growth factor-mediated mitogenic pathways. ECM collagens are known to both maintain cellular morphology and act as conduits between extracellular stimuli and cells by regulating proliferation, migration, differentiation, and survival [287]. Therefore, by the inhibition of collagen formation via ascorbate deprivation, not only the overall mass increase but also cell proliferation in the pellet is hindered. In articular cartilage, aggrecan is entrapped in the randomly aligned 3D collagen network. The GAG compartment of aggrecans strongly adhere to collagen fibrils via attractive mechanisms including van der Waals contacts, hydrophobicity, hydrogen bonding, physical entanglements, and electrostatic attraction between GAGs and the positively charged amino acids on collagen [288]. Therefore, it can be assumed that even if GAG synthesis itself is not compromised, no physical deposition will occur if there is no intact collagen scaffold in the defect. Without interaction to an anchor point, it is likely that free GAG will diffuse in the medium supernatant and no pellet growth is achievable. Transferred to the clinical situation of cartilage defect healing, this means that the deposition of a defect-bridging collagen scaffold or a capable biomaterial is needed to bind synthesized GAG at the interface that will contribute to a closure of the defect.

In clear contrast, it was found that when 50 µg/ml or 100 µg/ml ascorbate was added, there was a significant increase in pellet size and its cell number as compared to the initial values. After d28 of *in vitro* culture, a significantly higher collagen content was found for the 100 µg/ml group compared to 50 µg/ml. However, at d14, the highest collagen content was in the 50 µg/ml group. Normalized to the DNA content of the respective pellets, there were no significant differences in collagen content between the two applied ascorbate concentrations. However, at d28, normalized to the DNA content, a significantly higher GAG value was detected for the 50 µg/ml group. Histological examination of the pellets showed that tissue growth was based on the ECM components GAG and collagen type II, which are specific for hyaline cartilage. This also confirms that the culture conditions used were able to preserve the differentiated character of the chondrocytes. Based on the results of the pellet experiment in combination with previous experience in other experiments within the research group, a concentration of 50 µg/ml ascorbate was also used for the culture of native cartilage explants to ensure sufficient ECM synthesis and concomitant defect integration. Even though in the further course of this work a standard ascorbate concentration was used for the cultivation of chondrocytes and cartilage cultivation, there is in principle the possibility to easily adapt culture conditions in *in vitro* experimental models. Thus, potentially different clinical conditions in different patient populations or different symptoms can be simulated via the medium composition in order to investigate specific

influences on cartilage regeneration. For example, in the pellet model, the addition of cytokines to the medium can be used to investigate cartilage neosynthesis and therapeutic options in the inflammatory milieu [289]. In the future, it will be interesting to see which therapeutic approaches for cartilage integration work under certain environmental conditions or where performance differences can be expected. Findings from different culture conditions can be quickly transferred to other *in vitro* models such as the disc/ring model. As representative examples, the further consideration of inflammatory influences and the simulation of weight bearing can expand the versatility of *in vitro* models.

## 4.2 Lateral Cartilage Integration Facilitated by Fibrin Adhesives

In medical wound treatment the gold standard for wound closure is up to date still suturing. However, tissue adhesives are emerging in this field as they have some intrinsic benefits over sutures, for example by introducing a gap filling and thus tightening matrix at the defect interface. A frequently used natural derived tissue adhesive is fibrin glue. In this chapter the potential of fibrin glue for the enhancement of cartilage tissue integration will be evaluated on basis of *in vitro* models.

### 4.2.1 Application of Commercial Tissue Adhesives at Cartilage Disc/Ring Test Model

In the course of the experiments a porcine disc/ring cartilage model was used. Starting experiments were run with two different commercially available tissue glues. TissuCol (Baxter, Unterschleißheim, Germany) is a marketed fibrin glue and was compared against BioGlue® (CryoLife, Kennesaw, USA), an adhesive based on glutaraldehyde-crosslinked bovine serum albumin (BSA). Fibrin glue is a two-component material consisting of fibrinogen and thrombin. In the presence of calcium and factor XIII, thrombin converts fibrinogen (fibrin monomer) into insoluble fibrin, which has a stable form [226] (see also Chapter 1.1.5.1). BioGlue® is composed of 45 % BSA and 10 % glutaraldehyde. Glutaraldehyde exposure causes lysine molecules of bovine serum albumin, extracellular matrix proteins, and cell surfaces to bind to each other creating a strong scaffold [290]. The basic reaction principle of both adhesives and the application to the *in vitro* model is also illustrated in Figure 14.
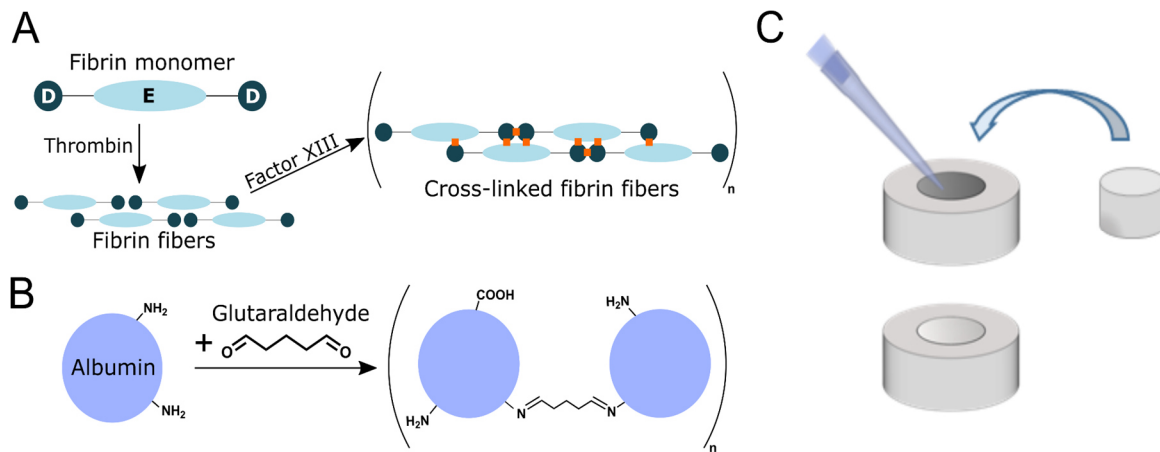
**Figure 14: Application of adhesives to the disc/ring model.**

Overview of the reaction mechanism of A) fibrin glue (see also Chapter 1.1.5.1) and B) BioGlue®. C) The premixed glue components are pipetted to the lumen of a cartilage disc before the cartilage disc/ring model is subsequently reassembled and the glued composite is investigated in further evaluations.

After application of the glue the to the disc/ring composites and curing, in both groups the disc was firmly attached to the ring. In untreated control constructs the plugged-in disc is loose and easily detached from the cartilage ring. The fibrin glue formed a translucent matrix at the defect interface, whereas BioGlue® immediately forms a yellowish glue matrix after mixing the two clear components together (see also Figure 15A upper row). A biomechanical push-out test was conducted with the glued constructs and referenced to non-glued controls (see Figure 15B). The measured strengths confirmed the loose character of the control samples where bonding strengths of 3.57 ± 1.78 kPa were obtained. Constructs treated with TissuCol achieved an immediate bonding strength of 13.54 ± 3.87 kPa. For BioGlue® samples the immediate bonding strength was 122.79 ± 43.91 kPa, which was significantly higher compared to the control and TissuCol groups.

Additionally, samples were stained for cell viability in the cartilage tissue after one day of *in vitro* culture (see also Figure 15A lower row). The untreated control group and samples treated with the fibrin glue showed a strong dark coloration, which indicates a high cell viability of the constructs. In clear contrast is the macroscopical impression of the BioGlue® treated constructs. The BioGlue® group samples remained bright after the MTT staining procedure similar to thermally devitalized cartilage constructs (freeze/thaw control). The cell viability was further evaluated colorimetrically by solubilization of the accumulated MTT stain in the tissue and measuring of the light absorbance at 570 nm. In the underlying analysis, the MTT formation was significantly higher in the TissuCol and control samples in comparison to the BioGlue® and freeze/thaw group (see Figure 15C).
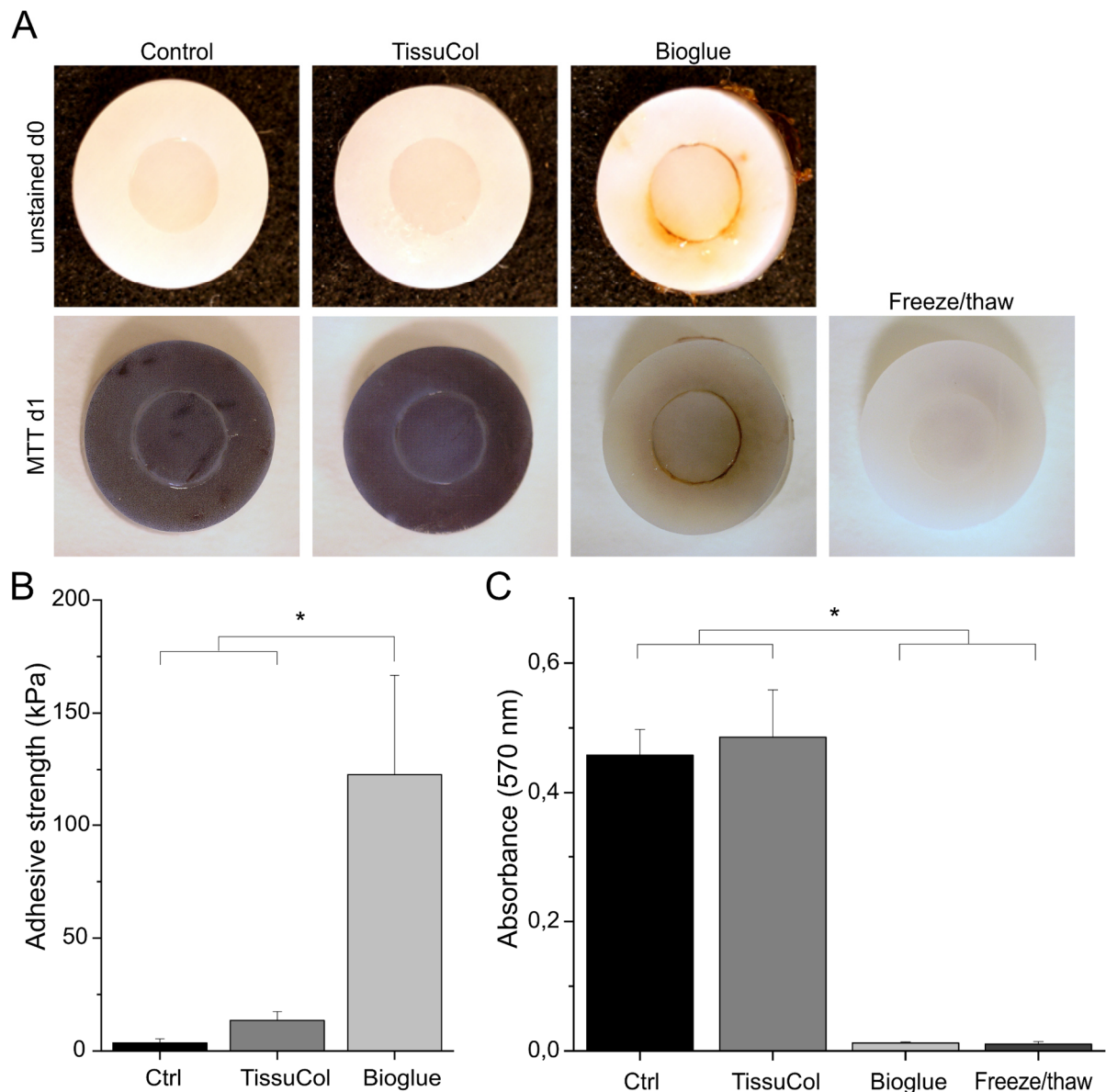
**Figure 15: Evaluation of TissuCol and BioGlue® *in vitro*.**

A) Macroscopical captures of assembled cartilage disc/ring constructs after application of glue or without glue treatment (control). Constructs were stained for cell viability (MTT) after one day *in vitro* culture. B) Immediate bonding strength values measured in a biomechanical push-out test. C) Colorimetrical evaluation of construct viability (MTT absorbance) after one day *in vitro* culture and MTT solubilization. Data are presented as means ± standard deviation (adhesive strength: n= 10-19; MTT absorbance n= 3-4). (* = p < 0.05 between groups).

## 4.2.2    Application of Long-Term Stable Fibrin at Cartilage Disc/Ring Model

To further assess the integrational capabilities of fibrin, additional experiments were conducted with the introduction of long-term stable fibrin gels as adhesives. In comparison to TissuCol the two

used long-term stable fibrin gels used are not commercially marketed but were established by our group. The crosslinking chemistry remains identical to TissuCol, however adaptions in the content of mainly calcium led to increased form stability *in vitro* when cultivated with cells [84,117,118,122]. The aim was to investigate the influence of long-term stability of fibrin both on immediate bonding and the course of cartilage integration *in vitro*. In addition, the influence of total fibrinogen content in the final adhesive hydrogel (25 vs. 50 mg/ml, stable fibrin (25) and stable fibrin (50)) was to be tested. The application and curing procedure of all tested fibrin formulations was identical. With the help of the biomechanical push-out test, the immediate bonding strength but also the integration strength after 7 and 21 days *in vitro* culture of the whole constructs was measured (see Figure 16A).

On day 0 (directly after glue curing) both long-term stable fibrin gels achieved slightly lower bonding strengths compared to TissuCol but still outperformed the untreated control group. The
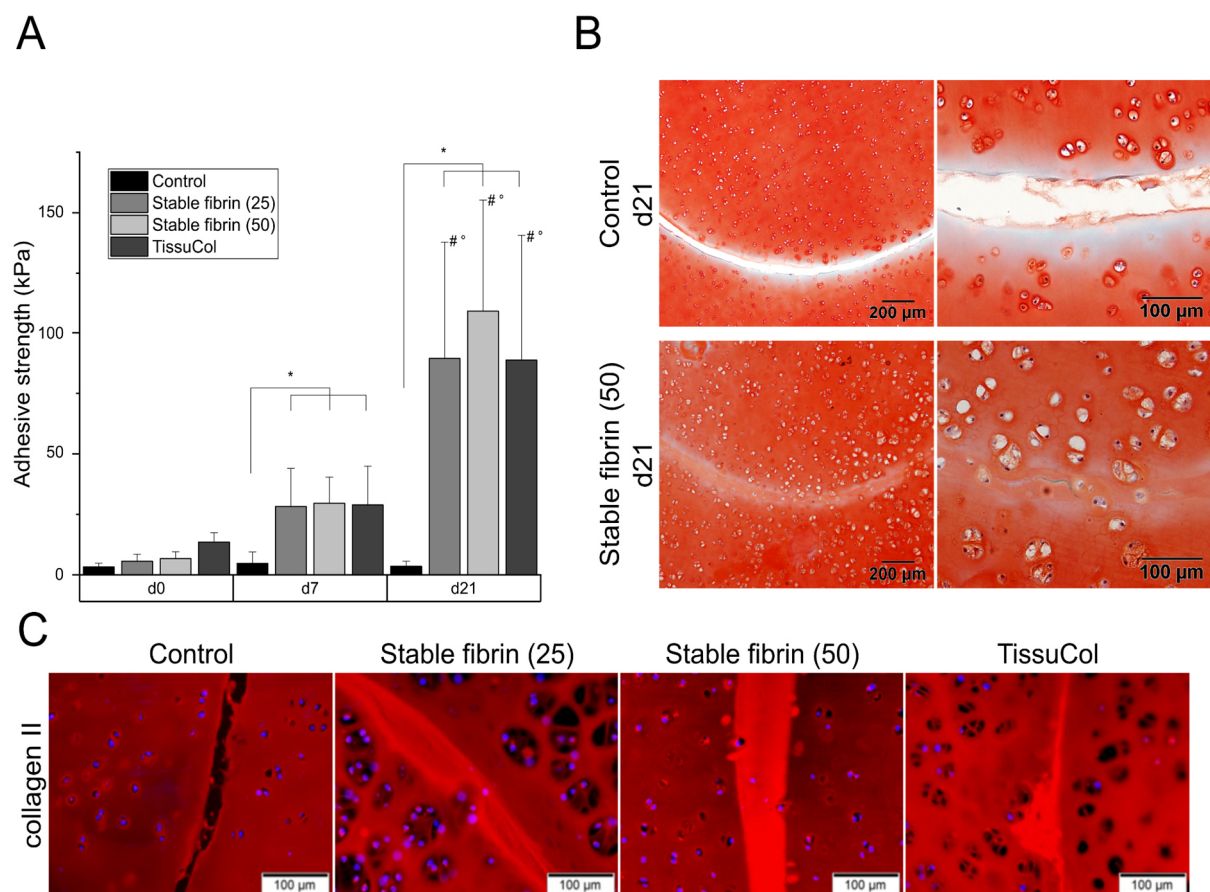


**Figure 16: Assessment of bonding strength and long-term cartilage integration in TissuCol and two long-term stable fibrin gels.**

A) diagram of the achieved push-out strengths. B) captures of SafO stainings for stable fibrin (50) and control samples at d21 in different magnifications. C) captures of immunofluorescence staining for collagen type II after d21 *in vitro* culture. Data are presented as means ± standard deviation (n= 7-16). (* = p < 0.05 between groups of different concentrations, # = p < 0.05 to d0 and ° = p < 0.05 between d7 and d21 of equal groups).

immediate bonding strength for the stable fibrin (25) was 5.66 ± 2.91 kPa and for stable fibrin (50) 6.74 ± 2.82 kPa. After seven days *in vitro* culture a second push-out test was performed with separate fabricated constructs. Remarkably, only in the three fibrin treated groups a clear increase in integration strength could be observed. The integration strength of the fibrin groups similarly rose to a level of slightly below 30 kPa (TissuCol at 28.84 ± 16.05 kPa; stable fibrin (25) at 28.27 ± 15.79 kPa; stable fibrin (50) at 29.57 ± 10.80 kPa). The control had a mean integration strength of 4.71 ± 4.74 kPa. This effect was even more pronounced after 21 days *in vitro* culture. Control samples remained with a low integration strength of 3.50 ± 2.18 kPa, whereas all three fibrin groups achieved significantly higher integration strength compared to the control and d7 values of the same group. No significant differences were obtained between the three different fibrin types. The highest strengths values had the stable fibrin (50) group with 108.95 ± 46.25 kPa. Stable fibrin (25) had a mean of 89.43 ± 48.44 kPa and TissuCol a mean of 88.70 ± 51.97 kPa.

The biomechanical results were well reflected by histology where it could be demonstrated that in all fibrin groups compared to the control a better filling of the interfacial defect gap with extracellular matrix was achieved (representative images for stable fibrin (50) and the control on d21 in Figure 16B). The Safranin O staining revealed that the matrix filling the defect gap in fibrin treated constructs is specific for articular cartilage and is rich in GAG. Other than in fibrin treated samples, in the control group less ECM deposition at the defect interface was observed that was also less frequently spanning over the complete defect interface. The remaining fibrin stains blueish to greenish in the SafO staining and partly small fibrin strings that run more or less parallel to the defect surface are visible. This leads to the assumption that fibrin serves as an anchor point for the interfacial deposition of newly synthesized ECM rather than just being filled with it. Along with an ECM-filled defect gap in fibrin treated constructs, there were also areas where cell migration into the defect zone was visible. These findings were also confirmed by immunofluorescence imaging (see Figure 16C). In all three fibrin glue groups an increased filling of the defect gap with articular cartilage specific collagen type II was observed. This again was accompanied by observations of cells that are in the process or already migrated into the filled defect gap.

## 4.2.3    Course of Integration Strength and Interfacial ECM Deposition

In a separate experiment the goal was to visualize the kinetics of interfacial ECM formation and cell migration in cartilage disc/ring constructs. For this, stable fibrin (50)-treated constructs were harvested immediately after gluing or after cultivation *in vitro* for 3, 7, 10, 14 and 21 days.
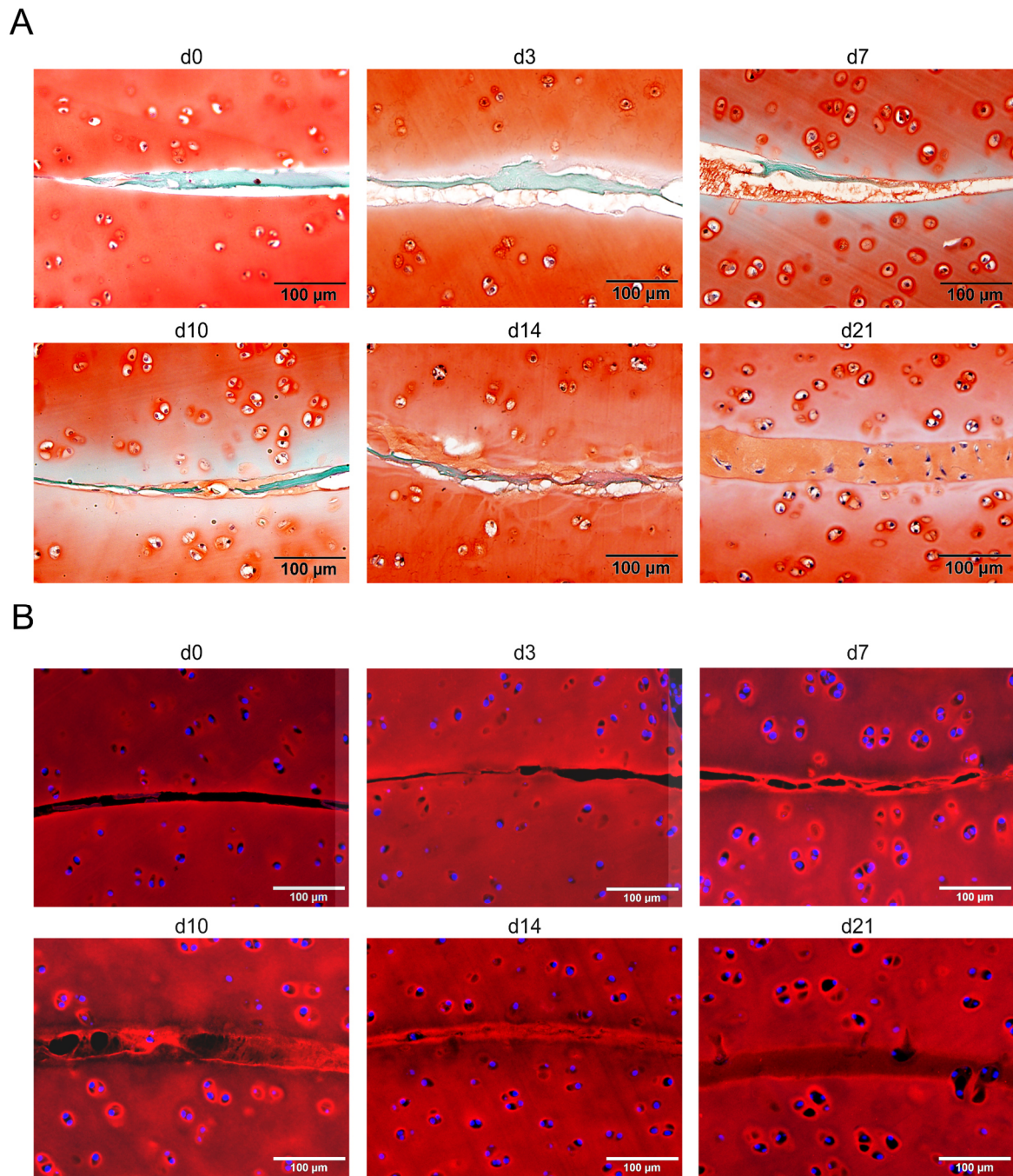
A



B



**Figure 17: Histological staining for GAG and immunofluorescence staining for collagen type II on stable fibrin (50)-treated cartilage disc/ring constructs.**

Samples were evaluated for GAG (A) and for collagen type II (B) immediately after glue treatment (d0) and after day 3, 7, 10, 14 and 21 of *in vitro* culture.

Histological analysis was conducted by means of Safranin O staining for glycosaminoglycans (see Figure 17A), immunofluorescence staining for collagen type II (see Figure 17B) and aggrecan (see Figure 18A). To investigate the formation of hyaline cartilage unspecific collagens, immunofluorescent staining for collagen type I was conducted (see Figure 18B). Representative images were chosen for illustration in the graphs.

In fibrin-treated composites, ECM deposition at the defect site was already obvious at day three and increased further over time. Interestingly, cell invasion was not detected before day ten to day 14 of *in vitro* culture. After three weeks cell invasion was even more distinct in many areas.

In the SafO images the fibrin glue stains bluish to greenish and it is visible that the fibrin glue is not totally attached to both opposing defect interfaces. The images also indicate that ECM synthesized from the cartilage tissue and secreted into the gap bind to the fibrin and, in the course of cultivation, increasingly enclose the fibrin glue. In parallel, the amount of remaining fibrin glue in the gap decreases over time. After 21 days *in vitro* culture, the defect gap is almost completely filled with articular cartilage specific ECM as confirmed by stainings for collagen type II and aggrecan. In addition, no positive staining for the chondrocyte dedifferentiation marker collagen type II was observed over the whole course of cultivation. In the DAPI signal of cell nuclei it was further recognizable that migrating cells originate from the surrounding bulk cartilage tissue and in this process initially form buds at the tissue/gap interface (for example see d21 in Figure 17B and Figure 18B). The increasing interfacial cell count from d14 to d21 indicates the capability of proliferation of these chondrocytes.
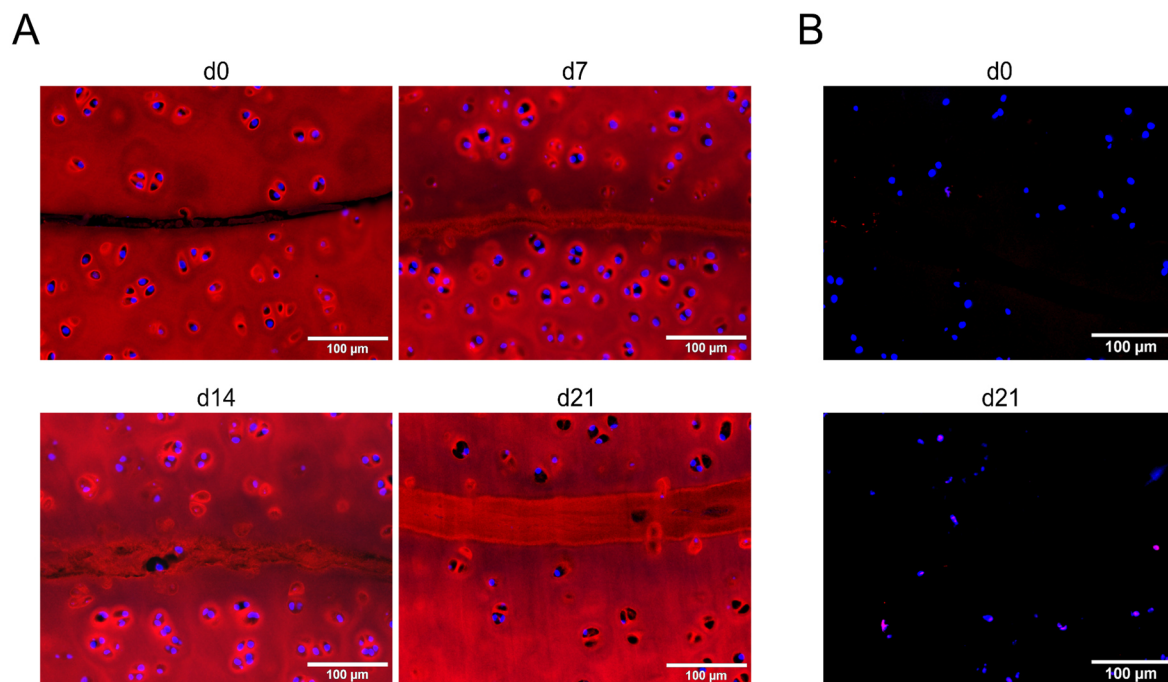


**Figure 18: Immunofluorescence staining for aggrecan (ACAN) and collagen type I on stable fibrin (50)-treated cartilage disc/ring constructs.**

A) Samples were evaluated for ACAN immediately after glue treatment (d0) and after day 7, 14 and 21 of *in vitro* culture. B) Immunofluorescence staining for collagen type I after d0 and d21.

## 4.2.4     Discussion

In traumatic cartilage defects such as lesions, damage occurs in the mechanically supporting scaffold of extracellular molecules. Stable regeneration requires a re-linking of these extracellular components, since progressive mechanical influences can mean an increasing deterioration of the defect up to arthrosis [12]. These processes can be initiated by age-related wear or by trauma to the cartilage. It is reported that even with current treatments more than 40 % of people who suffered traumatic knee joint injuries will develop OA [13]. Vital cartilage tissue is in a constant state of remodeling, and chondrocytes are able to build up new crosslinks by synthesizing and modulating macromolecules. However, this turnover occurs slowly and traumatic events can further reduce the cell density around defects and thus the intrinsic regenerative capacity of cartilage [14].

It appears obvious that the production of ECM is vital for integrative cartilage repair and it was shown that chemical inhibition of ECM synthesis or modulation inhibits the cartilage-to-cartilage integration. For example, collagen fibril formation is dependent on ascorbate and enzymatic actions. If the complex interplay in collagen formation is disturbed, cartilage integration is also strongly affected [170,190] (see also results from [196] in Chapter 4.2.4.3). These results indicate that not only the synthesis of cartilage specific ECM but also the formation of collagen crosslinks in cartilage explants is critical in integrative cartilage repair.

### 4.2.4.1     Push-Out Testing

In the underlying work, assessment of integration strength was done biomechanically by implementation of a push-out test with the cartilage disc/ring model. Another frequent applied model for biomechanical testing of adhesion is the lap-shear test using cartilage blocks. However, as reported in the literature, harvested cartilage blocks are approximately parallel to the articular surface. Accordingly, the simulating cartilage defect may be more relevant to fissures that extend horizontally in fractured or osteoarthritic cartilage. In contrast, human cartilage failure might occur more frequently because of joint loads in normal direction. Furthermore, *in vivo* experiments frequently highlight the missing cartilage integration at lateral defect interfaces [29,60–62,157,213]. Since the zonal structure of cartilage tissue and the orientation of collagen fibers may modulate the repair process, an integration model that mimics a lateral cartilage defect and simultaneously considers the hierarchical structure of cartilage tissue is very likely better suited for investigations on long-term cartilage repair processes [212].

In 2001, Obradovic et al. presented the disc/ring cartilage integration model with the aim to adapt the presentation of *in vivo* cartilage defects to better controllable *in vitro* conditions without systemic

effects [162]. These disc/ring constructs could easily be cultured for several weeks under variable conditions and the model also allowed histological analysis of the lateral defect interface both in the sagittal (cross-section) and the transverse plane (*en face*). To biomechanically quantify the integration strength at the disc-ring interface of the tissue composites, a plunger is used to separate the central disc from the cartilage annulus with a load cell recording the force until failure of the composite. One challenge of the model is to obtain an interface between the disc and ring that is perpendicular to both the top and bottom surfaces of the composites, which assures the collinearity of the interface axis with the mechanical testing device's plunger and eliminates potential artifacts [214].

Within the performed push-out measurements, all specimens were tested to failure with a displacement rate of 0.5 mm/min. This is in accordance with reported data in literature and provides a strain rate slow enough to ensure that equilibration of fluid essentially is achieved throughout the test and that the stress distribution within the cartilage is governed by the elastic properties of the solid matrix [160]. In order to allow evaluation of integration strength increases, a well-defined reference is mandatory. Unglued control samples achieved reproducibly low bonding strengths of 3.57 ± 1.78 kPa, thus serving as a base line. The detection sensitivity of the load cell is high and complete avoidance of detected adhesion is not possible due to capillary and frictional forces even in non-bonded constructs. This also illustrates the delicacy of the manufacturing method of the constructs, which uses special custom-made tools to enable precisely aligned cuts and punching channels. This in turn avoids canting during push-out and reduces measurement artifacts. Using the control group, the adhesive strength of a material on cartilage tissue can thus be well assessed.

### 4.2.4.2    **Fibrin vs. BioGlue®**

For an immediately resilient treatment and to prevent the progression of cartilage defects, immediate bonding means a promising option. The principle to fuse opposing cartilage pieces by chemical crosslinking the collagen fibers of the cartilage network was investigated in a single-lap cartilage model. Different chemical crosslinkers were applied before, either alone or in combination with a pretreatment of surface-degrading agents. Particularly crosslinking with glutaraldehyde and EDC/NHS achieved high bonding strengths which could be clearly enhanced by enzymatic pretreatment of the cartilage [197]. Another early approach used a photochemical crosslinking approach to achieve immediate bonding in a disc/ring cartilage model [211]. However, within the respective studies the outcome of bonding strength was highly dependent on the application of an additional compressive load during the bonding procedure, which underlines the necessity of direct contact of individual collagen fibers for successful bonding. Considering the scale of individual collagen molecules

and fibrils, an approximate distance of 1.3 -1.7 nm becomes the critical parameter for crosslinking using chemical reactants without a supporting molecular layer [291]. Regarding this, the possibility to apply load on the overlapping integration area during fabrication proved advantageous when chemical crosslinkers of small molecular size are used and intimate contact between both cartilage blocks is needed. Additionally, the application of small chemical reactants rises concerns regarding potential cytotoxic properties.

The use of an adhesive matrix in contrast to small crosslinkers allows not only the bridging of larger defect gaps, but also the spatial filling of defects. Binding crosslinkers in a matrix can also reduce the free diffusion of potentially critical reactants into the tissue. In clinical use, there are several surgical adhesives and sealants that vary widely in composition and reaction chemistry.

The combination of a chemical crosslinker with a protein matrix is applied in the commercially available BioGlue®. BioGlue® consists of two components: glutaraldehyde and bovine serum albumin. The main field of application of this substance is cardiothoracic surgery and the treatment of large vessels [290,292]. After mixing, the components polymerize within a few seconds, which requires rapid intraoperative application. BioGlue® is acknowledged to provide very good shear and tensile strength. Glutaraldehyde is present in a concentration of 10 % (w/v) and bovine serum albumin (BSA) in 45 % (w/v) in respective pecursor solutions. The syringe delivery system assures mixing of both components in a ratio of one part glutaraldehyde component to four parts BSA component. Glutaraldehyde corresponds to the reactive component and causes polymerization, in which BSA serves as a substrate. The reactive aldehyde groups crosslink the amine groups of albumin proteins with each other, leading to the formation of a stable matrix. In addition to these compounds, the adhesive is also able to bind to the surrounding endogenous tissue and the amine groups present there, thus achieving good tissue adhesion even on a moist substrate [290]. Despite the proven positive effects in vascular and cardiac surgery, the use of BioGlue®, according to the recommendation of Bhamidipati et al, remains limited to a selected patient clientele and should not be performed routinely [293]. This is due, on the one hand, to the known toxicity of glutaraldehyde and, on the other hand, to the inflammatory reaction that can potentially occur during application. In principle, the adhesive also appears suitable for other applications and was therefore included in experiments on immediate cartilage bonding.

Fibrin glue was the first agent approved as a hemostat, sealant and adhesive by the FDA [226]. Because of its natural origin and accompanying advantages, fibrin has become a prominent and well-known material for wound closure and tissue engineering applications. A number of crosslinking steps are involved during fibrin clot formation. In addition to its self-polymerization, the fibrin molecules crosslink with both collagen and adhesive glycoproteins at the wound site. The clot formation in fibrin glue also resembles the final step in physiological coagulation (see also Chapter 1.1.5.1). Via

attachment of plasmin inhibitors like α2 plasmin inhibitor (α2-PI), α2- macroglobulin, and plasminogen activator inhibitor 2 (PAI-2) to the α chain of fibrin, the clot is strengthened and fibrinolysis is reduced. Both autologous and homologous fibrin sealants have been developed based on whether the plasma is obtained from the same patient or another person, respectively. Fibrin glue was reported to be biocompatible, resorbable, and not causing tissue necrosis, fibrosis, or inflammation. The degradation time of fibrin glue can vary from a few days to months depending on the composition. Despite the use of fibrin glue as a hemostatic agent from xenogeneic sources for a range of surgeries and despite components undergo a battery of screening analysis and inactivation steps, the risk of virus transmission still prevails [226]. For the use in medical devices high quality and purity standards such as requested by Regulation (EU) No 722/2012 and ISO 22442-1 need to be fulfilled by materials of animal origin.

The mechanical strength of the fibrin clot is in general a function of the fibrinogen concentration, whereas the thrombin concentration directly relates to the speed of clotting. Therefore, an optimum concentration of both components is necessary to achieve rapid hemostasis as well as satisfying adhesion and mechanical properties. Adhesion strength of the fibrin glue depends on the substrate, composition of the glue, method of fibrinogen preparation, presence of water, fat, or collagen, and setting time, making it redundant to deduce a universal value for the adhesion strength of fibrin glue [95].

In the here described comparative experiment, the immediate adhesive strength on cartilage tissue of the two commercially available tissue adhesives TissuCol and BioGlue® were tested. Although an increase in integration strength as compared to the control group was obvious, the immediate bonding strength of TissuCol with 13.53 ± 3.87 kPa was significantly below the value achieved with BioGlue®, for which immediate bonding strengths of 122.79 ± 43.91 were achieved. The values achieved for TissuCol are consistent with literature values for fibrin glue [209]. The high concentration of the very reactive crosslinker glutaraldehyde in BioGlue® suggests that a large number of covalent bonds have occurred between adhesive components and the cartilage surface, leading to a sharp increase in integration strength. In contrast to the rather rigid appearance of cured BioGlue®, fibrin retains an elastic character, which can be attributed on the one hand to a lower number of covalent crosslinks within the adhesive and on the other hand to the fibrillar structure of the proteins. Although an existing elasticity may be beneficial to distribute mechanical forces to the adhesive matrix, it requires sufficient bonding to the tissue surface to prevent detachment of the adhesive from the interface.

Coupled to the enormous reactivity of small crosslinker molecules such as glutaraldehyde in the case of BioGlue®, is the high risk of toxic effects on cells and tissues. To investigate the influence of the adhesive materials and possible leachable substances on tissue viability, the disc/ring constructs were

stained with the viability dye MTT after the adhesive application. After only one day, it was noticeable that cartilage constructs treated with BioGlue® had enormously lost vitality. Since the vitality of the tissue not only decreased in the immediate vicinity of the adhesive interface, but extended over the entire construct, it can be concluded that considerable amounts of unbound glutaraldehyde were able to diffuse into the cartilage tissue. This process is probably enhanced by the very high water content in the cartilage tissue compared to other tissues. The European Chemicals Agency (ECHA) provides a toxicological database for chemical compounds. The approach for toxicological evaluations of medical devices is described in the ISO 10993-17 guideline. Generally speaking, to assess the toxicity of a compound, for example derived no effect levels (DNEL) can be determined for specific exposure routes, up to which concentration no toxicological hazard to the human body has to be expected. With regard to the parenteral application of adhesives to cartilage tissue, the derived DNEL by ECHA for the oral exposure route most closely reflects the clinical situation from a toxicological perspective. The DNEL of 70 µg/kg bw/day corresponds to a total amount of just 4.2 mg for a representative 60 kg adult, above which a risk for systemic toxicities is assumed. Under the simplified assumption that 1 ml of the final BioGlue® corresponds to 1000 mg and the final concentration of glutaraldehyde is 0.025 % (after 1:4 mixing of the 10 % stock solution), then already 1 ml of the adhesive contains a total amount of 25 mg glutaraldehyde. Of course, most of the crosslinker is chemicaly bound in the glue matrix and no immediate exposure as a leachable is probable, however this reflection underlines the high toxic potential of this substance not even considering local toxic effects (e.g. tissue irritation). Glutaraldehyde is classified as cytotoxic and as a strong irritant by the ECHA, whereby irritating properties have an enhanced effect in tissues that have a low regenerative capacity.

The here utilized viability stain MTT is also used as a dye in cytotoxicity tests for medical devices according to the ISO 10993-5 standard. Only recently, the principle of viability staining with MTT has also been approved for the *in vitro* irritation testing of medical devices. The ISO 10993-23 guideline describes *in vitro* irritation testing using MTT in a recombinant 3D skin model. However, the corresponding procedure may be transferred to other tissue models to better simulate clinical use. Thus, MTT staining in the disc/ring model well reflects the potential clinical use of the adhesive on cartilage defects. In addition, subsequent dissolution of the MTT dye allowed quantifiable analysis of cytotoxic or irritant properties of the adhesive material. According to ISO 10993-5, a reduction of cell viability by more than 30 % is classified as severe cytotoxicity. Although experience has shown that the presence of tissue components in a 3D model is protective against cytotoxic properties compared with 2D cell culture testing, a drastic decrease in viability was observed in BioGlue®-treated constructs similar to thermally killed constructs (freeze/thaw). In sharp contrast, the TissuCol treated constructs show viability on par with the untreated control constructs both macroscopically and quantitatively.

As expected, due to the physiological origin of the fibrin glue, no toxicological risk could be detected with the detection methods used. Assuming a high purity of the adhesive components used, no biological hazards are to be expected, as the components of fibrin are produced and metabolized physiologically in the human body. Also, the risk from transmissible viruses can theoretically be avoided by the possibility of autologous isolation. Successful long-term cartilage integration requires vital tissue to strengthen the bond at the defect interface through regenerative processes and to prevent cartilage defects from advancing. Due to the drastic toxic effects of BioGlue® at the application site, successful tissue regeneration of a cartilage defect with this treatment seems to be excluded despite the high adhesive strength. In contrast, the biological compatibility of the fibrin glue TissuCol allows potential cartilage regeneration and the development of long-term integration in treated lateral cartilage defects can be investigated in further experiments with the disc/ring model in combination with *in vitro* cultivation.

### 4.2.4.3 **Long-term cartilage integration with fibrin glues**

Repair tissue that forms at opposing cartilaginous surfaces can be defined as an adhesive, a material at "the surfaces of two solids [that] can join them together such that they resist separation" [294]. A prerequisite for repair tissue formation is the presence of viable cells at the application site. Experiments conducted before showed good biocompatibility of the commercial fibrin glue TissuCol by simultaneously providing a biomaterial matrix with immediate bonding capacities at the cartilage defect interface. As a natural material in physiological wound healing, fibrin can be remodeled by the body and intrinsically has the ability to be the basis for newly formed tissue.

One goal in tissue engineering is to use cell carriers that have a turnover rate that corresponds to the new synthesis of tissue. This would provide a balance of degradation and remodeling without, for example, causing spatial stress or tissue loss at the application site. Due to its properties, fibrin is frequently used not only as an adhesive but also as a cell carrier or hydrogel in tissue engineering approaches. Adjustments to the formulation of the fibrin components allow the mechanical properties as well as the resistance to degradation to be modified and adapted to the specific requirements of the intended use. Although fibrin is frequently used in treatments of cartilage defects, the specific requirements for fibrin stability to match optimal cartilage regeneration are unknown.

Within our research group, different formulations of long-term stable fibrin hydrogels for tissue engineering of cartilage and adipose tissue have been established. Mainly by adjusting the calcium and aprotinin concentration, transparent and long-term stable hydrogels can be produced, which allow a significantly better and longer shape stability when colonized with cells. The mechanical strength of

fibrin hydrogels can also be adjusted via the proportion of fibrinogen [84,117,118,122]. In the experiments performed with chondrocyte-populated fibrin gels, one of the observations was that cell proliferation and the amount of synthesized cartilage-specific ECM varied with fibrinogen content. Decreasing the fibrinogen concentration also reduced the stiffness of gels. Using a mechanically too strong fibrin gel, however, may immure the single chondrocyte, inhibiting cell proliferation and migration, and subsequently preventing ECM development. Only fibrin formulations with a final fibrinogen concentration of 25 mg/ml or higher, a $Ca^{2+}$ concentration of 20 mM and a pH between 6.8 and 9 were transparent and stable for three weeks. Related to the intended use as cell carrier for volume stable hydrogels for *in vitro* cartilage tissue engineering, optimized formulations had a final fibrinogen concentration of 50 mg/ml, a $Ca^{2+}$ concentration of 20 mM and a pH of 7.0. In comparison, commercial TissuCol has a final fibrin concentration of 35-50 mg/ml, a $Ca^{2+}$ concentration of 20 mM and a pH of 7.4. In the experiments to develop long-term stable fibrin, TissuCol was tested as a comparator, but colonized hydrogels of this material were completely dissolved after three weeks of culture [122]. To transfer these varying properties of different fibrin formulations to long-term integration in the disc/ring cartilage model, the optimized long-term stable fibrin gel with 50 mg/ml fibrinogen (stable fibrin (50)), a modification with 25 mg/ml fibrinogen (stable fibrin (25)) as well as TissuCol were applied as adhesive to the defect model and the course of integration over three weeks was evaluated. The goal was to determine if the potentially higher stability of the long-term stable formulations is superior for the development of repair tissue at the defect site. It was further to be shown how the interaction of the adhesives with synthesized ECM is and in what time course ECM is deposited at the defect gap.

In contrast to TissuCol, slightly lower immediate bonding values were obtained with the long-term stable formulation. Both stable fibrin formulation achieved similar values, stable fibrin (25) with 5.66 ± 2.91 kPa and stable fibrin (50) with 6.74 ± 2.82 kPa. Separate adhesive-treated cartilage constructs were transferred to *in vitro* culture and additional push-out tests were performed after seven and after 21 days. After seven days, there were no significant differences between the tested fibrin types and all showed an increase in integration strength to just below 30 kPa. In the further course until 21 days *in vitro* culture there was a steady increase of the integration strength. At the end of the test period, both TissuCol and stable fibrin (25) achieved values of about 90 kPa. The highest integration forces were observed with stable fibrin (50) at 108.95 ± 46.25 kPa, but the differences between the fibrin groups were without significance. However, it is striking that from day seven the increase in integration strength was significantly higher to untreated control constructs. Without the use of an adhesive, there was no significant increase in integration strength in the control group, which already indicates that the presence of a fibrin matrix in the defect gap has a positive effect on integrative repair processes. The group of Martin reported for comparable unglued samples

integration strengths of about 30 kPa up to 160 kPa after six weeks [214,215], however, much of this performance could be contributed to additional tissue layers that were deposited on top of the samples during the culture period. Restoring the disc/ring cylinders with smooth surfaces by selectively trimming the attached layers without compromising the actual punched defect surface provided a halving of the integration strength.

Using a single-lap model and bovine cartilage explants, integration strengths of 30-40 kPa were obtained in untreated constructs after three weeks in a serum-containing *in vitro* culture. However, in these experiments, the adhesive interface was weighted with a porous plate to ensure direct contact of the opposing cartilage surfaces [160,189,295]. Additionally, differences in integrations strength of untreated samples can be attributed in part to the difference in the orientation of the interface (lateral in disc/ring model vs. transversal in single-lap model) and to the differences in mechanical testing (push-out in disc/ring model vs. lap shear in single-lap model). The influence of collagenase treatment at the defect interface was investigated in a disc/ring model with cartilage isolated from calves of different age. Both the untreated control group and the collagenase-treated samples increased the histological integration score and integration strength values over a time course of four weeks *in vitro*. Interestingly, the additional enzymatic treatment initially slowed integration, but then had an accelerated increase after two weeks to levels similar of the control group and partly even higher after four weeks. However, both the histological integration increase and the increase in integration strength were strongly dependent on the age of donor calves. In cartilage explants from young calves (one to two months old), an integration strength of approximately 7 kPa was measured after two weeks and 28 kPa after four weeks in the control group. Constructs from older calves (six to eight months) already had values of approx. 33 kPa and 44 kPa after the same time in each case [164]. Moretti et al. also used the disc/ring model, however with a total *in vitro* cultivation time of 6 weeks. In their experimental set-up they compared the adhesive strength of untreated samples to samples from which the formed capsule of repair tissue formed on the surface of the cartilage cylinders was trimmed. Since in the biomechanical test the adhesive strength between cartilage explants must stretch or fracture any potential encapsulating layer on top of the composite's surface, the mechanical properties of this tissue would contribute to the actual stresses measured [214]. These examples show that even in the same experimental model with the culture over several weeks, variability in the integration increase is possible, which can arise, for example, from deviation in the age of the donor animals or the species [296], but also from changes in the test specimen geometry. The disc/ring model was also applied for meniscal tissue where integration strength with different adhesive materials were tested and *in vitro* cultivation of four weeks was conducted. The authors included fibrin as test material

and interestingly the initial integration strength of fibrin (about 20 kPa on meniscus) was reduced to less than half after 28 days [297].

Comparison of results obtained between publications using different starting material, different culture periods, or even different models is therefore difficult and co-testing of control samples within an experiment is essential to interpret the possible benefits of a treatment. No comparable *in vitro* long-term results in the disc/ring model with fibrin glue and similar culture conditions are available. In *in vivo* experiments, fibrin was used to fill osteochondral defects in the femoral grove of rabbits. In this experiment the fibrin treatment impaired the natural repair. Chondrocytes were observed to continuously grow on the fibrin adhesive but no cell migration was seen into the fibrin [298]. Contrary, the usage of fibrin adhesive for the treatment of chondral and osteochondral injuries in human patients was reported as beneficial earlier [227]. In the performed clinical follow-up examination it was found that for all observed injuries where fibrin adhesive was used, the wounds healed after twelve weeks, whereas in untreated group a distinct gap was still visible at the wound sites. In more detail, the fibrin stopped the retraction of the wound edges and the remaining gap was soon filled with a new matrix. These results are consistent with our findings observed at the scale of the *in vitro* model within three weeks.

As was already mentioned before, one necessity for successful long-term cartilage integration is the presence of viable tissue in the surrounding of the defect. Living chondrocytes within the native tissue secrete precursors of collagen and their subsequent deposition near the repair interface contributes to functional integration [189]. The fact that there is no or strongly reduced integration in vital cartilage tissue without additional support, e.g. in form of an adhesive matrix, has also been found in other studies. No signs of integration in a cartilage disc/ring model were reported in untreated samples after 28 days of culture. In these samples, either a gap between the wound edges was observed or the surgical cutting line remained visible [165]. In an approach to facilitate cartilage integration via enzymatic treatment (lysyl oxidase), gaps were seen after histological processing in the control group [217]. In another publication where a cartilage disc/ring model was utilized, no sign of integration was observed in the group without enzymatic treatment and a gap remained visible after four weeks of *in vitro* culture. In contrast to that, integration was observed in the enzymatic treatment (collagenase and thermolysin) group, and outgrowth of tissue in the interface was also noted. In addition, a higher cell density was found in the integrative interface [166]. Transmission electron microscopy analysis of disc/ring constructs after six weeks of culture indicated that interfacial collagen fibrils were well integrated into the collagen network of the cartilage disk and ring, whereas molecular bridging between opposing disk/ring cartilage surfaces was less pronounced and restricted to regions with narrow interfacial regions that have a gap width of less than two mm. At interfacial regions with

gaps of 1–1.7 mm in width, larger diameter fibers at a higher density were seen to bridge into the cartilaginous collagen network of the disk and ring [214].

In the experiment with different fibrin glues performed here, defect filling with ECM components was also found after 21 days, whereas a clear gap remained detectable in the control group similar to reports in the literature. Based on immunofluorescence and safranin O staining, the newly deposited ECM can also be assigned to cartilage-specific collagen type II and GAG. Histologic images also revealed the presence of cells in the defect interface in all three fibrin groups, which was pronounced to varying degrees at different sites of the defect regardless of fibrin type. The images show that chondrocytes from the surrounding cartilage tissue are moving into the defect interface. However, it remains unclear whether the cells in the interface result solely from migration from the surrounding tissue or also from proliferation *in situ*. The results show a clear dependence on fibrin as a filling matrix for increasing both integration strength and ECM deposition in the interface. However, the variance in biomechanical results also increases with the progression of culture duration. One reason for this may be the biological variability of the donor animals. In the experimental approach, cartilage from different animals was pooled. The starting material was obtained from a local slaughterhouse. Accordingly, it cannot be ruled out that there are variations in the processing time and age of the animals. In addition, the processing of the cartilage constructs with the fibrin glue is a potential source of variability. Once the fibrinogen and thrombin components are mixed, curing begins immediately. In practice, the small size dimension of the disc/ring constructs may result in temporal differences in the assembly of the two glued parts. It cannot be ruled out that certain variations in the curing or distribution of the fibrin glue components may occur due to differences in the spatial presentation of glue precursors combined with the fast reaction mechanism and thus directly influence the bonding capacity to the tissue. During the gluing process, the fibrin was mixed in the lumen of the cartilage ring and then the cartilage disc was inserted. During insertion, the cartilage disc inevitably pushes excess adhesive out of the defect interface. This can result in significant variations at the microscopic level in the local remaining adhesive thickness in the gap, and thus areas of more and less thick fibrin layers in the interface even within the same construct.

Due to the good outcome with the stable fibrin (50) in terms of integration strength and ECM deposition development as well as cell migration, further experiments were conducted with a focus on this material in the course of the presented experiments. The results shown here with stable fibrin (50) were also used as a basis for further experiments by a medical student in our research group [196]. In this work, a focus was set on the influence of collagen synthesis on the integration. The synthesis performance was modulated in two ways. In the disc/ring model the function of ascorbic acid was investigated. In addition, ethyl-3,4-dihydroxybenzoate (EDHB), which is a structural analogue
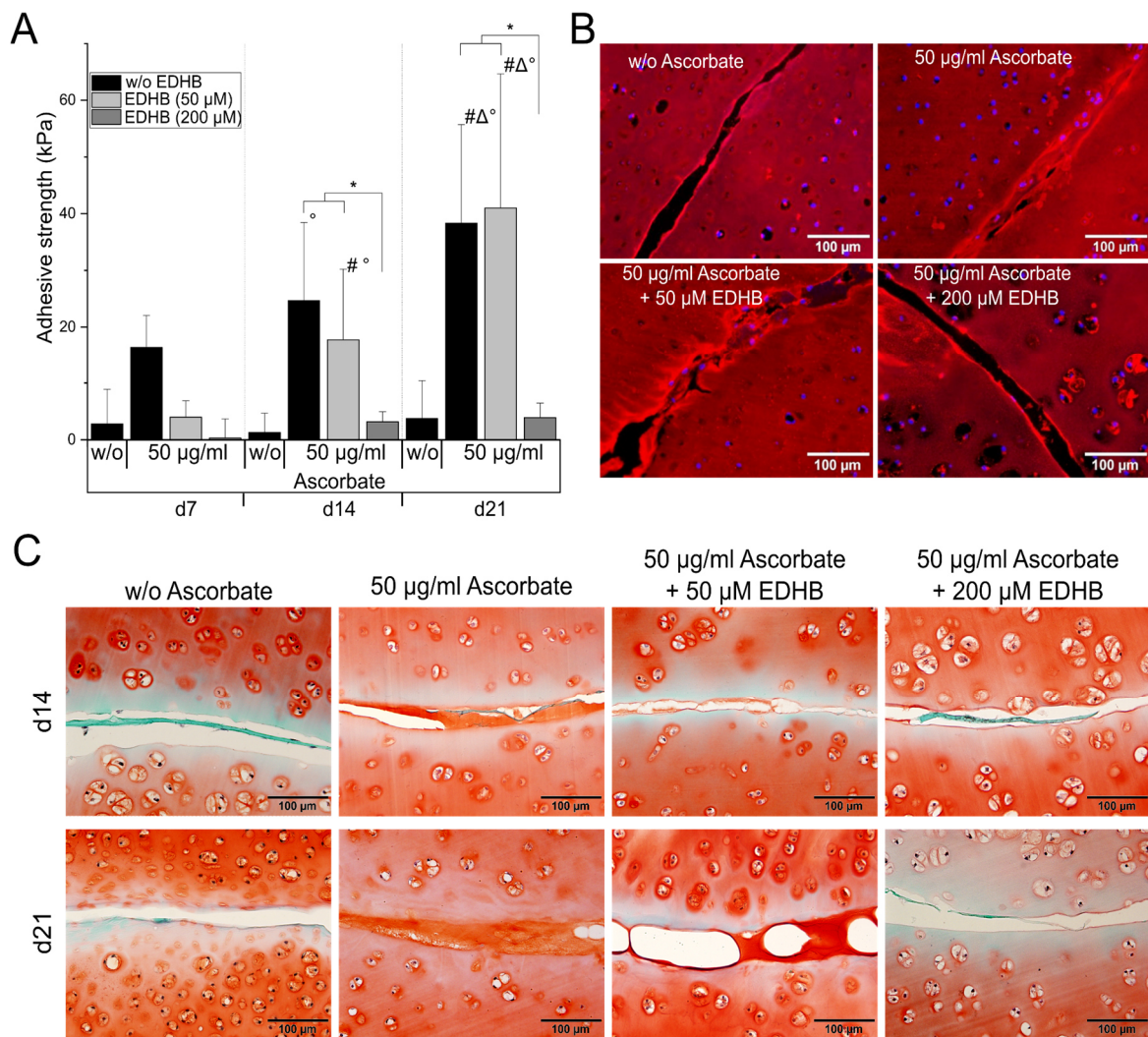
**Figure 19: Assessment of the integration process in stable fibrin (50) gels as a function of ascorbic acid and when collagen formation is blocked by EDHB.**

A) diagram of the achieved push-out strengths at different observation points. B) captures of immunofluorescence staining for collagen type II after d21 in vitro culture. C) captures of SafO stainings in the different test groups at d14 and d21. Data are presented as means ± standard deviation. Figure adapted from[196].

to ascorbic acid and can thereby block prolyl-4-hydroxylase-mediated collagen formation [192,193] was included in the experimental set-up. The test group with 50 µg/ml ascorbate corresponds to the stable fibrin (50) group described previously. Although over the 21-day *in vitro* culture the increase in integrating strength was less than in the results described earlier with stable fibrin (50) (see above), significant increases were observed after 14 and 21 days (see Figure 19A). The variation in outcome repeatedly shows that even in the standardizable *in vitro* model, other factors such as donor animal variability or handling may influence the results even if trends are reproducible. Both the withdrawal of ascorbic acid from the medium and, depending on the dose, EDHB significantly prevented the formation of integrative repair. Histologically and immunohistochemically, the groups without

ascorbate supplementation and with high-dose EDHB also showed significantly reduced ECM synthesis with failure to fill the defect zone with type II collagen and a glycosaminoglycan matrix during cultivation (see Figure 19B and C). In the groups without ascorbic acid supplementation or with high-dose EDHB, there were no signs of collagen synthesis and/or integration, either biomechanically or immunohistochemically. Thus, in the disc/ring model, ascorbic acid as a cofactor of collagen synthesis was shown to be an essential additive for cartilage tissue integration. This emphasizes the urgent need for interfacial ECM deposition to bridge defects for successful integrative repair. The development of biomaterials and cartilage adhesives must therefore focus on ensuring that this property is not inhibited or even favored.

### 4.2.4.4        Time course of lateral cartilage integration in fibrin glue

As a follow-up to the long-term integration experiment conducted with different fibrin formulations, stable fibrin (50) treated disc/ring constructs were cultivated similar to the experiment before, but constructs were harvested at additional timepoints to better track the regenerative development occurring at the defect. In a series of histological examinations, it was found that starting at day three of *in vitro* culture after assembly of the glued constructs a first interfacial ECM deposition occurs visible. At this time point no chondrocytes within the defect were observed. This means that the newly formed ECM molecules were secreted exclusively from the surrounding native tissue and can be enriched in the cleft. Since this effect was observed to a much lesser extent in control samples in previously performed experiments, it can be assumed that the fibrin matrix in the defect gap is conducive to the deposition of ECM components. In the SafO stain, the fibrin glue is bluish to greenish in color and can be distinguished from the orange-stained surrounding cartilage tissue (see also Figure 17A). It can be seen that already at the beginning the glue does not show a continuous connection to the opposite cartilage surfaces, which may be a reason for the relatively low immediate bonding strength values. In the further course of the *in vitro* culture between day three and day 14, ECM filaments increasingly form a bridge between the cartilage surface and the intermediate fibrin layer. It appears that the fibrin glue acts as an anchor point for secreted ECM components and thereby allows for better ECM deposition. This results in increased closure of gaps where the fibrin previously did not bind to the cartilage surface. Protein polymers and cartilage ECM molecules can adhere to each other and build strong interactions. ECM precursor molecules are secreted by the chondrocytes and assembly to the final three-dimensional network takes place in the extracellular space [299,300]. Between GAG und collagen molecular adherence was reported that is based on van der Waals contacts, hydrophobicity, hydrogen bonding, physical entanglements, and electrostatic attraction between

GAGs and the positively charged amino acids on collagen [288]. It is probable that the interfacial fibrin interferes with synthesized ECM components via identical attraction mechanisms and thus foster deposition of matrix components at the defect site. With proceeding culture duration this effect can facilitate defect filling and annealing of opposing cartilage surfaces.

From day ten, the first occurrences of chondrocytes in the gap can also be observed. In the further course, there is increased remodeling of fibrin as the defect progressively closes with newly synthesized ECM. At d21, only remnants of the original fibrin glue can be seen. It can therefore be concluded that using this *in vitro* model over the three-week period, the rate of degradation of fibrin corresponds to the capacity of tissue regeneration. A core aspect in tissue engineering is the balance of degradation of a biomaterial and concurrent tissue development. In this experiment, it was shown that the initial repair processes are initiated by secretion of macromolecules from the surrounding native tissue and that repopulation of the defect with cells is delayed. This initial effect is inevitably localized and thus limits the magnitude of potential defects that may take the observed integration course via application of cell-free fibrin glue. However, it can be stated in advance that fibrin in principle has the potential to be colonized with cells, which could enhance and accelerate the regenerative capacity in the disc/ring model when treated with fibrin glue. However, it must also be taken into account that degradation and regeneration processes *in situ* in the patient can be influenced by many other factors and that *in vitro* results can only be partially transferred.

Particularly in the immunofluorescence staining for aggrecan and collagen type II (see Figure 17A and B), it can be seen that cells from the surrounding cartilage tissue migrate into the defect gap. In some cases, the pericellular matrix surrounding a chondrocyte can be seen to bud into the defect gap. Due to the necrotic margin that is formed on the tissue during the creation of the defect, it can be ruled out that living chondrocytes were initially present in this region of the cartilage model. Since at this stage the gap has a less compact network of macromolecules compared to the native cartilage tissue, the environment there may favor the proliferation of chondrocytes once they have migrated into the defect. However, because a three-dimensional structure of ECM components is present, dedifferentiation of chondrocytes into a fibroblast-like cell type is prevented like it was reported before [152]. Without the presence of defect-filling ECM molecules, migrating chondrocytes could potentially also initially proliferate on the surface of the cartilage tissue at the interface. However, this is similar to the conditions found in a 2D culture of chondrocytes. In those cultures, dedifferentiation of chondrocytes including a change in secreted molecules and development of a hypertrophic phenotype was observed [285].

Over time the migration or proliferation of cells on surfaces of, or in gaps within the disc/ring composites principally may contribute to the repair process. This was also observed in another *in vitro*

model before where the effect was dependent on the serum content of the culture medium. It was reported in those experiments that outgrowth of chondrocytes from the cartilage tissue and repopulation of a laceration with cells after a timespan of three to six weeks was present. However, the magnitude of cellular response was discussed to be dependent on specific interactions between the cells and extracellular surfaces [160]. The benefit of a cell-adhesive scaffold was also demonstrated in a publication by Pabbruwe et al. Chondrocytes that were sandwiched between two cartilage discs improved fusion of the tissue specimens. The study showed that when cells alone were seeded to the interface there was some space filling with proliferating cells but little or no extracellular matrix to bind the pieces of cartilage together. However, when combining the chondrocytes with a collagen scaffold the histological analysis showed tissue continuum across the cartilage-scaffold interface and a drastically increased biomechanical integration strength. Also in scaffold-only constructs the migration out of the cartilage into the collagen scaffold was observed [168]. Improved cartilage tissue fusion that is based on the presence of matrix-bound chondrocytes is reported frequently in literature. Experiments using osteochondral explants and cell-seeded biphasic constructs also reported increasing integration strengths with ongoing *in vitro* culture. Unlike autologous osteochondral implant controls that were inserted into the explant, the tissue engineered constructs allowed for cell migration and therefore better integration with the surrounding host cartilage tissue [169]. This study expanded the findings of a previous *in vitro* work with an annulus-based explant model. There, calf chondrocytes were seeded to hyaluronan meshes that were press-fitted into adjacent rings of cartilage or bone tissue. Integration strength increased in all groups during *in vitro* culture. The authors suggested that cell migration out of the mesh is a main factor for tissue fusion and that the dense extracellular matrix, especially the high glycosaminoglycan content hinders cell mobility [219]. These results highlight that interfacial chondrocytes play a crucial role for the development of a functional repair tissue in means that they increase the availability of the molecular building blocks of extracellular matrix that is deposited at the defect interface and accelerate defect healing.

Especially in cell-free approaches of adhesives, glue materials that attract cells and simultaneously allow for cell proliferation would provide in theory a huge benefit concerning the speed of defect healing compared to inert materials. Using various growth factors, it has already been shown that the cell concentration at cartilage wounds interface can be specifically increased by cell migration [158,201,202,301,302]. However, for fibrin glue an intrinsic chemotactic potential was described. Using a co-culture assay to mimic matrix-induced ACI (MACI), chondrocytes were found to migrate from collagen membranes towards fibrin and the migration stimulation could be contributed to the thrombin component of the fibrin sealant. The molecular mechanisms underlying these thrombin-induced effects were triggered by activation of protease-activated receptors (PARs), established

thrombin receptors [303]. Contrary, higher amounts of thrombin result in a network of shorter and thinner fibers and smaller pores which again is a known inhibitor for cell invasion in fibrin gels. Thus, with varying thrombin concentration in available fibrin formulations, it is important to consider that not all fibrin adhesives equally allow cell invasion. Differences in cell invasion observed in varying fibrin formulations may have resulted from different degrees of fibrin crosslinking mediated by factor XIIIa, which requires thrombin for its activation. Factor XIIIa covalently links α-antiplasmin to fibrin and this renders the clot less resistant to plasmin degradation. A highly crosslinked fibrin clot may impede cell invasion by reducing the ability of cells to degrade the fibrin [304]. Moreover, it has been demonstrated that plasmin activity is a requirement for cells to migrate into fibrin gels [305]. Additionally, the protease inhibitor aprotinin can vary between fibrin formulations. Aprotinin is typically added to slow fibrinolysis and its action can accordingly influence cell migration as well. It is also open to debate whether or not cytokines present in the fibrin glue function as chemotactic stimuli and further clarification is needed to which extent chemotactic agents form during fibrin formation and degradation [304,306]. Cell density at the defect interface is affected not only by chemotaxis, but also by the dense network of native cartilage, which enormously affects the ability of cells to migrate. Especially glycosaminoglycan chains were reported as being an inhibitor for chondrocyte migration [163,211]. In contrast to the observations in our experiments, Andjelkov et al. found no cell outgrowth in particulated cartilage biopsies that were embedded in fibrin und cultivated *in vitro* up to five weeks [307]. The authors included non-treated as well as collagenase treated samples for their observation. However, there are also many conflicting reports in the literature about existing cell migration from native cartilage tissue that support our findings. Within those reports, different approaches aiming in softening of the native ECM in order to increase cell mobility and cell density at the defect were investigated, including enzymatic treatments, but also short-term inflammatory conditions [162–167,179,207].

One of the major difficulties of *in vitro* models is the translation of results for potential treatment approaches. The multitude of influencing factors on cartilage regeneration that may prevail *in situ* may also differ from patient to patient and cannot be completely simulated *in vitro*. For example, age and potential inflammatory reactions can have a major individual influence on the metabolism in cartilage tissue but also on the conversion of a biomaterial or adhesive. *In vivo*, fibrin is gradually degraded during wound healing by fibrinolysis and replaced by mature ECM. In this process, the fibrin matrix is locally degraded by the proteolytic activity of metalloproteinases and plasmin. Concentration differences of these factors between *in vitro* and *in vivo* inevitably cause differences in the outcome of a treatment. One potential adjustment of a material, as in this case with fibrin, is the rate of degradation, which can be controlled e.g. by incorporation of protease inhibitors. The influence of the

adhesive degradability was further demonstrated by our group with a fibrinogen-polyoxazoline hybrid adhesive (see discussion in Chapter 4.4).

## 4.3 Improvement Strategies for Cartilage Integration in Fibrinogen-Based Adhesives

Fibrin glue is a naturally derived adhesive that incorporates enzyme-driven crosslinking mechanisms that also take place in blood clot formation. For the application on cartilage defects with the respective mechanical requirements in the knee joint, particularly a high immediate bonding strength is desirable. Therefore, the goal of the following chapter was to investigate approaches to increase the interfacial bonding of fibrinogen-based adhesives by means of different crosslinking-mechanisms.

## 4.3.1 Diazirine Functionalization of Cartilage Tissue

In order to increase the immediate bonding strength of fibrin (here stable fibrin (50)), the goal was to increase the number of covalent bindings between the fibrin and the surrounding bulk cartilage tissue (see Figure 20A). Diazirines are heterocyclic organic chemical substances containing a triple ring consisting of two nitrogen atoms and one carbon atom, the two nitrogen atoms forming an azo group (-N=N-). Here, a bifunctional Sulfo-NHS-LC-diazirine was used to functionalize the cartilage tissue surface with reactive diazirine moieties (see also working principle illustrated in Figure 20B and C).

In order to functionalize the surface of the cartilage tissue preliminary tests revealed that an enzymatic pre-treatment facilitates binding of the diazirine molecule via the NHS moiety. Therefore, the cartilage disc/ring samples were incubated with Chondroitinase ABC (Ch-ABC) that is expected to erase superficial GAG and expose the collagen network of the cartilage tissue. Upon irradiation with ultraviolet light at 365 nm, the tissue-bound diazirine forms reactive carbenes, which can insert into C-H, N-H, and O-H bonds to build up covalent connections with the fibrin glue. Constructs treated with Ch-ABC (1 U/ml Ch-ABC for 20 min) with or without additional diazirine-functionalization were tested either in combination with fibrin glue (stable fibrin (50)) or without (Ctrl). The immediate bonding strength was determined in a biomechanical push-out test (see Figure 21A).

The enzymatic digestion of superficial GAG alone increased the immediate bonding strength both in the control and the fibrin samples. The mean integration strength of the Ch-ABC treated control was 12.87 ± 4.34 kPa. In the Ch-ABC treated fibrin samples a mean adhesive strength of 25.58 ± 8.45 kPa was achieved.

The introduction of the diazirine moieties in addition to the Ch-ABC treatment led to a further increase in bonding strengths of both the fibrin and control group. The immediate bonding strength of control samples with Ch-ABC and diazirine treatment was 20.51 ± 11.31 kPa. In the corresponding fibrin group 58.01 ± 19.02 kPa were measured. The combinational treatment of Ch-ABC digestion and diazirine functionalization led to significantly higher bonding strengths than without any defect treatment. Only when combined with fibrin glue this combinational treatment also resulted in significantly higher values than when treated with Ch-ABC alone.
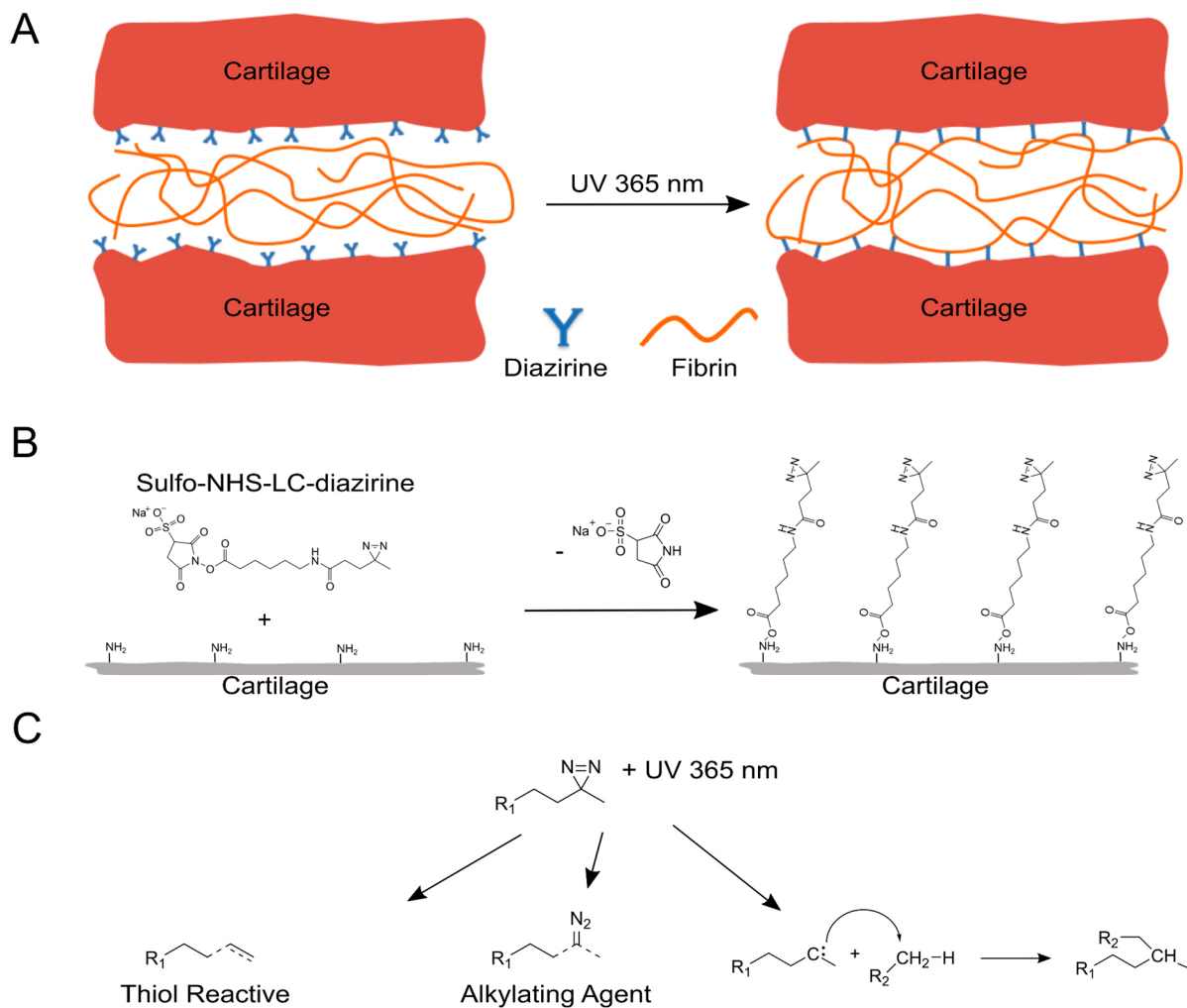


**Figure 20: Enhancement of the immediate bonding strength of fibrin glue to cartilage tissue via functionalization of the tissue surface with diazirine.**

A) Schematic illustration of the bonding mechanism B) Bonding mechanism of the bifunctional diazirine molecule to the cartilage surface via stable amid-bond formation after reaction of the molecule's NHS ester with primary amines of the tissue. C) Upon irradiation with UV light the diazirine forms reactive carbene species that possess different binding possibilities with the fibrin glue molecules.

The chondrocyte survival and viability in the surrounding of the defect after the different treatments was analyzed by means of live/dead and MTT staining (see Figure 21B). Resulting from the defect creation, a small necrotic band was formed at the defect edge (see also Chapter 4.1.1). No increased cell death or reduced viability was observed after Ch-ABC or diazirine treatment in comparison to the untreated control samples. The histological analysis well confirmed the impression
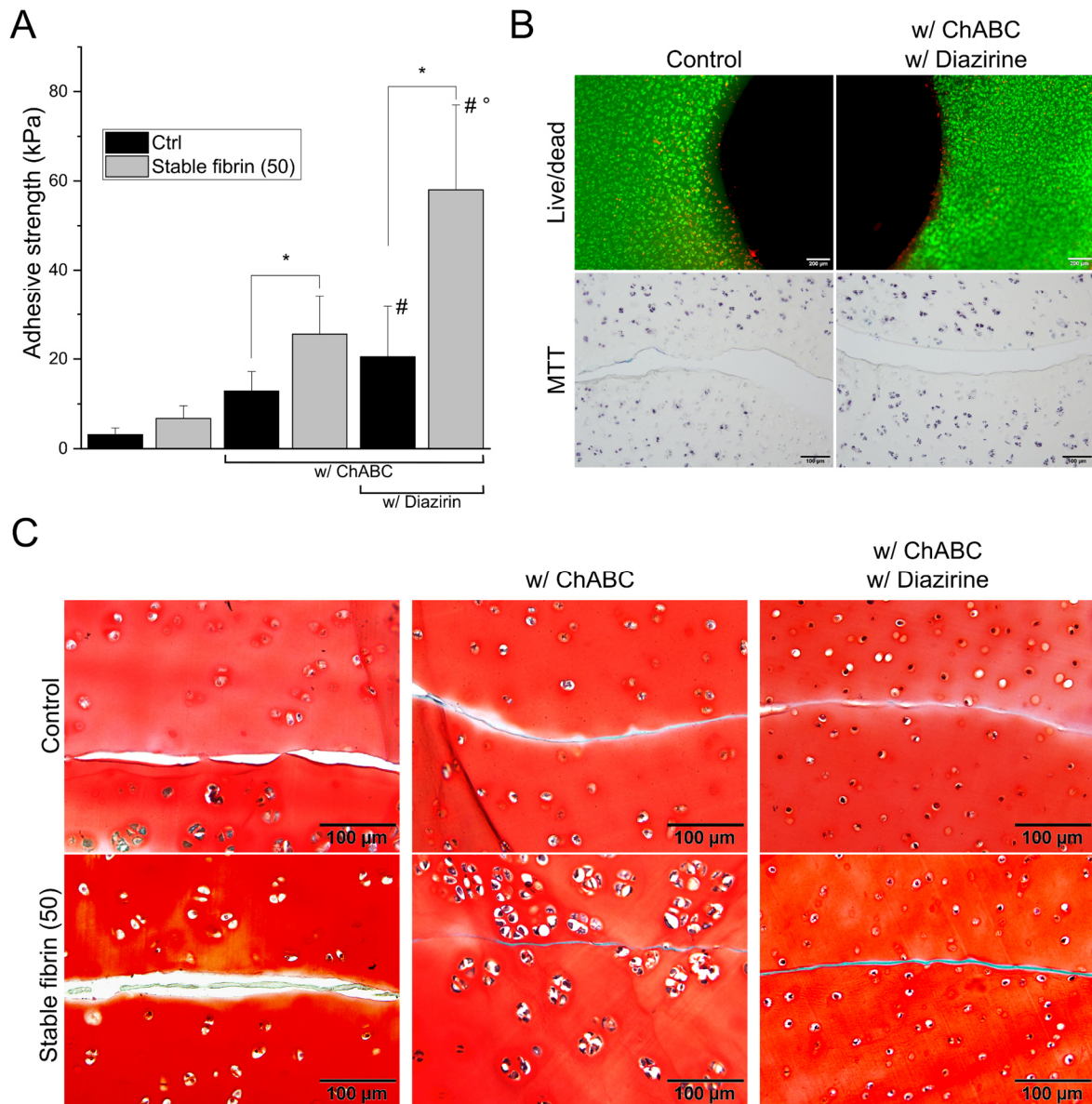


**Figure 21: Immediate bonding of non-glued or fibrin-glued (stable fibrin (50)) disc/ring composites after treatment with Chondroitinase-ABC (w/ ChABC) or combinations thereof with Sulfo-NHS-LC-Diazirine (w/ Diazirine).**

A) Immediate bonding strengths determined by a push-out test. B) Assessment of tissue viability at the defect interface by live/dead and MTT staining. C) Histological images (SafO) of the defect interface after treatment. Data are presented as means ± standard deviation (n= 6-13). (* = p < 0.05 between non-glued control and fibrin-glued samples of otherwise same treatment, # = p < 0.05 to same group w/o treatment, ° = p < 0.05 to same group w/ Ch-ABC treatment).

of the push-out test (see Figure 21C). In the SafO images it was identifiable that both the treatment of Ch-ABC and diazirine led to a firmer contact of opposing tissue surfaces.

## 4.3.2 Photocrosslinkable Fibrinogen as Cartilage Adhesive

An adhesive hydrogel with a fibrinogen content of 50 mg/ml utilizing the photoinitiator tris(2,2-bipyridyl)dichlororuthenium(II) hexahydrate ([RuII(bpy)3]$^{2+}$ complex (abbreviated as "ruthenium" or "Ru" in the course of this document) and sodium persulfate (SPS) was established. The curing was initiated via blue light to form di-tyrosine linkages in the fibrinogen (see also Figure 23A). The resulting hydrogel material was named RuFib50. For comparison of hydrogel stiffness with previously tested adhesive hydrogels, cylindrical hydrogels were cast. RuFib50, two formulations of long-term stable fibrin, namely stable (25) and stable fibrin (50), as well as the commercial fibrin TissuCol (see also Chapter 4.2) were included in the testing. Stable fibrin (50) contains the identical total fibrinogen content as RuFib50, however a thrombin-based crosslinking is used for curing instead of ruthenium. In a screening approach, the Young's modulus of the respective hydrogels (n=2 -4 per group) were obtained after manufacture (d0) and after seven days submerged in PBS (d7) in a compression set-up.
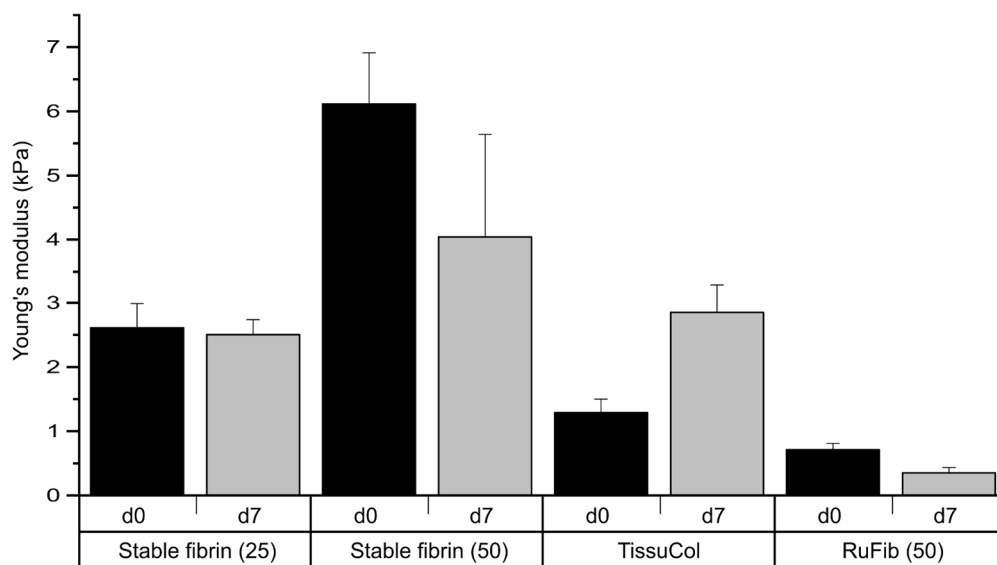


**Figure 22: Determination of the Young's modulus of different fibrinogen-based hydrogels.**

Samples were evaluated directly after fabrication (d0) and after seven days storage in PBS (d7). Data are presented as means ± standard deviation (n = 2-4).

Since no previous experience with the RuFib50 was available, this experiment was used to get an impression of differing physical properties and potential degradation over time in comparison with known materials. However, due to limited number of test samples, no statistic evaluation was applicable. Nonetheless, a trend of differences between the test groups is clearly visible

(see Figure 22). Ruthenium-crosslinked fibrinogen with a content of 25 mg/ml (RuFib25) showed visible solidification of the material, however no stable hydrogel cylinders were obtained after the irradiation. Accordingly, no RuFib25 hydrogels could be included in this evaluation. The lowest stiffness at d0 was obtained for RuFib50 with a mean Young's modulus of 0.71 ± 0.10 kPa. Both long-term stable fibrins resulted in higher Young's moduli (stable fibrin (50) with 6.11 ± 0.80 kPa, stable fibrin (25) with 2.61 ± 0.38 kPa) than TissuCol (1.29 ± 0.21 kPa).
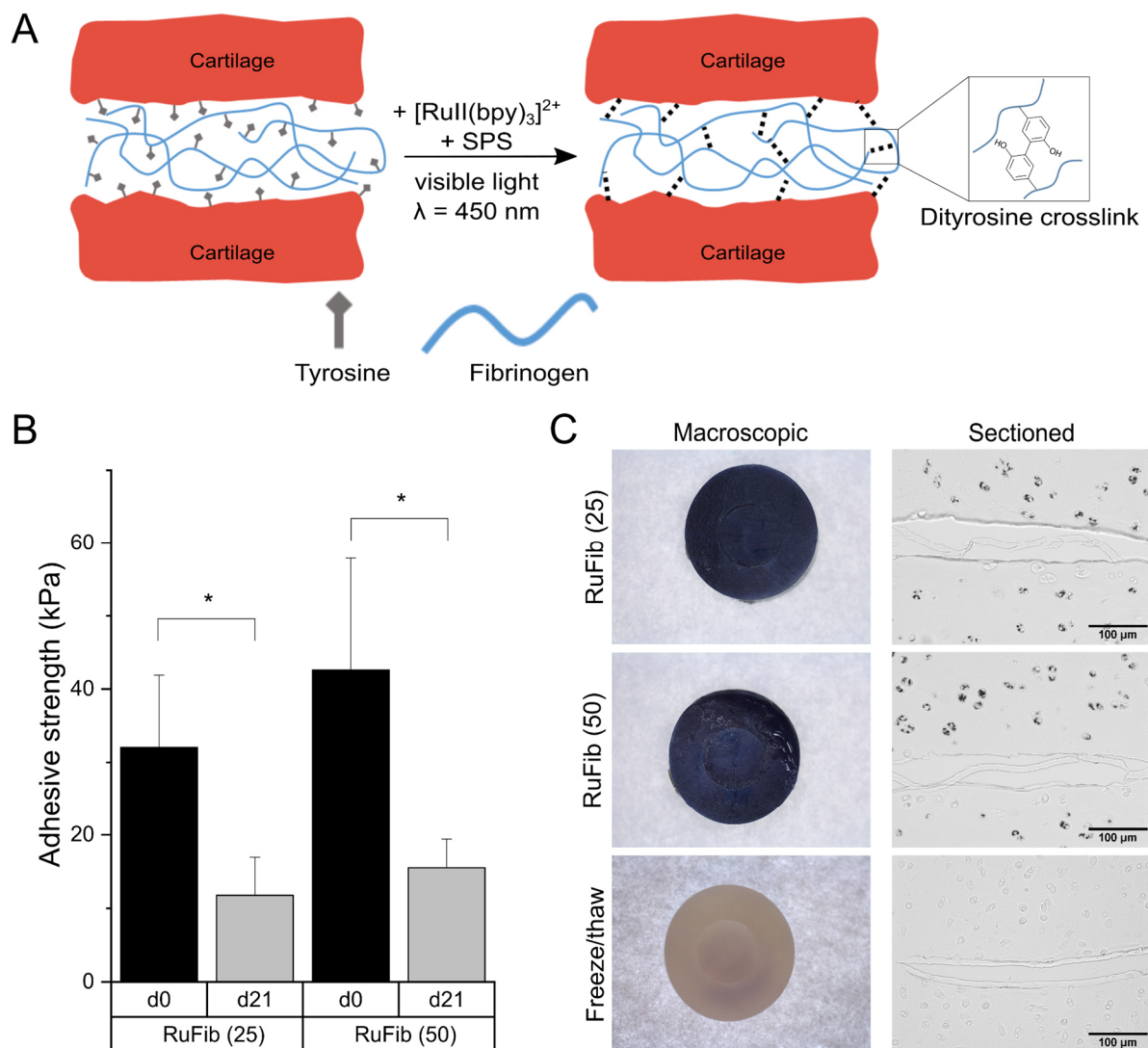


**Figure 23: Cartilage adhesion of ruthenium-crosslinked fibrinogen (RuFib).**

A) Schematic illustration of the bonding mechanism. After blue light irradiation a ruthenium complex mediates dityrosine bonds between fibrinogen and surface proteins of the cartilage matrix. B) Immediate bonding strength (d0) and adhesive strength after seven days (d7) of RuFib25 and RuFib50 determined by a push-out test. Data are presented as means ± standard deviation (n= 6-7). (* = p < 0.05 between same group at different time points). C) Assessment of tissue viability at the macroscopic level and microscopically at the defect interface by MTT staining.

The most pronounced reduction from the Young's modulus from d0 to d7 was seen with stable fibrin (50) (4.04 ± 1.60 kPa at d7). Stable fibrin (25) almost stagnated with 2.51 ± 0.23 kPa at d7. TissuCol

was initially softer than both long-term stable fibrin formulations, but the Young's modules raised to 2.85 ± 0.44 kPa during the seven-day incubation accompanied with visible shrinkage of the hydrogel cylinders. The softer RuFib50 resulted in decreased stiffness values of 0.35 ± 0.08 kPa at d7.

For the application as cartilage adhesive at the lateral defect site in the disc/ring model, both the RuFib25 and RuFib50 formulations could be tested, since in this set-up sufficient solidification of both materials for proper handling of the glued constructs was obtained. The immediate bonding strength after push-out testing was 32.04 ± 9.86 kPa for RuFib25 and 42.59 ± 15.32 kPa for RuFib50. The adhesive strength decreased significantly for both tested formulations after 21 days *in vitro* culture. The detected adhesive strength was 11.78 ± 5.16 kPa for RuFib25 and 15.51 ± 3.91 kPa for RuFib50 at d21 (see Figure 23B). MTT staining was performed to assess the chondrocyte viability in the glued constructs. High cell viability of the entire disc/ring construct was observable after MTT staining. In the thin section, no additional induced necrosis could be detected directly at the defect interface and thus in close proximity to the applied adhesive (see Figure 23C).

Histological staining with SafO was performed followed by sectioning of the constructs and microscopical evaluation of the defect interface. In the treated disc/ring constructs a qualitative
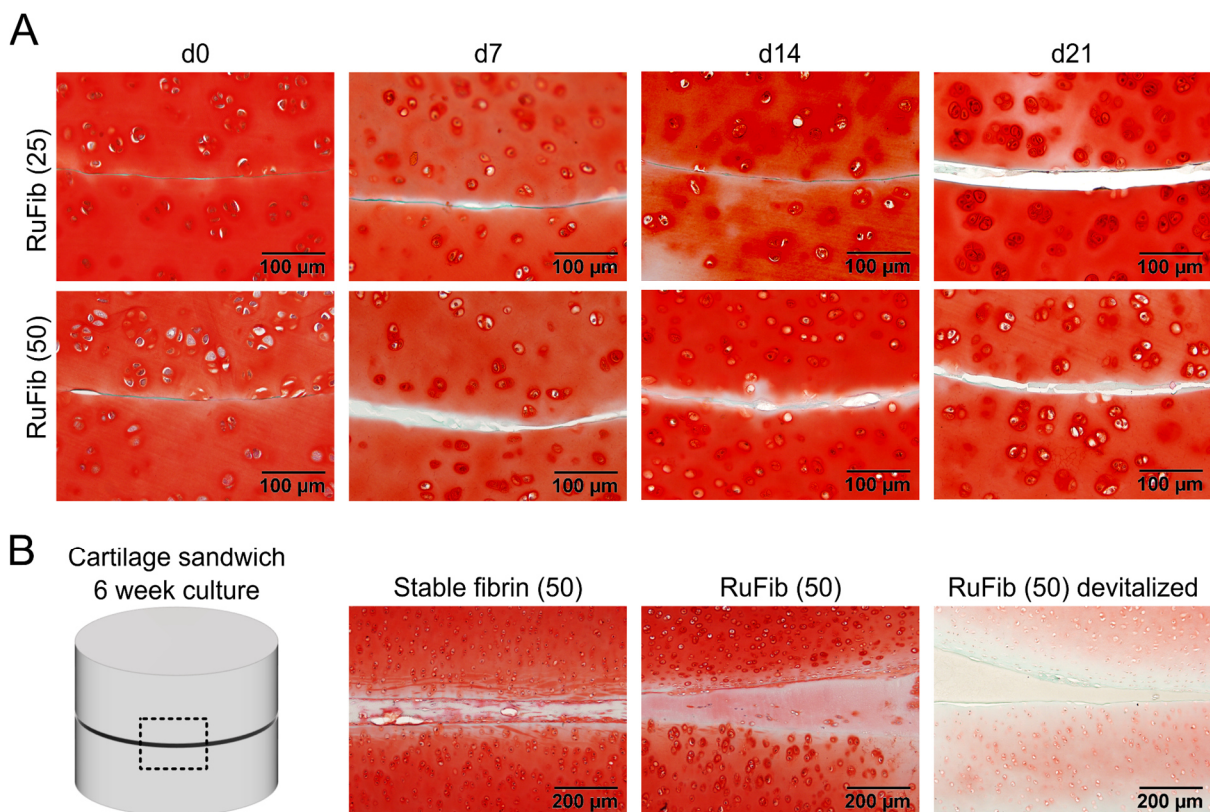


**Figure 24: Histological captures (SafO) of the defect interface after RuFib treatment.**

Disc/ring samples were evaluated directly after fabrication (d0), after seven (d7), 14 (d14) and 21 (d21) days in vitro culture (A) Sandwich construct samples were evaluated after six weeks *in vitro* culture (B).

decrease and to some extent delamination of the adhesive material from the cartilage surface was observable after 21 days *in vitro* culture. No significant deposition of ECM or migration of chondrocytes into the adhesive matrix was evident in cultured disc/ring constructs (see Figure 24A). As an additional approach for histological evaluation, sandwich constructs of 6 mm discs were prepared and cultured *in vitro* over a six-week period. Sandwich constructs were also fabricated with stable fibrin (50) to compare the long-term integration of the different materials in this *in vitro* model. Those constructs were vital after a total cultivation duration of six weeks. In both groups migrating cells from the surrounding native tissue into the respective hydrogel material was visible at the end of the observation period. ECM accumulation in both gap-filling hydrogels was visible. A qualitative overall tissue regeneration was observed in both groups without a clear difference between RuFib50 and stable fibrin (50) (see Figure 24B).

### 4.3.3    Discussion

In Photocrosslinking approaches, photons are absorbed in the presence of an activated photoinitiator and the formation of radicals is stimulated, which in turn covalently crosslink molecules by radical polymerization.

Due to their high reactivity, free radicals have a short half-life, on the order of milliseconds to seconds. However, even within this short lifetime, free radicals react with almost any polypeptide chain in the vicinity, immediately forming new covalent bonds. Free radicals are generally considered harmful because they contribute to cellular aging. However, proteins covalently immobilized by free radicals were found to retain their protein conformation and exhibit higher functionality [308]. This is an important factor for bioadhesives that aim incorporation of biological functions e.g. cell adhesion or coil flexibility capacities from biomacromolecules. In addition, lower local tissue toxicity and inflammation is likely with higher retained protein conformation. Although bioadhesives based on covalent binding of free radicals are promising, the complexity of plasma ovens and the short half-life of radicals themselves (most radicals are likely quenched upon entry into the atmosphere) make this plasma generation method impractical. This means that plasma treatment is a cumbersome and expensive procedure that cannot be performed in the clinical setting. To take advantage of covalent free radical binding and prevent toxic tissue attachment, a mechanism is needed that generates the radicals *in situ* (at the precise time and place where soft tissue binding is desired). For this purpose, radical activation by photoinitiators seems to be the right solution. For the activation of a photoinitiator in photocrosslinking approaches, a light source is required, for which UV light is usually used. Photocrosslinking has far-ranging applications including the development of drug delivery

vehicles, implant coatings, and tissue engineering scaffolds. Photocrosslinking also enables fast processing, as these reactions are often quite rapid. Furthermore, the use of focused light sources and photomasks facilitates exquisite spatial and temporal control of crosslinking reactions. Furthermore, many photoreactions have been proven cytocompatible, which allowed direct photo-encapsulation of cells [146,148].

Many photoactivatable compounds and functional groups that generate free radicals when activated by light, such as azides, diazo compounds, benzophenone, anthraquinone, diaryldiazomethanes, diazirine and psoraline, are known and commercially available. Nevertheless, careful selection of one of these compounds for soft tissue adhesion is not an easy task. The ideal photoactivatable compound should be biocompatible (i.e., have low variability, high purity, and no detectable biological reactivity as determined by biocompatibility testing). Diazirine molecules are considered biocompatible and allow *in situ* formation of a carbene, which can be viewed as a type of free bi-radical, without toxic by-products for relatively harmless covalent attachment to the protein scaffold (e.g. collagen of the cartilage ECM). Dankbar et al. [309] found that amongst several candidates diazirine has the highest photolinking efficiency with the fastest reaction times, which is a very strong argument for its utilization in a bioadhesive. It is rapidly converted to carbene and harmless nitrogen gas when exposed to long wavelength UV light (in the range of about 320-370 nm). The high reactivity of the carbene, which is similar to that of free radicals, allows immediate covalent bonding to a pre-existing C-H bond. This type of C-H insertion is relatively harmless within protein backbones, a fact that makes diazirines popular for photoaffinity labeling to study ligand-protein interactions [310,311]. A diazirine-based mechanism of adhesion has all general benefits of photocrosslinking and accordingly has many advantages over other adhesion mechanisms. For example, cyanoacrylate adhesives and BioGlue® cannot be cured on demand, their polymerization is moisture-sensitive and they have toxic properties (see also Chapter 4.2.4.2). Photoactivatable acrylate or epoxy polymerization-based bioadhesives tend to have high front temperatures (causing thermal damage) and can leave toxic monomer byproducts [312]. The photoactivatable diazirine functional group leaves no monomer byproducts and does not require a separate photoinitiator for cure.

In previous discussed experiments with fibrin glues, a promising long-term colonization with ECM and cells was observed in principle. Via introduction of additional binding sites via diazirine groups, the aim was to obtain additional adhesion capacity to the relatively low intrinsic adhesive property of fibrin without changing the fibrin glue itself and its biological properties. Therefore, an approach was chosen in which the surface of the native cartilage tissue is functionalized with diazirine instead of the polymeric components of the adhesive. Additional functionalization of fibrinogen with diazirine would lead to an altered crosslink density within the adhesive matrix, which in turn would have a strong

impact on the regenerative performance of the fibrin and would not allow comparability with previous results. Heterobifunctional diazirine molecules are commercially available for many research applications including the study of protein:protein interactions, isolating cell surface proteins and preparing labeled probes. Succinimidyldiazirine (SDA) reagents are a new class of crosslinkers that combine proven amine-reactive chemistry with innovative and efficient diazirine photochemistry for the conjugation of amine-containing molecules with virtually any other functional group via the diazirine residue. Six different SDA crosslinkers are commercially available (Thermo Fisher Scientific) that differ in spacer arm lengths between the two different functional groups, ability to cleave the crosslinked proteins, and the presence or absence of a charged group for membrane permeability. For the underlying experiments, Sulfo-NHS-LC-diazirine was chosen, since the negatively charged sulfate group improves water solubility and reduces cell membrane permeability, allowing them to be used for crosslinking extracellular proteins and in theory minimizes cytotoxicity. The longer spacer arm length (12.5 Å) in this structure may support approximation to a binding molecule. The NHS ester group reacts with primary amines at pH 7 to 9 and in this way the Sulfo-NHS-LC-diazirine is bound to the collagen framework of the cartilage to "functionalize" it. The diazirine compartment of the molecule subsequently reacts efficiently with each amino acid side chain or the peptide backbone of adjacent fibrin fibers in the presence of the fibrin glue upon activation with long-wavelength UV light (330 to -370 nm). Theoretically, two adjacent cartilage surfaces can also be directly bonded via this reaction mechanism, but this requires immediate molecular proximity of the collagen fibers, which cannot be assumed for lesions and larger chondral defects.

For integration approaches with small chemical crosslinker molecules ("zero-length process") it was reported that an approximate distance in the magnitude of only $1.3e^{1.7}$ nm is the critical parameter for crosslinking individual collagen molecules and fibrils [291]. The reactive capacity of the NHS functional group to cartilage tissue was demonstrated before and it was also utilized as the adhesive moiety in adhesive hydrogel polymers. In 2010 the group of Jennifer Elisseeff described a chondroitin sulfate-polyethylene glycol adhesive hydrogel (CS-PEG) for cartilage applications. They functionalized the chondroitin sulfate with N-hydroxysuccinimide (NHS) that can react with primary amines to form amide bonds. This reaction facilitates both bonding to the cartilage and polymerization with an amine-functionalized PEG (see Figure 25). In a lap-shear test the adhesive strength of the material with cartilage tissue was shown to be ten times higher than that of fibrin glue. Furthermore, the authors demonstrated good biocompatibility of the material and the possibility to encapsulate cells within the hydrogel [208]. NHS reaction chemistry is thus in principle suitable to achieve strong adhesion to cartilage in a biocompatible context. However, the approach of Strehin et al. described above differs in that a synthesized polymer is used as the adhesive matrix and both the adhesion and cohesion connections

are completed in one step via NHS. For an advanced conjugation of the cartilage with subsequent on-demand reactivity, it requires a second functional group, which in our approach is enabled by the light-activated diazirine.
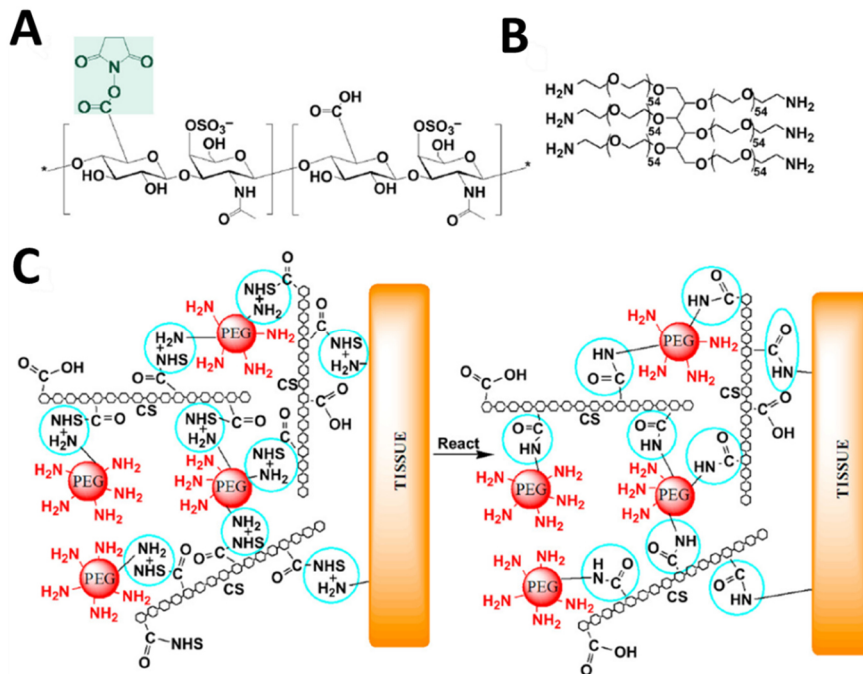


**Figure 25 Tissue adhesion mechanism via NHS functional groups.**

The NHS activated carboxyl groups of CS-NHS (A) react with the primary amines of PEG-$(NH_2)_6$ (B) and the primary amines of proteins in tissue (C, reactive groups circled). Modified with kind permission from[208].

In a similar approach, Li et al. reported a design of a two-layer adhesive based on modified alginate and chitosan. The adhesive surface layer can bond to the tissue substrate through electrostatic interactions, covalent bonds, and physical interpenetration. In cylindrical defects of explant porcine cartilage rings filled with the adhesive material it was possible to recover the compressive properties of the healthy native cartilage. However, interfacial bridging to the adhesive material relied on the cartilage priming with the chemical crosslinkers EDC/Sulfo-NHS to covalently bind their materials [218].

The push-out experiments with disc/ring cartilage constructs have shown that conjugating the cartilage surface with diazirine prior to treatment with fibrin glue can significantly enhance the adhesion strength. However, additional enzymatic pretreatment with chondroitinase ABC was necessary to allow considerable binding of the Sulfo-NHS-LC diazirine to the cartilage. This enzyme is capable of specifically digesting GAG components in the cartilage matrix and the results suggest that present GAG prevents NHS binding to the collagen scaffold and thus additional adhesion enhancement. Enzymatic digestion with chondroitinase ABC alone was able to significantly increase

the adhesion strength of fibrin-glued constructs as well as control constructs. Light-induced diazirine binding was then able to further enhance this effect, and the combination of chondroitinase ABC digestion, diazirine conjugation of cartilage, and fibrin glue achieved the highest adhesion strength in the experiment. Compared with unglued controls and fibrin glue alone, the adhesion force was significantly increased and multiplied. The histological images support the outcome of the biomechanical analysis and indicate improved gap bridging when enzymatic digestion alone or in combination with the diazirine linker were applied. Furthermore, the performed Live/dead and MTT imaging indicated that no cytotoxicity was introduced by neither the enzymatic treatment nor the diazirine coupling followedby the corresponding UV-irradiation. However, the necessary digestion step makes clear that the GAG in the native tissue functions as an anti-adhesive. Despite the spacer arm of the utilized Sulfo-NHS-LC-diazirine molecule, the chain length may be too short to overcome distances to the binding partner. The same effect was observed in another photochemical bonding approach on cartilage tissue by Sitterle et al. [211]. This group also utilized chondroitinase ABC treatment in combination with a photosensitizer molecule and hypothesized that enzymatic surface treatment of the tissue for proteoglycans removal and collagen exposur was required to form a photochemical bond to articular cartilage tissue. In contrast, meniscal tissue, with its significantly lower proteoglycan content, required no such modification. Furthermore, this group also observed that while chondroitinase ABC treatment was consistently effective, treatment with hyaluronidase did not facilitate tissue bonding. Besides for adhesive approaches, chondroitinase ABC was investigated in the context of cartilage regeneration before. Lee et al. demonstrated the utility of digestive rinses for improving cartilage integration by showing that treatment of cartilage explants with chondroitinase ABC for 5 to 15 minutes leads to enhanced chondrocyte adhesion, as measured by a micropipette micromanipulation system [313]. The biosafety of such enzymatic treatments has been investigated by Quinn and Hunziker with regard to changes in cell density, structure, and cell-mediated matrix deposition that result from chondroitinase ABC treatment [314]. While chondroitinase ABC exposure did appear to further decrease cell densities of the cartilage tissue within 100 µm of the defect surfaces, the decrease was small in relation to the effect of the defect itself and was contained to the area immediately adjacent to the defect (within 100 µm), demonstrating that digestive treatments can be spatially controlled to break down matrix within the zone of chondrocyte death. This is also consistent with our results, where no additional cell death was evident except for the inevitable necrotic margin mechanically induced by the punching defect. The ECM loosening effect by enzymes may theoretically also provide additional benefits for long-term cartilage integration by facilitating cell migration locally and enhancing repopulation of defects [8].

Despite the promising results and the potential favoring of cell repopulation by enzymatic treatment, there are some severely limiting factors to consider for the use of the combination presented here for adhesion enhancement. The Sulfo-NHS-LC-diazirine is actually used on a small scale in research for conjugation of certain proteins and antibodies. For such purposes, only small amounts of this cost-intensive molecule are needed. In contrast, much larger amounts of the molecule are needed to achieve full-coverage coating of the cartilage surface in larger defects. The experiments carried out are initial proof-of-concept experiments. In order to investigate the adhesive mechanism and its influencing factors (e.g. the interplay between different concentrations of diazirine and enzyme) in detail , a large number of experimental groups would be required. The number of samples needed for statistical significance and different experimental groups would increase the complexity. The replicability of the results would also have to be checked. The required scale of downstream experiments e.g. with different incubation times and long-term culture times limits feasibility of further investigation due to ecological concerns. The combination of the two costly compounds diazirine and chondroitinase enzyme is not economically available in sufficiently large quantities. In fact, even under consideration of upscaling factors, the high cost for this approach is also a huge obstacle to commercial clinical use. The scientific focus on more economical alternatives was recognized more goal-oriented, which is why other approaches were pursued further in this thesis instead. Nevertheless, the diazirine group with its versatile reactivity remains a very promising candidate for the development of novel tissue adhesives. One option to be investigated proactively for cost reduction in experimental approaches would be the replacement of the enzyme used. Commercial production of chondroitinase is usually of recombinant nature and costly. Trypsin is an abundant enzyme and could be a cost-effective alternative, especially since it has already been shown that short-term trypsin digestion can be used to selectively remove GAG from cartilage tissue [197].

The check for cytotoxicity by Live/dead and MTT staining was without any abnormalities. However, a large number of other toxicologically effects are relevant for such novel organic molecules without experience of safe clinical application. Surgical adhesives are generally classified as medical devices with long-term patient contact and the biological safety assessment of various endpoints must be checked in accordance with the ISO 10993 standard series. For the diazirine molecule used, no toxicological data are available in the prominent databases (e.g. European Chemicals Agency (ECHA) Database, US National Library of Medicine (NLM), OECD Chemical Database etc.) on the toxicological risk for local effects (e.g. irritation and sensitization), systemic toxicities and potential mutagenicity. In order to get a rough estimate of the potential toxicity of a substance, open source *in silico* tools such as ToxTree can be used. On the basis of the molecular structure, a classification according to Cramer can be carried out in order to derive limit values for daily exposure in humans [315]. Integrated models

of the quantitative structure-activity relationship (QSAR) can help to identify structure-related risks of a molecule. According to ToxTree analysis, non-genotoxic carcinogenicity cannot be ruled out for the sulfo-NHS-LC-diazirine. In addition, the Cramer prediction classified the compound as Cramer Class III, for which significant toxicity has to be assumed without the availability of further data. Tolerable intake amounts of released substances can be derived in accordance to the regulatory requirements of ISO 10993-17. For Cramer Class III substances daily exposures are to be restricted to a maximum of 90 µg/day for adult, 15 µg/day for pediatric and 5.25 µg/day for neonatal patients. Within the current experiments 10 µl of a 10 mM sulfo-NHS-LC-diazirine solution were applied to the lumen of a disc/ring construct. Based on the molecular weight of 440.4 g/mol this correlates to an applied amount of 44.04 µg for which a toxicological risk can therefore not be excluded, especially since no information on release kinetics are available and also larger cartilage defects that require higher amounts of this compound may need to be treated in clinics. Accordingly, further pre-clinical evaluation would need to be gathered to allow biocompatibility assessment and a safe clinical application of this approach.

The attachment of diazirine groups to larger carrier molecules is a possible approach in which potential toxicological properties could be achieved through the reduced ability of the molecule to migrate within the tissue. Diffusion of a reactive substance into the inner tissue away from the defect interface also reduces the presence of essential components for the adhesive reaction and thus the adhesive force. In addition, the density of functional groups on polymer backbones, degradation rates and other parameters can be controlled more specifically using chemical syntheses in suitable polymeric building blocks (see also Chapter 4.4). Grafting of diazirine molecules onto polymer chains offers many new possibilities for biomaterials design and processing. Good example of such technology was reported by Raphel et al. [316]. The Authors have demonstrated that diazirine conjugated elastin-like proteins can be produced in different forms such as micropatterned surfaces and porous scaffolds. In a further publication plasma post-irradiation grafting made it possible to graft diazirine onto PLGA substrates [317]. The polymeric adhesives were biomechanically tested on pre-wetted *ex vivo* swine aortas and adhesive strengths of up to 500 mN/cm² were achieved that correlate to 5 kPa, which is roughly in the same dimension of fibrin glue. Another study reported a hydrogel bioadhesive system based on poly amido amine (PAMAM) dendrimer, conjugated with diazirine. The diazirine grafting to the surface amine groups of PAMAM was achievable in a one-pot synthesis. The adhesive performance was tunable and as expected, adhesion strength and storage modulus both increased with diazirine conjugation percentage. Maximum adhesion strengths of almost 40 kPa to porcine blood vessels were obtained [318]. However, a direct comparison of the adhesive strength with the results presented here cannot be made, as there are significant differences between the tissues used as substrates. The severely higher proportion of water in the cartilage usually makes the bonding of adhesive

components more difficult and different mechanical properties must be taken into account. Nonetheless, it has been shown that diazirine bound to polymer chains can be a versatile approach for tissue adhesives and the door is open to developing potent cartilage adhesives, taking into account the relevant adaptation requirements.

In order to test the advantages of a photocrosslinking mechanism with another approach and to obtain as much overlap as possible with the previously tested fibrin glues, a way to crosslink fibrinogen using a photoinitiator instead of thrombin was investigated. Usually, fibrinogen, the precursor molecule of fibrin, is crosslinked by means of thrombin and factor XI according to the physiological model during blood clotting to form hydrogels and tissue adhesives. This reaction occurs spontaneously as soon as the components are mixed together, with only the thrombin concentration having a significant influence on the speed of curing. To achieve on-demand curing of a hydrogel, photoinitiators are often used [316,319–322]. Most commonly UV light-activated crosslinking using the photoinitiator Irgacure 2959 is applied [221]. However, this offers several disadvantages: it is oxygen sensitive, requiring the use of airtight barriers, which is clinically impractical, and the use of UV light carries the risk of inducing DNA damage in cells [323]. For these reasons, other crosslinker systems that absorb light from the visible spectrum are being investigated, for example, lithium phenyl 2,4,6-trimethylbenzoyl phosphinate (LAP) [324], eosin [325], or riboflavin [326]. However, these photoinitiators may possess disadvantages in terms of handling, reactivity, or toxicity [324,326]. Another crosslinker system consists of a water-soluble ruthenium (Ru) photoinitiator and sodium persulfate (SPS) and is activated by light from the visible spectrum. Lim et al. demonstrated that higher cell viability and metabolic activity can be achieved with this system, compared to UV light-activated systems such as Irgacure 2959, even at high Ru/SPS concentrations [327]. The method and mechanism behind it was first described by Fancy and Kodadek [328] and involves two steps: The $[RuII(bpy)3]^{2+}$ complex absorbs photons in the visible spectrum. Photolysis places it in an excited state where it can donate an electron to the persulfate, resulting in cleavage of the O-O bond. The products are the oxidized Ru(III), the sulfate radical, and a sulfate anion. In a second step, Ru(III) induces the formation of a tyrosine radical; polymerization is initiated by oxidative bonding of two tyrosines to form a di-tyrosine. This reaction process can be utilized to crosslink tyrosines originating from proteins within a hydrogel precursor solution, for example gelatin, collagen, or even fibrinogen [329]. This not only allows polymerization of a proteinaceous gel but also adhesion by means of covalent bond formation, since tyrosines from surrounding tissue are simultaneously targeted in the reaction.

Fibrinogen has already been used as bioactive supplement in hydrogel formulations [256,319,330], but the use of ruthenium as photoinitiator to crosslink fibrinogen fibrils directly eliminates the need for additional use of other polymeric hydrogel ingredients. In contrast to collagen/gelatin and other

fibrillar proteins, fibrinogen has a relatively high content of tyrosine. This is a prerequisite for adaptations of the mechanical strength via the crosslink density without the necessity of additional chemical modification to the protein. Two of the three protein chains of fibrinogen are particular rich in tyrosine (β-chain 4.9 % tyrosine; γ-chain 5.6 % tyrosine; α-chain 0.65 % tyrosine) and it was also reasoned that, because of its propensity to interact with other extracellular matrix proteins, fibrinogen is a superior candidate for ruthenium crosslinked proteinous adhesive hydrogels [235,331,332]. Elvin et al. found the mechanical properties of dumbbell-shaped strips of cross-linked fibrinogen compare favorably with the strength of a fibrin gel formed by treatment of fibrinogen (fibrinogen content 70 mg/ml) with thrombin/CaCl$_2$/Factor XIII, which had a tensile strength of 28 kPa and a strain at break of 104 %. The photochemically crosslinked fibrinogen material was stiffer and slightly less elastic than the comparative fibrin gels. In addition, the authors hypothesized that the binding capacities of fibrinogen to both fibronectin and vitronectin as well as collagen contributes to improved adhesion since fibrinogen chains are highly structured and relatively constrained in the degree of molecular associations possible between α-, β-, and γ- subunits in the native fibrin. It can be speculated that these intermolecular protein associations in combination with subsequent covalent dityrosine crosslinking of fibrinogen to various ECM proteins, could account for the superior adhesive properties of this photochemically-cured fibrinogen tissue adhesive. However, although the authors reported improved adhesion strength compared to ordinary fibrin glue, a direct transfer of the results to the performance as cartilage adhesive cannot be made. It should again be noted that the tissue type used can have an enormous influence on the adhesion strength and, in addition, the capacities for cartilage remodeling must also be appropriate. The group of Elvin et al. used relatively high fibrinogen concentrations (mostly 100 mg/ml) for application as a photo-crosslinked adhesive. In order to transfer the reported successful adhesion and crosslink mechanism to the application on cartilage tissue, a fibrinogen concentration of 25 and 50 mg/ml (named RuFib25 and RuFib50) were chosen in our experiments, which corresponds to the same final fibrinogen concentrations in the previously tested long-term stable fibrin glues (stable fibrin (25) and (50)). The aim was to determine whether the tyrosine density of the fibrinogen at those concentrations was sufficient to achieve both stable adhesion to the native cartilage and leads to sufficient intrinsic mechanical stability of the gel. In the mentioned fibrin gels with those fibrinogen concentrations, good repopulation of the defect interface with chondrocytes and newly synthesized ECM was observed in the disc/ring model (see Chapter 4.2). The exchange of the reaction mechanism at constant protein concentration thus theoretically allows a direct comparison of both approaches with respect to biological regeneration in addition to biomechanical properties.

To get a first impression of the material stability, a small group of different cylindrical test gels was prepared and observed over seven days in PBS to detect possible hydrolysis. The Young's modulus was determined from the gels initially and after seven days (see Figure 22). The results allow interpretation of a trend, but reproducibility and statistical significance would need to be tested in the future with a higher number of samples. For long-term stable fibrin gels, a higher fibrinogen content (25 vs. 50 mg/ml) resulted in higher strength, as was expected. However, a more pronounced reduction from the Young's modulus was also seen with stable fibrin (50). TissuCol was initially softer than both long-term stable fibrin formulations but hardened during the seven-day incubation, possibly due to shrinkage of the gel because it is not a dimensionally stable formulation. Relative to the fibrin gels, RuFib50 is a rather soft gel, which may indicate a lower crosslink density but may also be an advantage for cell invasion. Unfortunately, despite that for RuFib25 gelling was observable, the hydrogels were to soft to allow proper handling and determination of the Young's modulus. Incubation in PBS further worsened hydrogel integrity and accordingly no mechanical data could be obtained. In contrast to the fabrication of bulk hydrogels, application at the defect interface of both RuFib formulations resulted in stabile bonding of the cartilage disc, which allowed handling, biomechanical testing and further processing of the constructs. Because of the small volume in the gap and in proportion the large reaction surface of the native cartilage with its collagen content, it was assumed that sufficient reaction partners are present to obtain a cohesively stable adhesive matrix as well.

Dityrosine bonds that are also the resulting linkage in the applied ruthenium mechanism are easily formed *in vitro* via multiple physiologically relevant reactions, that are amenable to the incorporation of cells or *in situ* crosslinking for tissue regeneration. The reactivity of the phenolic side chain of the amino acid tyrosine, and its unique chemical reactivity, fosters its involvement in a number of molecular interactions. It has been known for decades that dityrosine bonds are a key component to many biopolymer materials in native tissues, however, these motifs are exploited in the development of new biomaterials only since few years [333]. While dityrosine-crosslinked proteins have been documented, the consequences of the dityrosine link on the structure and function of the thus modified proteins are yet to be understood. Tyrosine residues on the surface of the protein can form both intra- and intermolecular bonds. It was demonstrated that the structural stability of dityrosine-crosslinked molecules is lower than that of the parent native monomer [334]. However, the biphenyl bond that links two tyrosine molecules is generally acknowledged as chemically quite stable. In the marine environment for example such substrates can be degraded enzymatically only by select bacterial populations or through photoinduced scission of the biphenyl bond [335]. A precise cause for the decrease of adhesion strength in RuFib after *in vitro* culture cannot be stated with certainty. Even if the dityrosine bond has a high resistance to hydrolysis and enzymatic degradation, it cannot be

excluded that the mechanical stability of the individual fibrinogen chains suffers and thus the mechanical resilience of the adhesive matrix was reduced. It is therefore also conceivable that the biomechanically determined force values were limited by a cohesive rather than an adhesive failure.

Similar to previously conducted experiments with fibrin glue, the tissue regeneration at the glue interface is of particular interest for a potential suitability as cartilage glue. In histology it was observed that over a period of 21 days *in vitro* culture there was a qualitative decrease in defect bridging. Delamination of RuFib25 and RuFib50 adhesives from cartilage tissue was evident. Despite the lower stiffness of the RuFib material compared with fibrin, no significant deposition of ECM or migration of chondrocytes into the adhesive matrix was evident in cultured disc/ring constructs. Again, the altered structure of the fibrinogen molecule due to the formed intra- and intermolecular dityrosine bonds may be a trigger for the decrease in biological interaction with ECM components or cell adhesion receptors. As an additional approach for histological evaluation, sandwich constructs of 6 mm cartilage discs layered with the adhesive were prepared in one experiment and cultured *in vitro* over a six-week period. In contrast to the disc/ring construct, approximately twice the amount of native cartilage tissue per composite is transferred to *in vitro* culture. However, this also changes the direct comparability, since it must be assumed that secreted ECM components and also, for example, enzymes can have a different effect on adhesive metabolism or its colonization. It should also be noted that the interface considered in the sandwich model is not a lateral but a sagital defect and that cartilage regeneration may differ fundamentally, e.g. because of the different orientation of collagen fibers in the tissue. In principle, sagital cartilage defects are of higher clinical relevance, but here the sandwich model was utilized because of the advantage for easy application of larger adhesive volumes and an adjustable gap size. This, in turn, may facilitate histological assessment of cartilage regeneration and interaction with the bulk material. However, to allow a direct comparison of the RuFib50 material, sandwich constructs were also made with stable fibrin (50). In the evaluated sandwich constructs, the range of the defect width was significantly increased compared to the disc/ring constructs. After six weeks of culture, the sandwich constructs of both groups were vital and a very clear cell migration from the native tissue into the glue-filled gap, as well as ECM accumulation in the glue hydrogel were visible. Although there was no significant difference between fibrin (stable fibrin (50)) and RuFib50, these results show that ruthenium crosslinking does not, in principle, destroy the regenerative capacity from fibrinogen. The underlying kinetics and differences to fibrin glue concerning cell and ECM interactions in the lateral defect of the disc/ring model remain unknown and would need further investigation.

However, the good biocompatibility of the adhesive materials and the visible-light-induced reaction mechanism attracted positive attention. Staining with MTT showed very good viability of the entire disc/ring construct in both RuFib variants. In the thin section, no additional induced necrosis

could be detected directly at the defect interface and thus in close proximity to the applied adhesive. This reflects the findings in similar applications where identical concentrations of ruthenium and SPS were used. Since it is a very strong oxidizing agent, SPS can be assumed to be the most critical ingredient in terms of compatibility. However, SPS is tolerated by exposed cells even at levels far exceeding than used in the protein adhesive formulation [235]. Kodadek et al. mentioned that the ruthenium complex is of cell permeant nature but that the persulphate anion is of cell impermeant nature [336]. Since both of these water-soluble reagents are either consumed during the reaction, or diffuse from the hydrogel following crosslinking, the local concentrations of the low molecular weight components would be expected to drop rapidly when applied *in vivo*. In several *in vivo* studies, no compound-related incompatibilities were reported for those glue compartments [329,331,332,337].

From a toxicological perspective, in contrast to organic crosslinkers (e.g. like the described sulfo-NHS-LC-diazirin) the metabolic pathways and clearances of inorganic compounds are better characterizable, which allows derivation of allowable threshold limits for compounds designated to a distinct element. Within the ICH Q3D guideline the toxicological data for elemental compounds is summarized and permitted daily exposure values (PDEs) for medical and pharmaceutical products are reported with regard to different exposure routes [338]. For ruthenium compounds no health hazards are to be expected for the parenteral exposure of up to 10 µg/day. For long-term exposures above this daily limit, toxicological risks cannot be excluded. Based on the molecular weight of the ruthenium complex (640.53 g/mol and the final molarity of 2 mM) an adhesive volume of 500 µl would exemplary contain approximately 640 µg of the ruthenium complex. Accordingly, further investigation would be required if potentially hazardous amounts of this compound can migrate out of the applied adhesive under its clinical use and get exposed to the patient in order to exclude systemic and genotoxic effects. Unlike other photoinitiators, ruthenium is not excited via UV but with light in the visible-blue wavelength range. This means that no harmful effects from energy-intensive radiation are to be expected. No special equipment is required and curing can also be carried out via ordinary plant growth lamps. The experiments performed clearly show the potential of ruthenium crosslinking as a basis for adhesion chemistry. The mechanism also allows the easy use of abundant proteins such as fibrinogen and collagen or gelatin, whereby their versatile biological and mechanical advantages can be used directly in an adhesive material without complex synthesis steps. The irradiation with visible light results in fast on-demand curing with good adhesion capacities, which addresses limitations of current fibrin sealants that typically have relatively slow curing times and relatively low bonding strengths. The use of higher concentrated fibrinogen in combination with ruthenium crosslinking can potentially enhance mechanical properties, thus affecting integrative repair in the disc/ring cartilage construct. Appropriate experimental approaches have been pursued within our research group and

are described accordingly in the context of another doctoral thesis (see dissertation of Johannes Maximilian Meister [339]).

The versatility of the dityrosine bond and the inspiration from crosslinking reactions in the byssus thread of mussels and in the chitin shell of insects has also stimulated researchers to develop a tissue adhesive that is light-inducible and achieves good adhesion results even on moist tissue. Jeon et al. reported a mussel protein-based bioadhesive (LAMBA) crosslinked via a ruthenium complex. Compared to fibrin, LAMBA exhibited substantially stronger bulk wet tissue adhesion accompanied by good biocompatibility in both *in vitro* and *in vivo* studies. The glue was shown to be easily tunable and to allow an effective on-demand wound closure that facilitated wound healing [340]. In naturally occurring dityrosine forming, functional transformations include the enzymatic conversion of tyrosine into L-3-4-dihydroxyphenylalanine (DOPA), which acts as a precursor for crosslinking with other amino acid residues and provides adhesion to surfaces. The general mechanism of dityrosine formation involves removal of the hydrogen atom from the hydroxyl group on the phenoxy ring to form a free radical. For the DOPA-intermediate mechanism, oxidative conditions are required to generate a free radical allowing for the coupling of the residues [333]. Therefore, in approaches utilizing DOPA chemistry for adhesive formulations oxidizing chemicals are most frequently used in contrast to ruthenium crosslinking. However, DOPA can be easily attached to different synthetic polymeric molecules which offers a great toolbox for adapting an adhesive hydrogel. Such an approach was also undertaken in the context of this work and is discussed in detail in Chapter 4.4. In addition, synthetic hydrogel compartments can be loaded with drugs and other active proteins. It was only recently shown that chemical synthesis steps can also be used to attach antibacterial agents to hydrogel components, thereby improving wound healing [341]. The connection of chemically modifiable polymers with the properties of fibrillar proteins is therefore probably the most promising approach to combine targeted adaptation options and biological functionalities in adhesive hydrogels.

## 4.4 Synthetic Polyoxazolines Functionalized with Catecholic Adhesion Moieties and Equipped with Tunable Degradation for Cartilage Integration

As discussed in the previous chapter, chemically modifiable polymers possess various benefits that can be utilized for adhesive material formulations. The versatility in the design opportunities for polymeric backbone molecules promise adaptability to specific requirements like adhesion mechanism and strength, mechanical stability and cell interaction. The goal of the following chapter was to

investigate the potential for lateral cartilage repair of functionalized and modifiable POx polymers especially in combination with fibrinogen as bioactive agent, similar to prior experiments.

Parts of this chapter have been published in:

Oliver Berberich, Julia Blöhbaum, Stefanie Hölscher-Doht, Rainer Meffert, Jörg Teßmar, Torsten Blunk, Jürgen Groll; Catechol-modified Poly(oxazoline)s with Tunable Degradability Facilitate Cell Invasion and Lateral Cartilage Integration, Journal of Industrial and Engineering Chemistry 2019, 80, p. 757-769. Copyright © 2019 The Korean Society of Industrial and Engineering Chemistry

Data and excerpts from the publication are used with the kind permission of the journal and are described in the following.

## 4.4.1    Hydrogel Preparation

Chemical synthesis and potential design possibilities for POx polymers was conducted in cooperation with the Department for Functional Materials in Medicine and Dentistry (FMZ), University Hospital Würzburg. The chemical synthesis was part of a chemistry PhD thesis and details were published elsewhere [241,342].

Vinyl side chain functional poly(2-alkyl)oxazoline copolymers were synthesized by randomly copolymerizing MeOx or EtOx with ButEnOx in a microwave reactor. The polymers were successfully functionalized at the side chain double bond via thiol-ene reaction. Those intermediate products were then further functionalized with a self-synthesized catechol with protected hydroxyl functionalities. The protected catechol building block was synthesized with a free carboxylic acid that could react with hydroxyl or amino side functional polymers creating ester or amide linkages between the polymer side chain and the catechol moiety.

Under the presence of excess catechol and reagents the side chains could be functionalized with the protected catechol molecule to a degree of 58 to 70 %. The synthesis for the MeOx copolymers was slightly adapted by means of incorporating an additional carboxylic side functionality due to the high hydrophilicity and the accompanied limited binding of the catecholic dopamine residue. With this approach, 85.4 % of all side chains could be successfully functionalized with dopamine. Here, it was observable that it played a crucial role whether MeOx or EtOx is used as co-monomer regarding the solubility of the final catechol-functionalized copolymer. The catechol moiety increases the overall

hydrophobicity of the polymer so that synthetization of water-soluble polymers with a catechol functionalization was reduced based on the less hydrophilic co-monomer EtOx.
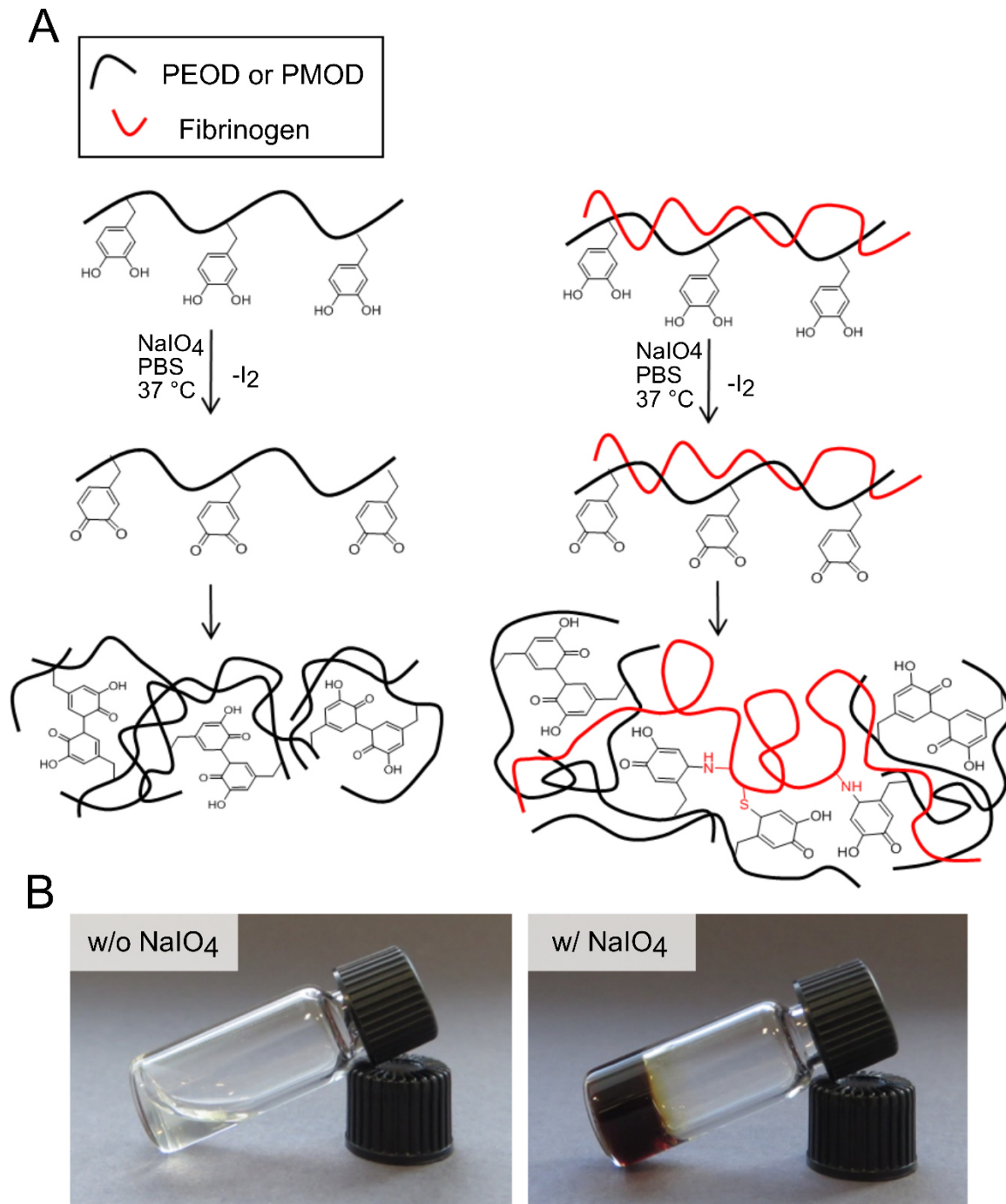


**Figure 26: Hydrogel formation mechanism of hydrogels based on catechol-functionalized POx.**

(A) Reaction scheme of hydrogel formation using catechol-functionalized POx polymers either alone or in combination with fibrinogen using sodium periodate and (B) hydrogel solution before (colorless, liquid) and after addition of sodium periodate (brown, solid).

**Table 9: Overview of synthesized catechol functional POx availalbe for hydrogel formulations.**

| Polymer Precursor | No. of repeating units | % Vinyl functionality | % Catechol functionality | Catechol chemistry | Abbreviation |
|---|---|---|---|---|---|
| PEtOx-*co*-ButEnOx | 91.5 | 6.6 | 4.6 | amide | PEOD$_{amide}$ |
| PEtOx-*co*-ButEnOx | 91.5 | 6.6 | 4.3 | ester | PEOD$_{ester}$ |
| PMeOx-*co*-ButEnOx | 79 | 10 | 8.7 | amide | PMOD$_{amide}$ |
| PMeOx-*co*-ButEnOx | 79 | 10 | 5.3 | ester | PMOD$_{ester}$ |

For initiative evaluation of the hydrogel formation capacity, the different catechol-functionalized POx polymers were used to form hydrogels either with or without addition of fibrinogen to the precursor solutions under oxidative conditions using sodium periodate (NaIO$_4$) in PBS (see Figure 26). Starting from the colorless precursor solutions, the hydrogel formation was initiated by the addition of colorless NaIO$_4$, the color immediately changed to brown as the catechol groups were oxidized and NaIO$_4$ was reduced to iodine. The formation of the hydrogel network took place within less than three minutes.

## 4.4.2    Mechanical Characteristics of Hydrogels

Hydrogels with and without fibrinogen were prepared in PBS using NaIO$_4$ as oxidizing agent. To determine the influence of fibrinogen on the elastic modulus and to evaluate the right ratio of polymer to fibrinogen for the intended application, hydrogels with 12.5 w/v% PEOD$_{amide}$ or PMOD$_{amide}$ only as well as 5, 7.5 and 10 w/v% PEOD$_{amide}$ or PMOD$_{amide}$ combined with 5 w/v% fibrinogen (denoted as PEOD-Fib and PMOD-Fib, respectively) each were prepared. During mechanical testing, it was observed that hydrogels without fibrinogen were less elastic than those containing 5 w/v% fibrinogen and were already destroyed after compression to 69 % of their original height (see Figure 27A).

The Young's modulus of the hydrogels with 12.5 w/v % pure synthetic polymer was 9.7 ± 0.6 kPa for PEOD and 49.0 ± 9.1 kPa for PMOD in contrast to 6.9 ± 2.4 kPa for 7.5 % PEOD-Fib and 15.3 ± 2.2 kPa for 7.5 % PMOD-Fib. These values show on the one hand that the almost doubled functionalization degree of the more hydrophilic PMOD (8.7 % catechol), compared to PEOD, results in gels which are five times stiffer. On the other hand, the addition of fibrinogen increased the elasticity, as expected, which obviously impacted the hydrogels made of PMOD to a greater degree than those based on PEOD. Compositions of only 5 w/v % PEOD-Fib were too soft to be analyzed. Hydrogels with the same composition, but based on PMOD were stable enough to be characterized and displayed a Young's modulus of 6.2 ± 0.7 kPa. As to be expected, the elastic modulus could be further increased using 10 w/v % polymer. 10 % PMOD-Fib hydrogels became rather stiff with a modulus of 45.1 ± 3.8 kPa compared to 10 % PEOD-Fib with a modulus of

12.5 ± 2.1 kPa (see Figure 27B). Based on these results, we decided to continue our experiments with the formulation containing 7.5 % of the synthetic polymers and 5 % fibrinogen as these hydrogels had shown an adequate elasticity and stability whilst keeping the material content as low as possible.
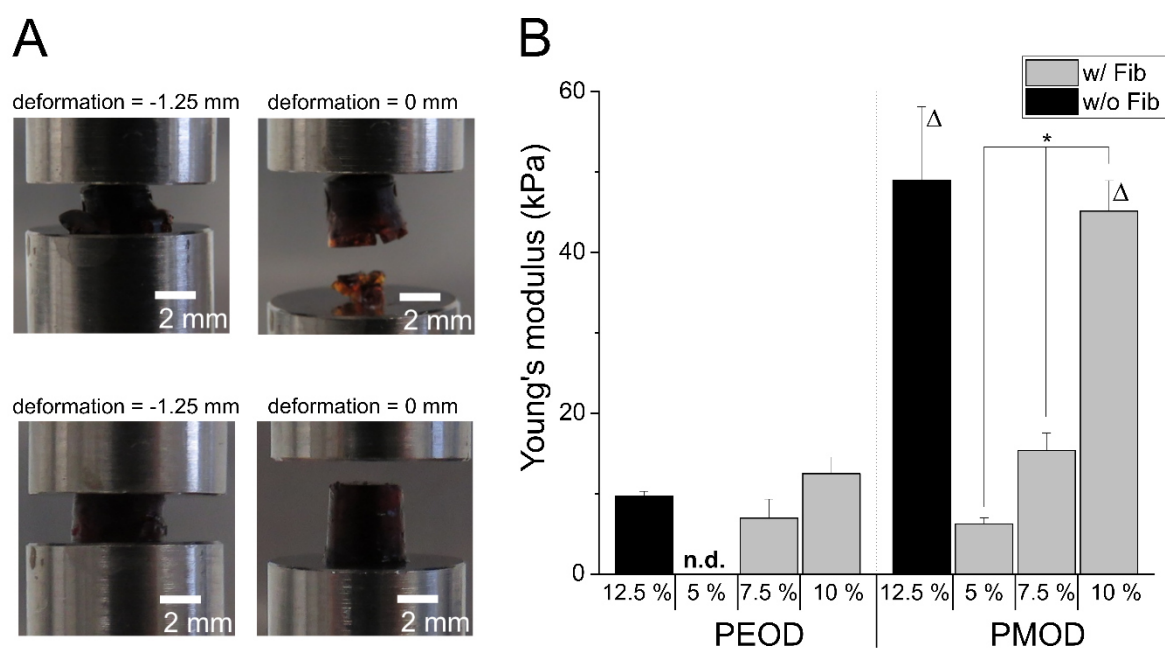


**Figure 27: Compression specification of hydrogels based on catechol-functionalized POx.**

A) Hydrogel with 12.5 w/v % mass content consisting of only synthetic polymer (top) and with 5 w/v% fibrinogen (bottom) illustrating an increased elasticity due to incorporation of fibrinogen and B) Young's moduli of PMOD or PEOD with and without fibrinogen after 24 h incubation at 37 °C. Because hydrogels were too soft, values of 5 % PEOD-Fib hydrogels could not be determined (n.d.) Data are presented as means ± standard deviation (n=3). (* = p<0.05 between groups of different concentrations, and Δ = p<0.05 between PEOD and PMOD of equal concentrations).

## 4.4.3    Tunable Hydrogel Degradation

For the degradation study hydrogels with 7.5 % PEOD-Fib containing 0, 25 and 50 % PEOD$_{ester}$ in the polymeric phase were prepared and incubated in PBS at 37 °C for 21 days. Precursor solutions solely consisting of PEOD$_{ester}$ showed instant clotting at the pipet tip used to transfer the NaIO$_4$ solution for initiation of crosslinking. Similar problems occurred for other hydrogels consisting of more than 50 % PEOD$_{ester}$. Moreover, up to 50 % PEOD$_{ester}$ content in the polymer phase of the gels, no significant changes in swelling and gel morphology could macroscopically be observed over a time period of three weeks, while gel specimens completely consisting out of PEOD$_{ester}$ disintegrated to a large extent (see Figure 28). Due to their rapid loss in shape fidelity, it was also not possible to record the change in Young's moduli over time for compositions with more than 50 % ester polymer.
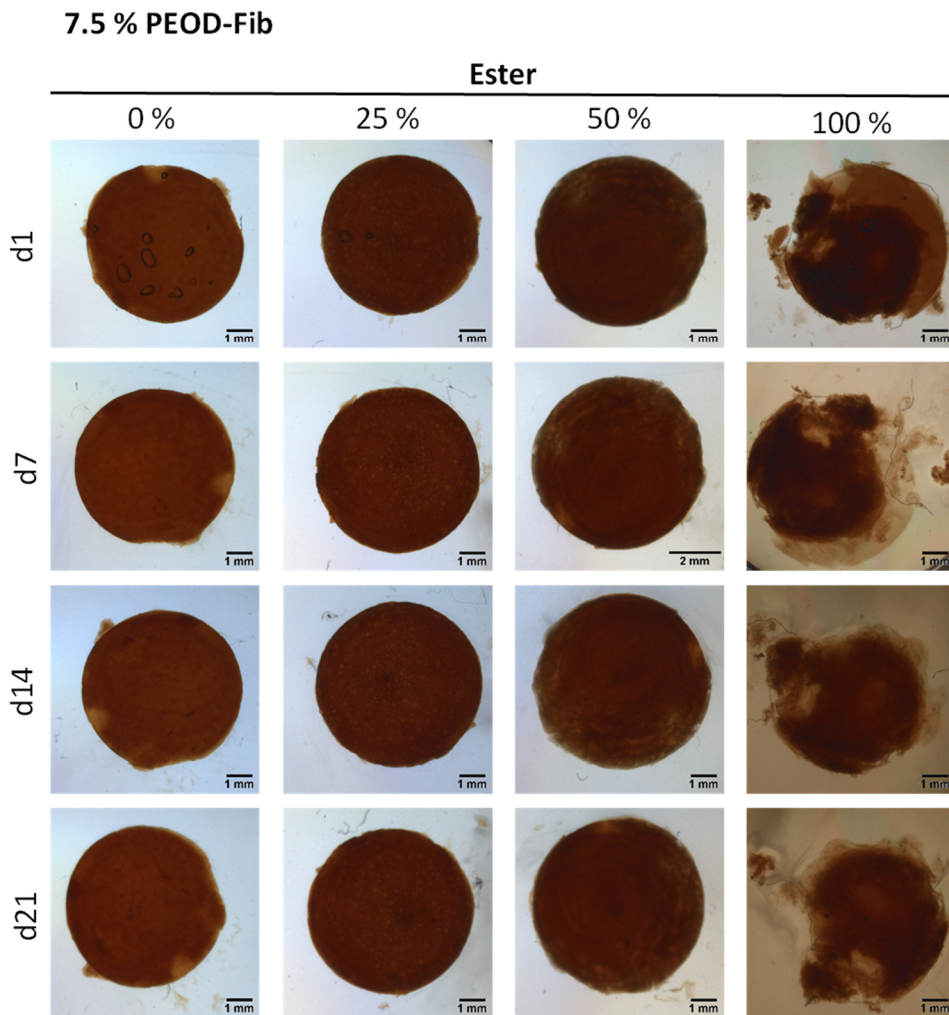
**7.5 % PEOD-Fib**



**Figure 28: Macroscopical captures of cast 7.5 % PEOD-Fib hydrogels with different concentrations of PEOD$_{ester}$.** Samples were evaluated after d1, d7, d14 and d21 in PBS at 37 °C. All hydrogels showed initial swelling. The higher the concentration of PEOD$_{ester}$ the more prominent is the mass loss due to hydrolysis over time

For this reason, quantitative degradation studies were conducted only for ester contents of 50 % and lower, which avoided clotting and inhomogeneity. It was observed that with proceeding hydrogel degradation higher contents of iodine diffused from the hydrogels to the supernatant. Thus, the release of iodine was recorded in UV/Vis measurements for 7.5 % PEOD-Fib hydrogels containing 0, 25 and 50 % PEOD$_{ester}$ over a time course of 21 days (see Figure 29). Most iodine was released for the hydrogel specimens with 50 % PEOD$_{ester}$. The release of iodine followed a steep increase during the first seven days reaching a plateau after 14 days for hydrogels without ester and with 25 % ester polymer. This implicates that the network degradation under physiological conditions is fast during the first seven days and then continues slowly until all ester bonds have been dissolved.

Swelling of separate hydrogels (both PEOD and PMOD variations with 7.5 % total POx content) was measured using gravimetric analysis and referenced to their initial weight before incubation in PBS over the time frame of three weeks. All hydrogels increased in mass after 24 h of incubation at 37°C reaching their equilibrium swelling. The higher the amount of degradable ester polymer, the higher was the observed mass increase. Hydrogels without and with 25 % PEOD$_{ester}$ did not further increase in mass after one day, whereas hydrogels with the highest PEOD$_{ester}$ content still increased in mass until week two (see Figure 30A).
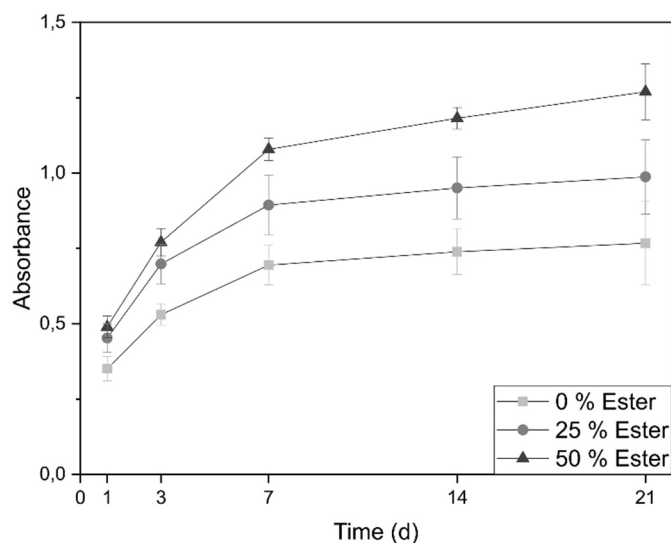


**Figure 29: Release of iodine analyzed by UV/Vis absorption of 7.5 w/v % hydrogels consisting of PEOD-Fib with 0, 25 and 50 % ester content.**

Samples were evaluated over the course of three weeks. Data are presented as means ± standard deviation (n=3).

A similar trend, but less initial swelling, caused by a denser network due to the higher polymer functionalization, could be observed for the hydrogels based on PMOD-Fib (see Figure 31A). In addition, the hydrogel specimens were further mechanically analyzed. In general, the elasticity of the hydrogels appeared to decrease over the course of three weeks, although this trend was not statistically significant (see Figure 30B). The same trend could be observed for hydrogels based on PMOD-Fib, see Figure 31B. Clear differences were observed between groups, with the hydrogels having the highest PEOD$_{ester}$ content showing the lowest Young's moduli. There was no initial difference between hydrogels without ester and 25 % ester, but the elasticity was significantly influenced when 50 % ester was added to the polymeric phase.

The results showed that the incorporation of ester-containing polymer alters hydrogel swelling and mechanical properties.
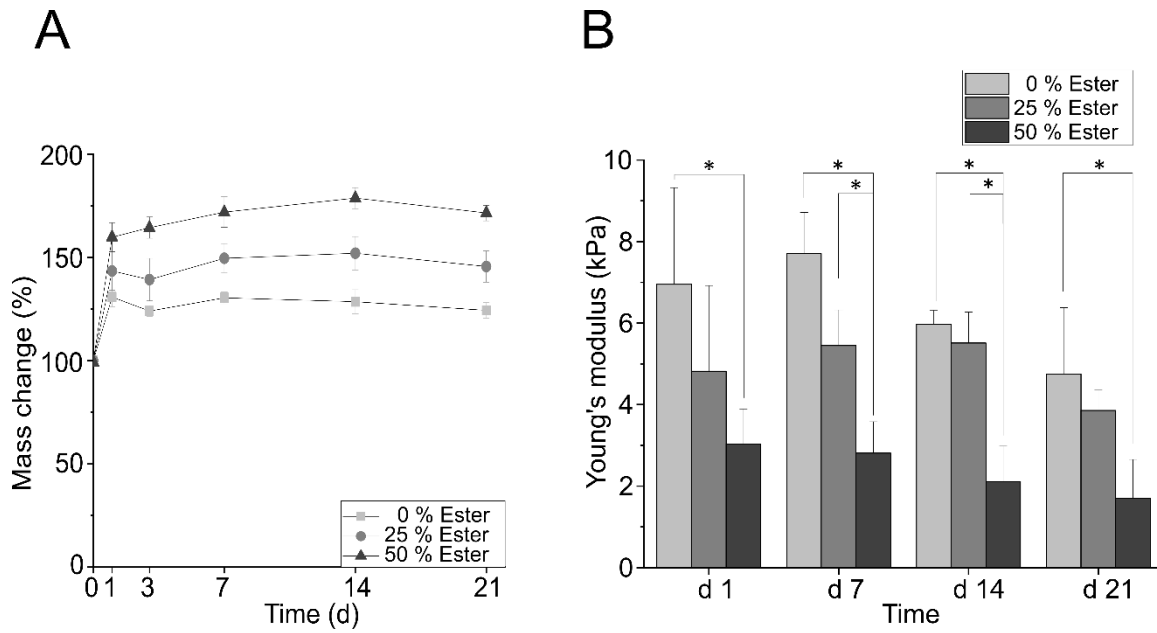
**Figure 30: Time dependent mass and compression specification of PEOD-Fib hydrogels.**

A) Mass change and B) Young's modulus of 7.5 w/v % hydrogels consisting of PEOD-Fib with 0, 25 and 50 % ester content over the course of three weeks. Data are presented as means ± standard deviation (n=3), (* = p<0.05).
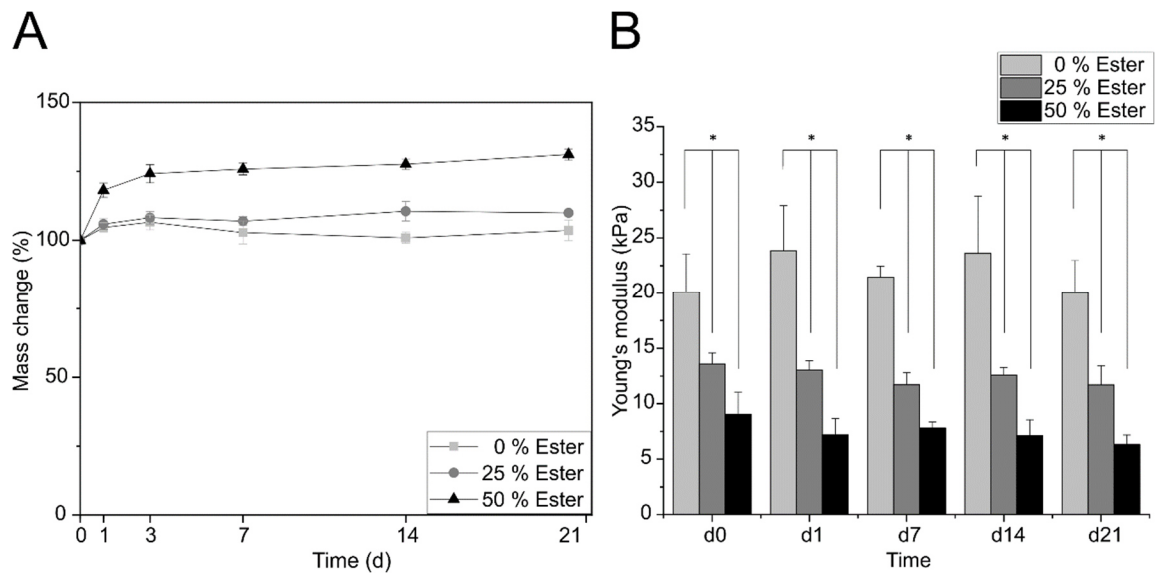


**Figure 31: Time dependent mass and compression specification of PMOD-Fib hydrogels.**

A) Mass change and B) Young's modulus of 7.5 w/v % hydrogels consisting of PMOD-Fib with 0, 25 and 50 % ester content over the course of three weeks. Data are presented as means ± standard deviation (n=3), (* = p<0.05).

### 4.4.4    Cartilage Tissue Adhesion of POx Crosslinked Fibrinogen

The adhesive strength, i.e. immediate bonding, of the hydrogels on cartilage tissue was assessed biomechanically via a push-out test. Upon initialization of the curing reaction by $NaIO_4$, a stable hydrogel formed from the POx and fibrinogen molecules that adhered to the cartilage tissue due to dicatechol crosslinking (see mechanism in Figure 32A). Thereby, it was examined how the catechol
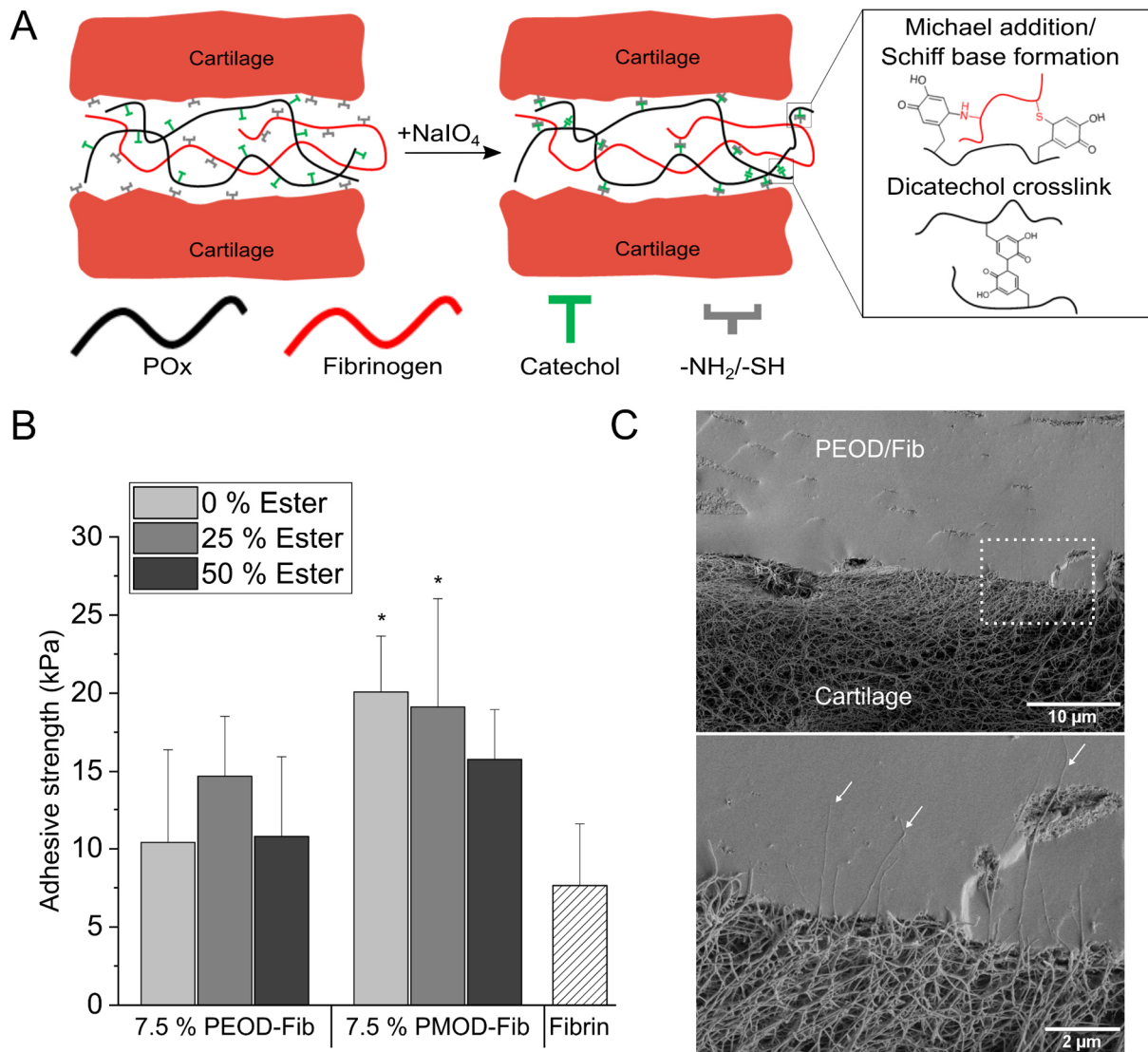


**Figure 32: Cartilage tissue adhesion of catechol-functionalized POx in combination with fibrinogen.**

A) Schematic illustration of the bonding mechanism. B) Adhesive strength of different compositions of PEOD-Fib, PMOD-Fib, and fibrin to cartilage tissue after one day in tissue culture. Data are presented as means ± standard deviation (n= 3-5), statistically significant differences between POx adhesives and fibrin are denoted with *(p< 0.05). C) Scanning electron microscopy of a cartilage disc treated with 7.5 % PEOD-Fib (25 % PEOD$_{ester}$ as representative). Adhesive is firmly integrated with cartilage surface (upper image). At higher magnification, collagen fibrils crossing the interface and fixed inside the adhesive hydrogel can be identified (lower image, highlighted with arrows).

functional POx, the presence of hydrolytically cleavable ester bonds, and the degree of functionalization have an impact on the adhesive properties (see Figure 32B).

As it has been shown in literature that catechol crosslinking can take up to several hours [343], the samples were allowed to cure overnight prior to testing. Although the solidification is relatively fast, the continuous oligomerization via catechol reaction can further increase stiffness and crosslink density as well as adhesion to the cartilage surface. After complete crosslinking of the different polymers, no significant differences were observable when the amide-containing polymer was substituted with the polymer containing hydrolyzable side chains (ester), both in PEOD-Fib and PMOD-Fib (see Figure 32B). This generally means that the reduced Young's moduli corresponding to increasing ester content did not significantly compromise the adhesive strength of the cartilage adhesive. The highest adhesive strength value was reached with 7.5 % PMOD-Fib solely containing $PMOD_{amide}$ (20.08 ± 3.57 kPa). For 7.5 % PEOD-Fib the highest value was obtained when 25 % $PEOD_{ester}$ were substituted (14.70 ± 3.82 kPa). It was observed that when applied on cartilage tissue, all tested adhesive compositions, at least by trend, resulted in higher adhesive strength than fibrin, with significant increase for 7.5 % PMOD-Fib when 0 % or 25 % $PMOD_{ester}$ were present. Due to the limited yield of PMOD polymers in the chemical synthetization and since the functionalization of the amide- and the ester-containing polymer was more consistent in PEOD compared to PMOD (see Table 9), further experiments on the integrative interaction and cytotoxicity assessment were restricted to the 7.5 % PEOD-Fib adhesive group.
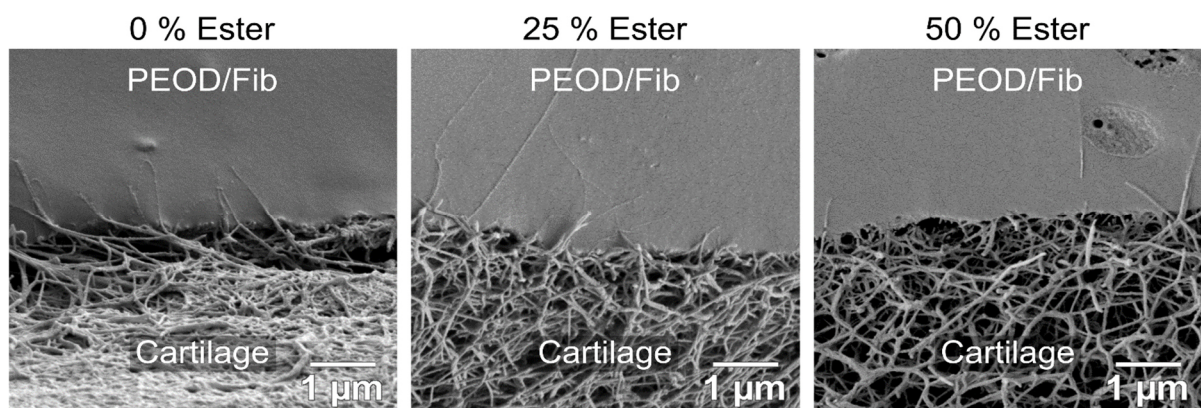


**Figure 33: Scanning electron microscopy of a cartilage disc treated with 7.5 % PEOD-Fib (0, 25 and 50 % $PEOD_{ester}$ ).**

Irrespective of ester content adhesives are firmly integrated with cartilage surface. In all groups, collagen fibrils crossing the interface and fixed inside the adhesive hydrogel can be identified. No differences in network structure related to the ester content of the adhesives could be detected immediately after adhesive application.

The fine structure of the bonding interfaces was further visualized by scanning electron microscopy (SEM). Independent of the ester content, all examined PEOD-Fib compositions revealed a tight and continuous adhesion to the fibrous collagen network of the cartilage ECM (see Figure 32C

and Figure 33). High magnification images revealed that the adhesive material smoothly penetrated the cartilage surface and that single collagen fibers were firmly attached within the hydrogel.

### 4.4.5 Evaluation of Cytotoxicity

The *in vitro* cytotoxicity of various PEOD-based adhesive hydrogels was determined using the MTT viability stain and microscopic evaluation. Potential cytotoxic effects within the cartilage tissue at the application site were examined microscopically (see Figure 34A) but the deposited MTT dye in the tissue was also quantified colorimetrically (see Figure 34B). Constructs without any adhesive treatment, the fibrin control and 7.5 % PEOD-Fib, irrespective of ester content, showed excellent cell viability. Remarkably, even cells in adjacent contact to the tested adhesives stained positive for viability (dark cell-associated MTT stain). In contrast, as a negative control, thermally devitalized constructs did not show metabolically transformation of MTT dye. The quantification of the accumulated MTT in the disc/ring samples confirmed the before mentioned evaluation. No adverse effects of PEOD-Fib on tissue viability could be detected, irrespective of ester content (see Figure 34B).
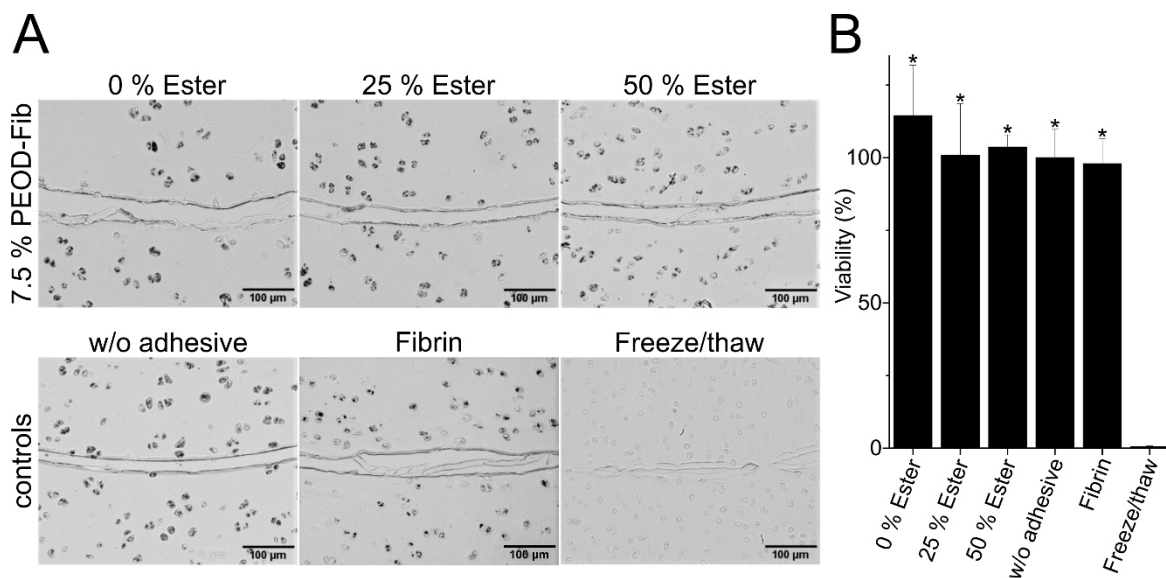


**Figure 34: In vitro cytotoxicity evaluation of 7.5 % PEOD-Fib with different contents of PEOD$_{ester}$.**

A) Adhesives were applied at the defect interface of disc/ring composites, stained with MTT viability stain and inspected microscopically. Composites without adhesive treatment or with fibrin showed comparable viability. Thermally devitalized cartilage as a negative control showed no MTT stain accumulation. B) MTT accumulated in cartilage constructs was solubilized and optical density was measured at 570 nm. % Viability was calculated in reference to mean of w/o adhesive control. Statistically significant differences to Freeze/thaw control are denoted with *(p< 0.05).

Additionally, cast cylindrical hydrogels of PEOD-Fib and stable fibrin (50) as a control were incubated in a chondrocyte suspension where good cell attachment was observable for gels containing fibrinogen (see Figure 35). There were no signs of harmed cells that would occur in case of cytotoxic byproducts in the sol content or leachable gel fractions.
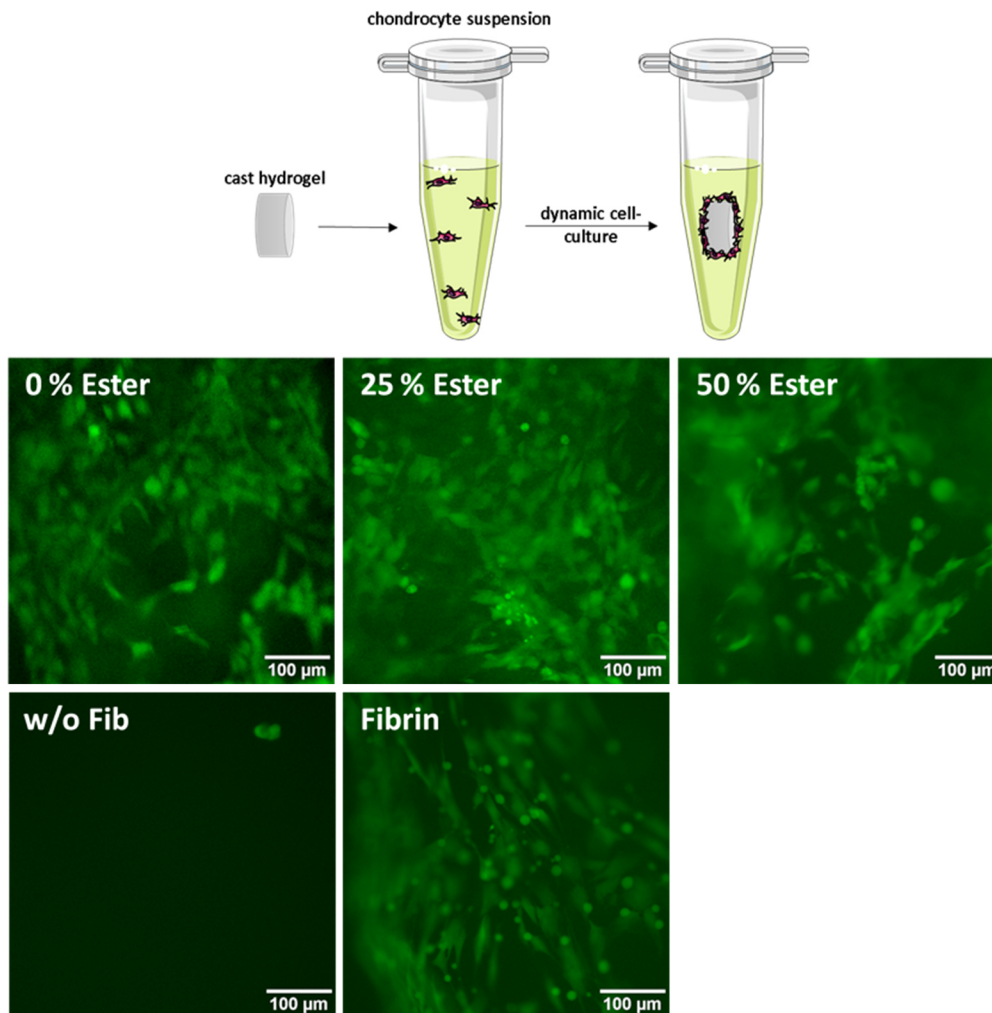


**Figure 35: Calcein fluorescence images of cast hydrogels incubated in a chondrocyte suspension at d7.**

Attached cells were stained with calcein. 7.5 % PEOD-Fib hydrogels with different concentrations of PEOD$_{ester}$ (upper row) revealed good cell attachment on the hydrogel surface, comparable to that of fibrin hydrogels (lower row, right). In contrast, 7.5 % PEOD hydrogels without fibrinogen showed no chondrocyte attachment.

## 4.4.6 Influence of Adhesive Degradation on Long-Term Cartilage Integration

To evaluate the influence of the different degradation and mechanisms on long-term *in vitro* cartilage integration, different PEOD-Fib adhesives were applied on cartilage disc/ring constructs. After three weeks *in vitro* tissue culture, biomechanical push-out tests showed an increase in adhesive
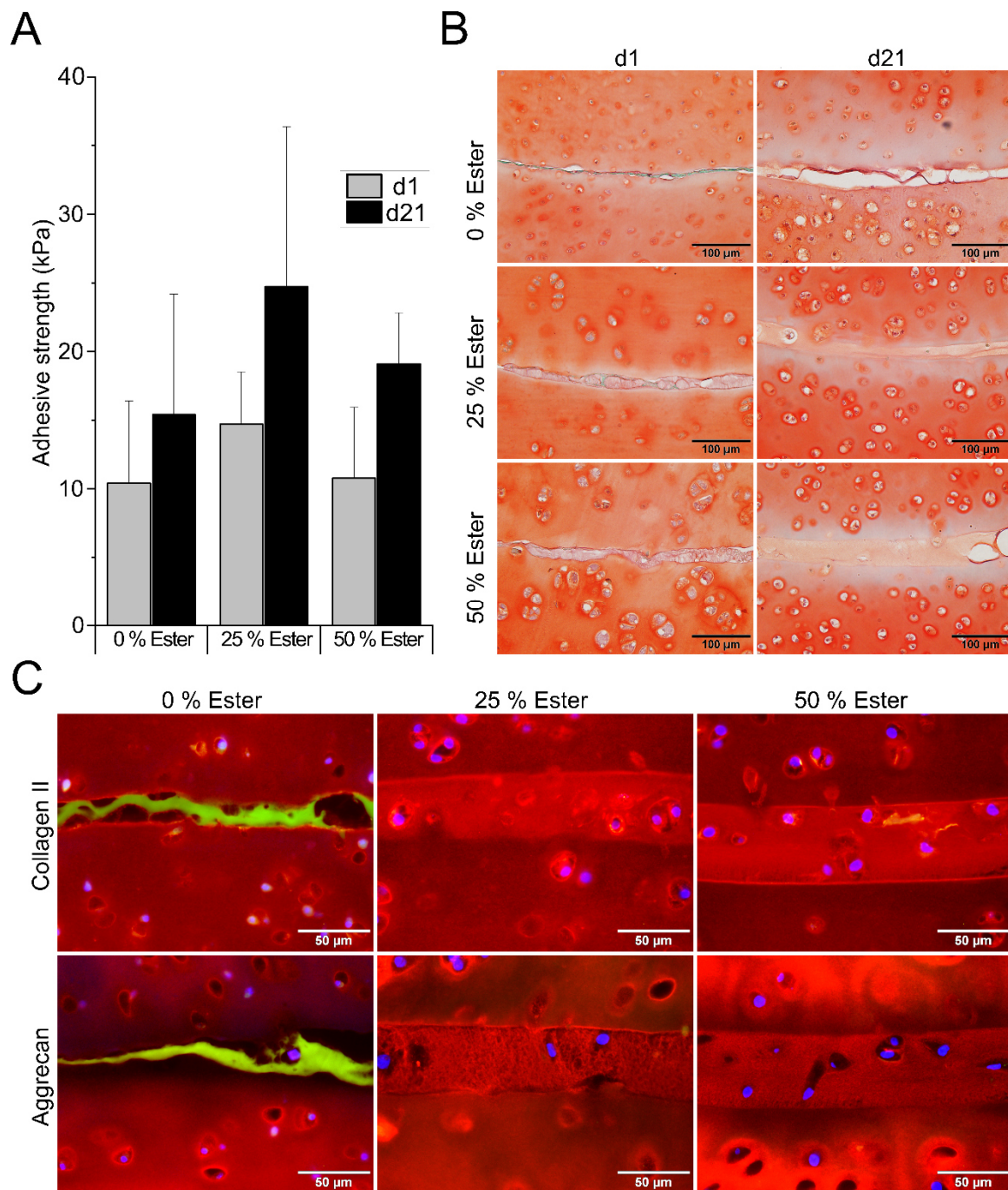
**Figure 36: Long-term cartilage integration with 7.5 % PEOD-Fib adhesives.**

A) Comparison of biomechanical integration strength of 7.5 % PEOD-Fib with different concentrations of PEOD$_{ester}$ after d1 and d21 in tissue culture. Data are presented as means ± standard deviation (n= 3-5). B) Histological SafO-staining for glycosaminoglycans (GAG) in 7.5 % PEOD-Fib with different concentrations of PEOD$_{ester}$ at d1 and d21 of tissue culture. C) Immunofluorescent staining for cartilage ECM markers collagen type II and aggrecan (red) at d21, epifluorescent signal of PEOD-Fib is seen as green fluorescence.

strength for all tested compositions of 7.5 % PEOD-Fib, as compared to the bonding at day one (see Figure 36A). The incorporation of 25 % PEOD$_{ester}$ as well as of 50 % PEOD$_{ester}$ of the total PEOD amount achieved higher adhesive strength values (24.73 ± 11.66 kPa and 19.10 ± 3.72 kPa,

respectively), as compared to constructs where only $PEOD_{amide}$ was used (15.41 ± 8.77 kPa), albeit these differences were not statistically significant. However, strikingly, microscopic analysis clearly demonstrated the benefit of an increased degradation for cell invasion and cartilage regeneration. Histological staining for glycosaminoglycans (SafO, see Figure 36B) and immunofluorescent staining for typical cartilage ECM components (aggrecan, collagen type II, see Figure 36C) showed an impaired cartilage integration after 21 days *in vitro* culture when the amide-containing adhesive was used.

In contrast, for the ester-containing adhesive, as the network of the hydrogel was loosened due to hydrolyzable crosslinks via the incorporation of either 25 % or 50 % $PEOD_{ester}$, a turnover of the adhesive along with neocartilage formation was observed. A homogeneous ECM deposition spanning the defect in combination with a high number of invaded cells was detected in the defect gap in adhesives with the hydrolyzable crosslinks.

## 4.4.7 Discussion

With the appropriate crosslinking chemistry, polymers have the ability to cure into hydrogels via reactive groups and to adhere directly to tissue surfaces. Despite the progressive increase in understanding of adhesion mechanisms, researchers face the extreme challenge to fabricate materials with adhesion to wet and dynamic surfaces that are in compliance with biocompatibility demands. Especially for the application on cartilage tissue with its wet environment and high mechanical forces, adhesives are needed that can withstand the strain. For this reason, scientists are inspired by organisms that achieve adhesion under the hardest conditions [344].

Specific organisms that attracted the interest of researchers worldwide are blue mussels. These small bivalves are capable of attaching to a wide range of organic and inorganic surfaces underwater and even in the harsh intertidal line. Analysis of secreted proteins at the byssal threads revealed that the underwater adhesive properties and the mechanical properties of the threads are linked to repeating residues of the catecholic amino acid 3,4-dihydroxyphenyl-alanine (DOPA) which has been reviewed before [345]. With the use of catechol-functionalized polymers it is possible to mimic the mussel adhesion via oxidation of containing catechol groups or reduction with metallic ions. The catechol group can form metal complexes in the presence of metal ions such as $Fe^{3+}$ or bind to inorganic surfaces via hydrogen bonds. Under oxidizing conditions, the catechol group becomes highly reactive and forms an o-quinone that can polymerize itself or react with a variety of nucleophiles such as amino or thiol groups by Michael addition or Schiff base formation [244]. This makes DOPA or other catechol molecules perfect candidates for reactions with nucleophiles (e.g. $-NH_2$, $-SH$) such as cysteinyl, histidyl or lysyl groups, which are present on many natural tissue surfaces [245,346].

The most common method is the polymerization of dopamine with other monomers. For example, Mehdizadeh et al. polymerized citric acid with PEG and dopamine in a condensation reaction to form a biodegradable polymer that could be used as a tissue adhesive for wound closure [347]. Moreover, catechol functionality has already been linked to amino- or NHS-functionalized PEG with 3,4-dihydroxyhydrocinnamic acid or dopamine HCl [246,247]. It has also been bound to biomacromolecules, for example, to carboxylated silk fibroin [248] or to gelatin by simple EDC/NHS chemistry [210]. Moreover, it has already been polymerized as dopamine acrylamide or dopamine hydrochloride to form three-dimensional networks [250,251].

A possible alternative are water soluble synthetic polymers like poly(2-alkyl-2-oxazoline)s (POx), which have become increasingly popular in the biomedical field due to their improved and accelerated synthesis using microwave heating. In contrast to the more prominent poly(ethylene glycol) (PEG), POx do not only offer end-terminal functionalization via functional initiators or terminating agents, but also allow for a tunable side chain functionalization, which can be varied through a range of different functional monomers or further post-polymerization functionalization [236]. POx has also been associated with good hemocompatibility, low cytotoxicity and low immunogenicity [237–239]. Accordingly, hydrogels based on different POx derivatives were already used for drug delivery, as cell culture scaffolds, or as hemostatic wound dressings [240,241].

### 4.4.7.1 Hydrogel Preparation and Mechanical Characteristics

For the present experiments, POx polymers were prepared, differing essentially in two building blocks used (MeOx vs. EtOx). The respective building block strongly affects the possibility of functionalizing POx with DOPA via its own hydrophilicity. The susceptibility to hydrolysis of the binding sites can also be adjusted via amide or ester binding to the DOPA residue. POx built on the less hydrophilic co-monomer EtOx achieved a less high functionalization rate with DOPA (finalized POx referred to as PEOD). However, the yield of functionalization was more consistent for PEOD containing either amide or ester linkages in contrast to functionalized POx polymers based on the MeOx co-monomer (PMOD).

The catechol-functionalized POx were used to form hydrogels under oxidative conditions using sodium periodate (NaIO$_4$) in PBS. As known from literature, catechol functionalities are oxidized to quinones, which will crosslink with other available quinones to form dicatechols [247]. Dicatechol formation with the used POx polymers results in covalent intra- and intermolecular bindings and thus contributes to curing into a hydrogel. For the application as biohybrid cartilage adhesive, fibrinogen was added to the hydrogel precursor solutions. Besides adding a biological macromolecule offering

several additional crosslinking points, we anticipated a better cell adherence on the hydrogel and only mild cellular response to the implant as it had been observed by Berdichevski *et al.* for comparable PEG- hydrogels *in vivo* [348]. To prove this assumption, we incubated cast hydrogels based on PEOD with and without fibrinogen in a chondrocyte suspension. After seven days, all hydrogels with fibrinogen were massively covered with cells and the specimen without fibrinogen did not show any attachment of cells. Besides an improved cell attachment, the supplementation with fibrinogen raised the elasticity of the hydrogel adhesive.

The biomechanical determination of the Young's modulus showed on the one hand that the almost doubled functionalization degree of the more hydrophilic PMOD (8.7 % catechol), compared to PEOD (4.6 % catechol), results in gels which are five times stiffer. On the other hand, the addition of fibrinogen increased the elasticity, as expected, which obviously impacted the hydrogels made of PMOD to a greater degree than those based on PEOD. The added fibrinogen is composed of a long α-helical coiled coil, which will convert into an extended β-strand conformation when force is applied, making it a stretchable and soft fiber [349] and, thus, may improve mechanical characteristics of the biohybrid materials. The ratio of free catechol groups from the POx to the fibrinogen concentration directly affects the crosslink density within the gel and accordingly its mechanical properties. In contrast to 5 w/v % PMOD-Fib, compositions of 5 w/v % PEOD-Fib were too soft to be analyzed, despite that the same fibrinogen concentration of 5 w/v % was present. This can be explained by the fact that this polymer precursor contained only 4.6 % catechol groups due to less efficient functionalization. In general, the assumption that a higher degree of functional catechol groups will result in a denser network and hence in a higher Young's modulus was confirmed. The results also demonstrate that a range of elastic moduli can be produced depending on the functionalization degree, which may be used to influence chondrocyte migration and neocartilage formation. Based on these results, we decided to continue our experiments with the formulation containing 7.5 % of the synthetic polymers and 5 % fibrinogen as these hydrogels had shown an adequate elasticity and stability whilst keeping the material content as low as possible. For all tested formulations, the formation of the hydrogel network took place within less than three minutes, which would be favorable for the later clinical application.

### 4.4.7.2 Degradation

In general, the elasticity of the hydrogels appeared to decrease over the course of three weeks which was shown by course of Young's moduli determination. There was no initial difference between hydrogels without ester and 25 % ester, but the elasticity was significantly influenced when 50 % ester

was added to the polymeric phase. This can be explained with the increased swelling and additional network inhomogeneities, which also lead to a reduced stiffness, which may be favorable for cell invasion.

During the oxidative curing reaction iodine is formed that is deposited within the gel. It was observed that with ongoing hydrolysis of the diverse produced hydrogel cylinders the supernatant PBS solution darkened due to corresponding iodine release into the PBS solution. The UV/Vis absorbance of iodine in the supernatant was taken as a measurement for the iodine release and therefore as an indication for the degradation degree of the gel over time. The release of iodine followed a steep increase during the first seven days reaching a plateau after 14 days for hydrogels without ester and with 25 % ester polymer. This implies that the network degradation under physiological conditions is fast during the first seven days and then continues slowly until all ester bonds have been dissolved. Constitution changes of hydrogel test specimens were also evaluated by means of macroscopic observation and mass change. The higher the amount of degradable ester polymer, the higher was the observed mass increase initially after fabrication of the gel and transfer to the PBS solution.

The results that the incorporation of ester-containing polymer alters hydrogel swelling and mechanical properties over time due to hydrolysis. A different degradation dynamic in biological settings *in vivo* or *in vitro* has to be considered, since the additional enzymatic degradation of fibrinogen plays another important role. Furthermore, it should be noted that the fabricated hydrogel specimens used for mechanical testing, iodine release determination and macroscopic evaluation were prepared in much larger dimensions than it would likely be necessary in clinical applications when used as an adhesive to fill cartilage lesions. From the obtained results we assumed that, when applied as cartilage adhesives, the incorporation of ester-containing polymer in the tested concentrations may be sufficient to create adequate space and, thus, facilitate cell invasion and ECM deposition, which was tested in subsequent experiments with long-term *in vitro* cultivation of disc/ring constructs.

### 4.4.7.3    Adhesive Strength

As it has been shown in literature that catechol crosslinking can take up to several hours [343], therefore the samples were allowed to cure overnight prior to testing to take into account the full reaction capacity. Although the solidification is relatively fast, the continuous oligomerization via catechol reaction can further increase stiffness and crosslink density as well as adhesion to the cartilage surface. After complete crosslinking of the different polymers, we could not observe significant differences when the amide-containing polymer was substituted with the polymer containing hydrolyzable side chains (ester linkages), both in PEOD-Fib and PMOD-Fib. This generally

means that the reduced Young's moduli corresponding to increasing ester content as described earlier did not significantly compromise the adhesive strength of the cartilage adhesive. Compared to PMOD-Fib, the reduced catechol functionalization in PEOD-Fib may compromise the adhesive performance due to competing crosslinking reactions and less catechol that is needed for intermolecular crosslinking and cohesive properties. A long-term stable fibrin formulation (stable fibrin (50)) that was investigated in prior experiments served as a control group. The fibrinogen concentration of the stable fibrin (50) is identical to the here examined POx adhesives as well as to photopolymerizable RuFib50 described in Chapter 4.3.2 [122]. All tested POx adhesive compositions possessed higher adhesive strength than the fibrin glue. The higher functionalized PMOD achieved the highest adhesive strength where the formulations of 7.5 % PMOD-Fib with 0 % or 25 % content of the hydrolyzable PMOD$_{ester}$ significantly outperformed the stable fibrin (50). The slight decline of adhesive strength in the 7.5 % PMOD-Fib group with the highest amount of PMOD$_{ester}$ (50 %) was most likely a result of the uneven catechol functionalization between PMOD$_{amide}$ and PMOD$_{ester}$ (8.7 % vs. 5.3 %, see Table 9). Nonetheless, these results clearly demonstrate that with the variation of the catechol functionalization degree, both the mechanical strength of the bulk hydrogel and the corresponding adhesive strength can be adapted.

When compared to other catechol-based hydrogels applied to tissues other than cartilage, the range of adhesive strength values obtained with our approach was comparable or even higher [245,247,350–352]. Here, we tested adhesive strength on cartilage tissue that is known for its anti-adhesive properties due to its high GAG content [197,313]. No enzymatic pre-treatment of the cartilage surface was performed to expose potential binding sites on the collagen scaffold of the cartilage as was necessary for diazirine functionalization (see Chapter 4.3.1) and photocrosslinking approaches in the literature [211]. In order to compare adhesive strength values, one must also consider differences in the biomechanical test set-up. Most other studies have utilized a biomechanical lap-shear test, whereas we have chosen to analyze integration in a disc/ring model, as the defect orientation resembles the common lateral defect interfaces in cartilage repair.

Due to the high GAG content of native cartilage tissue, high amounts of water are present in the disc/ring samples that are kept moist during fabrication steps. High magnification images from performed electron microscopy revealed that the POx-fibrinogen adhesive material smoothly penetrated the cartilage surface and that single collagen fibers were firmly attached within the hydrogel. These observations suggest good tissue wettability by the hydrogels as it has also been reported for other catechol-modified materials [344,353]. High surface wetting is necessary for intimate contact between the polymer and substrate prior to bond setting. It has also been shown that low molecular weight polymers favor interactions with a surface due to their higher mobility. However,

low molecular weight polymers may on the other hand lead to reduced cohesive strength of the hydrogel due to a reduced chain entanglement [354]. Therefore, increasing surface bonding at the possible expense of bulk cohesion is an important design aspect of creating underwater or wet-tissue adhesives and it has to be further clarified how the chain length of our POx derivatives influences this balance.

### 4.4.7.4 Cytotoxicity

For cartilage defects, it has been shown that a hypocellular region surrounding the defect imposes a significant hurdle for cartilage integration [8,157,165]. The mechanical stress after trauma to the cartilage results in reduced cell viability. As demonstrated in Chapter 4.1 punching of the cartilage during fabrication of the lateral defect interface in the disc/ring model resulted in a small necrotic band at the defect site despite the usage of sharp biopsy punches. However, leachable substances from an adhesive material can further decrease cell viability in the surrounding tissue and thus impede the long-term success of regenerative repair. The main components of the here evaluated adhesives are poly(oxazoline)s and fibrinogen that are generally considered as cytocompatible and are already applied in biomedical applications [330,355–359]. The formation of a hydrogel network using catechol groups and $NaIO_4$ as curing agent has already been used by other research groups for different applications. No cytotoxic effects were reported most probably because the potentially critical oxidizing agent only needs to be applied at very low concentrations [360,361]. The final $NaIO_4$ concentration in the adhesive formulations was 60 mM. Based on the molar mass of the single iodine (I) atom (126.9 g/mol) an exemplary clinical applied glue volume of 500 µl would contain 3.8 mg atomic I. Iodine is a naturally occurring trace element that is vital for human health. It serves the body's own build-up of the thyroid hormones thyroxine and triiodothyronine. These hormones control many processes in the body such as growth, bone formation, brain development and energy metabolism.

The German Federal Institute for Risk Assessment (BfR) has prepared a guideline for iodine exposure in humans and summarized existing health-relevant data [362]. The recommendations of the German Nutrition Society (DGE) for adequate iodine intake depend on age and increase from 40 to 80 micrograms per day for infants to 200 micrograms per day for adolescents and adults. Women need more iodine during pregnancy and lactation, so intakes of 230 and 260 micrograms per day are recommended. Data on the iodine supply of the German population were collected in the nationally representative studies "Study on the Health of Adults in Germany" (DEGS) and "Study on the Health of Children and Adolescents in Germany" (KIGGS). In Germany, a maximum daily intake of 500 micrograms of iodine is still considered safe, even for people who are sensitive to iodine exposure. As

shown by the iodine absorbance data und macroscopic images of hydrogel specimens, the iodine release is coupled to the degradation progress of the adhesive material and therefore iodine exposure to the patient is distributed throughout the shelf-life of the adhesive with no single critical acute dose. No toxicological risk has therefore to be expected for the released iodine from the adhesive in those applied concentrations. The BfR assessment even concluded that about 30 percent of the population still have an iodine intake below the estimated mean requirement and food supplementation e.g., via the use of iodized table salt is recommended.

This toxicological risk evaluation is supported by other working groups with studies in other tissues where DOPA-containing adhesives were cured with comparable doses of the oxidant sodium periodate [245,247,352,360,361]. Additionally, the already described experiments with cast cylindrical hydrogels of PEOD-Fib that were incubated in a chondrocyte suspension showed good cell attachment (see Figure 35). There were no signs of harmed cells that would occur in case of cytotoxic byproducts in the sol content or leachable gel fractions. As bovine fibrinogen was used for the presented adhesive compositions, there would still be risks of blood-borne diseases or hypersensitivity that has also been reported for commercial fibrin glue kits (e.g. Tisseel, Baxter, Inc.). Medical devices containing derivatives of animal origin are required to validate the absence of viruses and transmissible spongiform encephalopathy (TSE) agents in accordance with the ISO 22442 standard series. To bypass such risks, there are several preparation methods described how to extract autologous fibrinogen from patients [112,226], which could alternatively be used to allogenic fibrinogen. The good biocompatibility of the prepared POx adhesives is further indicated by the tolerance and remodeling of the adhesives by the disc/ring composites as observed in long-term cultivation experiments that will be discussed in detail in the following chapter.

### 4.4.7.5 Long-term lateral cartilage integration

Three different compositions of 7.5 % PEOD-Fib with regard to the content of hydrolyzable ester-based POx were included in long-term experiments in order to evaluate the influence of adhesive degradation on the lateral cartilage integration at the defect interface. In sharp contrast to the results obtained with the photopolymerized RuFib adhesive (see Chapter 4.3.2), the adhesive strength for all tested PEOD-Fib formulations increased after three weeks *in vitro* tissue culture as determined by the biomechanical push-out test. This already indicates that the dicatechol-based crosslinking of the hydrogel via the POx polymers is superior for the long-term integration process compared to the dityrosine formation via ruthenium activation. The increase in integration strength can thereby be related to more stable intra- and intermolecular bonding and/or an improved cell-based integration

via ECM remodeling. The tunable degradation rate of the PEOF-Fid adhesives by adaption of the content of ester-linages in the POx polymers further influenced the outcome of long-term integration. The incorporation of 25 % PEOD$_{ester}$ as well as of 50 % PEOD$_{ester}$ of the total PEOD amount achieved higher adhesive strength values and improved interfacial neocartilage formation as compared to constructs where only the stable PEOD$_{amide}$ was used. Lacking remodeling capacity of an adhesive may lead to delamination of the adhesive from the application surface when ECM synthesized in the bulk cartilage tissue pushes against a non-interacting adhesive. The inability of a proper degradation results in a barrier for migrating cells and gap-bridging neocartilage formation, as was also reported previously by Murphy et al. [363].

A homogeneous ECM deposition spanning the defect in combination with a high number of invaded cells was detected in the defect gap in adhesives with the hydrolyzable crosslinks. Synthesized components of cartilage ECM that integrate with native cartilage and chondrocytes that can freely migrate across the interface have been shown to enhance mechanical stability of tissue repair in cartilage, both in short-term and long-term [81,162,168,169,176,177,253]. Similar properties were observed in different fibrin glue formulations that allowed for cell migration and ECM deposition at the glue interface (see Chapter 4.2). It is likely that the formed repair tissue in the evaluated PEOD-Fib adhesives still lack sufficient cohesive strength to bear strong mechanical loading at day 21 and therefore the cohesive failure of the neocartilage limits the maximum stress in push-out experiments. However, as seen in Figure Figure 36B and Figure 36C, the advanced repair in the ester-containing adhesives after day 21 suggests a superior progress at later time-points of defect healing as compared to the adhesive with non-hydrolyzable crosslinks despite the counteracting effect of increased hydrolysis on cohesive strength. As the exact time course of hydrogel remodeling and development of cartilage ECM is still not fully understood, it needs further investigation of optimal degradation and mechanical characteristics of the hydrogels. The challenge will be to achieve a material composition with distinct immediate integration strength and a balanced course of degradation to fully meet the demands for successful long-term cartilage regeneration. Concerning this matter, the POx-based adhesives can easily be further modified, i.e. by altering crosslink density and variable incorporation of hydrolysis motifs, holding great potential for applications in wound closure or as sealant also in other types of tissue. In combination with fibrinogen and oxidative conditions we could produce adhesive hydrogels with tunable degradability. In principle, a higher functionalization rate of the POx polymers can lead to increased immediate bonding strengths as was shown for adhesive formulations based on PMOD. Higher available DOPA at the polymer backbone in combination with a suitable degradation kinetic may benefit the overall outcome of the adhesive. However, the difficulties in chemical synthesis of highly functionalized POx related to the high hydrophobicity of DOPA can limit the availability of

functional groups for this approach. More detailed considerations would have to be made as to whether maximization of the functionalization rate can be achieved by circumventing the polarity problems with alternative polymers without the loss of the ability for long-term regeneration. A group in Singapore already introduced a double crosslink mechanism of a gelatin-dopamine conjugate that achieved immediate bonding strengths of up to 200 kPa in a lap shear test with stripes of either porcine skin or cartilage [210]. However, despite the proven biocompatibility in *in vitro* cytotoxicity analysis and subcutaneously implantation in mice, long-term results regarding the interaction of the material with cartilage tissue remain missing. In future experiments on adhesive-mediated cartilage regeneration a focus must be set on the evaluation of opportunities to chemically modify adhesive polymers with regard to maximization of catechol residues and tunable degradation properties. Ideally, experiments include the application directly on cartilage tissue either *in vitro* or *in vivo*. The *in vitro* disc/ring model, however, provides the benefit of easily performable biomechanical assessment of integration strength over the course of several weeks without solely relying on qualitative interpretation via microscopical evaluation.

## 4.5 Lateral Cartilage Integration with Hydrogel Constructs

Besides the approach to enhance cartilage wound healing by means of gluing, there are other strategies to improve cartilage tissue healing with adhesive hydrogels. Among other things, adhesive hydrogel materials also offer advantages for larger defects, since the carrier material can be shape-specific and fill larger wound spaces. In tissue engineering approaches, carrier materials are seeded with cells with the aim to create newly formed tissue. Up to the formation of functional tissue, numerous factors influence the outcome. Even if tissue engineering can successfully be used to produce a tissue replacement that is similar in structure and function to the native tissue, it requires good integration between the tissue engineering construct and the native tissue in order to maintain long-term function. In the following, experiments are presented where different materials were used for the creation of cartilaginous tissue engineering constructs. Factors influencing the outcome of cartilage tissue formation within the constructs as well as their integration to the native cartilage were investigated.

## 4.5.1 Chondrocyte Isolation for Hydrogel Seeding

The enzymatical digestion of porcine cartilage samples allows isolation of chondrocytes. However, the harsh conditions during this process can have a result on cell viability. After the isolation procedure a relatively high number of dead cells was present that varied between different experiments. Chondrocytes attach to culture flasks under static *in vitro* cell culture, which allowed skimming of dead cells and non-adherent cell types via wash steps and/or medium exchange. In cell culture, after plate adhesion, the expression changesd from a spherical shape to spindle-shaped. Thus, *in vitro* culture had the possibility to increase the uniformity of living chondrocytes in addition to proliferation. The limitation to a short-term culture period of five days avoided a greater influence of dedifferentiation phenomena of chondrocytes in a 2D cell culture while at the same time it allowed the creation of a more uniform cell population for an increase of comparability between different experimental approaches. For monitoring the efficiency of the above described isolation, chondrocytes were labeled for the surface receptor CD44 that is strongly expressed in this cell type. While much debris and CD44 negative cell material was seen in the directly isolated chondrocytes without subsequent cell culture, the five-day cell culture increased the uniformity of the cell population with respect to CD44 expression (see Figure 37). Because of the previously mentioned advantages, those short-time cultivated chondrocytes were used for experiments with colonized hydrogels.
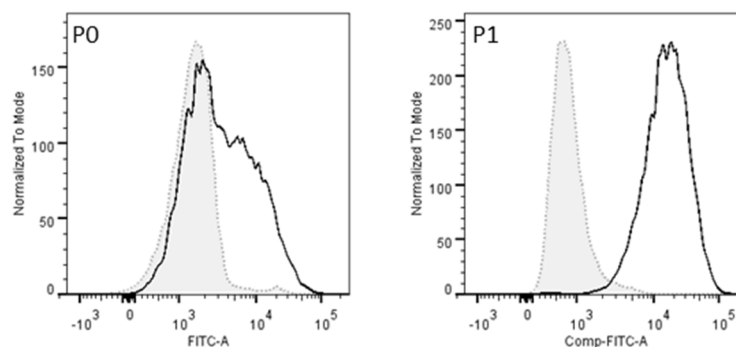


**Figure 37: Flow cytometry of porcine chondrocyte surface expression of CD44 directly after cell isolation (P0) and after short-time *in vitro* cultivation (P1).**

FITC intensity histograms are displayed. The gray-shaded histograms with dotted line represent the IgG control and the bold-lined histogram the experimental sample.

## 4.5.2 Integration of Cell-Laden Fibrin Hydrogels

In addition to the adhesive properties that make fibrin a candidate for use as cartilage adhesive, the material has further advantageous properties. As it is derived from natural wound closure, it is a

material that is compatible with cell colonization and is therefore also used clinically in the treatment of cartilage damage since many years [228]. In previous experiments it was demonstrated that long-term stable fibrin formulations allow the accumulation of cartilage-specific ECM when applied as an adhesive to lateral cartilage defects (see Chapter 4.2). Long-term stable fibrin formulations were already used before as cell carrier for cartilage tissue engineering constructs *in vitro* and *in vivo* [84,122], however it is has to be clarified if and how these constructs can integrate to native cartilage tissue. In order to investigate cartilage tissue formation by the encapsulated chondrocytes without the presence of native tissue, the hydrogels were cultivated *in vitro* for up to 21 days

### 4.5.2.1        Influence of native cartilage tissue on seeded chondrocytes

For the preparation of cell-seeded stable fibrin hydrogels, porcine chondrocytes were isolated and cultivated *in vitro* for five days with chondrocyte proliferation medium. Afterwards the cells were trypsinized and resuspended in fibrinogen solutions of different protein content. By addition of equal volumes thrombin solution to 20 µl of the cell-fibrinogen solutions prepared in silicone molds the crosslinking was initiated. At the end 40 µl hydrogels were obtained with approximately $6 \times 10^5$ cells/gel and a final fibrinogen concentration of 15 (stable fibrin (15)), 25 (stable fibrin (25)) and 50 mg/ml (stable fibrin (50)). In order to investigate cartilage tissue formation by the encapsulated chondrocytes without the presence of native tissue, the hydrogels were cultivated *in vitro* for up to 21 days and the presence of GAG within the hydrogels was analyzed biochemically and histologically over the time course of the cultivation period.

Additionally, the DNA content of the hydrogels was determined. In none of the three experimental groups a significant change of DNA concentration was observed between the d0, d14 and d21 timepoints. The GAG concentration increased in hydrogels of all three fibrinogen concentrations over 21 days. However, in the stable fibrin (15) group the increase in GAG was the most recognizable. Already on day 14, in the stable fibrin (15) and (25) the increase in GAG content was significantly higher than compared to d0 constructs. The GAG content in the stable fibrin (15) constructs at d14 and d21 was significantly higher than in the two groups with higher fibrinogen concentration. In the stable fibrin (50) group, the GAG increase was clearly lower that in the other groups and was significantly higher to the d0 value only at d21. This significance is lost when normalizing the GAG concentration to the DNA content of the hydrogel. The biochemical analysis clearly shows a negative correlation of GAG synthesis by encapsulated cells with increasing fibrinogen concentration in the hydrogels (see Figure 38A). The amount and distribution of newly synthesized GAG in the hydrogels was also analyzed via Safranin O staining. GAG synthesis was recognizable mostly pericellularly and more dominant in
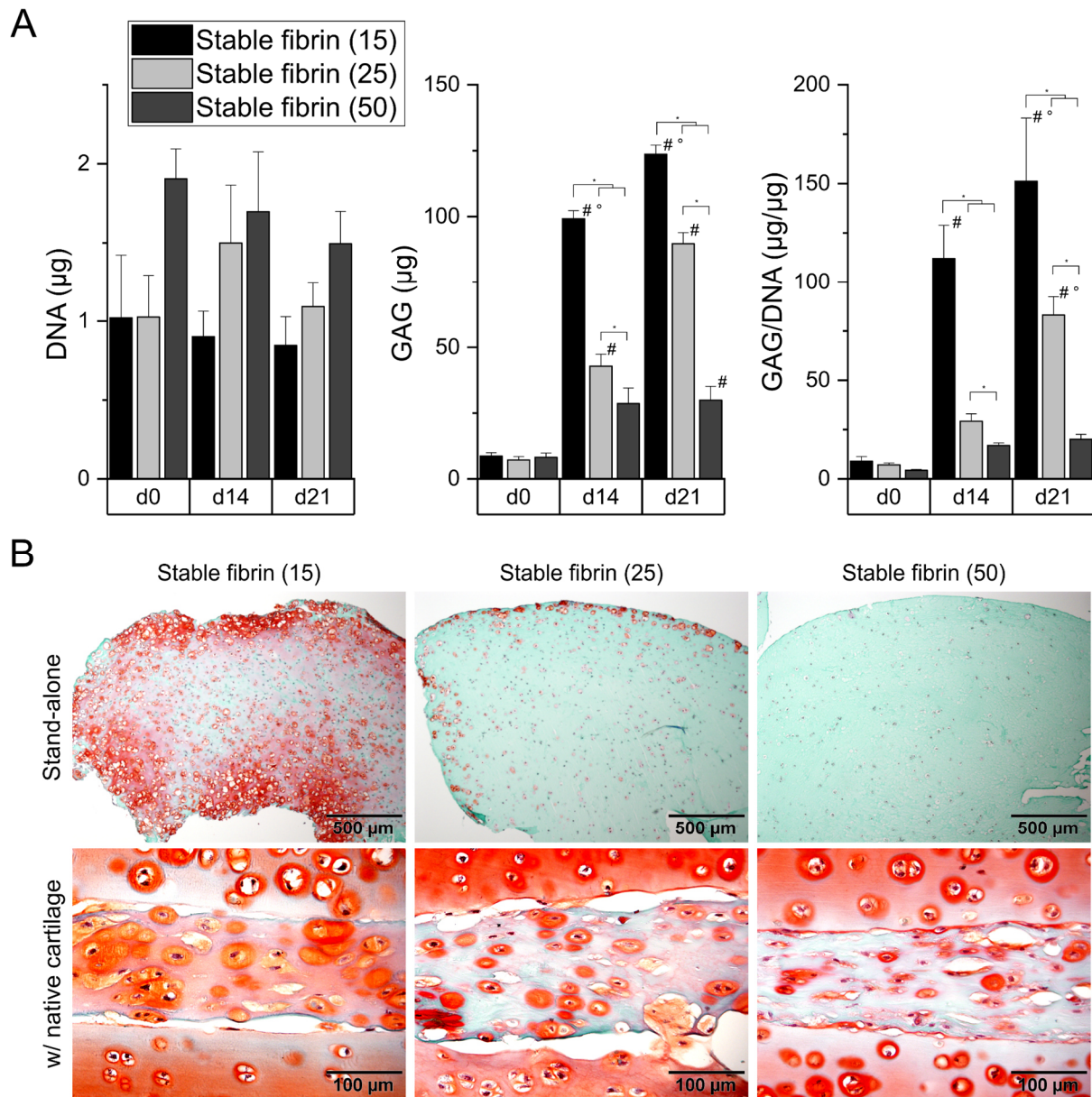
**Figure 38: Time dependent ECM development in long-term stable fibrin hydrogels.**

A) Biochemical analysis of the DNA and GAG content of *in vitro* cultivated long-term stable fibrin gels seeded with porcine chondrocytes. B) Safranin O staining of chondrocyte-seeded hydrogels cultivated *in vitro* for 21 days as stand-alone gels (upper row) or when prepared adjacent to two native cartilage discs (lower row). Data are presented as means ± standard deviation (n= 3-4). (* = $p < 0.05$ between groups of different concentrations, # = $p < 0.05$ to d0 value of same group , ° = $p < 0.05$ to d14 value of same group).

surface regions of the hydrogels. Only in the stable fibrin (15) group a deeper GAG deposition in the hydrogel could be observed, with an improved extracellular distribution of the GAG than in the other groups. The histological staining well reflected the results of the biochemical analysis showing a decrease of the GAG content with higher fibrinogen concentration in the fibrin gels (see Figure 38B, upper row). To investigate the influence of the presence of native cartilage tissue on ECM formation, separate experimental groups were cultivated simultaneously where the hydrogel solutions were

cured adjacent to two 6 mm native porcine cartilage discs. Histological images of these layered combination constructs (sandwich layering) clearly demonstrate a positive influence of contacting native cartilage tissue on GAG content and distribution in the cell-seeded fibrin gels (see Figure 38B, lower row). The best outcome was again obtained in the stable fibrin (15) group. But in sharp contrast to the gels without cartilage contact, increased GAG deposition and improved distribution within the gels can be observed even at higher fibrinogen concentrations when native cartilage tissue was contacting the hydrogel.

### 4.5.2.2 Long-term integration of cell-laden fibrin hydrogels

In the experiment described before a positive influence of native cartilage tissue on ECM synthesis within hydrogels was visible. Subsequent experiments aimed to investigate the differences between cell-laden and cell-free hydrogels that have contact with cartilage tissue. For this purpose, the 6 mm disc/ring model that was used before with native cartilage-only constructs was adapted. After preparation of the disc/ring model the inner 3 mm cartilage disc was discarded. Instead, the outer cartilage ring served as a mold for the preparation of cartilage-hydrogel composites. Stable fibrin (50) hydrogels, either cell free or chondrocyte-laden, were cured within the cartilage disc and the whole composite constructs were subsequently cultivated for 28 days. After the *in vitro* culture of 28 days the integration strength of the hydrogels to the native tissue was determined by a push-out test. Additionally, the DNA and GAG content of the pushed-out hydrogels were determined. Separate constructs were sectioned and analyzed histologically and immunohistochemically. As determined with the push-out test, only a slight non-significant increase in integration strength compared to d0 was obtained for both the cell-free and the cell-laden hydrogels on d28. Remarkably, an increase in DNA content within the hydrogels was observable in both groups over the 28 day time course. In addition, compared to the respective d0 value, a significant increase in GAG content was determined in hydrogels that were either prepared cell-free or encapsulated with chondrocytes (22.9 ± 10.8 µg/gel and 43.8 ± 24.6 µg/gel)(see Figure 39A). The increased accumulation of ECM in cell-seeded fibrin gels was also illustrated by an increased turbidity at d28 of the gels. In addition, MTT staining showed that both the native cartilage ring and the encapsulated cells were vital at the end of *in vitro* culture (see Figure 39B). A higher cartilage-specific ECM concentration in stable fibrin (50) gels compared to cell-free gels was also observable in the Safranin O and the collagen Type II immuno staining (see Figure 39C). Interestingly, even in the cell-free gels after 28 days a slight but relatively evenly distributed GAG coloration of the gels was visible. In comparison to the cell-laden hydrogels, no collagen type II was detected in the cell-free hydrogels after 28 days. When looking at the d0 images,

a gap is visible at the interface region of the hydrogels and the cartilage tissue, that resulted from a condensation of the hydrogels during the crosslinking process. However, particularly at the interfacial regions individual cells could be seen which migrated into the initially cell-free hydrogels at d28. In the interface region between hydrogel and cartilage ring, a region of less than 100 µm was also partially visible, in which an increased concentration of GAG can be seen, in the cell-seeded gels additionally collagen type II.
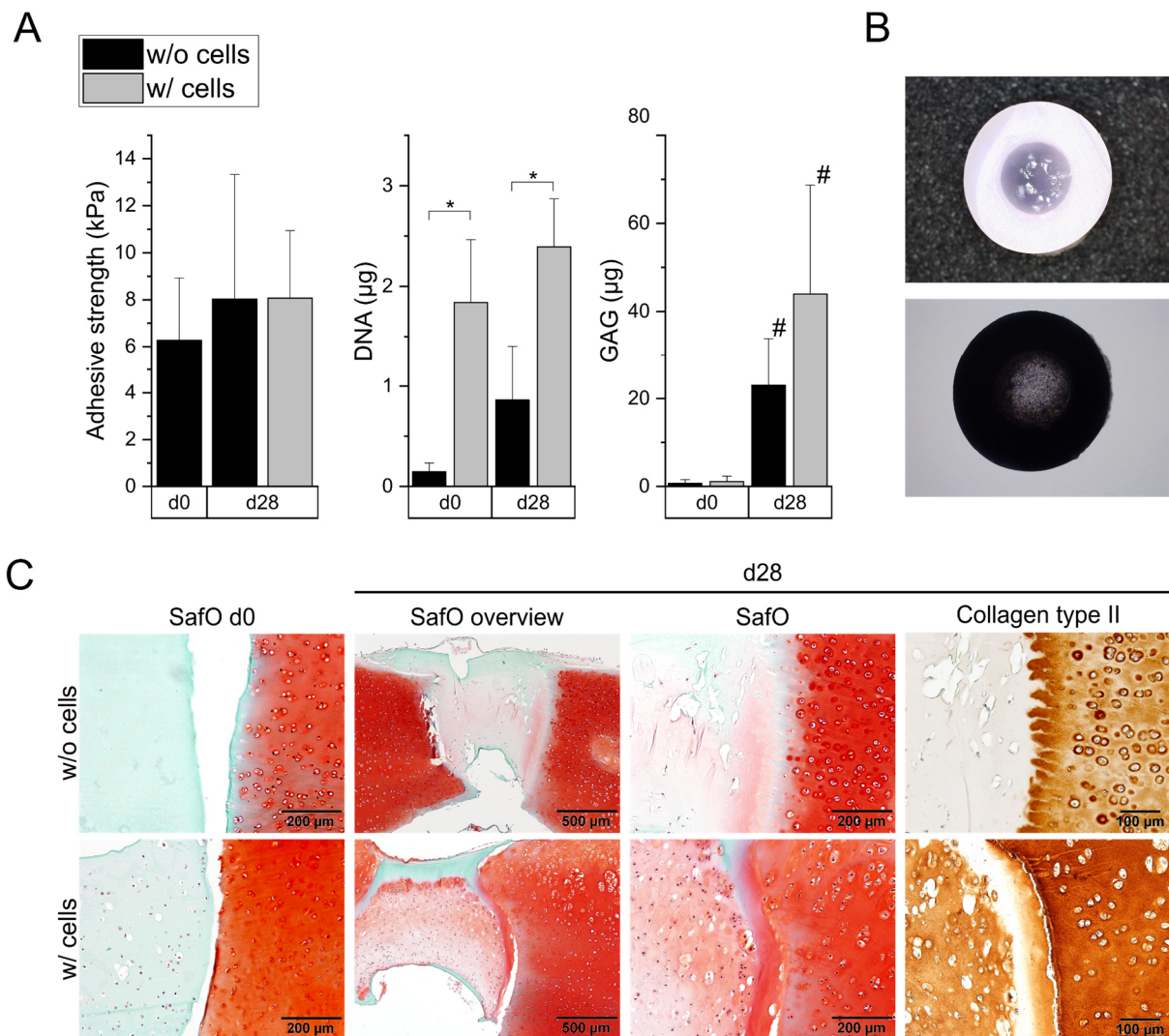


**Figure 39: Long-term cartilage integration of stable fibrin (50) hydrogel constructs.**

A) Integration strength determined with a push-out test and DNA and GAG concentration of cell-free and cell-laden fibrin gels cultivated in a cartilage tissue ring. B) Macroscopical images of an unstained and an MTT-stained cell-laden composite construct at d28. C) Safranin O and Collagen type II stainings of the interface region of cell-free and cell-laden hydrogel-cartilage composites. Data are presented as means ± standard deviation (n= 4-5). (* = $p < 0.05$ between groups, # = $p < 0.05$ to d0 value of same group.

### 4.5.3    Integration of Cell-Laden Agarose Hydrogels

In another approach to investigate the integration of tissue-engineered cartilage constructs into native cartilage tissue, agarose was used as cell carrier material. Agarose is a natural polysaccharide polymer that, unlike fibrin, gelates simply by cooling due to its thermal hysteresis properties. Agarose hydrogels are frequently used for cell encapsulation and for cartilage tissue engineering approaches. In contrast to fibrin, chondrocytes have no possibility for cell adhesion on or enzymatic degradation of agarose. These contrasts offer an interesting basis for the investigation of factors influencing the integration of tissue engineering constructs with the surrounding cartilage tissue.

#### 4.5.3.1    Long-term integration of cell-laden agarose hydrogels

For the preparation of cell-seeded agarose hydrogels, porcine chondrocytes were isolated and cultivated *in vitro* for five days with chondrocyte proliferation medium. Afterwards the cells were trypsinized and resuspended in a tempered agarose solution. For the experiments, a final agarose concentration of 2 % w/v was used with a cell density of approximately $1.5 \times 10^6$ cells/ml. For the preparation of the cartilage ring/hydrogel composites the agarose solution was transferred to the lumen of the ring and the constructs were stored in the refrigerator for ten minutes in order to allow gelation of the hydrogels. Simultaneously to experiments conducted with table fibrin 50 hydrogels, cell-free and cell-laden hydrogels were used as experimental groups and cultivated *in vitro* for 28 days.

After the *in vitro* culture of 28 days the integration strength of the hydrogels to the native tissue was determined by a push-out test. Additionally, the DNA and GAG content of the pushed-out hydrogels were determined. Separate constructs were sectioned and analyzed histologically and immunohistochemically. An increase in integration strength was only observable when the agarose hydrogels were seeded with chondrocytes ($3.8 \pm 0.7$ kPa for cell-laden vs. $1.2 \pm 0.9$ kPa for cell-free gels).

As seen before with stable fibrin (50) gels, the GAG content in both the cell-free and cell-laden hydrogels increased after the *in vitro* culture period. However, no increase in DNA content was determined in the cell-free group. For the cell-laden group a significant loss of DNA content was detected in the hydrogels at d28 compared to the d0 constructs. Despite the reduced number of cells, a significant increase of GAG was obtained in cell-laden agarose gels after 28 days ($113.8 \pm 1.1$ kPa)(see Figure 40A). The increased accumulation of ECM in cell-seeded agarose gels was also illustrated by an increased turbidity at d28 of the gels. The MTT staining showed good cell visibility in both the native cartilage ring and the encapsulated cells at the end of *in vitro* culture (see Figure 40B). The results as described for the biochemical analysis of the hydrogels was confirmed by the histological and

immunohistochemical staining. The agarose hydrogels have retained their shape and thus had almost direct contact with the adjacent cartilage tissue at d28. A slight and evenly distributed GAG content can be seen in the cell-free agarose gels after 28 days, whereas in the cell-laden constructs a strong pericellular and a lower distributed GAG concentration is visible. The same pattern is recognizable for the collagen type II signal in the cell-seeded gels (see Figure 40C). No cell migration was observable in the cell-free agarose gels.
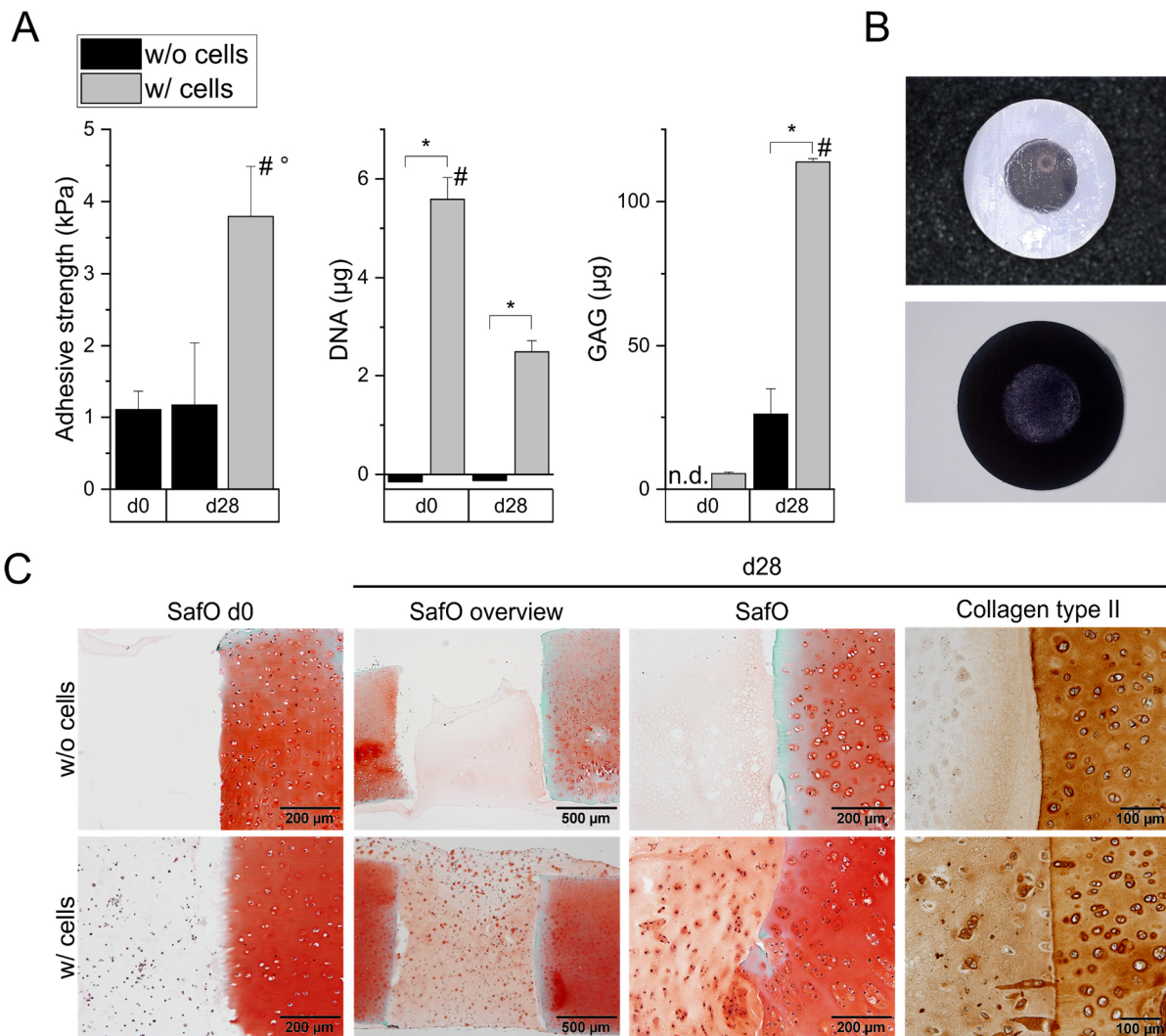


**Figure 40: Long-term cartilage integration of agarose hydrogel constructs.**

A) Integration strength determined with a push-out test and DNA and GAG concentration of cell-free and cell-laden agarose gels cultivated in a cartilage tissue ring. B) Macroscopical images of an unstained and an MTT-stained cell-laden composite construct at d28. C) Safranin O and Collagen type II stainings of the interface region of cell-free and cell-laden hydrogel-cartilage composites. Data are presented as means ± standard deviation (n= 4-5). (*;° = $p < 0.05$ between groups, # = $p < 0.05$ to different time-point of same group.

## 4.5.4 Integration of Cell-Laden HA-SH/P(AGE/G) Hydrogels

Experiments conducted before used the naturally derived materials fibrin and agarose as scaffold material for cell encapsulation. Synthetically produced materials offer additional possibilities for tissue engineering in terms of adaptability of material properties and the manufacturing process. A hydrogel based on functionalized hyaluronic acid (HA-SH) and polyglycidol (P(AGE/G)) was produced as part of the development of a bio-ink with the aim of 3D printed tissue engineered constructs for the treatment of cartilage defects [100,149]. The versatility of this material allows in principle the production of complex structures and the starting material hyaluronic acid is a natural component of native articular cartilage. As the material has only recently been developed, detailed knowledge about the potential for cartilage regeneration using chondrocytes as cell type and the integration of the material with native cartilage tissue is still missing. The following experiments used chondrocyte-laden HA-SH/P(AGE/G) hydrogels for *in vitro* tissue formation and integration observation in comparison the reference material agarose.

### 4.5.4.1 Influence of oxygen on seeded chondrocytes

As was also demonstrated recently by members of our group, the oxygen concentration during *in vitro* culture has an direct influence on cartilage tissue formation in agarose gels seeded with articular cartilage progenitor cells (ACPCs) and/or mesenchymal stromal cells (MSCs) [364]. Within the preliminary experiment presented in the following both agarose and HA-SH/P(AGE/G) hydrogels were seeded with chondrocytes (approx. $1.5 \times 10^6$ cells/ml) and cultivated either under normoxic or under hypoxic conditions for 21 days to investigate the relation of oxygen concentration on the formation of cartilage specific ECM. In both hydrogel types an increase in total GAG and collagen concentration per gel was obtained after 21 days *in vitro* culture (see Figure 41). Surprisingly, the net GAG content was significantly higher in agarose than in HA-SH/P(AGE/G) gels for both oxygen conditions, but the collagen content resulted on similar concentrations irrespective of oxygen concentration during cultivation. However, it has to be noted that DNA concentration in HA-SH/P(AGE/G) gels increased over the culture period in contrast to agarose. When normalizing the net GAG content to the DNA it is recognizable for cell-seeded HA-SH/P(AGE/G) hydrogels that a significant higher GAG amount per DNA was achieved under hypoxic condition and the difference to the amount achieved in agarose gels of both oxygen conditions was insignificant (see Figure 41A). When looking at the collagen concentration a significant higher amount was obtained only in the DNA normalized values for agarose under normoxic conditions.

Immunohistochemical staining was performed with sections of both hydrogel materials and the different oxygen conditioning. It was obviously, that agarose not only had a higher cell number but

also showed a much better distribution of aggrecan and collagen type II over the complete gel area (see Figure 42). In the HA-SH(PAGE/G) hydrogels in both oxygen conditions the deposition of the ECM components remained in restriction to the pericellular area. Within the immunohistochemistry no clear difference in cartilage specific ECM formation was found between normoxic and hypoxic conditions in both hydrogel types, which is why following experiments where these two hydrogel materials are compared against each other were performed under normoxic conditions.
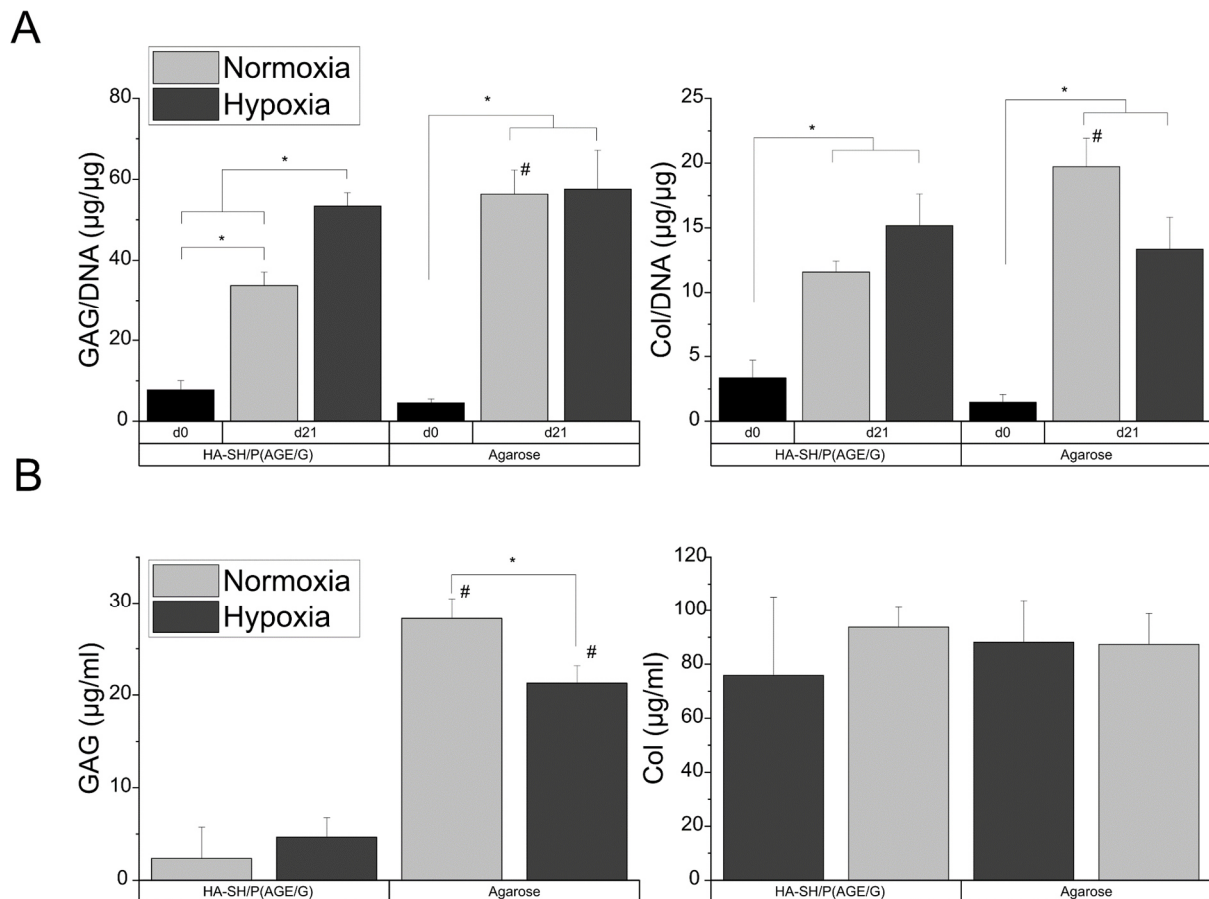


**Figure 41: Biochemical analysis of ECM deposition in dependency of atmospheric oxygen concentration in HA-SH(P(AGE/G) and agarose hydrogels.**

A) GAG and collagen concentration determined in hydrogels normated to the respective DNA content. B) Total GAG and collagen concentration in hydrogels after 21 days of culture. Data are presented as means ± standard deviation (n= 2-4). (* = p < 0.05 between values of same material group, # = p < 0.05 to different material group at same time-point)
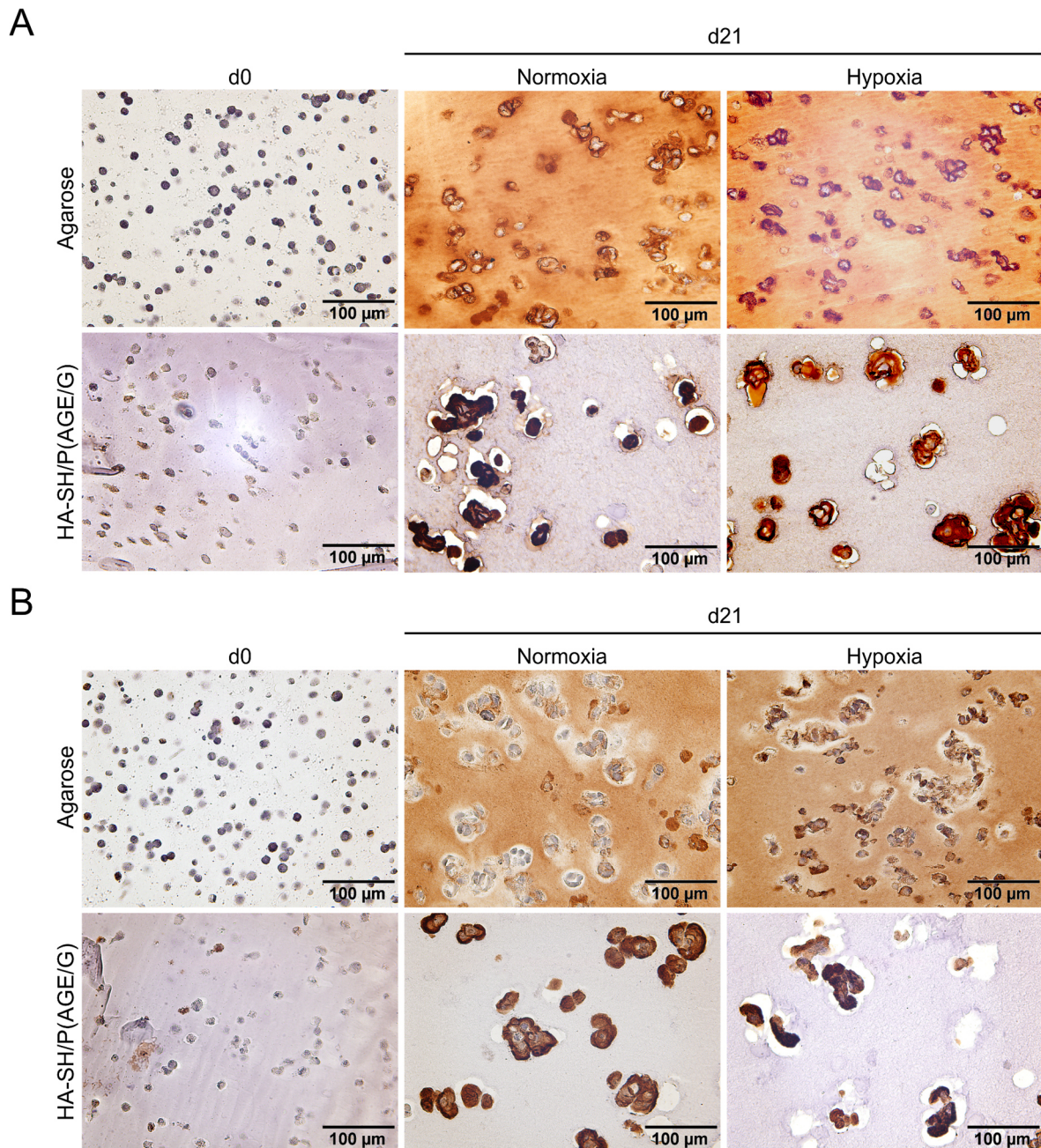
**Figure 42: Histological analysis of ECM deposition in dependency of atmospheric oxygen concentration in HA-SH(P(AGE/G) and agarose hydrogels.**

Immunohistochemical staining for A) aggrecan and B) collagen type II of agarose and HA-SH/P(AGE/G) hydrogels at d0 or after 21 days cultivation under normoxic or hypoxic conditions.

### 4.5.4.2 Long-term integration of cell-laden HA-SH/P(AGE/G) hydrogels

The gelation process of HA-SH/P(AGE/G) hydrogels is based on UV-initiated thiol-ene reaction [149]. In contrast to the thermal solidification of agarose, this reaction has the potential ability to react with surface molecules of the cartilage tissue, which would lead to a covalent binding of hydrogel

components with the cartilage and thus could directly initiate the integration to the native tissue. For this reason, an experiment with HA-SH/P(AGE/G) hydrogels fabricated as a composite with an articular cartilage ring was conducted to investigate the integration potential via push-out testing and histology of the interfacial zone. As this material was developed as a bioink for 3D printing of cartilage tissue engineering constructs where a double-printing approach with thermoplastic poly(ε-caprolactone)(PCL) is aimed to enhance the hydrogels mechanical resistance, separate constructs were created where a PCL grid was placed inside the cartilage ring prior to the addition of the hydrogel solutions and UV-irradiation. In a control group, hydrogels of the same diameter were prepared outside of the cartilage (pre-cast) and then inserted into the cartilage ring. As reference group agarose was used. Similar to experiments conducted before, a final chondrocyte density of approximately $1.5 \times 10^6$ cells/ml was used in the final hydrogels. Curing for ten minutes under UV light of 365 nm led to solidified HA-SH/P(AGE/G) gels in all groups. As expected, very low integration strengths were detected for agarose and pre-cast constructions. In comparison to agarose and pre-cast constructs, the HA-SH/P(AGE/G) without and with PCL reinforcement had a significant higher immediate integration strength (16.1 ± 0.9 kPa and 13.7 ± 7.7 kPa). However, after 21 days *in vitro* culture a decrease of the initial integration strength was observed for those two groups. A slight increase in integration strength was obtained for the pre-cast group and for agarose a comparatively strong
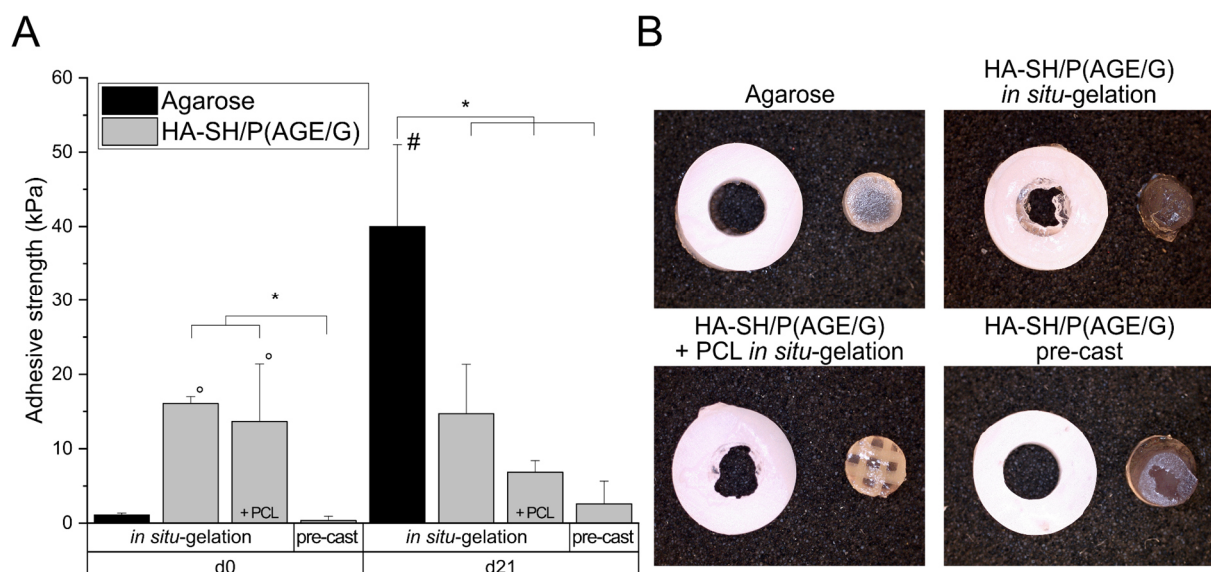


**Figure 43: Long-term cartilage integration of HA-SH/P(AGE/G) hydrogel constructs in comparison to agarose.**

A) Integration strength determined in a push-out test of agarose gels and HA-SH/P(AGE/G) that have either been crosslinked in situ within a cartilage ring or have been transferred to the cartilage after gelation in an external mold (pre-cast). In one group a rigid PCL grid was placed in the cartilage ring before the hydrogel solution was applied aiming to enhance mechanical properties. B) Macroscopical images of the hydrogel-cartilage composites after the push-out test. Data are presented as means ± standard deviation (n=6). (*= p < 0.05 between groups, # = p < 0.05 to d0 value of same group, ° = p < 0.05 to agarose value at same time point.
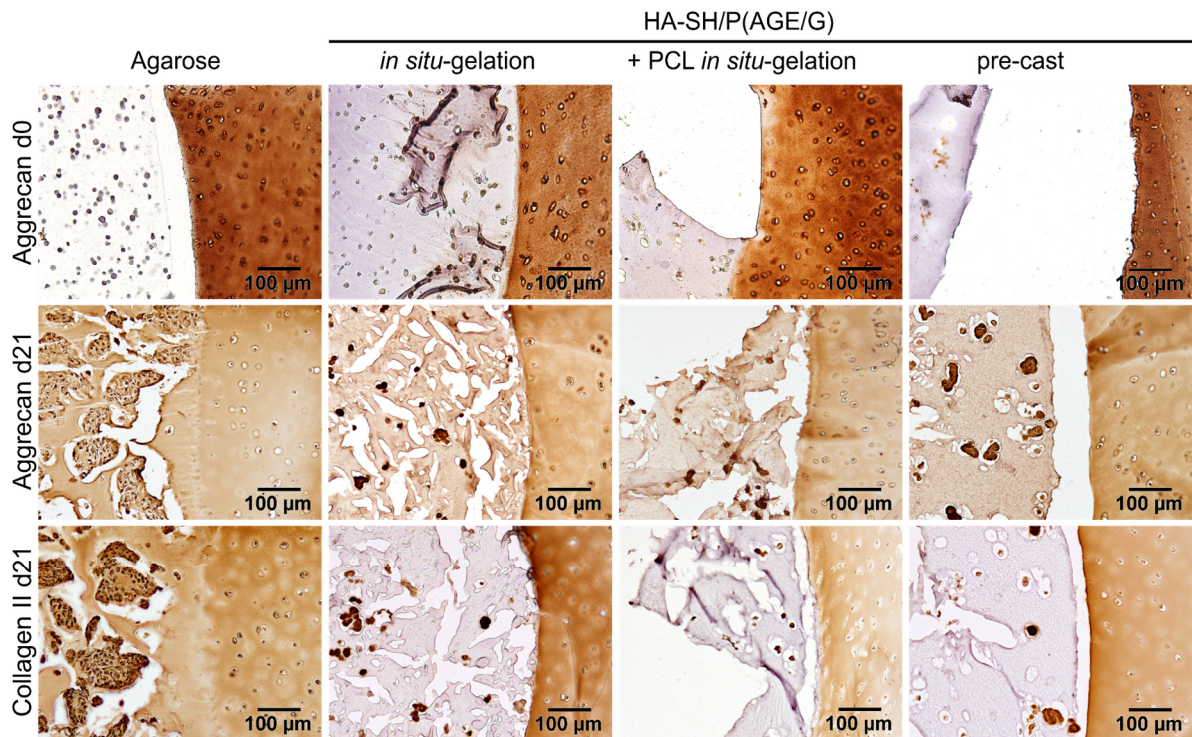
increase in integration strength up to $40.0 \pm 11.0$ kPa was detected. The integration strength value of agarose at d21 was significantly higher compared to its d0 value but also to the d21 values of all three groups using the HA-SH/P(AGE/G) hydrogel (see Figure 43A).

In sections of agarose-cartilage composites cell clusters in the hydrogel with a strong signal for cartilage specific ECM components was observed. Outside the cell clusters an even distribution of aggrecan and collagen type II in the agarose was observed at d21. In contrast, all HA-SH/P(AGE/G) hydrogels showed a lower cell concentration after *in vitro* cultivation. The collagen type II deposition in HA-SH/P(AGE/G) was strongly limited to the pericellular space. For aggrecan, a strong cell-bound signal as well as an increased deposition within the gel material could be detected.

In the agarose group there were no recognizable connections between tissue and hydrogel at d0, but at d21 numerous areas can be found where a good fusion of the tissue engineering construct with the cartilage ring can be seen. In sections of HA-SH/P(AGE/G) it appears as if the gel strength is decreased due to increased visible ruptures within the hydrogel. As expected, there is no immediate integration after construction in the pre-cast group. In contrast, HA-SH/P(AGE/G) gels that were crosslinked in contact with the native cartilage show an immediate firm connection to tissue. After 21 days, the integration of HA-SH/P(AGE/G) to the cartilage is less obvious and only fragments are adherently bound to the tissue. Due to processing with organic solvents during the staining procedure, the PCL Scaffold dissolves and could be recognized afterwards only as a negative with a sharp demarcation to the hydrogel within the cartilage ring lumen (see Figure 44A).

The quantification of the amount of DNA in pushed-out gels showed an initially comparable amount between the groups. After 21 days of *in vitro* culture, only agarose showed a significant increase in DNA amount per gel. The detected amount was also significantly higher than in the *in situ* prepared HA-SH/P(AGE/G) gels. However, an increase in DNA amount was also detected in the pre-cast group and after 21 days this amount was also significantly higher than in the *in situ* prepared gels of the same material. In the quantification of GAG and collagen a significant increase to d0 constructs was detected in agarose only and the d21 levels were significantly higher than in the HA-SH/P(AGE/G) groups. However, at least for GAG, a significant increase in the amount was detected in the group without PCL reinforcement and the pre-cast group (see Figure 44B).
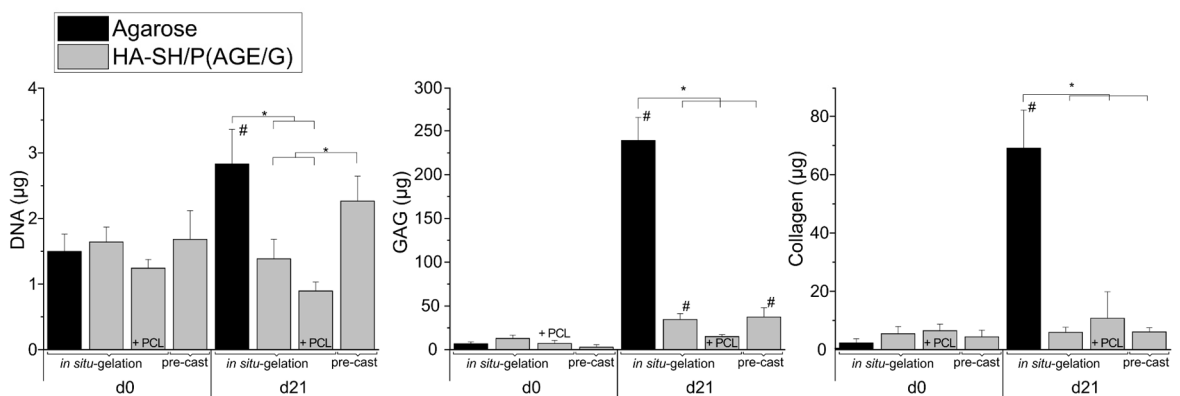
**Figure 44: Histological and biochemical evaluation of ECM formation in HA-SH/P(AGE/G) hydrogel constructs in comparison to agarose.**

A) Immunohistochemical staining for aggrecan and collagen type II of agarose and HA-SH/P(AGE/G) cartilage composites. HA-SH/P(AGE/G) has either been crosslinked *in situ* within a cartilage ring or has been transferred to the cartilage after gelation in an external mold (pre-cast). In one group a rigid PCL grid was placed in the cartilage ring before the hydrogel solution was applied aiming to enhance mechanical properties. B) Biochemical determination of DNA, GAG and collagen content in the hydrogels after a push-out test. Data are presented as means ± standard deviation (n=6). (*= p < 0.05 between groups, # = p < 0.05 to d0 value of same group.

### 4.5.5    Discussion

Tissue engineering is a promising approach for articular cartilage repair. It also enables versatile research into cartilage development, function and structure, which is essential for the development of successful treatments for cartilage defects. In principle, tissue engineering of tissue replacement implants requires a three-dimensional construct. Therefore, a widely used approach is the colonization of a carrier material with a suitable cell type to build up tissue-specific matrix. In addition to solid scaffolds, hydrogels are also frequently used as a carrier material, since their intrinsic properties provide a good basis for tissue engineering.

Although hydrogels lack the mechanical properties of rigid scaffolds, the use of these comparable softer materials has several advantages. Due to the direct encapsulation of cells, seeding efficiency is high and the seeding procedure is simple, resulting in homogeneous cell distribution. In addition, hydrogels can be used for delivery of sensitive molecules (e.g., bioactive peptides, growth factors, and DNA), and delivery of oxygen, nutrients, and additives to the encapsulated cells is excellent because hydrogels have high permeability to fluids. Various materials in different modifications are used for cartilage tissue engineering, which illustrates the versatility of this concept. In addition to protein-, polysaccharide- or protein-polysaccharide-based hydrogels or chemically modified proteins and polysaccharides, a variety of synthetic polymers or hybrids of biopolymers and synthetic polymers (composite hydrogels) are also being investigated.

However, hydrogels can be used not only for growing mature tissue under laboratory conditions, but also as space-filling materials for defects after trauma or injury that will be transformed into functional tissue over time. This treatment approach for cartilage defects is referred as matrix-induced autologous chondrocyte transplantation/implantation (MACT/MACI) and different set-ups are already approved for clinics [365,366]. Huang et al. extensively reviewed chondrocyte- and scaffold-based implants for cartilage repair that are currently used in clinical approaches [367]. Hydrogels are generally network systems consisting of macromolecular polymers. Their hydrophilic residues bond with water molecules and the hydrophobic residues expand with water to form crosslinked polymers that can absorb high amounts of water. The network of physically crosslinked hydrogels is aggregated by molecular entanglement, ionic bonding, hydrogen bonding, or hydrophobic interaction to form a reversible structure that gradually degrades in water and is generally non-uniform. The network formed by covalent bonds is called a chemically crosslinked hydrogel, which is stable, homogeneous, and difficult to degrade. The source of hydrogels is usually natural or synthetic polymers. Natural polymers have distinct biomedical applications and properties, such as nontoxicity and biodegradability, but poor stability; synthetic polymers are just the opposite. The compressive strength of hydrogels used for cartilage repair were reported to range from about 0.5 to 5.6 MPa. However, supplementation of

hydrogels with artificial polymers such as polylactic co-glycolic acid (PLGA), polymethyl methacrylate (PMMA), polycaprolactone (PCL), and poly(ethylene glycol) (PEG) can increase the compressive strength up to 20 - 120 MPa [368].

The mechanical properties of hydrogels can affect the stability of the material and the behavior of cells, including cell spreading, migration, and differentiation, by influencing the signal transformation process; for example, the mechanical signals are converted into biochemical signals. Thus, hydrogels with different mechanical properties can be chosen according to the specific requirements and the effects of different mechanical strengths on the explored cell behavior. The swelling rate of hydrogels is primarily determined by the hydrophilicity of the materials and the internal crosslink density. As a rule, the harder the hydrogels, the lower the swelling rates. The internal pore size and porosity of the hydrogels can directly affect the exchange capacity, swelling rate and mechanical properties. Thus, hydrogels with low swelling rate, mass transfer capacity and high elastic modulus have low pore size and porosity. Sufficient biodegradability is essential for the application of hydrogels in tissue engineering and clinical tissue regeneration. Compared to non-degradable hydrogels, the migration and intercellular interaction of cells are significantly enhanced in biodegradable hydrogels. Due to the lack of blood vessels, nerves, and lymphatics, mature cartilage cannot spontaneously heal the defects caused by osteoarthritis, aging, or joint injury [368].

Current cartilage tissue engineering strategies are not yet capable of producing artificial cartilage that is indistinguishable from native cartilage in terms of zonal organization, extracellular matrix (ECM), and mechanical properties. As an ideal strategy for repairing large chondral defects, the structure of the cartilage and eventually the subchondral bone must be regenerated layer by layer [8,31]. Layered hydrogel constructs were shown to achieve promising results with regard to the creation of hierarchical structures that can further be utilized in rapid prototyping via bioprinting [101,364,369]. In addition to the reconstruction structures, cell seeding, cell differentiation, and long-term safety of the implants are other difficulties that must be overcome. The usage of naturally derived hydrogels components may favor those requirements.

Another strong advantage of hydrogel approaches is the ability to perform minimally invasive surgeries by means of endoscopically filling precursor solutions into the defect and creating a defect-filling construct via respective curing mechanisms. The fluid nature of the hydrogel solution allows direct contact of the biomaterial to the complete articular surface, even with complex defect geometries. If compatible, chondrocytes or other cell types can be added to the solution to promote *in situ* maturation of new tissue in the hydrogel. Since integration with the cartilage is necessary for the long-term success of the therapy, many research groups are pursuing the goal of developing adhesive hydrogel materials that allow direct bonding to the native tissue, similar to the cartilage

adhesives already discussed (see Chapters 4.2 - 4.4). Ideally, such a material should have a strong adhesive strength to allow a certain mechanical stability and at the same time allow the deposition and remodeling of biomacromolecules in order to seamlessly transition to the native tissue over time.

The group around Elisseeff et al. developed different hydrogel materials where functionalized PEG polymers introduced a, reactive mechanism that both allowed tissue adhesion and hydrogel solidification [88,206,208]. Kazusa et al. described a biodegradable hydrogel glue that achieved 3.8 times higher adhesive strengths on articular cartilage than fibrin in an *ex vivo* pull-out setup [370]. Their adhesion mechanism based on the introduction of aldehyde groups into an α-glucan (e.g., dextran (polysaccharide) and starch) through oxidation, followed by a reaction with polylysine. Although these studies demonstrated high initial bond strength and good tissue regeneration *in vivo*, the chosen test systems do not allow biomechanical or histological investigation *in vitro* in a controllable milieu.

The disc/ring model that was described earlier and was successfully established for biomechanical integration strength assessment of cartilage glues allows also long-term *in vitro* cultivation. This model can be easily adapted to investigate integration of bulk biomaterial constructs [162]. The punched out inner cartilage disc is exchanged for an appropriate material, resulting in an annular interface of the construct with the surrounding cartilage ring. The integration force to the cartilage can be determined biomechanically by means of a push-out test. In principle, pre-matured tissue-engineered constructs can be used as the construct, and adhesive hydrogel materials can be pipetted in and cured in direct contact with the cartilage. The successful application of this model to studies of hydrogel integration with cartilage tissue has been reported previously in the literature. Broguiere et al. applied functionalized hyaluronic acid hydrogels to a cartilage ring followed by biomechanical push-out testing [220]. A further study using a cartilage disc/ring model adaption investigated the potential of the metallo-enzyme lysyl-oxidase (LOX) to form collagen crosslinks at the cartilage defect interface. In their experiments, the researchers used not only pure cartilage disc/ring constructs, but also pre-matured tissue engineered constructs that were centered in the cartilage ring instead of the cartilage disc. The investigators evaluated the bonding strength of the LOX-glued constructs over a four-week course *in vitro* culture. The results show that collagen crosslinking is a decisive factor for cartilage integration. However, a complete annealing of the opposing pieces was not achieved and histology indicated a narrowing gap at the cartilage interface, which shows the limits of crosslinking without a gap-filling matrix [217]. Therefore, approaches are needed to fill in deformities and cavities of cartilage damage and hydrogels are the most suitable candidates. Similar to the experiments performed by other groups, it was shown by here presented results that the disc/ring model is excellent for studying the interaction of biomaterials with cartilage and the time course of integration. In tissue engineering experiments, the capacity of tissue re-creation in a material is usually studied under simplified conditions and with

stand-alone constructs. The combination of the material with the target tissue for clinical application, as simulated here for cartilage defects, additionally allows the investigation of the influence of the surrounding tissue on tissue development in the respective biomaterial. Secreted substances and ECM building blocks from the cartilage can have a strong effect on the integration increase and correspondingly on the cartilage new synthesis in the construct. This allows targeted optimization of biomaterials in a standardized *in vitro* model closer to clinical application.

In the disc/ring model described, the surrounding tissue is exclusively articular cartilage and the influence of other tissues such as the subchondral bone and synovium are excluded. Although this set-up does not totally replicate the physiological environment and the multifactorial influence on cartilage regeneration, it can be assumed that the adjacent cartilage has the greatest influence on lateral integration. Supplementation of the culture medium can also be used to investigate specific factors and their influence on integrative repair. The group of Tuan et al. et al. were able to demonstrate that proinflammatory cytokines hinder the integration of cell-laden hydrogels to the adjacent cartilage ring [178] and that supplementation with growth factors can foster integration [216]. In addition to biomechanical determination of the integration strength, the expressed constructs can subsequently be subjected to standard tissue development studies, e.g. biochemical quantification of ECM molecules. In principle, the disc/ring model can also be adapted for other tissue types to investigate interfacial integration at defects. Besides cartilage rings, Tognana et al. used vital and devitalized bone rings to investigate integration of engineered constructs [371]. An extension of the disc/ring model described here with an attached subchondral plate has already been described in the context of integrative cartilage repair [222–225,372]. Osteochondral plugs can easily be retrieved from donor animals and chondral defect cavities can be created that reach up to the attached subchondral bone. In order to assess the lateral integration strength of an inserted material to the adjacent cartilage tissue, the chondral portions of the osteochondral explants can carefully be separated from the subchondral bone prior push-out testing [164,169,188]. To achieve improved cartilage regeneration, materials that resemble the natural cartilage ECM and allow cells to form and secrete new cartilaginous tissue while replacing the scaffold material appear desirable. The aim of the experiments performed was to investigate under controlled conditions in the cartilage disc/ring construct the integration of hydrogels with adhesive (fibrin) or non-adhesive properties (agarose) known from cartilage tissue-engineering, as well as a newly developed hyaluronic acid gel. The tested materials are cell compatible and the influence of encapsulated cells on the integration process in the respective hydrogel material was investigated.

In cartilage tissue engineering, different cell types are used to generate new cartilage tissue. Chondrocytes derived from cartilage or stem cells that can be differentiated into chondrocytes are

used to produce tissue that is intended to be as similar as possible to natural articular cartilage. When the right combination of cell type, scaffold, and other stimuli are used, cartilage can be produced that resembles natural tissue. MSCs are considered a potential cell source for cartilage repair because they can differentiate into chondrocytes and, unlike chondrocytes, do not lose this chondrogenic potential in with advancing *in vitro* expansion. However, they also tend to form fibrocartilage rather than articular cartilage and may undergo terminal differentiation and hypertrophy. This can lead to endochondral ossification and decreased functionality of the cartilage tissue [373]. Multipotent articular cartilage-resident chondroprogenitor cells (ACPCs) are a relatively new and promising cell source for cartilage repair found in the upper layer of articular cartilage [175]. They have the same advantage over chondrocytes as MSCs in that they can be expanded without losing their ability to undergo chondrogenic differentiation [374]. In addition, studies have found a high chondrogenic potential and no tendency to terminal differentiation [375,376].

In the experiments reported here, chondrocytes were used to seed the hydrogels because they can be isolated in large quantities from the same tissue of origin as the disc/ring model used. In addition, ACPCs and MSCs require specific culture conditions, e.g. addition of growth factors to induce chondrogenic differentiation [101,364]. In turn, optimizing culture conditions for a particular cell type may have implications or drawbacks for the native cartilage and its chondrocytes, which could complicate interpretations, especially for hybrid constructs of a hydrogel and a cartilage ring. A good understanding of the chondrocytes' interaction with a carrier material is also important for integrative cartilage regeneration. This assumption is further supported by observation in several here reported gluing experiments that chondrocytes from the surrounding native tissue migrate into the defect and contribute to regeneration.

### 4.5.5.1 Chondrocyte isolation and cultivation

When primary chondrocytes are grown in a monolayer culture, dedifferentiation occurs in which they lose their phenotype and ability to form cartilage. Dedifferentiation is an obstacle to cell therapy for cartilage degeneration. *In vitro* expanded human chondrocytes showed progressive changes in gene expression, affecting e.g. BMP- and ERK-signaling. A general decrease in overall gene expression was observed, which was both gradual and cumulative [377]. Overall, as a rule of thumb, the longer chondrocytes are kept under 2D culture conditions *in vitro*, the more they lose their chondrogenic potential.

To investigate the ability of chondrocytes to regenerate cartilage tissue *in vitro* and *in vivo*, researchers expanded chondrocytes *in vitro* up to a passage number of five, placed them on

biodegradable polymer scaffolds, and maintained them *in vitro* or implanted them in the subcutaneous areas of athymic mice for one month. It was found that passage two chondrocytes showed high expression of collagen type II and low expression of collagen type I. In contrast, passage five chondrocytes showed low expression of collagen type II and high expression of collagen type I, indicating dedifferentiation of chondrocytes. Histological and immunohistochemical analyses of cartilage tissue prepared *in vitro* and *in vivo* with passage one chondrocytes showed mature and well-formed cartilage and the presence of highly sulfated glycosaminoglycans and type II collagen, a type of collagen produced by differentiated chondrocytes. In contrast, tissues prepared *in vitro* and *in vivo* with passage five chondrocytes did not exhibit chondrocyte morphology or cartilage-specific extracellular matrices (i.e., glycosaminoglycans and type II collagen). The results of this study indicate that chondrocyte passage number is an important factor influencing the quality of cartilage tissue produced with chondrocytes and that chondrocytes [378].

Although the cell expansion step carries the risk of dedifferentiating isolated chondrocytes, potentially reducing the regenerative capacity toward functional hyaline cartilage tissue, short-term cell culture has major advantages. To allow efficient isolation of chondrocytes, tissue samples from an articular surface are usually mechanically minced prior to enzymatic digestion of the extracellular matrix. Even with the use of sharp instruments [14], this inevitably kills many cells, and the extent is difficult to determine in advance. Without a way to specifically filter out the dead cells from the resulting cell suspension, subsequently fabricated constructs can have a wide variation in overall cell viability. However, tissue formation is dependent on the cell density present [122,379] and comparability of, among other things, cartilage neosynthesis between different experimental approaches is hampered if a consistent cell density cannot be guaranteed. In addition, it remains unclear what influence dead cells have on the experimental process, e.g. through the release of cytokines [178]. Unlike dead cells, vital chondrocytes have the property of plastic adherence under normal cell culture conditions. Thus, dead cells can be easily removed with the supernatant from the culture by rinsing or changing the medium and thus a homogeneous solution of vital cells is obtained after detaching the 2D cell layer.

However, it must be noted that the use of chondrocytes for use in tissue engineering approaches also has limitations. A major advantage of other commonly used cell types, e.g. MSCs or ACPCs [369], is the possibility to obtain a high cell number from relatively little starting material via high cell culture passages. This is limited for chondrocytes at least with standardized 2D culture due to their dedifferentiation. In clinical applications, the use of autologous cells is a prerequisite. Conversely, this means that healthy cartilage tissue must be removed from the patient for the isolation of chondrocytes in order to treat a cartilage defect at a traumatized location. Even though the donor site is usually

taken from non-load bearing articular surfaces, an additional defect is still set. The short-term cultivation of isolated chondrocytes already allows the multiplication of the original cell number after a few days, which at least reduces the required starting material to achieve a certain cell number. In addition, several comparative studies revealed that chondrocytes cultured *in vitro* could produce more collagen type II than that of its stem cell counterparts [70].

Articular cartilage consists to large amounts of hyaluronic acid and chondrocytes can interfere with this extracellular component via the cell surface receptor CD44. The hyaluronan receptor CD44 serves as the critical link for the retention of hyaluronan-proteoglycan aggregates to the chondrocyte cell surface. Disruption of chondrocyte CD44-hyaluronan interaction triggers a cascade of events leading to activation of both catabolic and anabolic gene products. Fragments of hyaluronan generated in free radical processes have the potential to enhance nitric oxide production in a CD44-dependent mechanism. The data also support the emerging paradigm that CD44-mediated signaling influences both chondrocyte survival and apoptotic pathways [380]. Furthermore, it was shown that the expression of collagen type II and GAG is concomitant to a high CD44 signal on chondrocyte surfaces. The authors concluded that CD44 can function as a marker that allows characterization of the capacity of monolayer-expanded chondrocytes to form *in vitro* cartilaginous tissue [381].

For the experiments reported here, chondrocytes were isolated from porcine knees and used for subsequent experiments. In this way, it was achieved that the cells as well as the 3D cartilage tissue models used were taken from the same starting material from the local slaughterhouse. Although joints from different animals were randomly used, at least the same species and age of the animals can be assumed without large differences. Isolated chondrocytes were analyzed for CD44 by flow cytometry both immediately after isolation (P0) and after five days of *in vitro* expansion (P1). Both cell populations showed strong CD44 signals. However, in P0 chondrocytes, the CD44 signal was of lower intensity than in P1 cells (see Figure 37). As previously noted, there is also a high amount of dead cells and debris in the P0 population after isolation, which may have a negative impact on signal detection. Furthermore, it cannot be differentiated whether the enhanced CD44 signal is due to increased expression of the receptor in these cells or the altered cell morphology and increased homogeneity of the cell population after cell culture. However, due to the strong CD44 signal it could be assumed that the short-term cultured chondrocytes have the strong expression of collagen type II and GAG that is associated with CD44 presence. This, together with the increased cell number, the ethically acceptable porcine starting material and the possibility to obtain homogeneous cell populations, make the short-term cultured chondrocytes an ideal cell type for *in vitro* experiments in tissue engineering and regenerative cartilage research. Furthermore, for those porcine chondrocytes high synthesis rates of

articular cartilage specific matrix components were already demonstrated by our group in cell pellet experiments that investigated the influence of an inflammatory milieu on cartilage formation [289].

### 4.5.5.2 Chondrocyte-seeded fibrin hydrogels

Long-term stable fibrin was already tested as an adhesive in the disc/ring model with good results regarding cell migration and ECM deposition in the treated defect gap. Fibrin is also a suitable material for the filling of larger defects and the production of tissue-engineered cartilage, as it can be easily colonized with cells and has also been used clinically for many years in MACI applications with expanded chondrocytes [112,228].

In prior experiments using fibrin as cartilage glue material, no clear differences were observed between various long-term stable fibrin formulations and the commercial TissuCol (see also Chapter 4.2). For a successful treatment with a material, a solid integration of the material or construct to the native tissue is a prerequisite [8,152,169]. This in turn requires a certain dimensional stability of the material. Excessive swelling or shrinkage can loosen connections at the interface and thus negatively influence the course of integration. With the development of long-term stable fibrin formulations, it was shown that fibrin gels can be produced that maintain their size and shape over a period of several weeks [122]. As an originally physiological material, cells can remodel fibrin relatively rapidly and, particularly for cell-seeded TissuCol gels, severe shrinkage has been observed over time [117,118].

It is also known that the stiffness of the hydrogels has a strong influence on the performance of encapsulated cells [112]. In general, cells feel more comfortable in a less packed matrix and an increased expression of desired molecules is observed. However, softer gels are also less mechanically resilient and a good balance must be found where the applied material has sufficient mechanical integrity while maintaining high tissue synthesis. In the case of fibrin, the strength of the gels can be easily adjusted by the amount of fibrinogen in the precursor solutions.

Studies on the interactions of different hydrogel parameters are usually performed under simplified laboratory conditions by colonizing the different materials with cells and comparing the outcome after *in vitro* culture. In clinical application, however, the material is in a very complex environment and, in relation to cartilage defects, the adjacent cartilage tissue and synovium can have a strong influence on the cells encapsulated in the material. For this reason, experiments were performed in which long-term stable fibrin gels of different initial strength were seeded with chondrocytes and cultivated either as stand-alone constructs or the gels were placed between two discs of native cartilage and cultivated. The final fibrinogen concentration was either 15 (stable fibrin

(15)), 25 (stable fibrin (25)) or 50 mg/ml (stable fibrin (50)) and the constructs were cultivated *in vitro* for up to 21 days.

For the stand-alone gels biochemical analysis could be easily performed initially and after different time points of cultivation. The DNA content measurement revealed that initial cell densities can vary between the different stable fibrin gels. This may be due to varying viscosities of the respective fibrinogen precursor solutions that are used to resuspend chondrocyte pellets prior to gel formation and may thus complicate the homogenous distribution of the cells within the solution. Within the cured hydrogels, the DNA content remained consistent, indicating a lack of proliferation of cells in the fibrin gels. Nevertheless, it was obvious that despite lower initial cell densities, the GAG synthesis of encapsulated chondrocytes in stand-alone gels significantly increases the lower the fibrinogen content in the gel and thus the stiffness was (see Figure 38). This finding was also well reflected by the Safranin O staining for GAG. Microscopical images revealed that the distribution of synthesized ECM is not homogenous throughout the gels and with increasing fibrinogen concentration a trend is observable that the deposition of GAG is limited to the pericellular region of the encapsulated chondrocytes. The intensity of GAG signal was drastically higher in the softer stable fibrin (15) gels compared to stable fibrin (50) and also stable fibrin (25). It was also noticeable that the highest GAG intensity was found at the outer edge of the gels and was weaker towards the center of the gel. It is highly probable that this effect is due to a lack of supply of nutrients and oxygen to the cells located further in the interior. Due to the lack of capillary penetration of the hydrogels, the exchange of substances is based exclusively on diffusion. Although native cartilage tissue is avascular, constant compression forces promote hydrodynamic mass transfer even in deeper tissue layers. These compression forces as they occur in joints are also the reason why stiffer gels with higher mechanical load capacity would be an advantage for cartilage regeneration. Increasing stiffness of the hydrogel itself can be achieved by increasing the hydrogel crosslink density for example. Unfortunately, this also compromises formation of new tissue partly due to impaired diffusion coefficients of nutrients and waste products through the hydrogel system [106].

The fibrinogen content has a direct effect on the stiffness of a gel, and the denser the matrix, the more limited is the extent of diffusion of substances. In tissue engineering, various approaches are therefore being pursued to improve the supply of tissue constructs with the aid of blood vessels or inner structures and thus to circumvent a size limitation of the constructs. These approaches range from the use of growth factors to accelerate the ingrowth of blood vessels [382], to the use of co-cultures with vascular cells [117], to the additive manufacturing of constructs [103,106]. However, it is clear that *in vitro* cultures of stand-alone gel constructs allow only limited transfer to potential behavior under physiological conditions at the clinical site. Surrounding tissue and physiological conditions can act in

a variety of ways on a material and on interfacial cells and thus can also influence integration with the cartilage tissue [204,215,219]. DiMicco and Sah found that viable chondrocytes placed between to cartilage strips foster interfacial integration when both or a single of the cartilage stripes was vital but integration was completely hampered when the adjacent cartilage stripes were devitalized [189]. Theodoropopoulus et al. investigated the influence of mechanical loading on the integration of tissue-engineered cartilage constructs *in vitro* in a disc/ring model. Mechanical stimulation significantly improved the construct's integration to the native tissue and it was hypothesized that the correlating increase was either purely mechanically induced or secondarily due to an improved diffusion of nutrients [188]. To investigate the influence of native cartilage on the stable fibrin gels with different stiffness investigated here, additional constructs were made in which the respective colonized hydrogels were applied between two cylindrical cartilage discs. This sandwich-layered model, in contrast to the disc/ring model, allows an easy definable gel-filled interface via the amount of gel used and the spacing of the cartilage discs. Such sandwich-like constructs have been used previously for cartilage integration studies and in principle also allow biomechanical testing of integration strength [168,205]. Pabbruwe et al. investigated the integration of collagen/chondrocyte scaffolds sandwiched between two cartilage cylinders similar to the approach here with cell-seeded fibrin gels. With the model, excellent histological examination of the cartilage and scaffold continuum was possible. It was subsequently reported that integration was dependent on both the cells and the scaffold. Using originally cell-free scaffolds, it was demonstrated that chondrocytes from the surrounding tissue migrated into the scaffold and had a positive effect on integration [168]. In the here reported experiments of sandwich-like layered constructs with different stable fibrin formulations, a very different outcome was obtained compared to the stand-alone gels. It was clearly demonstrated that the surrounding cartilage leads to improved GAG deposition and distribution in the fibrin gels. Although, the strongest GAG signal and the highest GAG distribution was still observed in the stable fibrin (15), the negative effects of higher gel stiffness was strongly reduced. Histologic images show that, similar to previously reported results with fibrin as a cartilage glue (see Chapter 4.2), cells from the cartilage migrate into the interface and bud into the fibrin gel. However, gaps in the transition from tissue to gel were observable in all groups. It is unclear whether this is due to mechanically-induced detachment during histological preparation or a lack of material integration. Either way, this observation indicates insufficiently stable integration after three weeks of culture, which probably cannot withstand the strong mechanical forces under physiological conditions. Based on the comparison to the stand-alone gels, each with identical fibrinogen content, the hypothesis allows that surrounding cartilage tissue may cause an accelerated softening of the gels and thus a more homogeneous ECM synthesis, e.g. via the release of enzymes or other degrading factors.

To investigate the influence of surrounding cartilage tissue also on the material integration progress in cartilage defects lateral of orientation, further experiments with different hydrogel materials were investigated in the disc/ring model (see also the following subsections).

### 4.5.5.3 Lateral integration of different hydrogels

For the purpose of investigating the lateral integration capacity of different hydrogel materials, the disc/ring model that was used before with native cartilage-only constructs was adapted. Instead of assembling the *in vitro* model with both obtained cartilage parts, the outer cartilage ring served as a mold for the preparation of cartilage-hydrogel composites. A set of different hydrogel materials was chosen to include varying curing mechanisms and intrinsic gel properties on the integration outcome. A focus was set on materials that allow for cell-encapsulation and thus the potential administration of a cell-source to the cartilage defect. Due to gained experience in the course of prior conducted experiments, stable fibrin (50) was considered in further experiments. The direct curing of the hydrogels in the cartilage ring simulates a clinical application in which a liquid material is injected into the cartilage defect in a minimally invasive manner. The adhesive property of fibrin to tissue can also be accounted for in experimental observation in this way. The fact that stable fibrin (50) remains dimensionally stable even under prolonged *in vitro* cultivation continues to be seen as a good basic prerequisite for potentially maintaining the immediate bonding to the surrounding tissue and avoiding detachment by shrinkage as far as possible. Unlike fibrin, agarose solely solidifies by cooling down a pre-warmed hydrogel solution and does not require the formation of chemical crosslinks at the polymer backbone. As a biomaterial, agarose proved to be widely applicable. It is non-degradable but in general biocompatible, and with the same ease that a researcher can create a plate of agarose for electrophoresis, a more complex gel geometry can be formed that will retain its shape over time. In addition, agarose seeded with cells can be 3D printed in a variety of shapes [123]. Although no immediate covalent bonding of agarose to the adjacent cartilage can be expected, the material is known for its excellent neocartilage formation when seeded with chondrocytes for many years [133].

A novel hyaluronic acid and polyglycidol-based hydrogel was included in experiments as third material. The HA-SH/P(AGE/G) was developed by a cooperating working group as a bioink for 3D printing of cartilage constructs [100,149]. The allyl-functional linear polyglycidol can rapidly be polymerized with a thiol-functionalized hyaluronic acid polymer to a three-dimensionally crosslinked hydrogel network via UV mediated thiol-ene click reaction. It was hypothesized that free allyl and thiol groups can also be present in the macromolecular compounds of the cartilage matrix and thus lead to chemical bonding of the hydrogel to the adjacent tissue surface. Since only little experience of this

material with encapsulated chondrocytes was available, an additional experiment was conducted where chondrocytes were seeded to hydrogel cylinders either made of HA-SH/P(AGE/G) or agarose for comparative reasons. The obtained stand-alone constructs were cultivated for up to 21 days *in vitro* and newly synthesized ECM compounds were determined biochemically and histologically.

Under physiological conditions chondrocytes experience hypoxic conditions in their native environment. Contradictory results can be found in literature regarding chondrogenesis influenced by low oxygen tension in cartilage tissue engineering approaches both in agarose and hyaluronic acid hydrogels [364,383–385]. Therefore, this initial test was performed with stand-alone gels both under normoxic (21 % oxygen) and hypoxic (2 % oxygen) conditions with respect to chondrocyte-induced cartilage neosynthesis. Although no uniform cell density was obtained between agarose and HA-SH/P(AGE/G) gels in the experimental set-up and a direct comparison is unfortunately only possible to a limited extent, clear differences were discernible. Normalized to the respective DNA content in the gel, GAG and collagen type II depositions increased significantly in both hydrogel types irrespectively of the oxygen concentration. Agarose showed a much more homogenous distribution of aggrecan and collagen type II in the constructs (see Figure 42). In the HA-SH/P(AGE/G) hydrogels, the deposition of the ECM components remained in restriction to the pericellular area. Overall however, no clear difference in cartilage specific ECM formation was found between normoxic and hypoxic conditions in both hydrogel types, which is why further experiments concentrated on the standard cell culture with normoxic conditions, which was also applied in previous experiments and reflects the standard conditions used in most published works.

As mentioned before, the disc/ring model is suitable to further analyze both ECM deposition inside a hydrogel and the integrative process of the cartilage tissue with a filled biomaterial inside the cartilage ring. It can be hypothesized, that the development of tissue regeneration more closely resembles the clinical situation, since influencing factors of the native tissue are better considered compared to stand-alone culture of tissue engineered constructs.

By using the disc/ring model the influence of encapsulated chondrocytes within stable fibrin (50) gels on tissue formation and integration strength were directly compared to cell-free counterparts. The performed push-out tests revealed only a slight non-significant increase in integration strength for both the cell-free and the cell-laden hydrogels. However, it was observable in histology that large gaps were already visible at d0 at the transition from the fibrin gel to the cartilage, although the gels were pipetted into the ring and cured there. It cannot be completely ruled out that the handling of the constructs during histological preparation (e.g. fixation steps) leads to shrinkage accompanied by detachment of the gels from the adjacent cartilage surface. Compared to the small applied material amounts when gluing smaller defects, shrinkage would be even more pronounced in larger bulk

constructs. Once the cohesive force of a gel exceeds the integration force, shrinkage inevitably leads to detachment at the defect interface [212]. An enlarged defect gap, of course, significantly complicates the fusion of tissue and material in the long-term [386]. The long-term stable fibrin gels were also evaluated for their appearance and other physical properties [122]. Thereby, all gels were visually examined to assess turbidity and shrinkage, i.e., contraction directly after preparation as well as degradation and/or dissolution over time. Depending on the formulation and pH, a more or less pronounced shrinkage was observed in the different gels tested. Although the stable fibrin (50) formulation used here, in contrast to commercial fibrin, was among the candidates classified as dimensionally stable after manufacture, even minimal shrinkage of the material is sufficient to lose direct contact at the defect interface and it can be doubted that visual inspection is sufficiently sensitive to detect shrinkage in these relevant size dimensions. Despite the low increase in integration strength, the tested fibrin gels showed promising results in regard to tissue formation. After four weeks of *in vitro* culture an increase in DNA content within the hydrogels was observable in both groups. In colonized gels, cell proliferation of the encapsulated chondrocytes can in principle lead to an increase in DNA content. The increase in originally cell-free gels to the extent observed proved the migration of cells from the surrounding cartilage tissue. Histological staining also showed the presence of cells spanning over the whole previously cell-free gels, albeit at a much lower cell density than in the colonized gels. The migration of chondrocytes from adjacent cartilage tissue into fibrin gels was reported before [167]. The investigators were also able to demonstrate accelerated and empowered cell migration when the cartilage tissue was pre-treated with collagenase. Enzymatic softening of the dense cartilage matrix is known to be of strong influence on chondrocyte migration and can contribute to increasing integration strengths [162–166,207]. Seol et al. further reported that the potential of cell migration is dependent of the cell-layer in the surrounding cartilage tissue. Cells that migrated into fibrin mainly originated from the cartilage surface and subchondral bone. They showed different characteristics in terms of migratory and chondrogenic activity. The cells from the surface of cartilage had a high migratory ability. They also discussed that even with enzymatic treatment the cell migration is a rather slow process and significantly improved integration results are expectable when chondrocytes are directly inserted into the fibrin gel during gel preparation. Other studies confirmed the hypothesis of improved cartilage integration when cells are delivered to the defect zone within a biomaterial [168,169,177,221].

Histological images of the stable fibrin (50) constructs showed a slight accumulation of cartilage-specific ECM after four weeks in the initially cell-free gels. In the colonized gels, a distinctly higher concentration of ECM components within the gel was detectable both histologically and biochemically. An increased GAG signal and cell density was also observed in areas adjacent to deeper zones of the

explanted cartilage, again confirming the results of Seol et al. In the populated gels, a cell-free band was partially pronounced at the edges, where there is also significantly less ECM deposited. It is likely that this was due to the way the constructs were manufactured. The sequential pipetting of the two fibrin components into the cartilage ring may have caused one of the fluid solutions to bind to the edges by capillary forces and also partially migrate under the ring. Such effects can counteract homogeneous mixing with the subsequent component and may locally lead to altered gel characteristics at the edges (e.g. cell density, strength). By using collagen sheets placed between two layered cartilage discs, Pabbruwe et al. confirmed migration of chondrocytes from the surrounding tissue into the scaffold. More strikingly, they also demonstrated that when cells alone were allowed to adhere to the cartilage surface there was some filling of the space with proliferating cells but little or no extracellular matrix to bind the pieces of cartilage together. The alternative approach of delivering the chondrocytes within the scaffold led to drastically improved gap bridging [168].

The limited increase in measured integrative strength to an almost identical level in both groups supports the theory that shrinkage after gel curing creates a gap and the four-week culture period is not long enough to establish a stable bond to the fibrin. It can be speculated that poorer integrative results would be obtained with ordinary commercial fibrin or other fibrin formulations with observable shrinkage effects. However, the results showed that the fibrin formulation used has in principle good regenerative properties, especially in combination of encapsulated chondrocytes and the surrounding native tissue. It would be worthwhile in the future to evaluate possibilities or approaches that additionally prevent shrinkage of the gel material while supporting or even enhancing the positive properties of the fibrin, for example by using hybrid gels with additional polymeric components.

Unlike fibrin, agarose does not harden via chemical reactions but is thermoresponsive and solidifies by cooling. No shrinkage is to be expected afterwards and due to the lack of cell adhesion, encapsulated cells cannot directly influence the dimensional stability of agarose gels. This solidification mechanism also means that no firm bonds of the gel to the cartilage are to be expected despite curing in direct contact with the cartilage tissue [123]. This was also reflected in the measured immediate bonding values of approx. 1 kPa. The lack of adhesion motifs and the possibility of metabolic degradation of the agarose also prevent cell migration into the gel interior. Here, the difference to fibrin became clear, as in cell-free agarose gels after four weeks of *in vitro* culture no increase in integration strength was detected. The DNA measurement showed that there was no cell migration into agarose and also in the colonized gels there was a decrease in cell density during the course of the culture. However, the cell-free gels also showed a slight deposition of ECM after four weeks, but this was significantly increased in the colonized gels. Therefore, unlike fibrin, the increase in integration strength in the colonized agarose gels must have been mainly due to the encapsulated cells.

In subsequent experiments agarose was used as a reference material to HA-SH/P(AGE/G) hydrogels (see also Chapter 4.5.4.2). In those experiments, initial bonding strength of agarose was again virtually non-present despite curing in contact with the cartilage ring. However, despite the shorter *in vitro* cultivation period of 21 days, a dramatical increase in integration strength was observable (up to up to $40.0 \pm 11.0$ kPa, see also see Figure 43A). As in the prior experiment with agarose hydrogels, similar ECM formation and chondrocyte behavior in the hydrogels was observable after cultivation in presence of the adjacent cartilage ring. Both GAG and collagen type II were distributed over the whole gel, with particularly strong signal in formed cell clusters. These cell clusters were particularly strong in the interface zone at the lateral cartilage defect. A significant increase of DNA content in agarose gels after 21 days was also observed in this set of experiments (see Figure 44). However, no evidence of cell ingrowth from native cartilage was seen in the histological images, again illustrating that in this second approach with agarose, increased proliferation was stimulated within the gel near the cartilage interface and the high local cell density massively enhanced annealing. In contrast, within the first agarose approach the total amount of DNA in the gel decreased and the increase in integration was less pronounced, which illustrates the great influence of the presence of vital cells at the defect, apart from the material itself. However, it was also shown how variable experimental results can turn out in the same model, e.g. due to donor variability of the cell source. Conversely, this finding makes it difficult to compare different experiments and the use of interexperimental control groups is recommended for direct comparisons.

Agarose was considered as material for the conducted experiments because of its excellent intrinsic properties and positive experience in regenerative cartilage repair. Characteristics of agarose were well reviewed by Roach et al. with a focus on cartilage tissue engineering [123]. Already in 1998, agarose was implanted with chondrocytes into a rabbit model for the treatment of full-thickness defects. No graft-versus-host rejection was reported and hyaline tissue formation including the preservation of the chondrogenic phenotype was observed [387]. Especially a key study with chondrocyte-seeded agarose applied to a canine defect model reported great overall biocompatibility paired with the formation of functional cartilage tissue in the agarose grafts [125]. A hydrogel comprised of both agarose and alginate was also injected to 20 human patients within a clinical trial in the European Union [388]. In some of these patients, the hydrogel allowed for improved orientation and organization of the engineered tissue upon implantation, with the collagen fiber orientation closely mimicking that of native tissue. The group around Buschmann et al. concluded that the agarose network allows transmission of compression to the encapsulated cells and respective pericellular matrix, playing an important role in mechanotransduction [131]. The group further confirmed that chondrocytes cultured in an agarose hydrogel produce mechanically functional extracellular matrix [133].

The results shown here principally confirmed the very good capacity of agarose to form cartilage tissue. Encapsulated chondrocytes formed a pericellular halo of ECM, but also a homogeneous distribution of GAG and collagen type II can be observed throughout the gel. Compared to results that were obtained with stable fibrin (50), the GAG content in the agarose gels (first experiment) was almost tripled after four weeks of culture for the agarose group (ca. 44 µg/gel in fibrin vs. ca. 114 µg/gel in agarose). In the second agarose experiment (comparison to HA-SH/P(AGE/G), see also Figure 44) due to the increased cell proliferation and/or their performance even higher amounts of deposited ECM were found already after three weeks represented by GAG contents of nearly 250 µg in the pushed-out gels. The histological images are also consistent with data from the literature. For both stand-alone agarose gels (see Figure 42) and the agarose gels that were cultivated within the cartilage ring, obvious conglomerates of chondrocytes that indicate focal cell proliferation were observed (see Figure 40C). It can be found in literature that initially the spherical shape of encapsulated cells is maintained by the physical entrapment in the hydrophilic scaffold, rendering the cells unable to attach to the polysaccharide molecules. With culture time and elaboration of the pericellular matrix, however, cells can bind to the ECM that is trapped around them, which can influence cell behavior and morphology [389]. In the long term, however, a non-degradable material may be problematic and prevent a long-term balance of new synthesis and degradation by local chondrocytes. While it has been shown that additional treatment with the enzyme agarase can remove portions from the agarose scaffold to create new space for tissue formation, this approach is difficult to implement clinically and carries further risks [390]. In experiments with a disc/ring model with encapsulated mesenchymal stem cells in either agarose or biodegradable methacrylated gelatine hydrogels and *in vitro* cultivation up to six weeks, a superior progress of integration was reported for the gelatine-based gel after biomechanical push-out testing [221]. Regarding biodegradability *in situ*, the addition of crosslinks that are sensitive to cell-related enzymatic degradation to the agarose network may be required to circumvent those issues. It could be shown for hyaluronic acid-based hydrogels that evolving networks (hydrogels with mesh sizes that change over time due to crosslink degradation) can provide the control needed to enhance overall tissue formation when compared to static non-degradable scaffolds [391].

Unlike agarose, hyaluronic acid is a biomolecule that is also present in large quantities in the natural environment of cartilage. Chondrocytes have the ability to adhere to this polysaccharide via the CD44 surface receptor. In addition, hyaluronic acid can be degraded and metabolized by the body's own enzymes, as occurs physiologically. Fibrinogen- or hyaluronan-based hydrogels belong to the class of biomimetic scaffold materials that serve as cell carriers and consist of molecules naturally occurring in the ECM of various tissues. Their ECM molecules can interact with cells and affect cell shape, function, and differentiation. When these natural ECM molecules are used in tissue engineering, it is

targeted that they will create an environment that will positively influence cells and cause them to form the desired tissue [392]. To adjust the physicochemical properties of hydrogels, synthetic polymers such as poly(ethylene glycol) (PEG) or poly(glycidol) (PG) are used in combination with natural polymers [393].

In the respective experiment presented here, articular chondrocytes were tested either in HA-SH/P(AGE/G) or agarose in a single experimental approach for direct comparison. As mentioned previously, HA-SH/P(AGE/G) is a hybrid hydrogel composed of thiolated HA (HA-SH) and allyl-functionalized PG (P(AGE-co-G)). The components were crosslinked by UV-induced radical thiol-ene coupling between thiol and allyl groups. A total polymer concentration of 10 wt% was used as reported in previous experiments [100]. This hydrogel was developed at the Department for Functional Materials in Medicine and Dentistry, University of Würzburg within the framework of the EU research project HydroZONES for 3D printing of cartilage tissue engineering constructs where a double-printing approach with thermoplastic poly(ε-caprolactone)(PCL) is aimed to enhance the hydrogels mechanical resistance (Bioactivated hierarchical hydrogels as zonal implants for articular cartilage regeneration). In order to consider this approach of additional mechanical stabilization in the test design, one test group comprised of punched out round PCL scaffolds, which were presented in the cartilage rings followed by addition of the hydrogel solution and exposure to light. In principle, specific bioprinting techniques are developed that allow the *in situ* fabrication of constructs directly at the defect site [394]. Such a technique could combine the advantages of adhesive materials for immediate integration and the ability to form hierarchical structures by 3D printing. In order to allow assessment of the potential cartilage-adhesive effect by the crosslinking mechanism, one test group comprised of hydrogels of the same diameter hat were prepared outside of the cartilage (pre-cast) and then inserted into the cartilage ring as a reference. As expected, the pre-cast hydrogels showed virtually no detectable bonding strength immediately after construct assembly, as was similarly seen with agarose. HA-SH/P(AGE/G) without and with PCL reinforcement had a significantly higher immediate integration strength (16.1 ± 0.9 kPa and 13.7 ± 7.7 kPa). Accordingly, the immediate bonding is contributable to the presence of chemical bonding of the hydrogel polymers to allyl and/or thiol groups within the opposing cartilage tissue via the UV-mediated crosslinking reaction. Most remarkably, the detected immediate bonding values were more than doubled to prior results obtained with stable fibrin (50) in the same *in vitro* model. The group of Zenobi-Wong et al. published results with transglutaminase crosslinked hyaluronan hydrogels (HA-TG) [220]. They also applied the here described approach of curing the hydrogel within a cartilage ring followed by biomechanical push-out testing. For their transglutaminase-mediated reaction immediate bonding strengths of about 2 kPa were reported, 6 to 8 times less we were able to achieve with our hyaluronan hydrogel. Zenobi-Wong et al. were able to

achieve a three-fold increase in integration strength when the cartilage surface was pre-treated with a chondroitinase solution to remove anti-adhesive polysaccharides and expose the protein part of the cartilage matrix. Although unwanted side reactions and more cumbersome handling would be expected in the clinical setting, it would be interesting to investigate potential benefits of such enzymatic treatments on the integration capacity the here investigated hyaluronan hydrogel in the future.

However, it is probable that the measured integration strengths in our and other experiments were also limited by a cohesive rather than an adhesive error [212]. Both adhesive and cohesive interactions are based on mechanical interlocking, intermolecular bonding, electrostatic bonding, chain entanglement or the formation of crosslinks. For strong adhesive performance, it is essential to achieve an optimum balance between the adhesive and cohesive strengths of the material [95]. A possible higher intrinsic strength of our gel would accordingly also lead to higher values in the push-out test. Pushed-out agarose and pre-cast HA-SH/P(AGE/G) hydrogels had no visible remains of hydrogel attached to the cartilage ring after biomechanical testing. In sharp contrast, for the *in situ* cured HA-SH/P(AGE/G) the push-out plunger went through the bulk hydrogels leaving a remaining ring-shaped hydrogel remnant attached to the cartilage (see Figure 43B), which proved the limitation by cohesive failure of the hydrogel. Since the PCL scaffold is not forming covalent bonds to the cartilage it could not contribute to the tissue adhesion. Its inherent rigidity is intended to provide resistance to compression forces, a highly beneficial characteristic for the treatment of large cartilage defects with soft hydrogels [106,395]. However, this positive effect would be more likely to be detected via biomechanical compression tests. Nonetheless, since the compression forces are only distributed via the PCL scaffold, but the gel itself remains unchanged in its physical properties, the cohesive defect at the gel-to-cartilage transition also remains predominant. As can be seen in the histological images, the PCL material was partially in direct contact with the cartilage without chemically contributing to the bonding, but at the same time it also reduced the contact area of the cartilage with the adhesive hydrogel. This also explains the lower measured integration strength to the *in situ* cured HA-SH/P(AGE/G) gels without PCL.

Both histology and biochemical analyses showed that the amounts of ECM in the gel increased over the 21 days of culture, although significantly reduced compared to the previously described agarose comparison group. ECM deposition is also the likely origin of the slight increase in integration strength after 21 days in the pre-cast constructs. However, the extent of this influence does not come into play in the present time frame for the *in situ* cured constructs due to the dimension of the adhesion despite its detected decrease. Compared to GAG, the increase in collagen was less prominent in the HA-SH/P(AGE/G) gels. The clearest trend was in the PCL group. It is possible that locally mobile

chondrocytes may interact and adhere with the high tubular surface area of the scaffold in the gel. Since adherent chondrocyte layers tend to form fibroblast-like structures that preferentially express collagen type I [396], this would explain the biochemically detected increase in total collagen with no detectable increase in collagen type II in immunohistology.

Unfortunately, the integration strength slightly decreased in both groups over the 21 days observation period. As discussed before the agarose gels containing chondrocytes from the identical cell source significantly increased integration strength and outperformed the HA-SH/P(AGE/G) gels after 21 days (see Figure 43A). A likely cause is inadequate interface-bridging ECM deposition with concomitant decline of existing covalent bonds to cartilage tissue. As a natural molecule, hyaluronic acid is subject to continuous degradation, which can be influenced by the degree and type of crosslinking. It is conceivable that hydrolytic or enzymatic degradation occurred in the gel over the observation period and that the decrease in cohesive strength in turn led to the slight decrease in biomechanical results. The histologic images on day 21 showed gels that have a torn appearance to large extend (see Figure 44A), which may indicate decreased intrinsic gel strength. It must be said that histological preparation of HA-SH/P(AGE/G) is difficult, and the inclusion of solvents as usually used in the staining process can cause swelling and thus destroy structures. This would be particularly pronounced at interface sites if the adjacent body (here the cartilage) does not swell to the same extent.

As with the stand-alone hydrogels, high-magnification images of HA-SH/P(AGE/G) hydrogels incubated in contact with cartilage tissue showed the intracellular and mostly pericellular distribution of the ECM components aggrecan and type II collagen. However, the pericellular ECM distribution in the gels was not optimal, especially when compared with agarose, because it did not resemble natural ECM and did not result in a continuous tissue-like construct. This effect has been previously observed when high polymer content or network density in hydrogels limited the homogeneous ECM distribution of encapsulated cells [100,397–401]. The properties of crosslinked HA-SH/P(AGE/G) hydrogels also depend on the length of HA-SH used and the degree of its modification. In general, the shorter the HA-SH, the more polymer content is required to produce a stable hydrogel by crosslinking. If the polymer content is too low, gelation will be inhibited. The HA-SH used in the underlying experiments was relatively small, so a high polymer content was required to form a gel with it. In addition, the hydrogel composition used, with a total polymer content of 10 wt%, was originally chosen to produce a 3D printable hydrogel. A high concentration of polymers is often used for 3D printing materials to improve stability and shape retention during and after the printing process [106]. With a polymer content of 10 wt% and additional unmodified high molecular weight HA (1-2 MDa) to increase viscosity, it was possible to dual print the HA-SH/P(AGE/G) hydrogel together with polycaprolactone (PCL) in a previous

study [100]. In another study using a very similar hydrogel system, it was demonstrated that a reduction in polymer content resulted in improved ECM distribution [395]. Therefore, the investigated HA-SH/P(AGE/G) hydrogel should be further developed to find a solution for combining the needs of the utilized cells and, for example, the requirements for a stable hydrogel intended for bioprinting with high shape fidelity. The easy chemical adaptability of the allyl functionalized polyglycidol may play an important role here. Application of the HA-SH/P(AGE/G) hydrogel in an equine *in vivo* model resulted in sub-optimal quality of the repair tissue, despite co-application of an PCL scaffold for mechanical protection. The authors hypothesized that this outcome may be related to early loss of implanted cells, or inappropriate degradation rate of the hydrogel [402]. However, concerning gel degradation, variation of the hyaluronan-thiol component allowed the formation of two types of hydrogels, degradable and non-degradable. Degradation was induced by the additional presence of the hydrolytically degradable ester group [149]. The right balance of degradation that fits the needs *in situ* may improve the material's outcome, similar to results obtained with the biodegradable DOPA adhesive (see Chapter 4.4).

The comparison between agarose and HA-SH/P(AGE/G) in the present experiment with the usage the same cells and the same cultivation conditions for both hydrogels, demonstrated the distinct influence that the used hydrogel can have on the different cell types. It has also been observed in other studies that different cell types prefer certain hydrogels and a supposedly less well-functioning material harmonizes well with other cells. In different studies, the cell types of ACPCs and MSCs were compared in both the here used HA-SH/P(AGE/G) material or different gelatine-based hydrogel formulations (GelMA) [101,369] with regard to chondrogenesis and production of cartilage ECM. In these hydrogels, MSCs always outperformed ACPCs regarding ECM production. Compared to the here presented results, much better overall cartilage neosynthesis was obtained in HA-SH/P(AGE/G) gels when MSCs were used instead of chondrocytes.

Hydrogels like GelMA or HA-SH/P(AGE/G), which contain biopolymers such as collagen and hyaluronic acid, appear to promote chondrogenesis of MSCs. These more biomimetic hydrogels may have promoted chondrogenesis of MSCs through adhesion and signaling between the material and the cells. In contrast, agarose has no biological cues to which the cells could adhere. In other previous studies that compared cartilage ECM production of chondrocytes and MSCs in agarose or other materials without biological cues, chondrocytes performed better than MSCs [384,403,404]. Therefore, the agarose hydrogel seems to be a favorable environment for chondrocytes and ACPCs, which are a subpopulation of chondrocytes. MSCs had to undergo the whole process of differentiation into chondrocytes, and it seemed plausible that signals from the microenvironment support this process, as they do in normal embryonic development [405–407]. Chondrocytes, on the other hand, are already mature cells that benefit from an environment that preserves and supports their properties, such as

agarose. This clearly shows that the choice of the right microenvironment or hydrogel depending on the cell type used for cartilage regeneration treatment is of utmost importance to achieve the best performance.

However, considering the optimization of a biomaterial with respect to its use for 3D printing remains a necessity for next-generation therapies of cartilage defects. First promising 3D printing approaches were reported almost ten years ago. Cui et al. developed a bioprinting system with simultaneous photopolymerization capable for 3D cartilage tissue engineering. Poly(ethylene glycol) dimethacrylate (PEGDMA) with human chondrocytes were printed to repair defects in osteochondral plugs in layer-by-layer assembly followed by *in vitro* culture for up to six weeks [105105]. Depths of the defects ranged from 2 to 5mm. At the end of the observation period, the printed cartilage implant attached firmly with the surrounding tissue and good proteoglycan deposition was observed at the interface of implant and native cartilage in Safranin O staining. However, after careful separation of the subchondral bone from the cartilage part of the construct and subsequent push-out testing of the constructs, rather low integration strengths of ca. 1 kPa after six weeks were obtained. The study showed the potential of a direct micro-printing process for fabricating tissue engineering constructs with high maintained cell viability and increasing integration to the lesion site. The significantly higher detected failure strength with our HA-SH/P(AGE/G) holds promise that biomaterials with favorable immediate integration can be achieved for 3D printing processes. In the next step bioink formulations need to be optimized with regard to specific needs of the respective cell type to foster tissue neoformation [101,369]. An exciting approach in the future could be the use of hybrid gels consisting of a hydrophilic polysaccharide such as hyaluronic acid and a protein polymer such as collagen or fibrinogen. This mix would emulate the model of native cartilage tissue and could provide a good balance of mechanical stability, hydrodynamic properties and cell compatibility. Ideally, modifications to the gel properties such as degradation and adhesion motifs can also be adapted via chemical modifications. Chemically modified hyaluronic acid has already been successfully used not only in the results described and discussed here. Liu et al. reported an approach for adhesive hydrogels based on photoresponsive hyaluronic acid and platelet-rich plasma (PRP) [209]. PRP, similar to fibrin, is typically cured via thrombin and its beneficial applicability for cartilage repair is well known. Besides the containment of leukocytes and a mixture of growth factors, a main component of PRP is fibrinogen. The growth factor release from PRP was reported to enhance cartilage integration mechanisms [408]. The gelation mechanism of the HA/PRP hybrid gel established by Liu et al. is based on Schiff base formation via reaction of generated aldehyde groups and amino groups of the PRP components. This photosensitive reaction allows *in situ* on-demand crosslinking at the defect site. The cartilage tissue adhesive strength of about 25 kPa was promising and significantly above the fibrin glue control.

Furthermore, in a twelve week *in vivo* study, integrative hyaline cartilage integration was present and the therapeutic efficacy was better than for thrombin activated PRP gel in the rabbit full-thickness defect.

Accordingly, the chemical modifiability of biomaterials represents a vast playground with almost inexhaustible possibilities. Progressive adhesion reactions such as the mussel-mimetic reaction via catechol groups and fine-tunable degradation kinetics (see also Chapter 4.4) will further advance the promising treatment approach of cartilage defects with hydrogels in the future.

# 5 Conclusion and Outlook

Articular cartilage is of enormous importance for the functional maintenance of the musculoskeletal system. As a superficial layer in joints, it provides the necessary gliding properties and force distribution under load. Due to the strong mechanical forces that can prevail in the joint, defects in the cartilage tissue are common. Defects in the joint surface can lead to severe pain and considerable limitations in the quality of life. Lesions after trauma often occur in the lateral dimension and even small defects can become larger and more severe over time, leading to osteoarthritis. Osteoarthritis is already a widespread disease, especially in industrialized countries with a steadily increasing average age of the population, and will continue to gain importance in the future. Surgical placement of artificial joint prostheses is often the final treatment approach. The lack of vascularization of cartilage tissue and the low self-healing capacity make alternative regenerative treatment approaches difficult. A variety of different factors play a role in cartilage regeneration. *In vitro* models are becoming increasingly important to simulate the clinical situation and to investigate the influence of certain factors. In contrast to animal experiments, *in vitro* models represent an ethically acceptable alternative, which is also economical and efficient in the execution of experiments. The disc/ring model is increasingly being used for investigations of cartilage defects. By creating a lateral defect in native cartilage tissue, a common clinical outcome is simulated and integrative repair mechanisms at the defect interface can be assessed. In the course of the work presented here, among other things, the disc/ring model was established with the use of biomechanical measurements to determine interfacial integration strength. Porcine knee joints, which are easily and ethically available as a by-product of the slaughter industry, were used as donor tissue.

Despite advances in regenerative treatment approaches for cartilage defects in recent decades, a common reason for failure is lack of integration at the defect interface with the native tissue. Surgical adhesives allow immediate fixation of defect sites and, in theory, unlike sutures, do not contribute to any additional injury to the sensitive articular surface. In reality, however, adhesives can have cytotoxic properties and users often have to choose between good biocompatibility and high adhesive strength for available materials. Two representative clinically available adhesives were tested with the disc/ring model. One was the glutaraldehyde-based BioGlue® and the other was fibrin, a material that is also used in physiological wound closure. The results showed that BioGlue® achieved very high adhesive strength in the cartilage model, but it became clear that cytotoxic substances from the adhesive leach in the tissue and led to necrosis over large areas. Despite the supposed success in terms of immediate adhesive strength, enormous long-term damage to the cartilage would have to be expected, which self-explanatorily rules out clinical use for this purpose. For fibrin, both a commercially available and long-term stable formulations that were established by our group were investigated in the

experiments. In contrast to BioGlue®, significantly lower immediate bonding strengths were measured, but all fibrin formulations tested showed very good biocompatibility. In addition to mechanical testing, the disc/ring model also allowed for *in vitro* tissue culture. Due to the good compatibility of the fibrin, corresponding constructs could be observed over a long period of time after *in vitro* culture to investigate integrative processes in more detail. Over a period of three weeks, a strong increase in integration strength coupled with the new synthesis of cartilage matrix at the defect site was shown for the biocompatible fibrin glues. Representatively, using a long-term stable formulation (stable fibrin (50)), the process of integration was followed in more detail histologically. Interfacial deposition of cartilage ECM was observed after only a few days, followed by cell migration from the surrounding native tissue within 14 days. In the further course, annealing of the opposing cartilage surfaces by newly synthesized tissue increased. The results proved that the use of adhesives can be beneficial for the healing process of cartilage defects, but tissue vitality must not be compromised for long-term success.

The adhesive properties of a material are primarily subject to the respective crosslinking mechanism. Different chemical groups can enter into reactions with the cartilage matrix and thus contribute to bonding. Since a high immediate adhesive strength would in principle mean improved fixation of the defect, the aim was to investigate different crosslink approaches to achieve improved adhesive strength. Based on previous experience and the positive results regarding *in vitro* tissue formation in fibrin, the further focus was to improve the integrative performance of fibrinogen-containing hydrogel compositions. Surface functionalization of cartilage with photosensitive diazirine increased the adhesive strength of fibrin. A ruthenium crosslinked fibrinogen hydrogel achieved significantly increased adhesive strength with good biocompatibility. Even though an increase in adhesive strength was achieved for both approaches compared to fibrin, cumbersome process steps or lack of long-term integration were obstacles for further use. Lateral cartilage integration with a biomaterial requires a balance of ongoing material integration and remodeling toward functional cartilage tissue. Therefore, in a cross-group collaboration, POx polymers were synthesized that enabled strong binding to the tissue via functional catechol groups and, at the same time, enabled the production of a hydrogel adhesive with fibrinogen, for which the degradation rate is finetuneable. In the correct ratio, the initial adhesive strength could thus be increased over time as observed before with fibrin, without compromising the ability to form new cartilage at the defect interface.

Especially for the regenerative treatment of larger cartilage defects, it requires approaches that require the formation of mechanically functional hyaline tissue. Therefore, when using tissue engineering constructs to fill the defect, there is a strong focus on the biological performance of biomaterials. Many hydrogels are known from tissue engineering, and further or new developments

are constantly being made to meet the specific needs of cell and tissue types. Agarose is known to have good compatibility with chondrocytes and their initiated ECM synthesis in the material. By adapting the disc/ring model, in which a hydrogel is applied into the cartilage ring lumen, integrative effects could also be studied with larger constructs *in vitro*. Due to the strong tissue synthesis of embedded chondrocytes in agarose, there was also a concomitant strong increase in integrative strength observed over time. However, due to the mechanical stresses in the joint, adhesive hydrogel materials have advantages over non-adhesive materials such as agarose, since direct bonding to the cartilage on the one hand better fixes the material at the site of application and thus prevents loss, and on the other hand the direct contact can facilitate annealing with the native tissue. In further investigations, hydrogel materials possessing a crosslink mechanism that simultaneously provides direct binding to the cartilage tissue were included. As before, stable fibrin (50) was investigated as a cartilage adhesive hydrogel construct, as well as a hyaluronic acid-based material (HA-SH/P(AGE/G)). In contrast to agarose, both materials were shown to adhere to the tissue in biomechanical measurements. In the course of *in vitro* culture up to four weeks, however, the increase in integration strength was only low (stable fibrin (50)) or even slightly regressive (HA-SH/P(AGE/G)) to the initial value. Histological investigations showed that the lack of homogeneous distribution of synthesized ECM in the hydrogel and at the interface area in comparison to agarose impaired integrative repair during the observation period. The results highlighted the importance of tissue neosynthesis in the hydrogel for the long-term success of cartilage integration and thus the overall treatment. For the future, it therefore requires materials that are mechanically stable both in a cohesive and with an tissue-adhesive manner, but at the same time are biocompatible and allow good cartilage formation. The possibilities to adapt biomaterials accordingly are extremely versatile. For example, chemical modifications can influence adhesion and material degradation. However, adaptations must also take into account the specific requirements of the cell types used, the nature of the defect, and a variety of other biological factors. It therefore needs efficient possibilities to test potential candidates ethically and economically justifiable. The disc/ring model was shown to be very versatile in the experiments presented here, although the potential scope of testing is far from exhausted. In addition to the quantitative and qualitative assessment of integration, the model allows the evaluation of tissue engineering constructs in contact to viable tissue. Thus, a better simulation of the clinical situation is given. Future experiments using the disc/ring model may not only be used to evaluate material integration, but also to investigate growth factors, inflammatory cytokines and other biological cues via medium supplementation.

# References

1.  Schulz, R.M. and Bader, A. (2007). Cartilage tissue engineering and bioreactor systems for the cultivation and stimulation of chondrocytes. European Biophysics Journal : EBJ *36*, 539–568.

2.  Bernhard, J.C. and Vunjak-Novakovic, G. (2016). Should we use cells, biomaterials, or tissue engineering for cartilage regeneration? Stem Cell Research & Therapy *7*, 56.

3.  Buckwalter, J.A. and Mankin, H.J. (1998). Articular cartilage: tissue design and chondrocyte-matrix interactions. Instructional Course Lectures *47*, 477–86.

4.  Aigner, T. and Stöve, J. (2003). Collagens--major component of the physiological cartilage matrix, major target of cartilage degeneration, major tool in cartilage repair. Advanced Drug Delivery Reviews *55*, 1569–93.

5.  Demoor, M., Ollitrault, D., Gomez-Leduc, T., Bouyoucef, M., Hervieu, M., Fabre, H., Lafont, J., Denoix, J.-M., Audigié, F., Mallein-Gerin, F., Legendre, F., and Galera, P. (2014). Cartilage tissue engineering: Molecular control of chondrocyte differentiation for proper cartilage matrix reconstruction. Biochimica Et Biophysica Acta (BBA) - General Subjects *1840*, 2414–2440.

6.  Sophia Fox, A.J., Bedi, A., and Rodeo, S. a. (2009). The Basic Science of Articular Cartilage: Structure, Composition, and Function. Sports Health: A Multidisciplinary Approach *1*, 461–468.

7.  Schinagl, R.M., Gurskis, D., Chen, A.C., and Sah, R.L. (1997). Depth-dependent confined compression modulus of full-thickness bovine articular cartilage. Journal Of Orthopaedic Research *15*, 499–506.

8.  Boushell, M.K., Hung, C.T., Hunziker, E.B., Strauss, E.J., and Lu, H.H. (2016). Current strategies for integrative cartilage repair. Connective Tissue Research *58*, 393–406.

9.  Wachsmuth, L., Söder, S., Fan, Z., Finger, F., and Aigner, T. (2006). Immunolocalization of matrix proteins in different human cartilage subtypes. Histology And Histopathology *21*, 477–85.

10. Hayes, A.J., Hall, A., Brown, L., Tubo, R., and Caterson, B. (2007). Macromolecular organization and in vitro growth characteristics of scaffold-free neocartilage grafts. The Journal Of Histochemistry And Cytochemistry : Official Journal Of The Histochemistry Society *55*, 853–866.

11. Bos, P.K., Kops, N., Verhaar, J.A.N., and van Osch, G.J.V.M. (2008). Cellular origin of neocartilage formed at wound edges of articular cartilage in a tissue culture experiment. Osteoarthritis And Cartilage *16*, 204–11.

12. Vignon, E., Arlot, M., Patricot, L.M., and Vignon, G. (1976). The cell density of human femoral head cartilage. Clinical Orthopaedics And Related Research *121*, 303–308.

13. Anderson, D.D., Chubinskaya, S., Guilak, F., Martin, J.A., Oegema, T.R., Olson, S.A., and Buckwalter, J.A. (2011). Post-traumatic osteoarthritis: Improved understanding and opportunities for early intervention. Journal Of Orthopaedic Research *29*, 802–809.

14. Redman, S.N., Dowthwaite, G.P., Thomson, B.M., and Archer, C.W. (2004). The cellular responses of articular cartilage to sharp and blunt trauma. Osteoarthritis And Cartilage *12*, 106–16.

15. Buckwalter, J.A. (2002). Articular Cartilage Injuries. Clinical Orthopaedics And Related Research *402*, 21–37.

16. Dell'Accio, F. and Vincent, T. (2010). Joint surface defects: clinical course and cellular response

in spontaneous and experimental lesions. European Cells And Materials *20*, 210–217.

17. Masuda, K., Sah, R.L., Hejna, M.J., and Thonar, E.J.-M.A. (2003). A novel two-step method for the formation of tissue-engineered cartilage by mature bovine chondrocytes: the alginate-recovered-chondrocyte (ARC) method. Journal Of Orthopaedic Research : Official Publication Of The Orthopaedic Research Society *21*, 139–48.

18. Eyre, D.R., Weis, M.A., and Wu, J.-J. (2006). Articular cartilage collagen: an irreplaceable framework? European Cells & Materials *12*, 57–63.

19. Billinghurst, R.C., Dahlberg, L., Ionescu, M., Reiner, A., Bourne, R., Rorabeck, C., Mitchell, P., Hambor, J., Diekmann, O., Tschesche, H., Chen, J., Van Wart, H., and Poole, A.R. (1997). Enhanced cleavage of type II collagen by collagenases in osteoarthritic articular cartilage. Journal Of Clinical Investigation *99*, 1534–1545.

20. Aigner, T. and McKenna, L. (2002). Molecular pathology and pathobiology of osteoarthritic cartilage. Cellular And Molecular Life Sciences : CMLS *59*, 5–18.

21. Charni-Ben Tabassi, N., Desmarais, S., Bay-Jensen, A.C., Delaiss??, J.M., Percival, M.D., and Garnero, P. (2008). The type II collagen fragments Helix-II and CTX-II reveal different enzymatic pathways of human cartilage collagen degradation. Osteoarthritis And Cartilage *16*, 1183–1191.

22. Catterall, J., Parr, S.D., Fagerlund, K., and Caterson, B. (2013). CTX-II is a marker of cartilage degradation but not of bone turnover. Osteoarthritis And Cartilage *21*, S77.

23. Duclos, M.E., Roualdes, O., Cararo, R., Rousseau, J.C., Roger, T., and Hartmann, D.J. (2010). Significance of the serum CTX-II level in an osteoarthritis animal model: a 5-month longitudinal study. Osteoarthritis And Cartilage *18*, 1467–1476.

24. Fosang, A.J., Stanton, H., Little, C.B., and Atley, L.M. (2003). Neoepitopes as biomarkers of cartilage catabolism. Inflammation Research *52*, 277–282.

25. Little, C.B., Hughes, C.E., Curtis, C.L., Janusz, M.J., Bohne, R., Wang-Weigand, S., Taiwo, Y.O., Mitchell, P.G., Otterness, I.G., Flannery, C.R., and Caterson, B. (2002). Matrix metalloproteinases are involved in C-terminal and interglobular domain processing of cartilage aggrecan in late stage cartilage degradation. Matrix Biology : Journal Of The International Society For Matrix Biology *21*, 271–88.

26. Lieberthal, J., Sambamurthy, N., and Scanzello, C.R. (2015). Inflammation in Joint Injury and Post-Traumatic Osteoarthritis. Osteoarthritis And Cartilage / OARS, Osteoarthritis Research Society *23*, 1825.

27. Englund, M. and Lohmander, L.S. (2004). Risk factors for symptomatic knee osteoarthritis fifteen to twenty-two years after meniscectomy. Arthritis & Rheumatism *50*, 2811–2819.

28. Forriol, F., Longo, U.G., Hernández-Vaquero, D., Monllau, J.C., Montserrat, F., Valentí, J.R., Vaquero, J., Maffulli, N., and Denaro, V. The effects of previous meniscus and anterior cruciate ligament injuries in patients with total knee arthroplasty. Ortopedia, Traumatologia, Rehabilitacja *12*, 50–7.

29. Shapiro, F., Koide, S., and Glimcher, M.J. (1993). Cell origin and differentiation in the repair of full-thickness defects of articular cartilage. The Journal Of Bone And Joint Surgery. American Volume *75*, 532–53.

30. Jackson, D.W., Lalor, P.A., Aberman, H.M., and Simon, T.M. (2001). Spontaneous Repair of Full-Thickness Defects of Articular Cartilage in a Goat Model. The Journal Of Bone And Joint Surgery-American Volume *83*, 53–64.

31. Hunziker, E.B. (2002). Articular cartilage repair: basic science and clinical progress. A review of

the current status and prospects. Osteoarthritis And Cartilage *10*, 432–463.

32. Furukawa, T., Eyre, D.R., Koide, S., and Glimcher, M.J. (1980). Biochemical studies on repair cartilage resurfacing experimental defects in the rabbit knee. The Journal Of Bone And Joint Surgery. American Volume *62*, 79–89.

33. Strauss, E.J., Goodrich, L.R., Chen, C.-T., Hidaka, C., and Nixon, A.J. (2005). Biochemical and Biomechanical Properties of Lesion and Adjacent Articular Cartilage after Chondral Defect Repair in an Equine Model. The American Journal Of Sports Medicine *33*, 1647–1653.

34. Veronese, N., Stubbs, B., Solmi, M., Smith, T.O., Noale, M., Cooper, C., and Maggi, S. (2017). Association between lower limb osteoarthritis and incidence of depressive symptoms: data from the osteoarthritis initiative. Age And Ageing *46*, 470–476.

35. Cross, M., Smith, E., Hoy, D., Nolte, S., Ackerman, I., Fransen, M., Bridgett, L., Williams, S., Guillemin, F., Hill, C.L., Laslett, L.L., Jones, G., Cicuttini, F., Osborne, R., Vos, T., Buchbinder, R., Woolf, A., and March, L. (2014). The global burden of hip and knee osteoarthritis: estimates from the global burden of disease 2010 study. Annals Of The Rheumatic Diseases *73*, 1323–30.

36. EUMUSC (2014). Musculoskeletal Health in Women. In: Mody, E and Matzkin, E (eds.). European Musculoskeletal Health Surveillance And Information Network , Springer London, 12pp. doi:10.1007/978-1-4471-4712-1 <http://link.springer.com/10.1007/978-1-4471-4712-1>.

37. The United Nations on World Population in 2300 (2004). The United Nations on World Population in 2300. Population And Development Review *30*, 181–187.

38. Schieir, O., Tosevski, C., Glazier, R.H., Hogg-Johnson, S., and Badley, E.M. (2017). Incident myocardial infarction associated with major types of arthritis in the general population: a systematic review and meta-analysis. Annals Of The Rheumatic Diseases *76*, 1396–1404.

39. Chung, W.-S., Lin, H.-H., Ho, F.-M., Lai, C.-L., and Chao, C.-L. (2016). Risks of acute coronary syndrome in patients with osteoarthritis: a nationwide population-based cohort study. Clinical Rheumatology *35*, 2807–2813.

40. Courties, A., Sellam, J., Maheu, E., Cadet, C., Barthe, Y., Carrat, F., and Berenbaum, F. (2017). Coronary heart disease is associated with a worse clinical outcome of hand osteoarthritis: a cross-sectional and longitudinal study. RMD Open *3*, e000344.

41. Puig-Junoy, J. and Ruiz Zamora, A. (2015). Socio-economic costs of osteoarthritis: A systematic review of cost-of-illness studies. Seminars In Arthritis And Rheumatism *44*, 531–541.

42. Vina, E.R. and Kwoh, C.K. (2018). Epidemiology of osteoarthritis: Literature update. Current Opinion In Rheumatology *30*, 160–167.

43. Sharif, B., Kopec, J.A., Wong, H., and Anis, A.H. (2017). Distribution and Drivers of Average Direct Cost of Osteoarthritis in Canada From 2003 to 2010. Arthritis Care & Research *69*, 243–251.

44. Xie, F., Kovic, B., Jin, X., He, X., Wang, M., and Silvestre, C. (2016). Economic and Humanistic Burden of Osteoarthritis: A Systematic Review of Large Sample Studies. PharmacoEconomics *34*, 1087–1100.

45. Outerbridge, R.E. (1964). Further Studies on the Etiology of Chondromalacia Patellae. The Journal Of Bone And Joint Surgery. British Volume *46-B*, 179–190.

46. Curl, W.W., Krome, J., Gordon, E.S., Rushing, J., Smith, B.P., and Poehling, G.G. (1997). Cartilage injuries: a review of 31,516 knee arthroscopies. Arthroscopy : The Journal Of Arthroscopic & Related Surgery : Official Publication Of The Arthroscopy Association Of North

America And The International Arthroscopy Association *13*, 456–60.

47.  Widuchowski, W., Widuchowski, J., and Trzaska, T. (2007). Articular cartilage defects: Study of 25,124 knee arthroscopies. The Knee *14*, 177–182.

48.  Årøen, A., Løken, S., Heir, S., Alvik, E., Ekeland, A., Granlund, O.G., and Engebretsen, L. (2004). Articular Cartilage Lesions in 993 Consecutive Knee Arthroscopies. The American Journal Of Sports Medicine *32*, 211–215.

49.  Rackwitz, L., Schneider, U., Andereya, S., Siebenlist, S., Reichert, J.C., Fensky, F., Arnholdt, J., Arnhold, J., Löer, I., Grossstück, R., Zinser, W., Barthel, T., Rudert, M., and Nöth, U. (2012). [Reconstruction of osteochondral defects with a collagen I hydrogel. Results of a prospective multicenter study]. Der Orthopäde *41*, 268–79.

50.  Rinonapoli, E., Mancini, G.B., Azzara, A., and Aglietti, P. (1992). Long-term results and survivorship analysis of 89 total condylar knee prostheses. The Journal Of Arthroplasty *7*, 241–246.

51.  Attar, F.G., Khaw, F.M., Kirk, L.M.G., and Gregg, P.J. (2008). Survivorship Analysis at 15 Years of Cemented Press-Fit Condylar Total Knee Arthroplasty. The Journal Of Arthroplasty *23*, 344–349.

52.  Vessely, M.B., Whaley, A.L., Harmsen, W.S., Schleck, C.D., and Berry, D.J. (2006). The Chitranjan Ranawat Award: Long-term survivorship and failure modes of 1000 cemented condylar total knee arthroplasties. Clinical Orthopaedics And Related Research *452*, 28–34.

53.  Robert, H. (2011). Chondral repair of the knee joint using mosaicplasty. Orthopaedics & Traumatology: Surgery & Research *97*, 418–429.

54.  Brittberg, M., Lindahl, A., Nilsson, A., Ohlsson, C., Isaksson, O., and Peterson, L. (1994). Treatment of Deep Cartilage Defects in the Knee with Autologous Chondrocyte Transplantation. New England Journal Of Medicine *331*, 889–895.

55.  Corpus, K.T., Bajaj, S., Daley, E.L., Lee, A., Kercher, J.S., Salata, M.J., Verma, N.N., and Cole, B.J. (2012). Long-Term Evaluation of Autologous Chondrocyte Implantation: Minimum 7-Year Follow-Up. Cartilage *3*, 342–50.

56.  Briggs, T.W.R., Mahroof, S., David, L.A., Flannelly, J., Pringle, J., and Bayliss, M. (2003). Histological evaluation of chondral defects after autologous chondrocyte implantation of the knee. The Journal Of Bone And Joint Surgery. British Volume *85*, 1077–83.

57.  Peterson, L., Brittberg, M., Kiviranta, I., Åkerlund, E.L., and Lindahl, A. (2002). Autologous Chondrocyte Transplantation. The American Journal Of Sports Medicine *30*, 2–12.

58.  Guney, A., Yurdakul, E., Karaman, I., Bilal, O., Kafadar, I.H., and Oner, M. (2016). Medium-term outcomes of mosaicplasty versus arthroscopic microfracture with or without platelet-rich plasma in the treatment of osteochondral lesions of the talus. Knee Surgery, Sports Traumatology, Arthroscopy *24*, 1293–1298.

59.  Zarnett, R., Delaney, J.P., Driscoll, S.W.O., and Salter, R.B. (1987). Cellular origin and evolution of neochondrogenesis in major full-thickness defects of a joint surface treated by free autogenous periosteal grafts and subjected to continuous passive motion in rabbits. Clinical Orthopaedics And Related Research *222*, 267–274.

60.  Akens, M.K., von Rechenberg, B., Bittmann, P., Nadler, D., Zlinszky, K., and Auer, J.A. (2001). Long term in-vivo studies of a photo-oxidized bovine osteochondral transplant in sheep. BMC Musculoskeletal Disorders *2*, 9.

61.  Waselau, A.C., Nadler, D., Müller, J.M. V, Zlinszky, K., Hilbe, M., Auer, J.A., and von Rechenberg, B. (2005). The effect of cartilage and bone density of mushroom-shaped,

photooxidized, osteochondral transplants: an experimental study on graft performance in sheep using transplants originating from different species. BMC Musculoskeletal Disorders *6*, 60.

62. Lane, J.G., Massie, J.B., Ball, S.T., Amiel, M.E., Chen, A.C., Bae, W.C., Sah, R.L., and Amiel, D. (2004). Follow-up of osteochondral plug transfers in a goat model: a 6-month study. The American Journal Of Sports Medicine *32*, 1440–50.

63. Bentley, G., Biant, L.C., Vijayan, S., Macmull, S., Skinner, J.A., and Carrington, R.W.J. (2012). Minimum ten-year results of a prospective randomised study of autologous chondrocyte implantation *versus* mosaicplasty for symptomatic articular cartilage lesions of the knee. The Journal Of Bone And Joint Surgery. British Volume *94-B*, 504–509.

64. Macmull, S., Parratt, M.T.R., Bentley, G., Skinner, J.A., Carrington, R.W.J., Morris, T., and Briggs, T.W.R. (2011). Autologous chondrocyte implantation in the adolescent knee. The American Journal Of Sports Medicine *39*, 1723–30.

65. Shekkeris, A.S., Perera, J.R., Bentley, G., Flanagan, A.M., Miles, J., Carrington, R.W.J., Skinner, J.A., and Briggs, T.W.R. (2012). Histological results of 406 biopsies following ACI/MACI procedures for osteochondral defects in the knee. Orthopaedic Proceedings *94-B*, 12.

66. Harris, J.D., Siston, R.A., Brophy, R.H., Lattermann, C., Carey, J.L., and Flanigan, D.C. (2011). Failures, re-operations, and complications after autologous chondrocyte implantation – a systematic review. Osteoarthritis And Cartilage *19*, 779–791.

67. Dell'Accio, F., Vanlauwe, J., Bellemans, J., Neys, J., De Bari, C., and Luyten, F.P. (2003). Expanded phenotypically stable chondrocytes persist in the repair tissue and contribute to cartilage matrix formation and structural integration in a goat model of autologous chondrocyte implantation. Journal Of Orthopaedic Research *21*, 123–131.

68. Russlies, M., Behrens, P., Wünsch, L., Gille, J., and Ehlers, E.-M. (2002). A cell-seeded biocomposite for cartilage repair. Annals Of Anatomy - Anatomischer Anzeiger *184*, 317–323.

69. Orth, P., Rey-Rico, A., Venkatesan, J.K., Madry, H., and Cucchiarini, M. (2014). Current perspectives in stem cell research for knee cartilage repair. Stem Cells And Cloning : Advances And Applications *7*, 1–17.

70. Chen, J.-L., Duan, L., Zhu, W., Xiong, J., and Wang, D. (2014). Extracellular matrix production in vitro in cartilage tissue engineering. Journal Of Translational Medicine *12*, 88.

71. Mauck, R.L., Byers, B.A., Yuan, X., and Tuan, R.S. (2007). Regulation of Cartilaginous ECM Gene Transcription by Chondrocytes and MSCs in 3D Culture in Response to Dynamic Loading. Biomechanics And Modeling In Mechanobiology *6*, 113–125.

72. Terraciano, V., Hwang, N., Moroni, L., Park, H. Bin, Zhang, Z., Mizrahi, J., Seliktar, D., and Elisseeff, J. (2007). Differential Response of Adult and Embryonic Mesenchymal Progenitor Cells to Mechanical Compression in Hydrogels. Stem Cells *25*, 2730–2738.

73. Li, Z., Kupcsik, L., Yao, S.-J., Alini, M., and Stoddart, M.J. (2010). Mechanical load modulates chondrogenesis of human mesenchymal stem cells through the TGF-β pathway. Journal Of Cellular And Molecular Medicine *14*, 1338–1346.

74. Frenkel, S.R., Toolan, B., Menche, D., Pitman, M.I., and Pachence, J.M. (1997). Chondrocyte transplantation using a collagen bilayer matrix for cartilage repair. The Journal Of Bone And Joint Surgery. British Volume *79*, 831–6.

75. Iwasa, J., Engebretsen, L., Shima, Y., and Ochi, M. (2009). Clinical application of scaffolds for cartilage tissue engineering. Knee Surgery, Sports Traumatology, Arthroscopy *17*, 561–577.

76. Eleftherios A. Makris, Andreas H. Gomoll, Konstantinos N. Malizos, J.C.H. and Athanasiou, K.A.

(2015). Repair and tissue engineering techniques for articular cartilage. Nat Rev Rheumatol *11*, 21–34.

77. Marlovits, S., Aldrian, S., Wondrasch, B., Zak, L., Albrecht, C., Welsch, G., and Trattnig, S. (2012). Clinical and Radiological Outcomes 5 Years After Matrix-Induced Autologous Chondrocyte Implantation in Patients With Symptomatic, Traumatic Chondral Defects. The American Journal Of Sports Medicine *40*, 2273–2280.

78. Zheng, M.-H., Willers, C., Kirilak, L., Yates, P., Xu, J., Wood, D., and Shimmin, A. (2007). Matrix-induced autologous chondrocyte implantation (MACI): biological and histological assessment. Tissue Engineering *13*, 737–46.

79. Bartlett, W., Skinner, J.A., Gooding, C.R., Carrington, R.W.J., Flanagan, A.M., Briggs, T.W.R., and Bentley, G. (2005). Autologous chondrocyte implantation *versus* matrix-induced autologous chondrocyte implantation for osteochondral defects of the knee. The Journal Of Bone And Joint Surgery. British Volume *87-B*, 640–645.

80. Zeifang, F., Oberle, D., Nierhoff, C., Richter, W., Moradi, B., and Schmitt, H. (2010). Autologous Chondrocyte Implantation Using the Original Periosteum-Cover Technique versus Matrix-Associated Autologous Chondrocyte Implantation. The American Journal Of Sports Medicine *38*, 924–933.

81. Ge, Z., Li, C., Heng, B.C., Cao, G., and Yang, Z. (2012). Functional biomaterials for cartilage regeneration. Journal Of Biomedical Materials Research. Part A *100*, 2526–36.

82. Groll, J., Burdick, J.A., Cho, D.-W., Derby, B., Gelinsky, M., Heilshorn, S.C., Jüngst, T., Malda, J., Mironov, V.A., Nakayama, K., Ovsianikov, A., Sun, W., Takeuchi, S., Yoo, J.J., and Woodfield, T.B.F. (2018). A definition of bioinks and their distinction from biomaterial inks. Biofabrication *11*, 013001.

83. Böck, T., Schill, V., Krähnke, M., Steinert, A.F., Tessmar, J., Blunk, T., and Groll, J. (2018). TGF-β1-Modified Hyaluronic Acid/Poly(glycidol) Hydrogels for Chondrogenic Differentiation of Human Mesenchymal Stromal Cells. Macromolecular Bioscience *18*, e1700390.

84. Eyrich, D., Wiese, H., Maier, G., Skodacek, D., Appel, B., Sarhan, H., Tessmar, J., Staudenmaier, R., Wenzel, M.M., Goepferich, A., and Blunk, T. (2007). In vitro and in vivo cartilage engineering using a combination of chondrocyte-seeded long-term stable fibrin gels and polycaprolactone-based polyurethane scaffolds. Tissue Engineering *13*, 2207–18.

85. Spiller, K.L., Maher, S.A., and Lowman, A.M. (2011). Hydrogels for the repair of articular cartilage defects. Tissue Engineering. Part B, Reviews *17*, 281–99.

86. Ahmed, T.A.E. and Hincke, M.T. (2010). Strategies for articular cartilage lesion repair and functional restoration. Tissue Engineering. Part B, Reviews *16*, 305–29.

87. Khan, F. and Ahmad, S.R. (2013). Polysaccharides and their derivatives for versatile tissue engineering application. Macromolecular Bioscience *13*, 395–421.

88. Sharma, B., Fermanian, S., Gibson, M., Unterman, S., Herzka, D.A., Cascio, B., Coburn, J., Hui, A.Y., Marcus, N., Gold, G.E., and Elisseeff, J.H. (2013). Human cartilage repair with a photoreactive adhesive-hydrogel composite. Science Translational Medicine *5*, 167ra6.

89. Kim, I.L., Pfeifer, C.G., Fisher, M.B., Saxena, V., Meloni, G.R., Kwon, M.Y., Kim, M., Steinberg, D.R., Mauck, R.L., and Burdick, J.A. (2015). Fibrous Scaffolds with Varied Fiber Chemistry and Growth Factor Delivery Promote Repair in a Porcine Cartilage Defect Model. Tissue Engineering. Part A *21*, 2680–90.

90. Liu, M., Zeng, X., Ma, C., Yi, H., Ali, Z., Mou, X., Li, S., Deng, Y., and He, N. (2017). Injectable hydrogels for cartilage and bone tissue engineering. Bone Research *5*, 17014.

91. Sánchez-Téllez, D.A., Téllez-Jurado, L., and Rodríguez-Lorenzo, L.M. (2017). Hydrogels for cartilage regeneration, from polysaccharides to hybrids. Polymers *9*, 1–32.

92. Nair, L.S. and Laurencin, C.T. (2007). Biodegradable polymers as biomaterials. Progress In Polymer Science *32*, 762–798.

93. Bhardwaj, N., Devi, D., and Mandal, B.B. (2015). Tissue-Engineered Cartilage: The Crossroads of Biomaterials, Cells and Stimulating Factors. Macromolecular Bioscience *15*, 153–182.

94. Matsiko, A., Levingstone, T., O'Brien, F., Matsiko, A., Levingstone, T.J., and O'Brien, F.J. (2013). Advanced Strategies for Articular Cartilage Defect Repair. Materials *6*, 637–668.

95. Bhagat, V. and Becker, M.L. (2017). Degradable Adhesives for Surgery and Tissue Engineering. Biomacromolecules *18*, 3009–3039.

96. Balakrishnan, B. and Jayakrishnan, A. (2005). Self-cross-linking biopolymers as injectable in situ forming biodegradable scaffolds. Biomaterials *26*, 3941–51.

97. Hou, Q., De Bank, P.A., and Shakesheff, K.M. (2004). Injectable scaffolds for tissue regeneration. Journal Of Materials Chemistry *14*, 1915.

98. Critchley, S.E. and Kelly, D.J. (2017). Bioinks for bioprinting functional meniscus and articular cartilage. Journal Of 3D Printing In Medicine *1*, 269–290.

99. Daly, A.C., Cunniffe, G.M., Sathy, B.N., Jeon, O., Alsberg, E., and Kelly, D.J. (2016). 3D Bioprinting of Developmentally Inspired Templates for Whole Bone Organ Engineering. Advanced Healthcare Materials *5*, 2353–2362.

100. Stichler, S., Böck, T., Paxton, N., Bertlein, S., Levato, R., Schill, V., Smolan, W., Malda, J., Teßmar, J., Blunk, T., and Groll, J. (2017). Double printing of hyaluronic acid/poly(glycidol) hybrid hydrogels with poly( ε -caprolactone) for MSC chondrogenesis. Biofabrication *9*, 044108.

101. Levato, R., Webb, W.R., Otto, I.A., Mensinga, A., Zhang, Y., van Rijen, M., van Weeren, R., Khan, I.M., and Malda, J. (2017). The bio in the ink: cartilage regeneration with bioprintable hydrogels and articular cartilage-derived progenitor cells. Acta Biomaterialia *61*, 41–53.

102. Klein, T.J., Malda, J., Sah, R.L., and Hutmacher, D.W. (2009). Tissue Engineering of Articular Cartilage with Biomimetic Zones. Tissue Engineering Part B: Reviews *15*, 143–157.

103. Melchels, F.P.W., Domingos, M.A.N., Klein, T.J., Malda, J., Bartolo, P.J., and Hutmacher, D.W. (2012). Additive manufacturing of tissues and organs. Progress In Polymer Science *37*, 1079–1104.

104. Schuurman, W., Klein, T.J., Dhert, W.J.A., van Weeren, P.R., Hutmacher, D.W., and Malda, J. (2015). Cartilage regeneration using zonal chondrocyte subpopulations: a promising approach or an overcomplicated strategy? Journal Of Tissue Engineering And Regenerative Medicine *9*, 669–78.

105. Cui, X., Breitenkamp, K., Finn, M.G., Lotz, M., and D'Lima, D.D. (2012). Direct Human Cartilage Repair Using Three-Dimensional Bioprinting Technology. Tissue Engineering Part A *18*, 1304–1312.

106. Malda, J., Visser, J., Melchels, F.P., Jüngst, T., Hennink, W.E., Dhert, W.J.A., Groll, J., and Hutmacher, D.W. (2013). 25th Anniversary Article: Engineering Hydrogels for Biofabrication. Advanced Materials *25*, 5011–5028.

107. Zhu, J. and Marchant, R.E. (2011). Design properties of hydrogel tissue-engineering scaffolds. Expert Review Of Medical Devices *8*, 607–626.

108. Woodfield, T.B.F., Malda, J., de Wijn, J., Péters, F., Riesle, J., and van Blitterswijk, C.A. (2004).

Design of porous scaffolds for cartilage tissue engineering using a three-dimensional fiber-deposition technique. Biomaterials *25*, 4149–4161.

109. Cronkite, E.P., Lozner, E.L., and Deaver, J.M. (1944). Use of thrombin and fibrinogen in skin grafting: Preliminary report. Journal Of The American Medical Association *124*, 976–978.

110. Mosesson, M.W. (2009). Structure and Functions of Fibrinogen and Fibrin. Recent Advances In Thrombosis And Hemostasis 2008 , Springer Japan, Tokyo, pp 3–26. doi:10.1007/978-4-431-78847-8_1.

111. Broche, L.M., Ismail, S.R., Booth, N.A., and Lurie, D.J. (2012). Measurement of fibrin concentration by fast field-cycling NMR. Magnetic Resonance In Medicine *67*, 1453–1457.

112. Eyrich, D., Göpferich, A., and Blunk, T. (2006). Fibrin in tissue engineering. Advances In Experimental Medicine And Biology *585*, 379–92.

113. Homminga, G.N., Buma, P., Koot, H.W.J., van der Kraan, P.M., and van den Berg, W.B. (1993). Chondrocyte behavior in fibrin glue in vitro. Acta Orthopaedica *64*, 441–445.

114. Sidelmann, J.J., Gram, J., Jespersen, J., and Kluft, C. (2000). Fibrin Clot Formation and Lysis: Basic Mechanisms. Seminars In Thrombosis And Hemostasis *26*, 605–618.

115. Helgerson, S.L., Seelich, T., DiOrio, J.P., Tawil, B., Bittner, K., and Spaethe, R. (2015). Fibrin. Encyclopedia Of Biomedical Polymers And Polymeric Biomaterials, 11 Volume Set , CRC Press, pp 3393–3399.

116. Weisel, J.W. (2005). Fibrinogen and Fibrin. Advances In Protein Chemistry *70*, Academic Press, pp 247–299.

117. Wittmann, K., Dietl, S., Ludwig, N., Berberich, O., Hoefner, C., Storck, K., Blunk, T., and Bauer-Kreisel, P. (2015). Engineering vascularized adipose tissue using the stromal-vascular fraction and fibrin hydrogels. Tissue Engineering - Part A *21*, 1343–1353.

118. Wittmann, K., Storck, K., Muhr, C., Mayer, H., Regn, S., Staudenmaier, R., Wiese, H., Maier, G., Bauer-Kreisel, P., and Blunk, T. (2016). Development of volume-stable adipose tissue constructs using polycaprolactone-based polyurethane scaffolds and fibrin hydrogels. Journal Of Tissue Engineering And Regenerative Medicine *10*, E409–E418.

119. Meinhart, J., Fussenegger, M., and Höbling, W. (1999). Stabilization of fibrin-chondrocyte constructs for cartilage reconstruction. Annals Of Plastic Surgery *42*, 673–8.

120. Fussenegger, M., Meinhart, J., Höbling, W., Kullich, W., Funk, S., and Bernatzky, G. (2003). Stabilized Autologous Fibrin-Chondrocyte Constructs for Cartilage Repair in Vivo. Annals Of Plastic Surgery *51*, 493–498.

121. Ting, V., Sims, C.D., Brecht, L.E., McCarthy, J.G., Kasabian, A.K., Connelly, P.R., Elisseeff, J., Gittes, G.K., and Longaker, M.T. (1998). In vitro prefabrication of human cartilage shapes using fibrin glue and human chondrocytes. Annals Of Plastic Surgery *40*, 413–20; discussion 420-1.

122. Eyrich, D., Brandl, F., Appel, B., Wiese, H., Maier, G., Wenzel, M., Staudenmaier, R., Goepferich, A., and Blunk, T. (2007). Long-term stable fibrin gels for cartilage engineering. Biomaterials *28*, 55–65.

123. Roach, B.L., Nover, A.B., Ateshian, G.A., and Hung, C.T. (2016). Agarose Hydrogel Characterization for Regenerative Medicine Applications: Focus on Engineering Cartilage. Biomaterials From Nature For Advanced Devices And Therapies , John Wiley & Sons, Inc., Hoboken, New Jersey, pp 258–273. doi:10.1002/9781119126218.ch16 <https://onlinelibrary.wiley.com/doi/abs/10.1002/9781119126218.ch16>.

124. Hung, C.T., Mauck, R.L., Wang, C.C.B., Lima, E.G., and Ateshian, G.A. (2004). A paradigm for functional tissue engineering of articular cartilage via applied physiologic deformational loading. Annals Of Biomedical Engineering *32*, 35–49.

125. Ng, K.W., Lima, E.G., Bian, L., O'Conor, C.J., Jayabalan, P.S., Stoker, A.M., Kuroki, K., Cook, C.R., Ateshian, G.A., Cook, J.L., and Hung, C.T. (2010). Passaged adult chondrocytes can form engineered cartilage with functional mechanical properties: a canine model. Tissue Engineering. Part A *16*, 1041–51.

126. Ng, K.W., Wang, C.C.-B., Mauck, R.L., Kelly, T.-A.N., Chahine, N.O., Costa, K.D., Ateshian, G.A., and Hung, C.T. (2005). A layered agarose approach to fabricate depth-dependent inhomogeneity in chondrocyte-seeded constructs. Journal Of Orthopaedic Research *23*, 134–141.

127. Albro, M.B., Rajan, V., Li, R., Hung, C.T., and Ateshian, G.A. (2009). Characterization of the Concentration-Dependence of Solute Diffusivity and Partitioning in a Model Dextran–Agarose Transport System. Cellular And Molecular Bioengineering *2*, 295–305.

128. Lima, E.G., Durney, K.M., Sirsi, S.R., Nover, A.B., Ateshian, G.A., Borden, M.A., and Hung, C.T. (2012). Microbubbles as biocompatible porogens for hydrogel scaffolds. Acta Biomaterialia *8*, 4334–41.

129. Scandiucci de Freitas, P., Wirz, D., Stolz, M., Göpfert, B., Friederich, N.-F., and Daniels, A.U. (2006). Pulsatile dynamic stiffness of cartilage-like materials and use of agarose gels to validate mechanical methods and models. Journal Of Biomedical Materials Research Part B: Applied Biomaterials *78B*, 347–357.

130. Mauck, R.L., Soltz, M.A., Wang, C.C., Wong, D.D., Chao, P.H., Valhmu, W.B., Hung, C.T., and Ateshian, G.A. (2000). Functional tissue engineering of articular cartilage through dynamic loading of chondrocyte-seeded agarose gels. Journal Of Biomechanical Engineering *122*, 252–60.

131. Buschmann, M.D., Gluzband, Y.A., Grodzinsky, A.J., and Hunziker, E.B. (1995). Mechanical compression modulates matrix biosynthesis in chondrocyte/agarose culture. Journal Of Cell Science *108 ( Pt 4*, 1497–508.

132. Benya, P.D. and Shaffer, J.D. (1982). Dedifferentiated chondrocytes reexpress the differentiated collagen phenotype when cultured in agarose gels. Cell *30*, 215–24.

133. Buschmann, M.D., Gluzband, Y.A., Grodzinsky, A.J., Kimura, J.H., and Hunziker, E.B. (1992). Chondrocytes in agarose culture synthesize a mechanically functional extracellular matrix. Journal Of Orthopaedic Research *10*, 745–758.

134. Lee, D.A. and Bader, D.L. (1995). The development and characterization of anin vitro system to study strain-induced cell deformation in isolated chondrocytes. In Vitro Cellular & Developmental Biology - Animal *31*, 828–835.

135. Lee, D.A. and Bader, D.L. (1997). Compressive strains at physiological frequencies influence the metabolism of chondrocytes seeded in agarose. Journal Of Orthopaedic Research *15*, 181–188.

136. Cai, Y., López-Ruiz, E., Wengel, J., Creemers, L.B., and Howard, K.A. (2017). A hyaluronic acid-based hydrogel enabling CD44-mediated chondrocyte binding and gapmer oligonucleotide release for modulation of gene expression in osteoarthritis. Journal Of Controlled Release *253*, 153–159.

137. Menzel, E.J. and Farr, C. (1998). Hyaluronidase and its substrate hyaluronan: biochemistry, biological activities and therapeutic uses. Cancer Letters *131*, 3–11.

138.  Chung, C. and Burdick, J.A. (2009). Influence of Three-Dimensional Hyaluronic Acid Microenvironments on Mesenchymal Stem Cell Chondrogenesis. Tissue Engineering Part A *15*, 243–254.

139.  Goldberg, V.M. and Buckwalter, J.A. (2005). Hyaluronans in the treatment of osteoarthritis of the knee: evidence for disease-modifying activity. Osteoarthritis And Cartilage *13*, 216–224.

140.  Burdick, J.A. and Prestwich, G.D. (2011). Hyaluronic Acid Hydrogels for Biomedical Applications. Advanced Materials *23*, H41–H56.

141.  Tan, H., Ramirez, C.M., Miljkovic, N., Li, H., Rubin, J.P., and Marra, K.G. (2009). Thermosensitive injectable hyaluronic acid hydrogel for adipose tissue engineering. Biomaterials *30*, 6844–6853.

142.  Nagaya, H., Ymagata, T., Ymagata, S., Iyoda, K., Ito, H., Hasegawa, Y., and Iwata, H. (1999). Examination of synovial fluid and serum hyaluronidase activity as a joint marker in rheumatoid arthritis and osteoarthritis patients (by zymography). Annals Of The Rheumatic Diseases *58*, 186–188.

143.  Park, S.-H., Park, S.R., Chung, S. Il, Pai, K.S., and Min, B.-H. (2005). Tissue-engineered Cartilage Using Fibrin/Hyaluronan Composite Gel and Its In Vivo Implantation. Artificial Organs *29*, 838–845.

144.  Smeds, K.A., Pfister-Serres, A., Miki, D., Dastgheib, K., Inoue, M., Hatchell, D.L., and Grinstaff, M.W. (2001). Photocrosslinkable polysaccharides for in situ hydrogel formation. Journal Of Biomedical Materials Research *55*, 254–255.

145.  Nettles, D.L., Vail, T.P., Morgan, M.T., Grinstaff, M.W., and Setton, L.A. (2004). Photocrosslinkable Hyaluronan as a Scaffold for Articular Cartilage Repair. Annals Of Biomedical Engineering *32*, 391–397.

146.  Anderson, D.G., Tweedie, C.A., Hossain, N., Navarro, S.M., Brey, D.M., Van Vliet, K.J., Langer, R., and Burdick, J.A. (2006). A Combinatorial Library of Photocrosslinkable and Degradable Materials. Advanced Materials *18*, 2614–2618.

147.  Sabnis, A., Rahimi, M., Chapman, C., and Nguyen, K.T. (2009). Cytocompatibility studies of an in situ photopolymerized thermoresponsive hydrogel nanoparticle system using human aortic smooth muscle cells. Journal Of Biomedical Materials Research Part A *91A*, 52–59.

148.  Nguyen, K.T. and West, J.L. (2002). Photopolymerizable hydrogels for tissue engineering applications. Biomaterials *23*, 4307–14.

149.  Stichler, S., Jungst, T., Schamel, M., Zilkowski, I., Kuhlmann, M., Böck, T., Blunk, T., Teßmar, J., and Groll, J. (2017). Thiol-ene Clickable Poly(glycidol) Hydrogels for Biofabrication. Annals Of Biomedical Engineering *45*, 273–285.

150.  Dworak, A., Slomkowski, S., Basinska, T., Gosecka, M., Walach, W., and Trzebicka, B. (2013). Polyglycidol - how is it synthesized and what is it used for? Polimery *58*, 641–649.

151.  Thomas, A., Müller, S.S., and Frey, H. (2014). Beyond Poly(ethylene glycol): Linear Polyglycerol as a Multifunctional Polyether for Biomedical and Pharmaceutical Applications. Biomacromolecules *15*, 1935–1954.

152.  Khan, I.M., Gilbert, S.J., Singhrao, S.K., Duance, V.C., and Archer, C.W. (2008). Cartilage integration: evaluation of the reasons for failure of integration during cartilage repair. A review. European Cells & Materials *16*, 26–39.

153.  Wakitani, S., Goto, T., Pineda, S.J., Young, R.G., Mansour, J.M., Caplan, A.I., and Goldberg, V.M. (1994). Mesenchymal cell-based repair of large, full-thickness defects of articular cartilage. The Journal Of Bone And Joint Surgery. American Volume *76*, 579–92.

154. Horas, U., Pelinkovic, D., Herr, G., Aigner, T., and Schnettler, R. (2003). Autologous chondrocyte implantation and osteochondral cylinder transplantation in cartilage repair of the knee joint. A prospective, comparative trial. The Journal Of Bone And Joint Surgery. American Volume *85-A*, 185–92.

155. Tew, S.R., Kwan, A.P.L., Hann, A., Thomson, B.M., and Archer, C.W. (2000). The reactions of articular cartilage to experimental wounding: Role of apoptosis. Arthritis And Rheumatism *43*, 215–225.

156. Zscharnack, M., Hepp, P., Richter, R., Aigner, T., Schulz, R., Somerson, J., Josten, C., Bader, A., and Marquass, B. (2010). Repair of Chronic Osteochondral Defects Using Predifferentiated Mesenchymal Stem Cells in an Ovine Model. The American Journal Of Sports Medicine *38*, 1857–1869.

157. Gelse, K., Riedel, D., Pachowsky, M., Hennig, F.F., Trattnig, S., and Welsch, G.H. (2015). Limited integrative repair capacity of native cartilage autografts within cartilage defects in a sheep model. Journal Of Orthopaedic Research : Official Publication Of The Orthopaedic Research Society *33*, 390–7.

158. McGregor, A.J., Amsden, B.G., and Waldman, S.D. (2011). Chondrocyte repopulation of the zone of death induced by osteochondral harvest. Osteoarthritis And Cartilage *19*, 242–8.

159. van de Breevaart Bravenboer, J., In der Maur, C.D., Bos, P.K., Feenstra, L., Verhaar, J. a N., Weinans, H., and van Osch, G.J.V.M. (2004). Improved cartilage integration and interfacial strength after enzymatic treatment in a cartilage transplantation model. Arthritis Research & Therapy *6*, R469-76.

160. Reindel, E.S., Ayroso, A.M., Chen, A.C., Chun, D.M., Schinagl, R.M., and Sah, R.L. (1995). Integrative repair of articular cartilage in vitro: adhesive strength of the interface region. Journal Of Orthopaedic Research : Official Publication Of The Orthopaedic Research Society *13*, 751–60.

161. Gilbert, S.J., Singhrao, S.K., Khan, I.M., Gonzalez, L.G., Thomson, B.M., Burdon, D., Duance, V.C., and Archer, C.W. (2009). Enhanced tissue integration during cartilage repair in vitro can be achieved by inhibiting chondrocyte death at the wound edge. Tissue Engineering. Part A *15*, 1739–49.

162. Obradovic, B., Martin, I., Padera, R.F., Treppo, S., Freed, L.E., and Vunjak-Novakovic, G. (2001). Integration of engineered cartilage. Journal Of Orthopaedic Research : Official Publication Of The Orthopaedic Research Society *19*, 1089–97.

163. Davies, L.C., Blain, E.J., Caterson, B., and Duance, V.C. (2008). Chondroitin sulphate impedes the migration of a sub-population of articular cartilage chondrocytes. Osteoarthritis And Cartilage *16*, 855–64.

164. Tam, H.K., Srivastava, A., Colwell, C.W., and D'Lima, D.D. (2007). In vitro model of full-thickness cartilage defect healing. Journal Of Orthopaedic Research : Official Publication Of The Orthopaedic Research Society *25*, 1136–44.

165. Bos, P.K., DeGroot, J., Budde, M., Verhaar, J.A.N., and van Osch, G.J.V.M. (2002). Specific enzymatic treatment of bovine and human articular cartilage: Implications for integrative cartilage repair. Arthritis & Rheumatism *46*, 976–985.

166. Lee, P., Chen, C., Mcnally, A., Chapman, C., Sly, K., and Lin, S. (2016). Partially enzymatic treatment to improve integrative repair of cartilage. Frontiers In Bioengineering And Biotechnology. Conference Abstract: 10th World Biomaterials Congress *4*.

167. Seol, D., Yu, Y., Choe, H., Jang, K., Brouillette, M.J., Zheng, H., Lim, T.-H., Buckwalter, J.A., and Martin, J.A. (2014). Effect of short-term enzymatic treatment on cell migration and cartilage

regeneration: in vitro organ culture of bovine articular cartilage. Tissue Engineering. Part A *20*, 1807–14.

168. Pabbruwe, M.B., Esfandiari, E., Kafienah, W., Tarlton, J.F., and Hollander, A.P. (2009). Induction of cartilage integration by a chondrocyte/collagen-scaffold implant. Biomaterials *30*, 4277–86.

169. Theodoropoulos, J.S., De Croos, J.N.A., Park, S.S., Pilliar, R., and Kandel, R.A. (2011). Integration of tissue-engineered cartilage with host cartilage: an in vitro model. Clinical Orthopaedics And Related Research *469*, 2785–95.

170. DiMicco, M.A., Waters, S.N., Akeson, W.H., and Sah, R.L. (2002). Integrative articular cartilage repair: dependence on developmental stage and collagen metabolism. Osteoarthritis And Cartilage *10*, 218–25.

171. Brittberg, M., Gomoll, A.H., Canseco, J.A., Far, J., Lind, M., and Hui, J. (2016). Cartilage repair in the degenerative ageing knee. Acta Orthopaedica *87*, 26–38.

172. Barbero, A., Grogan, S., Schäfer, D., Heberer, M., Mainil-Varlet, P., and Martin, I. (2004). Age related changes in human articular chondrocyte yield, proliferation and post-expansion chondrogenic capacity. Osteoarthritis And Cartilage *12*, 476–484.

173. Blaney Davidson, E., Scharstuhl, A., Vitters, E., van der Kraan, P., and van den Berg, W. (2005). Reduced transforming growth factor-beta signaling in cartilage of old mice: role in impaired repair capacity. Arthritis Research & Therapy *7*, R1338.

174. Tew, S., Redman, S., Kwan, A., Walker, E., Khan, I., Dowthwaite, G., Thomson, B., and Archer, C.W. (2001). Differences in Repair Responses Between Immature and Mature Cartilage. Clinical Orthopaedics And Related Research *391*, S142–S152.

175. Dowthwaite, G.P., Bishop, J.C., Redman, S.N., Khan, I.M., Rooney, P., Evans, D.J.R., Haughton, L., Bayram, Z., Boyer, S., Thomson, B., Wolfe, M.S., and Archer, C.W. (2004). The surface of articular cartilage contains a progenitor cell population. Journal Of Cell Science *117*, 889–97.

176. Englert, C., Blunk, T., Fierlbeck, J., Kaiser, J., Stosiek, W., Angele, P., Hammer, J., and Straub, R.H. (2006). Steroid hormones strongly support bovine articular cartilage integration in the absence of interleukin-1beta. Arthritis And Rheumatism *54*, 3890–7.

177. Maher, S.A., Mauck, R.L., Rackwitz, L., and Tuan, R.S. (2010). A nanofibrous cell-seeded hydrogel promotes integration in a cartilage gap model. Journal Of Tissue Engineering And Regenerative Medicine *4*, 25–9.

178. Djouad, F., Rackwitz, L., Song, Y., Janjanin, S., and Tuan, R.S. (2009). ERK1/2 activation induced by inflammatory cytokines compromises effective host tissue integration of engineered cartilage. Tissue Engineering. Part A *15*, 2825–35.

179. Khan, I.M., Gonzalez, L.G., Francis, L., Conlan, R.S., Gilbert, S.J., Singhrao, S.K., Burdon, D., Hollander, A.P., Duance, V.C., and Archer, C.W. (2011). Interleukin-1β enhances cartilage-to-cartilage integration. European Cells & Materials *22*, 190–201.

180. Carver, S.E. and Heath, C.A. (1999). Influence of intermittent pressure, fluid flow, and mixing on the regenerative properties of articular chondrocytes. Biotechnology And Bioengineering *65*, 274–81.

181. Waldman, S.D., Spiteri, C.G., Grynpas, M.D., Pilliar, R.M., and Kandel, R.A. (2004). Long-term intermittent compressive stimulation improves the composition and mechanical properties of tissue-engineered cartilage. Tissue Engineering *10*, 1323–31.

182. Dunkelman, N.S., Zimber, M.P., LeBaron, R.G., Pavelec, R., Kwan, M., and Purchio, A.F. (1995). Cartilage production by rabbit articular chondrocytes on polyglycolic acid scaffolds in a closed

bioreactor system. Biotechnology And Bioengineering *46*, 299–305.

183. Waldman, S.D., Spiteri, C.G., Grynpas, M.D., Pilliar, R.M., Hong, J., and Kandel, R.A. (2003). Effect of biomechanical conditioning on cartilaginous tissue formation in vitro. The Journal Of Bone And Joint Surgery. American Volume *85-A Suppl*, 101–5.

184. Smith, R.L., Donlon, B.S., Gupta, M.K., Mohtai, M., Das, P., Carter, D.R., Cooke, J., Gibbons, G., Hutchinson, N., and Schurman, D.J. (1995). Effects of fluid-induced shear on articular chondrocyte morphology and metabolism in vitro. Journal Of Orthopaedic Research : Official Publication Of The Orthopaedic Research Society *13*, 824–31.

185. Kiviranta, I., Tammi, M., Jurvelin, J., Säämänen, A.-M., and Helminen, H.J. (1988). Moderate running exercise augments glycosaminoglycans and thickness of articular cartilage in the knee joint of young beagle dogs. Journal Of Orthopaedic Research *6*, 188–195.

186. Vunjak-Novakovic, G., Martin, I., Obradovic, B., Treppo, S., Grodzinsky, A.J., Langer, R., and Freed, L.E. (1999). Bioreactor cultivation conditions modulate the composition and mechanical properties of tissue-engineered cartilage. Journal Of Orthopaedic Research : Official Publication Of The Orthopaedic Research Society *17*, 130–8.

187. Darling, E.M. and Athanasiou, K.A. (2003). Biomechanical strategies for articular cartilage regeneration. Annals Of Biomedical Engineering *31*, 1114–24.

188. Theodoropoulos, J.S., DeCroos, A.J.N., Petrera, M., Park, S., and Kandel, R.A. (2016). Mechanical stimulation enhances integration in an in vitro model of cartilage repair. Knee Surgery, Sports Traumatology, Arthroscopy : Official Journal Of The ESSKA *24*, 2055–64.

189. DiMicco, M.A. and Sah, R.L. (2001). Integrative cartilage repair: adhesive strength is correlated with collagen deposition. Journal Of Orthopaedic Research : Official Publication Of The Orthopaedic Research Society *19*, 1105–12.

190. Kagan, H.M. (1994). Lysyl Oxidase: Mechanism, Regulation and Relationship to Liver Fibrosis. Pathology - Research And Practice *190*, 910–919.

191. Ahsan, T., Lottman, L.M., Harwood, F., Amiel, D., and Sah, R.L. (1999). Integrative cartilage repair: inhibition by beta-aminopropionitrile. Journal Of Orthopaedic Research : Official Publication Of The Orthopaedic Research Society *17*, 850–7.

192. Sasaki, T., Majamaa, K., and Uitto, J. (1987). Reduction of collagen production in keloid fibroblast cultures by ethyl-3,4-dihydroxybenzoate. Inhibition of prolyl hydroxylase activity as a mechanism of action. The Journal Of Biological Chemistry *262*, 9397–403.

193. Kivirikko, K.I., Myllylä, R., and Pihlajaniemi, T. (1989). Protein hydroxylation: prolyl 4-hydroxylase, an enzyme with four cosubstrates and a multifunctional subunit. FASEB Journal : Official Publication Of The Federation Of American Societies For Experimental Biology *3*, 1609–17.

194. Nandan, D., Clarke, E.P., Ball, E.H., and Sanwal, B.D. (1990). Ethyl-3,4-dihydroxybenzoate inhibits myoblast differentiation: evidence for an essential role of collagen. The Journal Of Cell Biology *110*, 1673–1679.

195. Majamaa, K., Sasaki, T., and Uitto, J. (1987). Inhibition of Prolyl Hydroxylation During Collagen Biosynthesis in Human Skin Fibroblast Cultures by Ethyl 3,4-Dihydroxybenzoate. Journal Of Investigative Dermatology *89*, 405–409.

196. Kiepe, F. (2021). Dissertation: Knorpelintegration unter Hemmung der Kollagensynthese im Disc-Ring-Modell: eine In-vitro-Studie. doi:10.25972/OPUS-23761 <https://opus.bibliothek.uni-wuerzburg.de/frontdoor/index/index/docId/23761>.

197. Englert, C., Blunk, T., Müller, R., von Glasser, S.S., Baumer, J., Fierlbeck, J., Heid, I.M., Nerlich,

M., and Hammer, J. (2007). Bonding of articular cartilage using a combination of biochemical degradation and surface cross-linking. Arthritis Research & Therapy *9*, R47.

198. Meng, X., Ziadlou, R., Grad, S., Alini, M., Wen, C., Lai, Y., Qin, L., Zhao, Y., and Wang, X. (2020). Animal Models of Osteochondral Defect for Testing Biomaterials. Biochemistry Research International *2020*, 1–12.

199. Peretti, G.M., Bonassar, L.J., Caruso, E.M., Randolph, M.A., Trahan, C.A., and Zaleske, D.J. (1999). Biomechanical analysis of a chondrocyte-based repair model of articular cartilage. Tissue Engineering *5*, 317–26.

200. Peretti, G.M., Zaporojan, V., Spangenberg, K.M., Randolph, M. a, Fellers, J., and Bonassar, L.J. (2003). Cell-based bonding of articular cartilage: An extended study. Journal Of Biomedical Materials Research. Part A *64*, 517–24.

201. Silverman, R.P., Bonasser, L., Passaretti, D., Randolph, M.A., and Yaremchuk, M.J. (2000). Adhesion of tissue-engineered cartilage to native cartilage. Plastic And Reconstructive Surgery *105*, 1393–8.

202. Johnson, T.S., Xu, J.-W., Zaporojan, V. V, Mesa, J.M., Weinand, C., Randolph, M. a, Bonassar, L.J., Winograd, J.M., and Yaremchuk, M.J. (2004). Integrative repair of cartilage with articular and nonarticular chondrocytes. Tissue Engineering *10*, 1308–1315.

203. Gratz, K.R., Wong, V.W., Chen, A.C., Fortier, L.A., Nixon, A.J., and Sah, R.L. (2006). Biomechanical assessment of tissue retrieved after in vivo cartilage defect repair: Tensile modulus of repair tissue and integration with host cartilage. Journal Of Biomechanics *39*, 138–146.

204. Zhang, Z., McCaffery, J.M., Spencer, R.G.S., and Francomano, C.A. (2005). Growth and integration of neocartilage with native cartilage in vitro. Journal Of Orthopaedic Research : Official Publication Of The Orthopaedic Research Society *23*, 433–9.

205. Jürgensen, K., Aeschlimann, D., Cavin, V., Genge, M., and Hunziker, E.B. (1997). A new biological glue for cartilage-cartilage interfaces: tissue transglutaminase. The Journal Of Bone And Joint Surgery. American Volume *79*, 185–93.

206. Wang, D.-A., Varghese, S., Sharma, B., Strehin, I., Fermanian, S., Gorham, J., Fairbrother, D.H., Cascio, B., and Elisseeff, J.H. (2007). Multifunctional chondroitin sulphate for cartilage tissue-biomaterial integration. Nature Materials *6*, 385–92.

207. Englert, C., McGowan, K.B., Klein, T.J., Giurea, A., Schumacher, B.L., and Sah, R.L. (2005). Inhibition of integrative cartilage repair by proteoglycan 4 in synovial fluid. Arthritis And Rheumatism *52*, 1091–9.

208. Strehin, I., Nahas, Z., Arora, K., Nguyen, T., and Elisseeff, J. (2010). A versatile pH sensitive chondroitin sulfate-PEG tissue adhesive and hydrogel. Biomaterials *31*, 2788–2797.

209. Liu, X., Yang, Y., Niu, X., Lin, Q., Zhao, B., Wang, Y., and Zhu, L. (2017). An in situ photocrosslinkable platelet rich plasma – Complexed hydrogel glue with growth factor controlled release ability to promote cartilage defect repair. Acta Biomaterialia *62*, 179–187.

210. Fan, C., Fu, J., Zhu, W., and Wang, D.-A. (2016). A mussel-inspired double-crosslinked tissue adhesive intended for internal medical use. Acta Biomaterialia *33*, 51–63.

211. Sitterle, V.B., Nishimuta, J.F., and Levenston, M.E. (2009). Photochemical approaches for bonding of cartilage tissues. Osteoarthritis And Cartilage / OARS, Osteoarthritis Research Society *17*, 1649–56.

212. Ahsan, T. and Sah, R.L. (1999). Biomechanics of integrative cartilage repair. Osteoarthritis And Cartilage *7*, 29–40.

# References

213. Xu, X., Shi, D., Shen, Y., Xu, Z., Dai, J., Chen, D., Teng, H., and Jiang, Q. (2015). Full-thickness cartilage defects are repaired via a microfracture technique and intraarticular injection of the small-molecule compound kartogenin. Arthritis Research & Therapy *17*, 20.

214. Moretti, M., Wendt, D., Schaefer, D., Jakob, M., Hunziker, E.B., Heberer, M., and Martin, I. (2005). Structural characterization and reliable biomechanical assessment of integrative cartilage repair. Journal Of Biomechanics *38*, 1846–54.

215. Schaefer, D.B., Wendt, D., Moretti, M., Jakob, M., Jay, G.D., Heberer, M., and Martin, I. (2004). Lubricin reduces cartilage--cartilage integration. Biorheology *41*, 503–8.

216. Rackwitz, L., Djouad, F., Janjanin, S., Nöth, U., and Tuan, R.S. (2014). Functional cartilage repair capacity of de-differentiated, chondrocyte- and mesenchymal stem cell-laden hydrogels in vitro. Osteoarthritis And Cartilage *22*, 1148–57.

217. Athens, A. a, Makris, E. a, and Hu, J.C. (2013). Induced collagen cross-links enhance cartilage integration. PloS One *8*, e60719.

218. Li, J., Celiz, A.D., Yang, J., Yang, Q., Wamala, I., Whyte, W., Seo, B.R., Vasilyev, N. V., Vlassak, J.J., Suo, Z., and Mooney, D.J. (2017). Tough adhesives for diverse wet surfaces. Science (New York, N.Y.) *357*, 378–381.

219. Tognana, E., Chen, F., Padera, R.F., Leddy, H.A., Christensen, S.E., Guilak, F., Vunjak-Novakovic, G., and Freed, L.E. (2005). Adjacent tissues (cartilage, bone) affect the functional integration of engineered calf cartilage in vitro. Osteoarthritis And Cartilage *13*, 129–138.

220. Broguiere, N., Cavalli, E., Salzmann, G.M., Applegate, L.A., and Zenobi-Wong, M. (2016). Factor XIII Cross-Linked Hyaluronan Hydrogels for Cartilage Tissue Engineering. ACS Biomaterials Science & Engineering *2*, 2176–2184.

221. Lin, H., Cheng, A.W., Alexander, P.G., Beck, A.M., and Tuan, R.S. (2014). Cartilage Tissue Engineering Application of Injectable Gelatin Hydrogel with In Situ Visible-Light-Activated Gelation Capability in both Air and Aqueous Solution. Tissue Engineering. Part A *20*, 2402–2411.

222. de Vries-van Melle, M.L., Mandl, E.W., Kops, N., Koevoet, W.J.L.M., Verhaar, J. a N., and van Osch, G.J.V.M. (2012). An osteochondral culture model to study mechanisms involved in articular cartilage repair. Tissue Engineering. Part C, Methods *18*, 45–53.

223. de Vries-van Melle, M.L., Narcisi, R., Kops, N., Koevoet, W.J.L.M., Bos, P.K., Murphy, J.M., Verhaar, J.A.N., van der Kraan, P.M., and van Osch, G.J.V.M. (2014). Chondrogenesis of mesenchymal stem cells in an osteochondral environment is mediated by the subchondral bone. Tissue Engineering. Part A *20*, 23–33.

224. Schwab, A. (2017). Ex vivo culture platform for assessment of cartilage repair treatment strategies. ALTEX *34*, 267–277.

225. Mouser, V. (2018). Ex vivo model unravelling cell distribution effect in hydrogels for cartilage repair. ALTEX *35*, 65–76.

226. Spotnitz, W.D. (2014). Fibrin Sealant: The Only Approved Hemostat, Sealant, and Adhesive-a Laboratory and Clinical Perspective. ISRN Surgery *2014*, 203943.

227. Kaplonyi, G., Zimmerman, I., Frenyo, A.D., Farkas, T., and Nemes, G. (1988). The use of fibrin adhesive in the repair of chondral and osteochondral injuries. Injury *19*, 267–72.

228. Patel, S., Rodriguez-Merchan, E.C., and Haddad, F.S. (2010). The use of fibrin glue in surgery of the knee. The Journal Of Bone And Joint Surgery. British Volume *92*, 1325–31.

229. Sierra, D.H., Feldman, D.S., Saltz, R., and Huang, S. (1992). A method to determine shear

adhesive strength of fibrin sealants. Journal Of Applied Biomaterials *3*, 147–151.

230. Fürst, W. and Banerjee, A. (2005). Release of glutaraldehyde from an albumin-glutaraldehyde tissue adhesive causes significant in vitro and in vivo toxicity. The Annals Of Thoracic Surgery *79*, 1522–8; discussion 1529.

231. Bruns, T.B. and Worthington, J.M. (2000). Using tissue adhesive for wound repair: a practical guide to dermabond. American Family Physician *61*, 1383–8.

232. Strehin, I., Ambrose, W.M., Schein, O., Salahuddin, A., and Elisseeff, J. (2009). Synthesis and characterization of a chondroitin sulfate-polyethylene glycol corneal adhesive. Journal Of Cataract And Refractive Surgery *35*, 567–76.

233. Mehdizadeh, M. and Yang, J. (2013). Design strategies and applications of tissue bioadhesives. Macromolecular Bioscience *13*, 271–88.

234. Bouten, P.J.M., Zonjee, M., Bender, J., Yauw, S.T.K., Van Goor, H., Van Hest, J.C.M., and Hoogenboom, R. (2014). The chemistry of tissue adhesive materials. Progress In Polymer Science *39*, 1375–1405.

235. Elvin, C.M., Brownlee, A.G., Huson, M.G., Tebb, T.A., Kim, M., Lyons, R.E., Vuocolo, T., Liyou, N.E., Hughes, T.C., Ramshaw, J.A.M., and Werkmeister, J.A. (2009). The development of photochemically crosslinked native fibrinogen as a rapidly formed and mechanically strong surgical tissue sealant. Biomaterials *30*, 2059–2065.

236. Verbraeken, B., Monnery, B.D., Lava, K., and Hoogenboom, R. (2017). The chemistry of poly(2-oxazoline)s. European Polymer Journal *88*, 451–469.

237. Mero, A., Pasut, G., Via, L.D., Fijten, M.W.M., Schubert, U.S., Hoogenboom, R., and Veronese, F.M. (2008). Synthesis and characterization of poly(2-ethyl 2-oxazoline)-conjugates with proteins and drugs: Suitable alternatives to PEG-conjugates? Journal Of Controlled Release *125*, 87–95.

238. Goddard, P., Hutchinson, L.E., Brown, J., and Brookman, L.J. (1989). Soluble polymeric carriers for drug delivery. Part 2. Preparation and in vivo behaviour of N-acylethylenimine copolymers. Journal Of Controlled Release *10*, 5–16.

239. Gaertner, F.C., Luxenhofer, R., Blechert, B., Jordan, R., and Essler, M. (2007). Synthesis, biodistribution and excretion of radiolabeled poly(2-alkyl-2-oxazoline)s. Journal Of Controlled Release *119*, 291–300.

240. Dargaville, T.R., Park, J.-R., and Hoogenboom, R. (2018). Poly(2-oxazoline) Hydrogels: State-of-the-Art and Emerging Applications. Macromolecular Bioscience *18*, e1800070.

241. Blöhbaum, J., Paulus, I., Pöppler, A.-C., Tessmar, J., and Groll, J. (2019). Influence of charged groups on the cross-linking efficiency and release of guest molecules from thiol–ene cross-linked poly(2-oxazoline) hydrogels. Journal Of Materials Chemistry B *7*, 1782–1794.

242. Lee, H., Dellatore, S.M., Miller, W.M., and Messersmith, P.B. (2007). Mussel-inspired surface chemistry for multifunctional coatings. Science (New York, N.Y.) *318*, 426–30.

243. Lee, H., Rho, J., and Messersmith, P.B. (2009). Facile Conjugation of Biomolecules onto Surfaces via Mussel Adhesive Protein Inspired Coatings. Advanced Materials *21*, 431–434.

244. Li, L., Smitthipong, W., and Zeng, H. (2015). Mussel-inspired hydrogels for biomedical and environmental applications. Polym. Chem *6*, 353.

245. Li, Y., Meng, H., Liu, Y., Narkar, A., and Lee, B.P. (2016). Gelatin Microgel Incorporated Poly(ethylene glycol)-Based Bioadhesive with Enhanced Adhesive Property and Bioactivity. ACS Applied Materials & Interfaces *8*, 11980–11989.

246. Brubaker, C.E. and Messersmith, P.B. (2011). Enzymatically degradable mussel-inspired adhesive hydrogel. Biomacromolecules *12*, 4326–4334.

247. Cencer, M., Liu, Y., Winter, A., Murley, M., Meng, H., and Lee, B.P. (2014). Effect of pH on the rate of curing and bioadhesive properties of dopamine functionalized poly(ethylene glycol) hydrogels. Biomacromolecules *15*, 2861–9.

248. Burke, K.A., Roberts, D.C., and Kaplan, D.L. (2016). Silk Fibroin Aqueous-Based Adhesives Inspired by Mussel Adhesive Proteins. Biomacromolecules *17*, 237–45.

249. Sparks, B.J., Hoff, E.F.T., Hayes, L.P., and Patton, D.L. (2012). Mussel-Inspired Thiol–Ene Polymer Networks: Influencing Network Properties and Adhesion with Catechol Functionality. Chemistry Of Materials *24*, 3633–3642.

250. Han, L., Wang, M., Li, P., Gan, D., Yan, L., Xu, J., Wang, K., Fang, L., Chan, C.W., Zhang, H., Yuan, H., and Lu, X. (2018). Mussel-Inspired Tissue-Adhesive Hydrogel Based on the Polydopamine-Chondroitin Sulfate Complex for Growth-Factor-Free Cartilage Regeneration. ACS Applied Materials And Interfaces *10*, American Chemical Society, 28015–28026pp.

251. Scognamiglio, F., Travan, A., Rustighi, I., Tarchi, P., Palmisano, S., Marsich, E., Borgogna, M., Donati, I., de Manzini, N., and Paoletti, S. (2016). Adhesive and sealant interfaces for general surgery applications. Journal Of Biomedical Materials Research. Part B, Applied Biomaterials *104*, 626–39.

252. Artzi, N., Zeiger, A., Boehning, F., Bon Ramos, A., Van Vliet, K., and Edelman, E.R. (2011). Tuning adhesion failure strength for tissue-specific applications. Acta Biomaterialia *7*, 67–74.

253. Madl, C.M., LeSavage, B.L., Dewi, R.E., Dinh, C.B., Stowers, R.S., Khariton, M., Lampe, K.J., Nguyen, D., Chaudhuri, O., Enejder, A., and Heilshorn, S.C. (2017). Maintenance of neural progenitor cell stemness in 3D hydrogels requires matrix remodelling. Nature Materials *16*, 1233–1242.

254. Kossmann, A. (2019). Dissertation: Knorpelintegration - Etablierung eines Push-out-Modells und Untersuchung von BioGlue® als Knorpeladhäsivum. doi:10.25972/OPUS-18606 <https://opus.bibliothek.uni-wuerzburg.de/frontdoor/index/index/docId/18606>.

255. Scheibler, A.G., Götschi, T., Widmer, J., Holenstein, C., Steffen, T., Camenzind, R.S., Snedeker, J.G., and Farshad, M. (2018). Feasibility of the annulus fibrosus repair with in situ gelating hydrogels – A biomechanical study. PLoS ONE *13*, 1–15.

256. Berberich, O., Blöhbaum, J., Hölscher-Doht, S., Meffert, R.H., Teßmar, J., Blunk, T., and Groll, J. (2019). Catechol-modified poly(oxazoline)s with tunable degradability facilitate cell invasion and lateral cartilage integration. Journal Of Industrial And Engineering Chemistry *80*, 757–769.

257. Martin, I., Obradovic, B., Freed, L.E., and Vunjak-Novakovic, G. (1999). Method for Quantitative Analysis of Glycosaminoglycan Distribution in Cultured Natural and Engineered Cartilage. Annals Of Biomedical Engineering *27*, 656–662.

258. Kim, Y.J., Sah, R.L.Y., Doong, J.Y.H., and Grodzinsky, A.J. (1988). Fluorometric assay of DNA in cartilage explants using Hoechst 33258. Analytical Biochemistry *174*, 168–176.

259. Farndale, R.W., Buttle, D.J., and Barrett, A.J. (1986). Improved quantitation and discrimination of sulphated glycosaminoglycans by use of dimethylmethylene blue. BBA - General Subjects *883*, 173–177.

260. Woessner, J.F. (1961). The determination of hydroxyproline in tissue and protein samples containing small proportions of this imino acid. Archives Of Biochemistry And Biophysics *93*, 440–447.

261. Hollander, A.P., Heathfield, T.F., Webber, C., Iwata, Y., Bourne, R., Rorabeck, C., and Poole,

A.R. (1994). Increased damage to type II collagen in osteoarthritic articular cartilage detected by a new immunoassay. Journal Of Clinical Investigation *93*, 1722–1732.

262. Peretti, G.M., Campo-Ruiz, V., Gonzalez, S., Randolph, M. a, Wei Xu, J., Morse, K.R., Roses, R.E., and Yaremchuk, M.J. (2006). Tissue engineered cartilage integration to live and devitalized cartilage: a study by reflectance mode confocal microscopy and standard histology. Connective Tissue Research *47*, 190–9.

263. Mueller, M.B., Blunk, T., Appel, B., Maschke, A., Goepferich, A., Zellner, J., Englert, C., Prantl, L., Kujat, R., Nerlich, M., and Angele, P. (2013). Insulin is essential for in vitro chondrogenesis of mesenchymal progenitor cells and influences chondrogenesis in a dose-dependent manner. International Orthopaedics *37*, 153–8.

264. Hunter, C.J. and Levenston, M.E. (2002). The influence of repair tissue maturation on the response to oscillatory compression in a cartilage defect repair model. Biorheology *39*, 79–88.

265. Hunziker, E.B. and Quinn, T.M. (2003). Surgical removal of articular cartilage leads to loss of chondrocytes from cartilage bordering the wound edge. The Journal Of Bone And Joint Surgery. American Volume *85-A Suppl*, 85–92.

266. Lewis, J.L., Deloria, L.B., Oyen-Tiesma, M., Thompson, R.C., Ericson, M., and Oegema, T.R. (2003). Cell death after cartilage impact occurs around matrix cracks. Journal Of Orthopaedic Research *21*, 881–887.

267. Luyten, F.P., Hascall, V.C., Nissley, S.P., Morales, T.I., and Reddi, A.H. (1988). Insulin-like growth factors maintain steady-state metabolism of proteoglycans in bovine articular cartilage explants. Archives Of Biochemistry And Biophysics *267*, 416–25.

268. Fortier, L.A., Mohammed, H.O., Lust, G., and Nixon, A.J. (2002). Insulin-like growth factor-I enhances cell-based repair of articular cartilage. The Journal Of Bone And Joint Surgery. British Volume *84*, 276–88.

269. Hayami, T., Pickarski, M., Zhuo, Y., Wesolowski, G.A., Rodan, G.A., and Duong, L.T. (2006). Characterization of articular cartilage and subchondral bone changes in the rat anterior cruciate ligament transection and meniscectomized models of osteoarthritis. Bone *38*, 234–243.

270. Pacifici, M., Koyama, E., and Iwamoto, M. (2005). Mechanisms of synovial joint and articular cartilage formation: Recent advances, but many lingering mysteries. Birth Defects Research Part C - Embryo Today: Reviews *75*, 237–248.

271. Chen-An, P., Andreassen, K.V., Henriksen, K., Li, Y., Karsdal, M.A., and Bay-Jensen, A.C. (2012). The inhibitory effect of Salmon Calcitonin on Tri-Iodothyronine induction of early hypertrophy in articular cartilage. PLoS ONE *7*, 1–8.

272. Byers, B.A., Mauck, R.L., Chiang, I.E., and Tuan, R.S. (2008). Transient exposure to transforming growth factor beta 3 under serum-free conditions enhances the biomechanical and biochemical maturation of tissue-engineered cartilage. Tissue Engineering. Part A *14*, 1821–34.

273. Chua, K.H., Aminuddin, B.S., Fuzina, N.H., and Ruszymah, B.H.I. (2005). Insulin-Transferrin-Selenium prevent human chondrocyte dedifferentiation and promote the formation of high quality tissue engineered human hyaline cartilage. European Cells And Materials *9*, 58–67.

274. Muir, H. (1995). The chondrocyte, architect of cartilage. Biomechanics, structure, function and molecular biology of cartilage matrix macromolecules. BioEssays *17*, 1039–1048.

275. Grant, M.E. and Prockop, D.J. (1972). The Biosynthesis of Collagen. New England Journal Of Medicine *286*, 242–249.

276. Vasta, J.D. and Raines, R.T. (2015). Selective inhibition of prolyl 4-hydroxylases by bipyridinedicarboxylates. Bioorganic And Medicinal Chemistry *23*, 3081–3090.

277. Vasta, J.D. and Raines, R.T. (2016). Human Collagen Prolyl 4-Hydroxylase Is Activated by Ligands for Its Iron Center. Biochemistry *55*, 3224–3233.

278. De Jong, L., Albracht, S.P.J., and Kemp, A. (1982). Prolyl 4-hydroxylase activity in relation to the oxidation state of enzyme-bound iron. The role of ascorbate in peptidyl proline hydroxylation. Biochimica Et Biophysica Acta (BBA)/Protein Structure And Molecular *704*, 326–332.

279. Wang, J., Buss, J.L., Chen, G., Ponka, P., and Pantopoulos, K. (2002). The prolyl 4-hydroxylase inhibitor ethyl-3,4-dihydroxybenzoate generates effective iron deficiency in cultured cells. FEBS Letters *529*, 309–312.

280. Maličev, E., Wozniak, G., Knežević, M., Radosavljević, D., and Jeras, M. (2000). Vitamin C induced apoptosis in human articular chondrocytes. Pflugers Archiv : European Journal Of Physiology *440*, R046–R048.

281. Chang, Z., Huo, L., Li, P., Wu, Y., and Zhang, P. (2015). Ascorbic acid provides protection for human chondrocytes against oxidative stress. Molecular Medicine Reports *12*, 7086–7092.

282. Grigull, N.P., Redeker, J.I., Schmitt, B., Saller, M.M., Schönitzer, V., and Mayer-Wagner, S. (2020). Chondrogenic Potential of Pellet Culture Compared to High-Density Culture on a Bacterial Cellulose Hydrogel. International Journal Of Molecular Sciences *21*, 2785.

283. Huang, B.J., Hu, J.C., and Athanasiou, K.A. (2016). Effects of passage number and post-expansion aggregate culture on tissue engineered, self-assembled neocartilage. Acta Biomaterialia *43*, 150–159.

284. Bianchi, V.J., Lee, A., Anderson, J., Parreno, J., Theodoropoulos, J., Backstein, D., and Kandel, R. (2019). Redifferentiated Chondrocytes in Fibrin Gel for the Repair of Articular Cartilage Lesions. American Journal Of Sports Medicine *47*, 2348–2359.

285. Caron, M.M.J., Emans, P.J., Coolsen, M.M.E., Voss, L., Surtel, D.A.M., Cremers, A., van Rhijn, L.W., and Welting, T.J.M. (2012). Redifferentiation of dedifferentiated human articular chondrocytes: Comparison of 2D and 3D cultures. Osteoarthritis And Cartilage *20*, 1170–1178.

286. Ibold, Y., Lübke, C., Pelz, S., Augst, H., Kaps, C., Ringe, J., and Sittinger, M. (2009). Effect of different ascorbate supplementations on in vitro cartilage formation in porcine high-density pellet cultures. Tissue & Cell *41*, 249–56.

287. Koohestani, F., Braundmeier, A.G., Mahdian, A., Seo, J., Bi, J.J., and Nowak, R.A. (2013). Extracellular matrix collagen alters cell proliferation and cell cycle progression of human uterine leiomyoma smooth muscle cells. PLoS ONE *8*, 75844.

288. Rojas, F.P., Batista, M.A., Lindburg, C.A., Dean, D., Grodzinsky, A.J., Ortiz, C., and Han, L. (2014). Molecular Adhesion between Cartilage ExtracellularMatrix Macromolecules. Biomacromolecules *15*, 772.

289. Frischholz, S., Berberich, O., Böck, T., Meffert, R.H., and Blunk, T. (2020). Resveratrol counteracts IL-1β-mediated impairment of extracellular matrix deposition in 3D articular chondrocyte constructs. Journal Of Tissue Engineering And Regenerative Medicine *14*, 897–908.

290. Raanani, E., Latter, D. a, Errett, L.E., Bonneau, D.B., Leclerc, Y., and Salasidis, G.C. (2001). Use of "BioGlue" in aortic surgical repair. The Annals Of Thoracic Surgery *72*, 638–640.

291. Sung, H.W., Chang, W.H., Ma, C.Y., and Lee, M.H. (2003). Crosslinking of biological tissues using genipin and/or carbodiimide, 427–438at.

292. Chao, H.-H. and Torchiana, D.F. (2003). BioGlue: Albumin/Glutaraldehyde Sealant in Cardiac Surgery. Journal Of Cardiac Surgery *18*, 500–503.

293. Bhamidipati, C.M., Coselli, J.S., and LeMaire, S.A. (2012). BioGlue® in 2011: What is its role in cardiac surgery? Journal Of Extra-Corporeal Technology *44*, P6-12.

294. Vincent, J.F. V. (1992). Biomechanics--materials : a practical approach, IRL Press at Oxford University Press, 247pp.

295. Ahsan, T., Lottman, L.M., Harwood, F., Amiel, D., and Sah, R.L. (1999). Integrative cartilage repair: inhibition by beta-aminopropionitrile. Journal Of Orthopaedic Research : Official Publication Of The Orthopaedic Research Society *17*, 850–7.

296. Pfeifer, C.G., Fisher, M.B., Saxena, V., Kim, M., Henning, E.A., Steinberg, D.A., Dodge, G.R., and Mauck, R.L. (2017). Age-Dependent Subchondral Bone Remodeling and Cartilage Repair in a Minipig Defect Model. Tissue Engineering - Part C: Methods *23*, 745–753.

297. Izabela Bochyńska, A., Hannink, G., Verhoeven, R., Grijpma, D.W., and Buma, P. (2017). The effect of tissue surface modification with collagenase and addition of TGF-Î²3 on the healing potential of meniscal tears repaired with tissue glues in vitro. J Mater Sci: Mater Med *28*.

298. Brittberg, M., Sjögren-Jansson, E., Lindahl, A., and Peterson, L. (1997). Influence of fibrin sealant (Tisseel) on osteochondral defect repair in the rabbit knee. Biomaterials *18*, 235–42.

299. Peng, Z., Sun, H., Bunpetch, V., Koh, Y., Wen, Y., Wu, D., and Ouyang, H. (2021). The regulation of cartilage extracellular matrix homeostasis in joint cartilage degeneration and regeneration. Biomaterials *268*, 120555.

300. Fresquet, M., Jowitt, T.A., Stephen, L.A., Ylöstalo, J., and Briggs, M.D. (2010). Structural and functional investigations of matrilin-1 A-domains reveal insights into their role in cartilage ECM assembly. Journal Of Biological Chemistry *285*, 34048–34061.

301. Liebesny, P.H., Mroszczyk, K., Zlotnick, H., Hung, H.-H., Frank, E., Kurz, B., Zanotto, G., Frisbie, D., and Grodzinsky, A.J. (2019). Enzyme Pretreatment plus Locally Delivered HB-IGF-1 Stimulate Integrative Cartilage Repair In Vitro. Tissue Engineering. Part A *25*, 1191–1201.

302. Marmotti, A., Bonasia, D.E., Bruzzone, M., Rossi, R., Castoldi, F., Collo, G., Realmuto, C., Tarella, C., and Peretti, G.M. (2013). Human cartilage fragments in a composite scaffold for single-stage cartilage repair: an in vitro study of the chondrocyte migration and the influence of TGF-β1 and G-CSF. Knee Surgery, Sports Traumatology, Arthroscopy *21*, 1819–1833.

303. Kirilak, Y., Pavlos, N.J., Willers, C.R., Han, R., Feng, H., Xu, J., Asokananthan, N., Stewart, G.A., Henry, P., Wood, D., and Zheng, M.H. (2006). Fibrin sealant promotes migration and proliferation of human articular chondrocytes: Possible involvement of thrombin and protease-activated receptors. International Journal Of Molecular Medicine *17*, 551–558.

304. Karp, J.M., Sarraf, F., Shoichet, M.S., and Davies, J.E. (2004). Fibrin-filled scaffolds for bone-tissue engineering: Anin vivo study. Journal Of Biomedical Materials Research *71A*, 162–171.

305. Knox, P., Crooks, S., Scaife, M.C., and Patel, S. (1987). Role of plasminogen, plasmin, and plasminogen activators in the migration of fibroblasts into plasma clots. Journal Of Cellular Physiology *132*, 501–508.

306. Gille, J., Meisner, U., Ehlers, E.M., Müller, A., Russlies, M., and Behrens, P. (2005). Migration pattern, morphology and viability of cells suspended in or sealed with fibrin glue: A histomorphologic study. Tissue And Cell *37*, 339–348.

307. Andjelkov, N., Hamberg, H., and Bjellerup, P. (2016). No outgrowth of chondrocytes from non-digested particulated articular cartilage embedded in commercially available fibrin matrix: an in vitro study. Journal Of Orthopaedic Surgery And Research *11*, 23.

# References

308. Hirsh, S.L., Bilek, M.M.M., Bax, D. V., Kondyurin, A., Kosobrodova, E., Tsoutas, K., Tran, C.T.H., Waterhouse, A., Yin, Y., Nosworthy, N.J., McKenzie, D.R., Dos Remedios, C.G., Ng, M.K.C., and Weiss, A.S. (2013). Ion implanted, radical-rich surfaces for the rapid covalent immobilization of active biomolecules. AIP Conference Proceedings *1525*, 364–369.

309. Dankbar, D.M. and Gauglitz, G. (2006). A study on photolinkers used for biomolecule attachment to polymer surfaces. Analytical And Bioanalytical Chemistry 2006 386:7 *386*, 1967–1974.

310. Dubinsky, L., Krom, B.P., and Meijler, M.M. (2012). Diazirine based photoaffinity labeling. Bioorganic & Medicinal Chemistry *20*, 554–570.

311. Chee, G.L., Yalowich, J.C., Bodner, A., Wu, X., and Hasinoff, B.B. (2010). A diazirine-based photoaffinity etoposide probe for labeling topoisomerase II. Bioorganic & Medicinal Chemistry *18*, 830.

312. Viner, V. and Viner, G. (2011). Effect of filler choice on a binary frontal polymerization system. The Journal Of Physical Chemistry. B *115*, 6862–6867.

313. Lee, M.C., Sung, K.L.P., Kurtis, M.S., Akeson, W.H., and Sah, R.L. (2000). Adhesive Force of Chondrocytes to Cartilage. Clinical Orthopaedics And Related Research *370*, 286–294.

314. Quinn, T.M. and Hunziker, E.B. (2002). Controlled enzymatic matrix degradation for integrative cartilage repair: effects on viable cell density and proteoglycan deposition. Tissue Engineering *8*, 799–806.

315. Munro, I.C., Renwick, A.G., and Danielewska-Nikiel, B. (2008). The Threshold of Toxicological Concern (TTC) in risk assessment. Toxicology Letters *180*, 151–156.

316. Raphel, J., Parisi-Amon, A., and Heilshorn, S. (2012). Photoreactive elastin-like proteins for use as versatile bioactive materials and surface coatings. Journal Of Materials Chemistry *22*, 19429–19437.

317. Mogal, V., Papper, V., Chaurasia, A., Feng, G., Marks, R., and Steele, T. (2014). Novel on-demand bioadhesion to soft tissue in wet environments. Macromolecular Bioscience *14*, 478–484.

318. Feng, G., Djordjevic, I., Mogal, V., O'Rorke, R., Pokholenko, O., and Steele, T.W.J. (2016). Elastic Light Tunable Tissue Adhesive Dendrimers. Macromolecular Bioscience *16*, 1072–1082.

319. Appelman, T.P., Mizrahi, J., Elisseeff, J.H., and Seliktar, D. (2011). The influence of biological motifs and dynamic mechanical stimulation in hydrogel scaffold systems on the phenotype of chondrocytes. Biomaterials *32*, 1508–1516.

320. Yang, Y., Zhang, J., Liu, Z., Lin, Q., Liu, X., Bao, C., Wang, Y., and Zhu, L. (2016). Tissue-Integratable and Biocompatible Photogelation by the Imine Crosslinking Reaction. Advanced Materials (Deerfield Beach, Fla.) *28*, 2724–30.

321. Lu, M., Liu, Y., Huang, Y.C., Huang, C.J., and Tsai, W.B. (2018). Fabrication of photo-crosslinkable glycol chitosan hydrogel as a tissue adhesive. Carbohydrate Polymers *181*, 668–674.

322. Liang, J., Guo, Z., Timmerman, A., Grijpma, D., and Poot, A. (2019). Enhanced mechanical and cell adhesive properties of photo-crosslinked PEG hydrogels by incorporation of gelatin in the networks. Biomedical Materials *14*, 024102.

323. Sinha, R.P. and Häder, D.P. (2002). UV-induced DNA damage and repair: a review. Photochemical & Photobiological Sciences *1*, 225–236.

324. Fairbanks, B.D., Schwartz, M.P., Bowman, C.N., and Anseth, K.S. (2009). Photoinitiated

polymerization of PEG-diacrylate with lithium phenyl-2,4,6-trimethylbenzoylphosphinate: polymerization rate and cytocompatibility. Biomaterials *30*, 6702–6707.

325. Shih, H. and Lin, C.C. (2013). Visible-Light-Mediated Thiol-Ene Hydrogelation Using Eosin-Y as the Only Photoinitiator. Macromolecular Rapid Communications *34*, 269–273.

326. Hu, J., Hou, Y., Park, H., Choi, B., Hou, S., Chung, A., and Lee, M. (2012). Visible light crosslinkable chitosan hydrogels for tissue engineering. Acta Biomaterialia *8*, 1730–1738.

327. Lim, K.S., Schon, B.S., Mekhileri, N. V., Brown, G.C.J., Chia, C.M., Prabakar, S., Hooper, G.J., and Woodfield, T.B.F. (2016). New Visible-Light Photoinitiating System for Improved Print Fidelity in Gelatin-Based Bioinks. ACS Biomaterials Science And Engineering *2*, 1752–1762.

328. Fancy, D.A. and Kodadek, T. (1999). Chemistry for the analysis of protein–protein interactions: Rapid and efficient cross-linking triggered by long wavelength light. Chemistry Biochemistry *96*, 6020–6024.

329. Sando, L., Danon, S., Brownlee, A.G., McCulloch, R.J., Ramshaw, J.A.M., Elvin, C.M., and Werkmeister, J.A. (2011). Photochemically crosslinked matrices of gelatin and fibrinogen promote rapid cell proliferation. Journal Of Tissue Engineering And Regenerative Medicine *5*, 337–46.

330. Huang, S., Wang, C., Xu, J., Ma, L., and Gao, C. (2017). In situ assembly of fibrinogen/hyaluronic acid hydrogel via knob-hole interaction for 3D cellular engineering. Bioactive Materials *2*, 253–259.

331. Elvin, C.M., Danon, S.J., Brownlee, A.G., White, J.F., Hickey, M., Liyou, N.E., Edwards, G.A., Ramshaw, J.A.M., and Werkmeister, J.A. (2010). Evaluation of photo-crosslinked fibrinogen as a rapid and strong tissue adhesive. Journal Of Biomedical Materials Research. Part A *93*, 687–95.

332. Elvin, C. and Vuocolo, T. (2011). Photochemical Crosslinking of Proteins To Make Novel Biomedical Materials. Australian Biochemist *42*, 15–18.

333. Partlow, B.P., Applegate, M.B., Omenetto, F.G., and Kaplan, D.L. (2016). Dityrosine Cross-Linking in Designing Biomaterials. ACS Biomaterials Science And Engineering *2*, 2108–2121.

334. Balasubramanian, D. and Kanwar, R. (2002). Molecular pathology of dityrosine cross-links in proteins: Structural and functional analysis of four proteins. Molecular And Cellular Biochemistry 2002 234:1 *234*, 27–38.

335. Paerl, R.W., Claudio, I.M., Shields, M.R., Bianchi, T.S., and Osburn, C.L. (2020). Dityrosine formation via reactive oxygen consumption yields increasingly recalcitrant humic-like fluorescent organic matter in the ocean. Limnology And Oceanography Letters *5*, 337–345.

336. Liu, B., Burdine, L., and Kodadek, T. (2006). Chemistry of periodate-mediated cross-linking of 3,4-dihydroxylphenylalanine-containing molecules to proteins. Journal Of The American Chemical Society *128*, 15228–35.

337. Vuocolo, T., Haddad, R., Edwards, G.A., Lyons, R.E., Liyou, N.E., Werkmeister, J.A., Ramshaw, J.A.M., and Elvin, C.M. (2012). A Highly Elastic and Adhesive Gelatin Tissue Sealant for Gastrointestinal Surgery and Colon Anastomosis. Journal Of Gastrointestinal Surgery *16*, 744–752.

338. ICH Expert Working Group (2019). ICH harmonised guideline, Guideline for elemental impurities Q3D (R1). ICH Guideline Q3D (R1) On Elemental Impurities *31*.

339. Meister, J.M. (2022). Dissertation: Untersuchung zweier Gewebekleber auf Basis von Fibrinogen und Gelatine zur Knorpeladhäsion und -integration in einem In vitro Push-out-Modell. doi:10.25972/OPUS-28007 <https://opus.bibliothek.uni-

wuerzburg.de/frontdoor/index/index/year/2022/docId/28007>.

340. Jeon, E.Y., Hwang, B.H., Yang, Y.J., Kim, B.J., Choi, B.-H., Jung, G.Y., and Cha, H.J. (2015). Rapidly light-activated surgical protein glue inspired by mussel adhesion and insect structural crosslinking. Biomaterials *67*, 11–19.

341. Jin, L., Park, K., Yoon, Y., Kim, H.S., Kim, H.J., Choi, J.W., Lee, D.Y., Chun, H.J., and Yang, D.H. (2021). Visible light-cured antibacterial collagen hydrogel containing water-solubilized triclosan for improved wound healing. Materials *14*.

342. Liebscher (née Blöhbaum), J. (2020). Dissertation: Side chain functional poly(2-oxazoline)s for biomedical applications. doi:10.25972/OPUS-20396 <https://opus.bibliothek.uni-wuerzburg.de/frontdoor/index/index/docId/20396>.

343. Lee, B.P., Dalsin, J.L., and Messersmith, P.B. (2002). Synthesis and Gelation of DOPA-Modified Poly(ethylene glycol) Hydrogels. Biomacromolecules *3*, 1038–1047.

344. Bré, L.P., Zheng, Y., Pêgo, A.P., and Wang, W. (2013). Taking tissue adhesives to the future: From traditional synthetic to new biomimetic approaches. Biomaterials Science *1*, 239–253.

345. Waite, J.H. (2017). Mussel adhesion - essential footwork. The Journal Of Experimental Biology *220*, 517–530.

346. Lee, B.P., Messersmith, P.B., Israelachvili, J.N., and Waite, J.H. (2011). Mussel-Inspired Adhesives and Coatings. Annual Review Of Materials Research *41*, 99–132.

347. Mehdizadeh, M., Weng, H., Gyawali, D., Tang, L., and Yang, J. (2012). Injectable citrate-based mussel-inspired tissue bioadhesives with high wet strength for sutureless wound closure. Biomaterials *33*, 7972–83.

348. Berdichevski, A., Shachaf, Y., Wechsler, R., and Seliktar, D. (2015). Protein composition alters in vivo resorption of PEG-based hydrogels as monitored by contrast-enhanced MRI. Biomaterials *42*, 1–10.

349. Guthold, M., Liu, W., Sparks, E.A., Jawerth, L.M., Peng, L., Falvo, M., Superfine, R., Hantgan, R.R., and Lord, S.T. (2007). A comparison of the mechanical and structural properties of fibrin fibers with other protein fibers. Cell Biochemistry And Biophysics *49*, 165–81.

350. Barrett, D.G., Bushnell, G.G., and Messersmith, P.B. (2013). Mechanically Robust, Negative-Swelling, Mussel-Inspired Tissue Adhesives. Advanced Healthcare Materials *2*, 745–755.

351. Chung, H. and Grubbs, R.H. (2012). Rapidly Cross-Linkable DOPA Containing Terpolymer Adhesives and PEG-Based Cross-Linkers for Biomedical Applications. Macromolecules *45*, 9666–9673.

352. Shin, J., Lee, J.S., Lee, C., Park, H.-J., Yang, K., Jin, Y., Ryu, J.H., Hong, K.S., Moon, S.-H., Chung, H.-M., Yang, H.S., Um, S.H., Oh, J.-W., Kim, D.-I., Lee, H., and Cho, S.-W. (2015). Tissue Adhesive Catechol-Modified Hyaluronic Acid Hydrogel for Effective, Minimally Invasive Cell Therapy. Advanced Functional Materials *25*, 3814–3824.

353. Jenkins, C.L., Meredith, H.J., and Wilker, J.J. (2013). Molecular weight effects upon the adhesive bonding of a mussel mimetic polymer. ACS Applied Materials & Interfaces *5*, 5091–6.

354. North, M.A., Del Grosso, C.A., and Wilker, J.J. (2017). High Strength Underwater Bonding with Polymer Mimics of Mussel Adhesive Proteins. ACS Applied Materials & Interfaces *9*, 7866–7872.

355. Šrámková, P., Zahoranová, A., Kroneková, Z., Šišková, A., and Kronek, J. (2017). Poly(2-oxazoline) hydrogels by photoinduced thiol-ene "click" reaction using different dithiol crosslinkers. Journal Of Polymer Research *24*, 82.

356. Farrugia, B.L., Kempe, K., Schubert, U.S., Hoogenboom, R., and Dargaville, T.R. (2013). Poly(2-oxazoline) Hydrogels for Controlled Fibroblast Attachment. Biomacromolecules *14*, 2724–2732.

357. Viegas, T.X., Bentley, M.D., Harris, J.M., Fang, Z., Yoon, K., Dizman, B., Weimer, R., Mero, A., Pasut, G., and Veronese, F.M. (2011). Polyoxazoline: Chemistry, Properties, and Applications in Drug Delivery. Bioconjugate Chemistry *22*, 976–986.

358. Luxenhofer, R., Sahay, G., Schulz, A., Alakhova, D., Bronich, T.K., Jordan, R., and Kabanov, A. V (2011). Structure-property relationship in cytotoxicity and cell uptake of poly(2-oxazoline) amphiphiles. Journal Of Controlled Release : Official Journal Of The Controlled Release Society *153*, 73–82.

359. Bauer, M., Lautenschlaeger, C., Kempe, K., Tauhardt, L., Schubert, U.S., and Fischer, D. (2012). Poly(2-ethyl-2-oxazoline) as alternative for the stealth polymer poly(ethylene glycol): comparison of in vitro cytotoxicity and hemocompatibility. Macromolecular Bioscience *12*, 986–98.

360. Brubaker, C.E., Kissler, H., Wang, L.-J.J., Kaufman, D.B., and Messersmith, P.B. (2010). Biological performance of mussel-inspired adhesive in extrahepatic islet transplantation. Biomaterials *31*, 420–427.

361. Zhang, H., Bré, L.P., Zhao, T., Zheng, Y., Newland, B., and Wang, W. (2014). Mussel-inspired hyperbranched poly(amino ester) polymer as strong wet tissue adhesive. Biomaterials *35*, 711–9.

362. Bundesinstitut für Risikobewertung (BfR) (2021). Höchstmengenvorschläge für Vitamin B12 in Lebensmitteln inklusive Nahrungsergänzungsmittelnat.

363. Murphy, M.K., Arzi, B., Prouty, S.M., Hu, J.C., and Athanasiou, K. a (2015). Neocartilage integration in temporomandibular joint discs: physical and enzymatic methods. Journal Of The Royal Society, Interface *12*.

364. Schmidt, S., Abinzano, F., Mensinga, A., Teßmar, J., Groll, J., Malda, J., Levato, R., and Blunk, T. (2020). Differential production of cartilage ECM in 3D agarose constructs by equine articular cartilage progenitor cells and mesenchymal stromal cells. International Journal Of Molecular Sciences *21*, 1–19.

365. Madeira, C., Santhagunam, A., Salgueiro, J.B., and Cabral, J.M. (2015). Advanced cell therapies for articular cartilage regeneration. Trends In Biotechnology *33*, 35–42.

366. Kwon, H., Brown, W.E., Lee, C.A., Wang, D., Paschos, N., Hu, J.C., and Athanasiou, K.A. (2019). Surgical and tissue engineering strategies for articular cartilage and meniscus repair. Nature Reviews Rheumatology *15*, 550–570.

367. Huang, B.J., Hu, J.C., and Athanasiou, K.A. (2016). Cell-based tissue engineering strategies used in the clinical repair of articular cartilage. Biomaterials *98*, 1–22.

368. Li, L., Yu, F., Zheng, L., Wang, R., Yan, W., Wang, Z., Xu, J., Wu, J., Shi, D., Zhu, L., Wang, X., and Jiang, Q. (2019). Natural hydrogels for cartilage regeneration: Modification, preparation and application. Journal Of Orthopaedic Translation *17*, 26–41.

369. Mouser, V.H.M.M., Levato, R., Mensinga, A., Dhert, W.J.A.A., Gawlitta, D., and Malda, J. (2020). Bio-ink development for three-dimensional bioprinting of hetero-cellular cartilage constructs. Connective Tissue Research *61*, 137–151.

370. Kazusa, H., Nakasa, T., Shibuya, H., Ohkawa, S., Kamei, G., Adachi, N., Deie, M., Nakajima, N., Hyon, S.-H., and Ochi, M. (2013). Strong adhesiveness of a new biodegradable hydrogel glue, LYDEX, for use on articular cartilage. Journal Of Applied Biomaterials & Functional Materials

*11*, 180–186.

371. Tognana, E., Padera, R.F., Chen, F., Vunjak-Novakovic, G., and Freed, L.E. (2005). Development and remodeling of engineered cartilage-explant composites in vitro and in vivo. Osteoarthritis And Cartilage *13*, 896–905.

372. Vainieri, M.L., Wahl, D., Alini, M., van Osch, G.J.V.M., and Grad, S. (2018). Mechanically stimulated osteochondral organ culture for evaluation of biomaterials in cartilage repair studies. Acta Biomaterialia *81*, 256–266.

373. Pittenger, M.F., Mosca, J.D., and McIntosh, K.R. (2000). Human mesenchymal stem cells: progenitor cells for cartilage, bone, fat and stroma. Current Topics In Microbiology And Immunology *251*, 3–11.

374. Khan, I.M., Bishop, J.C., Gilbert, S., and Archer, C.W. (2009). Clonal chondroprogenitors maintain telomerase activity and Sox9 expression during extended monolayer culture and retain chondrogenic potential. Osteoarthritis And Cartilage *17*, 518–528.

375. Williams, R., Khan, I.M., Richardson, K., Nelson, L., McCarthy, H.E., Analbelsi, T., Singhrao, S.K., Dowthwaite, G.P., Jones, R.E., Baird, D.M., Lewis, H., Roberts, S., Shaw, H.M., Dudhia, J., Fairclough, J., Briggs, T., and Archer, C.W. (2010). Identification and clonal characterisation of a progenitor cell sub-population in normal human articular cartilage. PloS One *5*.

376. McCarthy, H.E., Bara, J.J., Brakspear, K., Singhrao, S.K., and Archer, C.W. (2012). The comparison of equine articular cartilage progenitor cells and bone marrow-derived stromal cells as potential cell sources for cartilage repair in the horse. Veterinary Journal (London, England : 1997) *192*, 345–351.

377. Ma, B., Leijten, J.C.H., Wu, L., Kip, M., van Blitterswijk, C.A., Post, J.N., and Karperien, M. (2013). Gene expression profiling of dedifferentiated human articular chondrocytes in monolayer culture. Osteoarthritis And Cartilage *21*, 599–603.

378. Kang, S.-W., Yoo, S.P., and Kim, B.-S. (2007). Effect of chondrocyte passage number on histological aspects of tissue-engineered cartilage. Bio-Medical Materials And Engineering *17*, 269–276.

379. Shamsul, B., Chowdhury, S., Hamdan, M.Y., and Ruszymah, B.H.I. (2019). Effect of cell density on formation of three-dimensional cartilaginous constructs using fibrin & human osteoarthritic chondrocytes. Indian Journal Of Medical Research *149*, 641–649.

380. Knudson, C.B. and Knudson, W. (2004). Hyaluronan and CD44: modulators of chondrocyte metabolism. Clinical Orthopaedics And Related Research *427*, S152-62.

381. Grogan, S.P., Barbero, A., Diaz-Romero, J., Cleton-Jansen, A.-M., Soeder, S., Whiteside, R., Hogendoorn, P.C.W., Farhadi, J., Aigner, T., Martin, I., and Mainil-Varlet, P. (2007). Identification of markers to characterize and sort human articular chondrocytes with enhanced in vitro chondrogenic capacity. Arthritis And Rheumatism *56*, 586–95.

382. Hall, H. (2007). Modified fibrin hydrogel matrices: both, 3D-scaffolds and local and controlled release systems to stimulate angiogenesis. Current Pharmaceutical Design *13*, 3597–3607.

383. Zhu, M., Feng, Q., and Bian, L. (2014). Differential effect of hypoxia on human mesenchymal stem cell chondrogenesis and hypertrophy in hyaluronic acid hydrogels. Acta Biomaterialia *10*, 1333–1340.

384. Meretoja, V. V., Dahlin, R.L., Wright, S., Kasper, F.K., and Mikos, A.G. (2013). The effect of hypoxia on the chondrogenic differentiation of co-cultured articular chondrocytes and mesenchymal stem cells in scaffolds. Biomaterials *34*, 4266–4273.

385. Desancé, M., Contentin, R., Bertoni, L., Gomez-Leduc, T., Branly, T., Jacquet, S., Betsch, J.M.,

Batho, A., Legendre, F., Audigié, F., Galéra, P., and Demoor, M. (2018). Chondrogenic Differentiation of Defined Equine Mesenchymal Stem Cells Derived from Umbilical Cord Blood for Use in Cartilage Repair Therapy. International Journal Of Molecular Sciences 2018, Vol. 19, Page 537 *19*, 537.

386. Yodmuang, S., Guo, H., Brial, C., Warren, R.F., Torzilli, P.A., Chen, T., and Maher, S.A. (2019). Effect of interface mechanical discontinuities on scaffold-cartilage integration. Journal Of Orthopaedic Research *37*, 845–854.

387. Rahfoth, B., Weisser, J., Sternkopf, F., Aigner, T., Von Der Mark, K., and Bräuer, R. (1998). Transplantation of allograft chondrocytes embedded in agarose gel into cartilage defects of rabbits. Osteoarthritis And Cartilage *6*, 50–65.

388. Ait Si Selmi, T., Neyret, P., Verdonk, P.C.M., and Barnouin, L. (2007). Autologous chondrocyte transplantation in combination with an alginate-agarose based hydrogel (Cartipatch). Techniques In Knee Surgery *6*, 253–258.

389. Kelly, T.-A.N., Wang, C.C.B., Mauck, R.L., Ateshian, G.A., and Hung, C.T. (2004). Role of cell-associated matrix in the development of free-swelling and dynamically loaded chondrocyte-seeded agarose gels. Biorheology *41*, 223–37.

390. Ng, K.W., Kugler, L.E., Doty, S.B., Ateshian, G.A., and Hung, C.T. (2009). Scaffold degradation elevates the collagen content and dynamic compressive modulus in engineered articular cartilage. Osteoarthritis And Cartilage *17*, 220–227.

391. Chung, C., Beecham, M., Mauck, R.L., and Burdick, J.A. (2009). The influence of degradation characteristics of hyaluronic acid hydrogels on in vitro neocartilage formation by mesenchymal stem cells. Biomaterials *30*, 4287–4296.

392. Armiento, A.R., Stoddart, M.J., Alini, M., and Eglin, D. (2018). Biomaterials for articular cartilage tissue engineering: Learning from biology. Acta Biomaterialia *65*, 1–20.

393. Wasyłeczko, M., Sikorska, W., and Chwojnowski, A. (2020). Review of Synthetic and Hybrid Scaffolds in Cartilage Tissue Engineering. Membranes 2020, Vol. 10, Page 348 *10*, 348.

394. Singh, S., Choudhury, D., Yu, F., Mironov, V., and Naing, M.W. (2020). In situ bioprinting – Bioprinting from benchside to bedside? Acta Biomaterialia *101*, 14–25.

395. Hauptstein, J., Böck, T., Bartolf-Kopp, M., Forster, L., Stahlhut, P., Nadernezhad, A., Blahetek, G., Zernecke-Madsen, A., Detsch, R., Jüngst, T., Groll, J., Teßmar, J., and Blunk, T. (2020). Hyaluronic Acid-Based Bioink Composition Enabling 3D Bioprinting and Improving Quality of Deposited Cartilaginous Extracellular Matrix. Advanced Healthcare Materials *9*, 2000737.

396. Roberts, S., Menage, J., Sandell, L.J., Evans, E.H., and Richardson, J.B. (2009). Immunohistochemical study of collagen types I and II and procollagen IIA in human cartilage repair tissue following autologous chondrocyte implantation. The Knee *16*, 398–404.

397. Vainieri, M.L., Lolli, A., Kops, N., D'Atri, D., Eglin, D., Yayon, A., Alini, M., Grad, S., Sivasubramaniyan, K., and van Osch, G.J.V.M. (2020). Evaluation of biomimetic hyaluronic-based hydrogels with enhanced endogenous cell recruitment and cartilage matrix formation. Acta Biomaterialia *101*, 293–303.

398. Richardson, B.M., Wilcox, D.G., Randolph, M.A., and Anseth, K.S. (2019). Hydrazone covalent adaptable networks modulate extracellular matrix deposition for cartilage tissue engineering. Acta Biomaterialia *83*, 71–82.

399. Bryant, S.J., Chowdhury, T.T., Lee, D.A., Bader, D.L., and Anseth, K.S. (2004). Crosslinking Density Influences Chondrocyte Metabolism in Dynamically Loaded Photocrosslinked Poly(ethylene glycol) Hydrogels. Annals Of Biomedical Engineering 2004 32:3 *32*, 407–417.

400.  Erickson, I.E., Huang, A.H., Sengupta, S., Kestle, S., Burdick, J.A., and Mauck, R.L. (2009). Macromer density influences mesenchymal stem cell chondrogenesis and maturation in photocrosslinked hyaluronic acid hydrogels. Osteoarthritis And Cartilage *17*, 1639–1648.

401.  Bian, L., Hou, C., Tous, E., Rai, R., Mauck, R.L., and Burdick, J.A. (2013). The influence of hyaluronic acid hydrogel crosslinking density and macromolecular diffusivity on human MSC chondrogenesis and hypertrophy. Biomaterials *34*, 413–421.

402.  Mancini, I.A.D., Schmidt, S., Brommer, H., Pouran, B., Schäfer, S., Tessmar, J., Mensinga, A., Van Rijen, M.H.P., Groll, J., Blunk, T., Levato, R., Malda, J., and Van Weeren, P.R. (2020). A composite hydrogel-3D printed thermoplast osteochondral anchor as example for a zonal approach to cartilage repair: in vivo performance in a long-term equine model. Biofabrication *12*, 035028.

403.  Mauck, R.L., Yuan, X., and Tuan, R.S. (2006). Chondrogenic differentiation and functional maturation of bovine mesenchymal stem cells in long-term agarose culture. Osteoarthritis And Cartilage *14*, 179–189.

404.  Huang, X., Hou, Y., Zhong, L., Huang, D., Qian, H., Karperien, M., and Chen, W. (2018). Promoted Chondrogenesis of Cocultured Chondrocytes and Mesenchymal Stem Cells under Hypoxia Using In-situ Forming Degradable Hydrogel Scaffolds. Biomacromolecules *19*, 94–102.

405.  Camarero-Espinosa, S., Rothen-Rutishauser, B., Foster, E.J., and Weder, C. (2016). Articular cartilage: from formation to tissue engineering. Biomaterials Science *4*, 734–767.

406.  Richardson, S.M., Kalamegam, G., Pushparaj, P.N., Matta, C., Memic, A., Khademhosseini, A., Mobasheri, R., Poletti, F.L., Hoyland, J.A., and Mobasheri, A. (2016). Mesenchymal stem cells in regenerative medicine: Focus on articular cartilage and intervertebral disc regeneration. Methods (San Diego, Calif.) *99*, 69–80.

407.  Decker, R.S. (2017). Articular cartilage and joint development from embryogenesis to adulthood. Seminars In Cell & Developmental Biology *62*, 50–56.

408.  Sermer, C., Kandel, R., Anderson, J., Hurtig, M., and Theodoropoulos, J. (2018). Platelet-rich plasma enhances the integration of bioengineered cartilage with native tissue in an in vitro model. Journal Of Tissue Engineering And Regenerative Medicine *12*, 427–436.

409.  Tuan, R.S. and Chen, F.H. (2006). Stem cell and gene-based therapy: frontiers in regenerative medicine. In: Battler, A and Leor, J (eds.). Stem Cell And Gene-Based Therapy: Frontiers In Regenerative Medicine , Springer, pp 179–193.

# List of Figures

# List of Tables

# List of Abbreviations

The specification of physical quantities is based on the guidelines of the international system of units.

Special abbreviations for technical terms that are not included in the list are explained in the text.

| Abbreviation | Prefix | Factor |
|:---:|:---:|:---:|
| p | pico- | $10^{-12}$ |
| n | nano- | $10^{-9}$ |
| μ | micro- | $10^{-6}$ |
| m | milli- | $10^{-3}$ |
| c | centi- | $10^{-2}$ |
| k | kilo- | $10^{3}$ |

| | |
|---|---|
| $[RuII(bpy)_3]^{2+}$ | Ruthenium trisbipyridyl chloride |
| °C | Degrees Celsius |
| 2D | Two-dimensional |
| 3D | Three-dimensional |
| ACI | Autologous chondrocyte implantation |
| ACPC | Articular cartilage-resident chondroprogenitor cells |
| ADAMTS | A Disintegrin and Metalloproteinase with Thrombospondin motifs |
| ANOVA | Analysis of variance |
| BAPN | B-aminopropionitrile |
| BMP | Bone morphogenic protein |
| BMSC | Bone marrow-derived mesenchymal stem cell(s) |
| BSA | Bovine serum albumin |
| ButEnOx | 2-Butenyl-2-oxazoline |
| bw | Body weight |
| Ca. | Circa |
| Ch-ABC | Chondroitinase ABC |
| $CO_2$ | Carbon dioxide |
| CTX-II | Human Cross Linked C-Telopeptide of Type II Collagen |
| DAB | P-dimethylamino-benzaldehyde |
| DAPI | 4',6-diamidino-2-phenylindole |
| $dH_2O$ | Distilled water |

| | |
|---|---|
| DIPEN | Aggrecan, N-terminal neoepitope |
| DMEM/F-12 | Dulbecco's modified eagle's medium/ham's f-12 |
| DMMB | Dimethylmethylene blue |
| DMSO | Dimethyl sulfoxide |
| DNA | Deoxyribonucleic acid |
| DNEL | Derived no effect level |
| DOPA | Dihydroxyphenylalanine |
| e.g. | Exempli gratia (Latin "for example") |
| ECM | Extracellular matrix |
| EDHB | Ethyl-3,4-dihydroxybenzoate |
| EDTA | Ethylenediaminetetraacetic acid |
| ERK | Extracellular signal-regulated kinase |
| EthD-III | Ethidium bromide homodimer III |
| EtOH | Ethanol |
| EtOx | 2-ethyl-2-oxazoline |
| FBS | Fetal bovine serum |
| FC | Flow cytometry |
| FDA | Food and Drug Administration |
| FFA | Free fatty acid(s) |
| FGF | Fibroblast growth factor |
| Fib | Fibrinogen |
| g | Gram |
| GF | Growth factor |
| HA-SH | Thiol-functionalized hyaluronic acid |
| HEPES | 4-(2-hydroxyethyl)-1-piperazineethanesulfonic acid |
| HRP | Horseradish peroxidase |
| i.e. | Id est (Latin "that is") |
| IGF | Insulin-like growth factor |
| IgG | Immunoglobulin G |
| IHC | Immunohistochemistry |
| IL-1$\beta$ | Interleukin 1 beta |
| ITS | Insulin-transferrin-selenium |
| KIU | Kallikrein inhibitory unit(s) |

| | |
|---|---|
| L | Liter |
| M | Molarity |
| m | Meter |
| MACI | Matrix-induced chondrocyte implantation |
| MeOx | 2-methyl-2-oxazoline |
| MMP | Matrix metalloproteinase(s) |
| MSC | Mesenchymal stem cell(s) |
| MTT | 3-(4,5-dimethylthiazol-2-yl)-2,5-diphenyltetrazoliumbromid |
| NHS | N-hydroxysuccinimide |
| NITEGE | Aggrecan, C-terminal neoepitope |
| OA | Osteoathritis |
| P(AGE/G) | Allyl-functionalized poly(glycidol)s (P(AGE/G)) |
| PBS | Phosphate-buffered saline |
| PCL | Poly(caprolactone) |
| PCR | Polymerase chain reaction |
| PEG | Poly(ethylene glycol) |
| PEOD | Petox-co-butenox (poly(oxazolines)) |
| PG | Poly(glycidol)s |
| PMOD | Pmeox-co-butenox (poly(oxazolines)) |
| POx | Poly(oxazoline)s |
| PRP | Platelet-rich plasma |
| QSAR | Quantitative structure-activity relationship |
| RNA | Ribonucleic acid |
| SafO | Safranin O |
| SD | Standard deviation |
| SEM | Scanning electron microscopy |
| SPS | Sodium persulfate |
| TE | Tissue engineering |
| TGF-β | Transforming growth factor-beta |
| TNF- α | Tumor-necrosis factor-alpha |
| U | Unit |
| v/v | Volume/volume % |
| w/o | Without |

| | |
|---|---|
| w/v | Weight/volume % |
| x g | Fold gravitational acceleration (g = 9.81 m/s$^2$) |

## Affidavit

I hereby confirm that my thesis entitled ''Lateral cartilage tissue integration - Evaluation of Bonding Strength and Tissue Integration *in vitro* Utilizing Biomaterials and Adhesives'' is the result of my own work. I did not receive any help or support from commercial consultants. All sources and/or materials applied are listed and specified in the thesis.

Furthermore, I confirm that this thesis has not been submitted as part of another examination process neither in identical nor in similar form.

_____     _____

Place, date     Signature

## Eidesstattliche Erklärung

Hiermit erkläre ich an Eides statt, die Dissertation „ Laterale Knorpelintegration - Beurteilung der Adhäsionskraft und der Gewebeintegration *in vitro* unter Verwendung verschiedener Biomaterialien und Gewebekleber" eigenständig, d.h. insbesondere selbständig und ohne Hilfe eines kommerziellen Promotionsberaters, angefertigt und keine anderen als die von mir angegebenen Quellen und Hilfsmittel verwendet zu haben.

Ich erkläre außerdem, dass die Dissertation weder in gleicher noch in ähnlicher Form bereits in einem anderen Prüfungsverfahren vorgelegen hat.

_____     _____

Ort, Datum     Unterschrift

# Statement on Copyright and Self-Plagiarism

The data presented in this thesis have been partially published in the Journal of Industrial and Engineering Chemistry as an original article entitled "Catechol-modified Poly(oxazoline)s with Tunable Degradability Facilitate Cell Invasion and Lateral Cartilage Integration". In accordance with the regulations of the parent publisher Elsevier, data, text passages and illustrations from the manuscript were used in identical or modified form in this thesis.

## Statement of individual author contributions and of legal second publication rights

Oliver Berberich[1], Julia Blöhbaum[1], Stefanie Hölscher-Doht, Rainer Meffert, Jörg Teßmar, Torsten Blunk, Jürgen Groll; Catechol-modified Poly(oxazoline)s with Tunable Degradability Facilitate Cell Invasion and Lateral Cartilage Integration, Journal of Industrial and Engineering Chemistry 2019, 80, p. 757-769. Copyright © 2019 The Korean Society of Industrial and Engineering Chemistry

[1] These authors contributed equally.

I, O. Berberich, was co-responsible for the production of all data and the preparation of all Figures that were reused from this original article if not otherwise stated at the respective illustration. J. Blöhbaum was equally contributing to this publication and was responsible for synthesis/characterization of POx polymers, Young's modulus and UV/Vis measurements. S. Hölscher-Doht and R. Meffert were consulted for physiological and biomechanical interpretations. T. Blunk, J. Teßmar and J. Groll were the principal investigators and were involved in the study design, writing of the manuscript and the proofreading.

# Acknowledgement